

**Investigation of Multiple Tank Car Rollover Derailments – Standard Type E
Double-shelf Coupler, and Modified Rotary Coupler**

Phase 2

Prepared for
Transport Dangerous Goods Directorate
of
Transport Canada

by
Centre for Surface Transportation Technology
National Research Council Canada

December 17, 2012

CSTT-RVC-TR-216

Investigation of Multiple Tank Car Rollover Derailments – Standard Type E Double-shelf
Coupler, and Modified Rotary Coupler

Phase 2

Albert Wahba, P. Eng.,
Yan Liu, P. Eng.,
Rebecca Mann, B.Sc., PMP,
Jon Preston-Thomas, P.Eng,
Robert Caldwell, P.Eng
and Alexandre Woelfle

Centre for Surface Transportation Technology
National Research Council Canada

December 17, 2012

REPORT PREPARED BY:



Albert Wahba, P.Eng.

Dec 10, 2012

Date



Yan Liu, P.Eng.

Dec. 10, 2012

Date



Rebecca Mann, B.Sc., PMP

Dec 10, 2012

Date



Jon Preston-Thomas, P.Eng.

10 Dec 2012

Date



Robert Caldwell, P.Eng.

Dec 10, 2012

Date



Alexandre Woelfle

Dec 10, 2012

Date

APPROVED BY:



Paul Treboutat
[General Manager]

10 Dec 2012

Date

NOTES:

This report reflects the views of the authors and not necessarily the official views or policies of the Transportation Technology and Innovation Directorate of Transport Canada or the co-sponsoring organizations.

The Transportation Technology and Innovation Directorate and the co-sponsoring agencies do not endorse products or manufacturers. Trade or manufacturers' names appear in this report only because they are essential to its objectives.

Since some of the accepted measures in the industry are imperial, metric measures are not always used in this report. Prices are given in Canadian dollars unless otherwise noted, and may have been converted from foreign currencies at the time of writing.

The National Research Council renamed the Centre for Surface Transportation Technology NRC-CSTT to Surface Transportation Portfolio NRC-ST on April 1, 2012. Since this project began and the report was published in draft form before that date, the old naming convention and report number have been retained.

Un sommaire français se trouve avant la table des matières.

PUBLICATION DATA FORM

| | | | | | |
|---|--|--------------------------------------|----------------------------------|--|--|
| 1. Transport Canada Publication No. TP | | 2. Project No. | | 3. Recipient's Catalogue No. | |
| 4. Title and Subtitle Investigation of Multiple Tank Car Rollover Derailments – Standard Type E Double-shelf Coupler, and Modified Rotary Coupler | | | | 5. Publication Date December 17, 2012 | |
| | | | | 6. Performing Organization Document No. CSTT-RVC-TR-216 | |
| 7. Author(s) Albert Wahba, P. Eng., Yan Liu, P. Eng., Rebecca Mann, B.Sc., PMP, Jon Preston-Thomas, P.Eng., Robert Caldwell, P.Eng., and Alexandre Woelfle | | | | 8. Transport Canada File No. | |
| 9. Performing Organization Name and Address Centre for Surface Transportation Technology (CSTT) National Research Council (NRC) U89 Lester Road, Ottawa ON K1A 0R6 | | | | 10. PWGSC File No. --- | |
| | | | | 11. PWGSC or Transport Canada Contract No. --- | |
| 12. Sponsoring Agency Name and Address Transport Dangerous Goods Directorate 330 Sparks Street, 9th Floor, Tower C Ottawa, ON K1A 0N5 | | | | 13. Type of Publication and Period Covered | |
| | | | | 14. Project Officer | |
| 15. Supplementary Notes (Funding programs, titles of related publications, etc.) | | | | | |
| 16. Abstract A review of TSB and NTSB reports did not give any indications that multiple tank car derailments, sometimes referred to as domino derailments, are related to the use of double-shelf couplers. An energy analysis determined the car body roll angle at which loaded and empty tank cars become unstable and roll off their trucks, alone and in a consist. Dynamic simulations of empty tank cars connected with Type E couplers with and without shelves supports historical observations that these rollovers did not occur prior to the implementation of double-shelf couplers. Full scale, zero-speed, physical testing of a short string of empty tank cars with double-shelf couplers showed that all cars rolled over without shelf-to-knuckle contact occurring. A subsequent test involving a rotary coupler with a double-shelf Type E head installed in the end of the car that faced the oncoming rollover was successful in stopping the rollover with very little roll of the car so equipped. Knuckle-to-shelf contact occurred at the coupling with the rotary coupler. When the rotary coupler was positioned at the opposite end of the car, it prevented the next car from completely rolling over although it did roll to 30°. Knuckle-to-shelf contact occurred again at the coupling with the rotary coupler. This performance difference is due to delayed transmission of vertical lift to the downstream (driven) car, when the rotary coupler is installed in the upstream (driving) car. | | | | | |
| 17. Key Words Railway, couplers, domino-effect, rollover, simulation, physical testing, literature survey, tank car, energy analysis, double-shelf coupler, truck, side frame, truck bolster, car body bolster | | | | 18. Distribution Statement . | |
| 19. Security Classification (of this publication) Unclassified | 20. Security Classification (of this page) Unclassified | 21. Declassification (date) - | 22. No. of Pages xvi, 131 | 23. Price Shipping/ handling | |

FORMULE DE DONNÉES POUR PUBLICATION

| | | | | | |
|--|--|---|---------------------|--|--|
| 1. No de la publication de Transports Canada | | 2. No de l'étude | | 3. N° de catalogue du destinataire | |
| 4. Titre et sous-titre | | 5. Date de la publication | | le 17 decembre, 2012 | |
| | | 6. N° de document de l'organisme exécutant | | CSTT-RVC-TR-216 | |
| 7. Auteur(s) | | 8. N° de dossier - Transports Canada | | Albert Wahba, P. Eng., Yan Liu, P. Eng., Rebecca Mann, B.Sc., PMP, Jon Preston-Thomas, P.Eng., Robert Caldwell, P.Eng. and Alexandre Woelfle | |
| 9. Nom et adresses de l'organisme parrain | | 10. N° de dossier – TPSGC | | Centre de technologie des transports de surface Conseil national de recherches Canada (CNRC) U89, chemin Lester, Ottawa (Ontario) K1A 0R6 | |
| | | 11. N° de contrat - TPSGC ou Transports Canada | | | |
| 12. Nom et adresse de l'organisme parrain | | 13. Genre de publication et période visée | | Transport des marchandises dangereuses 330 rue Sparks, 9 ^{ième} étage, Tour C Ottawa, ON K1A 0N5 | |
| | | 14. Agent de projet | | | |
| 15. Remarque additionnelles (programmes de financement, titres de publications connexes, etc.) | | | | | |
| 16. Résumé | | | | | |
| 17. Mots clés | | 18. Diffusion | | | |
| | | Le Centre de développement des transports dispose d'un nombre limité d'exemplaires. | | | |
| 19. Classification de sécurité (de cette publication) | 20. Classification de sécurité (de cette page) | 21. Déclassification (date) | 22. Nombre de pages | 23. Prix | |
| Non classifiée | Non classifiée | - | xvi, 131 | Port et manutention | |

EXECUTIVE SUMMARY

Purpose

This report was prepared by the National Research Council Canada's Centre for Surface Transportation Technology for the second phase of the investigation of multiple tank car rollover derailments, sometimes referred to as domino derailments. This phenomenon has been reported to occur for empty tank cars. An excellent example of such a derailment is the one that occurred in Clara City, Minnesota in October 2007. In a domino derailment, two or more tank cars must be coupled together. If one empty tank car rolls off its trucks, the tank car to which this initiating car is coupled also rolls off its trucks, causing the next tank car to do the same. The use of double-shelf couplers on tank cars prevents vertical disengagement of the couplers, so there is no means for the tank cars to separate during the derailment process unless component failure occurs.

Method

This phase of the investigation was performed in two parts. The first part included:

- a literature survey to check for incidents of domino derailments of loaded tank cars; if such incidents were to occur, the potential consequences could be far greater than for a domino rollover of empty tank cars,
- a basic analysis to examine the change of potential energies when a single empty tank car and a single loaded tank car roll over; the analysis was then extended to include several empty tank cars and several loaded tank cars,
- multi-body dynamic simulations of tank cars equipped with Type E couplers (without double-shelf) and with standard (non-rotary) Type F double-shelf couplers.

The second part of this phase of the investigation was the performance of full-scale physical tests on a short string of empty tank cars that underwent a domino derailment. The purpose of the test was to carry out measurements to support the simulation work and to test a potential solution to the domino derailment problem.

This report discusses the work that was done for both parts of the second phase of the investigation.

Results

The results of the literature survey are that reports from the United States' National Transportation Safety Board provide no information about the nature of loaded tank car derailments with respect to the domino derailment phenomenon. Twenty-four reports from 1993 to 2010 were reviewed. These reports seldom mention double-shelf couplers except to say that they are standard equipment on tank cars.

Seventy-three reports (1993 – 2010) were examined from Canada's Transportation Safety Board, and seventeen of these concern derailments of loaded tanks cars. There are two cases in which double-shelf couplers are stated as the reason for the rollover of some of the loaded cars, seven cases where it seems likely that loaded cars rolled over in domino-type fashion, and eight cases where the details of the report are insufficient to draw a conclusion. In most cases, the number of rolled loaded tank cars is relatively

small (2 – 4). There is one derailment in which four loaded tank cars rolled over at near zero-speed, similar to the Clara City incident (although on smaller scale).

The energy analysis shows that when a single empty tank car begins to roll over, the potential energy increases and reaches a maximum at 41° of body roll angle and then decreases as the roll angle continues to increase. The system potential energy of a string of empty tank cars undergoing a domino rollover reaches a maximum once the first car body rolls to a 64° angle and only decreases after that. If the differential roll angle, or roll slack, between cars is 18° (as it is during the physical tests described in this report), the system potential energy peaks before the fifth car body begins to roll, so only four empty tank cars are actively propagating the domino event. Leading cars continuously transfer energy to subsequent cars; this is what enables the rollover derailment to propagate through a train of empty tank cars.

A necessary condition for the domino effect to begin is that sufficient energy must be transferred to the undisturbed system to roll the first empty tank car to 64°; this puts the system at the point of maximum energy (a system metastable point). This energy transfer could result from a sideswipe impact with another train. The kinetic energy in a single empty or loaded tank car moving at speeds that are typical in rail yards is equivalent to the change in potential energy needed to reach the system meta-stable point.

The energy analysis also shows that when a single loaded tank car begins to roll over, its potential energy increases until the car body roll angle reaches 25°. The system potential energy of a string of loaded tank cars reaches its maximum when the first car has rolled to 32°. With roll slack of 18° between cars, the second car has only rolled to 14° and the third car has not yet moved, therefore only two loaded tank cars are responsible for starting the domino progression.

A necessary condition for the domino effect to begin is that sufficient energy must be transferred to the undisturbed system to roll the first loaded tank car to 32°; this puts the system at the point of maximum energy (a system meta-stable point). As with the empty tank cars, the kinetic energy of empty or loaded tank cars moving at speeds common in rail yards is equivalent to the energy needed to reach the system meta-stable point.

The results of the multi-body dynamic simulations are that cars equipped with Type E couplers (without double-shelf) are that domino derailment does not occur, due to coupler disengagement. This supports historical observations that domino derailments of tank cars did not occur prior to the introduction of double-shelf couplers. Simulations of tank cars equipped with Type E double-shelf couplers did result in domino rollover, supporting the general observation that domino rollovers do occur on tank cars fitted with this equipment.

A dry run test was conducted, followed by four dynamic tests. The dry run was needed to determine how best to pull on the first (initiating) car to start off the domino progression, and to decide where instrumentation and video cameras could be installed so that they would not get damaged during subsequent tests.

The first test was a full dynamic test at zero speed, using Type E double-shelf couplers between all cars. Four cars were involved, but the first car was used only as an initiating car and the remaining cars were the ones from which data was captured. All four cars rolled over during the test.

The second test involved the same four cars, but the second test car had a Type E double-shelf coupler that was modified to be a rotary coupler. This modified coupler was

installed in the end of the car closest to the initiating car (the near end of the second test car). The initiating car rolled over the first test car, but the domino progression halted at the second test car. The second test car remained upright in a yawed position, its near end still coupled to and supported by the far-end coupler of the first test car. The far end of the second test car was still sitting on its truck. The second test car only displaced very slightly in roll during the test.

The third test involved the same four cars as before, but with a fifth car added at the end of the consist to provide rollover resistance (if needed). The orientation of the second test car was reversed so the rotary Type E double-shelf coupler was now at the far end of the car. The domino derailment was initiated as before and this time the first and second test cars rolled over. The third test car did not roll over, but its body rolled significantly before the rollover event stopped.

The fourth test was a repeat of the third test, but with a modification to the draft sill at the far end of the second test car. This car was originally equipped with Type F couplers, and the original couplers were supported on a spring-loaded carrier iron. For the final test, the carrier iron was welded in place to make it functionally equivalent to the carrier iron on rail cars equipped with Type E couplers. The intent was to check if the carrier iron springs had influenced the manner in which the domino progression had halted during the third test. Despite this change, the result of the fourth test was essentially the same as that of the third test.

Conclusions

Based on the results of the literature survey domino-type rollovers for loaded trains cannot be ruled out, although the possibility of a large-scale incident seems remote.

The kinetic energy that must be added to the system to initiate a loaded car domino rollover is 1.6 times that required for the empty car case. Reducing the roll slack between coupled cars can significantly increase the energy required for a string of empty tank cars to reach the meta-stable point. If the roll slack is decreased from 18° to 11° , the change in potential energy required for a string of empty cars to reach its meta-stable point becomes the same as required for a string of loaded tank cars. Such an increase in potential energy could result in component failure and car separation, acting as a fuse between tank cars so as to halt the domino progression. An examination of this possibility is beyond the scope of this project.

The simulations of tank cars with double-shelf couplers showed that rollover was caused mainly by torque transfer between adjacent cars through the couplers.

Since a rotary coupler is free to roll within the sill of the car on which it is installed, it is unable to transmit a roll torque to its own car body or through the coupler to which it is joined.

The rolling motion of a driving car's body causes both lateral and vertical displacement at the adjacent, or driven, car body.

Lateral displacement that occurs in advance of vertical displacement causes the driven car's body and truck to roll together as an assembly until the truck slides off the track. This frees the car body from the truck and stops the domino effect from rolling the driven car body further. The zero-speed derailment ends with the driven car body rolled at a significant angle, partially supported by its trucks and possibly by the coupler on the driving car. **This is the domino-halting mechanism in the third and fourth physical tests.**

Vertical displacement that occurs in advance of lateral displacement helps to partially free the driven car's near-end centre plate from its truck before lateral motion causes the driven car's truck to roll about the wheel/rail contact points. The driven car's body does not roll with its truck, and no roll moment is applied to the driven car's body through the rotary coupler. Therefore, the driven car body does not roll. The zero-speed derailment ends when the driven car's centre plate drags the pin out of the near-end truck, which falls back to the rails. The driven car is suspended by its near end coupler, and sits on its undisturbed far-end truck. **This is the domino-halting mechanism in the second test.**

In the second, third and fourth physical tests, the rotary coupler:

- Absorbed the differential roll between the driving car and the driven car
- Did not transmit a roll torque to either the driving or driven car body

In contrast, standard Type E double-shelf couplers:

- Can only absorb roughly 18° of differential roll (based on angular slack in the coupling system)
- Always transmit a roll torque from the driving car to the driven car's body

Insufficient vertical lift at the near end of the driven car forced the near-end truck of the driven car to roll in order for the near-end car body to follow the lateral motion of the driving car. Since the driven car body was still connected to its near-end truck, the body rolled with the truck. This made the third and fourth tests appear less successful than the second, but the rotary coupler was nonetheless successful at stopping the domino progression in all three tests where it was used.

TABLE OF CONTENTS

| | |
|---|-------|
| EXECUTIVE SUMMARY | xi |
| TABLE OF CONTENTS | xv |
| LIST OF FIGURES | xviii |
| LIST OF TABLES..... | xxiv |
| GLOSSARY | xxv |
| 1. INTRODUCTION – PART 2 | 27 |
| 2. LITERATURE SURVEY ON LOADED TANK CAR ROLLOVERS | 28 |
| 2.1 Background..... | 28 |
| 2.2 NTSB Reports..... | 28 |
| 2.3 TSB Reports | 28 |
| 3. ENERGY ANALYSIS OF TANK CAR DOMINO ROLLOVERS..... | 33 |
| 3.1 Introduction | 33 |
| 3.2 Stages – Empty Tank Car | 34 |
| 3.2.1 Stage 1 | 35 |
| 3.2.2 Stage 2 | 36 |
| 3.2.3 Stage 3 | 37 |
| 3.2.4 Stage 4 | 39 |
| 3.2.5 Stage 5 | 40 |
| 3.2.6 Stage 6 | 41 |
| 3.2.7 Stage 7 | 42 |
| 3.3 Analysis – Empty Tank Car | 43 |
| 3.4 Stages – Loaded Tank Car..... | 45 |
| 3.4.1 Stage 1 | 47 |
| 3.4.2 Stage 2 | 48 |
| 3.4.3 Stage 3 | 49 |
| 3.4.4 Stage 4 | 50 |
| 3.4.5 Stage 5 | 52 |
| 3.4.6 Stage 6 | 53 |
| 3.4.7 Stage 7 | 54 |
| 3.4.8 Stage 8 | 55 |
| 3.5 Analysis – Loaded Tank Car | 56 |
| 3.6 Comparison of Empty and Loaded Cases | 57 |
| 4. VAMPIRE SIMULATION | 61 |

| | | |
|-------|--|-----|
| 4.1 | Introduction | 61 |
| 4.2 | Simulation Approach | 61 |
| 4.3 | Simulation Results | 64 |
| 4.4 | Proposed Dynamic Simulation Work for Future Consideration | 70 |
| 4.5 | Capabilities and Limitations of the Future Simulation Models | 73 |
| 5. | PHYSICAL TESTING..... | 77 |
| 5.1 | Introduction | 77 |
| 5.2 | Objectives | 78 |
| 5.3 | Test Results | 81 |
| 5.3.1 | Dry Run Testing | 81 |
| 5.3.2 | Test Preparation | 84 |
| 5.3.3 | Instrumentation | 87 |
| 5.3.4 | Test #1: Baseline Dynamic Testing | 92 |
| 5.3.5 | Test #2: Dynamic Testing With Modified Rotary Coupler – 4 Cars | 112 |
| 5.3.6 | Test #3: Dynamic Testing With Modified Rotary Coupler – 5 Cars | 126 |
| 5.3.7 | Test #4: Dynamic Testing With Modified Rotary Coupler – Blocked Carrier Springs | 138 |
| 5.4 | Explanation of the Domino Rollover Phenomenon and Rotary Coupler Effect | 147 |
| 5.4.1 | Domino Rollover Phenomenon – Standard Type E Double-Shelf Couplers | 147 |
| 5.4.2 | Rotary Coupler Effect – Facing the Oncoming Domino Wave..... | 147 |
| 5.4.3 | Rotary Coupler Effect – Facing Away from the Oncoming Domino Wave | 148 |
| 5.4.4 | Comparison of the Rotary Coupler Effectiveness in Tests #2, #3 and #4 | 150 |
| 5.4.5 | Study Limitations..... | 153 |
| 6. | CONCLUSIONS..... | 155 |
| 6.1 | Literature Survey On Loaded Tank Car Rollovers | 155 |
| 6.2 | Energy Analysis – Unloaded and Loaded Cases..... | 155 |
| 6.3 | Vampire Simulation | 156 |
| 6.4 | Physical Testing | 156 |
| 6.4.1 | Dry-Run Test..... | 156 |
| 6.4.2 | Dynamic Test #1 - Baseline with Standard Type E Double-Shelf Couplers – 4 Cars..... | 157 |

| | | |
|------------|---|------|
| 6.4.3 | Dynamic Test #2 with Modified Rotary Coupler – 4 Cars..... | 158 |
| 6.4.4 | Dynamic Tests #3 and #4 with Modified Rotary Coupler– 5 Cars | 159 |
| 6.4.5 | Physical Test Summary | 159 |
| 7. | REFERENCES | 167 |
| APPENDIX A | INSTRUMENTATION LIST | A-1 |
| APPENDIX B | TANK CAR DRAFT SILL CALIBRATIONS | B-1 |
| | B.1 Strain Gauges Location Investigation | B-2 |
| | B.2 Final Strain Gauge Locations | B-4 |
| | B.3 Calibration Procedure | B-5 |
| | <i>B.3.1</i> Calibration Beam..... | B-5 |
| | <i>B.3.2</i> Vertical Calibration Procedure..... | B-6 |
| | <i>B.3.3</i> Torque Calibration Procedure | B-7 |
| | B.4 Calibration Results | B-9 |
| | B.4.1 Disclaimer | B-9 |
| | B.4.2 Vertical Force Calibration Results | B-9 |
| | B.4.3 Torque Calibration Results | B-12 |
| APPENDIX C | MODIFIED ROTARY COUPLER MANUFACTURING AND INSTALLATION..... | C-15 |
| | C.1 Coupler Modification | C-16 |
| | C.2 Coupler Installation | C-17 |
| APPENDIX D | TANK CAR WEIGHTS AND DIMENSIONS..... | D-1 |
| APPENDIX E | TANK CAR AND TRUCK COMPONENT TERMINOLOGY | E-1 |

LIST OF FIGURES

| | | |
|------------|--|----|
| Figure 1: | Tank car sitting undisturbed on level track. | 35 |
| Figure 2: | Car body rolled onto the side bearings. | 36 |
| Figure 3: | Car body rolls about the side bearings until contact occurs with the side frame. | 37 |
| Figure 4: | Car body rolled contacting the side frame at the end of Stage 3. | 38 |
| Figure 5: | Car body has rolled about the inside corner of the side frame, until the body bolster lies flat on the side frame. | 40 |
| Figure 6: | Car body carried on the outside corner of the side frame. | 41 |
| Figure 7: | Car body has rolled about the wheel/rail contact points until the body contacts the ground below the TOR. | 42 |
| Figure 8: | Truck falls back on the rails after the car body has rolled sufficiently far away on the ground. | 43 |
| Figure 9: | Change in potential energies of empty tank cars and change in total potential energy of a system, as a function of the car body roll angle of the first car. | 45 |
| Figure 10: | Tank car sitting undisturbed on level track. | 47 |
| Figure 11: | Car body compresses truck suspension springs. | 48 |
| Figure 12: | Car body load transferred to side bearing from centre plate. | 49 |
| Figure 13: | Car body rolls about the side bearing until contacting the side frame. | 50 |
| Figure 14: | Final position of Stage 4 - car body just contacts inside corner of side frame without loading it. | 51 |
| Figure 15: | Car body load transferred to inside corner of the side frame. | 52 |
| Figure 16: | Car body rolls about the side frame until the system becomes unstable. | 53 |
| Figure 17: | Car body has rolled about the wheel/rail contact points until the body contacts the ground below the TOR. | 54 |
| Figure 18: | Truck falls back on the rails after the car body has rolled sufficiently far away on the ground. | 55 |
| Figure 19: | Change in potential energies of loaded tank cars and change in total potential energy of a system, as a function of the car body roll angle of the first car. | 57 |
| Figure 20: | Comparison of system variation in potential energy between loaded and unloaded tank cars. | 58 |
| Figure 21: | Effect of reducing coupler slack on system energy. | 59 |
| Figure 22: | Sample of measured torque vs angular displacement for a shelf (S1) coupler mated with a second shelf coupler (S2), from Trent et al [2]. | 63 |

| | | |
|------------|--|----|
| Figure 23: | Assumed impact scenario..... | 64 |
| Figure 24: | Animations of simulation results for regular Type E coupler case..... | 67 |
| Figure 25: | Car body roll angles obtained by simulation for regular Type E coupler case. | 68 |
| Figure 26: | Animations of simulation results for double-shelf coupler case..... | 69 |
| Figure 27: | Car body roll angles obtained by simulation for double-shelf coupler case. | 70 |
| Figure 28: | Test #1, dynamic testing - test setup schematic..... | 78 |
| Figure 29: | Test #2, dynamic testing - test setup schematic..... | 79 |
| Figure 30: | Test #3, dynamic testing - test setup schematic..... | 79 |
| Figure 31: | Test #4, dynamic testing - test setup schematic..... | 80 |
| Figure 32: | Pulling laterally at the end of the car from centre..... | 81 |
| Figure 33: | Pulling laterally at the end of the car from top. | 82 |
| Figure 34: | Pulling laterally at the middle of the car from top. | 82 |
| Figure 35: | Pulling vertically at the end of the car from jacking pad..... | 83 |
| Figure 36: | Pulling vertically at the end of the car using a custom-made beam. | 83 |
| Figure 37: | Truck almost touching the concrete during the dry-run test (left); and holes in the concrete during testing (right)..... | 84 |
| Figure 38: | Track support..... | 85 |
| Figure 39: | Cars landing on tires. | 85 |
| Figure 40: | Tires under Car #II after the rollover occurred..... | 86 |
| Figure 41: | Typical inclinometer location to measure coupler rotation angle..... | 87 |
| Figure 42: | Typical inclinometer location to measure car body rotation angle..... | 88 |
| Figure 43: | Typical inclinometer location to measure car body pitching angle. | 88 |
| Figure 44: | Typical inclinometer location to measure truck bolster rotation angle..... | 89 |
| Figure 45: | Typical event sensor location to detect contact of body bolster to side bearings, and contact of body bolster to truck side frame (rolled side)..... | 89 |
| Figure 46: | Typical event sensor location to detect shelf/knuckle contact..... | 90 |
| Figure 47: | Typical displacement sensor location to measure the height of the draft sill above top of the rail. | 90 |
| Figure 48: | Typical displacement sensor location to measure draft sill horizontal displacement across track. | 91 |
| Figure 49: | Typical strain gauge locations to measure car vertical load and torque. | 91 |
| Figure 50: | Test #1, dynamic baseline testing - test setup schematic..... | 92 |
| Figure 51: | Test #1, dynamic baseline testing – test setup..... | 93 |

| | | |
|------------|---|-----|
| Figure 52: | Test #1, initiating car on ground, failed rollover attempt. | 93 |
| Figure 53: | Test #1, pulling laterally at the near end of Car #I from top. | 94 |
| Figure 54: | Test #1, cars after test – side view. | 95 |
| Figure 55: | Test #1, cars after test – tail end view. | 95 |
| Figure 56: | Test #1, cars after test – initiating end view. | 96 |
| Figure 57: | Test #1, cars after test – close up of trucks. | 96 |
| Figure 58: | Test #1, cars after test – linked coupler. | 97 |
| Figure 59: | Test #1, broken coupler key of Car #II A-end. | 97 |
| Figure 60: | Test #1 first roll attempt, events on Car #III. | 99 |
| Figure 61: | Test #1 second roll attempt, events on Car #III. | 99 |
| Figure 62: | Gouge on wall of far end coupler of Car #I after Test #1. | 100 |
| Figure 63: | Test #1 first roll attempt, displacements for Car #II. | 101 |
| Figure 64: | Test #1 first roll attempt, displacements for Car #III. | 101 |
| Figure 65: | Test #1 second roll attempt, displacements for Car #II. | 102 |
| Figure 66: | Test #1 second roll attempt, displacement for Car #III. | 102 |
| Figure 67: | Test #1 first roll attempt, vertical forces on near-end car sills. | 103 |
| Figure 68: | Test #1 second roll attempt, vertical forces on near-end car sills. | 104 |
| Figure 69: | Test #1 first roll attempt, torques on near-end car sills. | 104 |
| Figure 70: | Test #1 second roll attempt, torques on near-end car sills. | 105 |
| Figure 71: | Test #1 second roll attempt, Car #III roll and side bearing contact at near end. | 106 |
| Figure 72: | Test #1 second roll attempt, centre pin in Car #III near truck. | 107 |
| Figure 73: | Test #1 second roll attempt, Car #III truck and body roll. | 108 |
| Figure 74: | Test #1 second roll attempt, Car #III roll and side bearing contact at far end. | 109 |
| Figure 75: | Test #2, dynamic testing with one modified rotary coupler and 4 tank cars - test setup schematic. | 112 |
| Figure 76: | Test #2, dynamic testing with one modified rotary coupler and 4 tank cars - test setup. | 113 |
| Figure 77: | Test #2, cars after test, initiating end – rotary coupler stopped the rollover propagation. | 114 |
| Figure 78: | Test #2, cars after test, tail end – rotary coupler stopped the rollover propagation. | 114 |
| Figure 79: | Test #2, cars after test, north side – modified rotary coupler junction. | 115 |
| Figure 80: | Test #2, cars after test, south side – modified rotary coupler junction. | 115 |

| | | |
|-------------|---|-----|
| Figure 81: | Test #2, rotary coupler after test. | 116 |
| Figure 82: | Test #2, rotary coupler orientation after test. | 116 |
| Figure 83: | Test #2, events on Car #III. | 118 |
| Figure 84: | Test #2, displacements on Car #I. | 118 |
| Figure 85: | Test #2, displacements on Car #III. | 119 |
| Figure 86: | Test #2, vertical forces on car sills. | 120 |
| Figure 87: | Test #2, torques on car sills. | 121 |
| Figure 88: | Test #2, motion at the near end of Car #III. | 123 |
| Figure 89: | Damage to Car #III centre bowl on near truck. | 124 |
| Figure 90: | Test #3, dynamic testing with one modified rotary coupler and 5 tank cars - test setup schematic. | 126 |
| Figure 91: | Test #3, dynamic testing with one modified rotary coupler and 5 tank cars - test setup. | 127 |
| Figure 92: | Test #3, lateral force applied at the middle of the initiating car from the top. | 127 |
| Figure 93: | Test #3, cars after test – rotary coupler stopped the rollover propagation. | 128 |
| Figure 94: | Test #3, rotary coupler after test. | 128 |
| Figure 95: | Test #3, rotary coupler partially opened after test, release arm hit ground. | 129 |
| Figure 96: | Test #3, rotary coupler partially opened after test. | 129 |
| Figure 97: | Comparison between rotary coupler position (before lifting the following car) in Test #2 (left) and Test #3 (right). | 130 |
| Figure 98: | Rotary coupler resting on the bottom springs (left); rotary coupler not touching the springs (fully compressed) (right). | 131 |
| Figure 99: | Top gap (left); bottom gap (right). | 131 |
| Figure 100: | Rear assembly of the rotary coupler. | 132 |
| Figure 101: | Rotary coupler assembly. | 133 |
| Figure 102: | Car #II near-end truck. | 134 |
| Figure 103: | Car #II near-end truck. | 134 |
| Figure 104: | Car #II after testing. | 135 |
| Figure 105: | Car #II far-end truck after testing. | 135 |
| Figure 106: | Test #4, dynamic testing with one modified rotary coupler and 5 tank cars - test setup schematic. | 138 |
| Figure 107: | Test setup showing rollover force application. | 139 |
| Figure 108: | Rotary coupler with isolated carrier system. | 140 |
| Figure 109: | Test #4 – five car test consist prior to rollover. | 140 |

| | | |
|-------------|---|------|
| Figure 110: | Test #4, five car test consist after rollover – rotary coupler stopped the rollover. | 141 |
| Figure 111: | Test #4, dynamic testing with one modified rotary coupler and five tank cars. | 141 |
| Figure 112: | Test #4, Car #II near-end truck. | 142 |
| Figure 113: | Test #4, Car #II far-end truck. | 143 |
| Figure 114: | Consist after test, from rolled end. | 143 |
| Figure 115: | Final position of modified rotary coupler. | 144 |
| Figure 116: | Test #4 modified rotary coupler partially opened after test, release arm hit ground..... | 145 |
| Figure 117: | Draft sill vertical force and torque measurements..... | A-5 |
| Figure 118: | Draft sill displacement measurements..... | A-5 |
| Figure 119: | Contact between a knuckle and shelf..... | A-6 |
| Figure 120: | Contact of body bolster to truck side frame and side bearings. | A-6 |
| Figure 121: | Car body pitching..... | A-7 |
| Figure 122: | Car body and truck bolster rotation angle..... | A-7 |
| Figure 123: | Coupler rotation angle..... | A-8 |
| Figure 124: | Preliminary strain gauge locations on draft sill. | B-2 |
| Figure 125: | Preliminary strain gauge bridge wiring diagrams. | B-3 |
| Figure 126: | Typical strain gauge locations on draft sill. | B-4 |
| Figure 127: | Strain gauge locations on Car #III draft sill. | B-4 |
| Figure 128: | Strain gauges SG3 & SG4 on Car #II draft sill..... | B-5 |
| Figure 129: | Calibration beam..... | B-6 |
| Figure 130: | Typical vertical force calibration setup..... | B-6 |
| Figure 131: | Torque calibration setup..... | B-7 |
| Figure 132: | Torque calculations - beam at angle zero..... | B-8 |
| Figure 133: | Torque calculations - beam at angle θ | B-8 |
| Figure 134: | Calculated and applied vertical forces – Car #I A-end..... | B-10 |
| Figure 135: | Percent error in calculated vertical force measurements – Car #I B-end. | B-10 |
| Figure 136: | Percent crosstalk error in torque measurements – Car #I B-end. | B-11 |
| Figure 137: | Calculated and applied torque – Car #I A-end..... | B-13 |
| Figure 138: | Percent error in calculated torque measurements – Car #I B-end. | B-14 |
| Figure 139: | Percent crosstalk error in vertical force measurements – Car #I A-end..... | B-14 |
| Figure 140: | Rotary coupler modification schematic..... | C-16 |

| | | |
|-------------|---|------|
| Figure 141: | Modified rotary coupler manufacturing. | C-17 |
| Figure 142: | Modified rotary coupler inside Type E sill/striker..... | C-18 |
| Figure 143: | Modified rotary coupler inside Type F sill/striker..... | C-18 |
| Figure 144: | Sill before modification. | C-19 |
| Figure 145: | Sill after modification. | C-19 |
| Figure 146: | Insertion of 1 in. spacer below the yoke | C-19 |

LIST OF TABLES

| | | |
|-----------|--|------|
| Table 1: | Empty car energy with respect to the top of the rails, Stage 1..... | 35 |
| Table 2: | Empty car energy with respect to the top of the rails, Stage 2..... | 36 |
| Table 3: | Empty car energy with respect to the top of the rails, Stage 3..... | 38 |
| Table 4: | Empty car energy with respect to the top of the rails, Stage 4..... | 39 |
| Table 5: | Empty car energy with respect to the top of the rails, Stage 6..... | 42 |
| Table 6: | Empty car energy with respect to the top of the rails, Stage 7..... | 43 |
| Table 7: | Loaded car energy with respect to the top of the rails, Stage 1..... | 47 |
| Table 8: | Loaded car energy with respect to the top of the rails, Stage 2..... | 48 |
| Table 9: | Loaded car energy with respect to the top of the rails, Stage 4..... | 51 |
| Table 10: | Loaded car energy with respect to the top of the rails, Stage 6..... | 53 |
| Table 11: | Loaded car energy with respect to the top of the rails, Stage 7..... | 54 |
| Table 12: | Loaded car energy with respect to the top of the rails, Stage 8..... | 55 |
| Table 13: | Major parameters for dynamic simulation..... | 65 |
| Table 14: | Capabilities and limitations of the developed simulation models..... | 74 |
| Table 15: | List of instruments..... | 87 |
| Table 16: | Comparison of key observations from full-scale tests..... | 160 |
| Table 17: | Instrumentation channels and sensors..... | A-2 |
| Table 18: | Tank car draft sill vertical force calibration results..... | B-9 |
| Table 19: | Tank car draft sill torque calibration results..... | B-12 |
| Table 20: | Tank car weights and dimensions used in simulation..... | D-2 |

GLOSSARY

| | |
|------|--|
| CSTT | Centre for Surface Transportation Technology |
| NRC | National Research Council |
| NTSB | National Transportation Safety Board |
| TC | Transport Canada |
| TDG | Transport Dangerous Goods Directorate |
| TOR | Top of Rails |
| TSB | Transportation Safety Board |

1. INTRODUCTION – PART 2

Transport Canada – Transport Dangerous Goods Directorate (TC-TDG) contracted the National Research Council Canada, Centre for Surface Transportation Technology (NRC-CSTT) to investigate multiple tank car rollover derailments, sometimes referred to as domino derailments. Part 2 of this project involved two phases.

The first phase included a literature survey to check for incidents of domino derailments involving loaded tank cars to determine if such derailments had occurred. The consequences from a domino derailment involving loaded tank cars could be far more serious than those from a similar derailment involving empty cars.

This phase also included a basic analysis of rollover derailment of a single empty tank car and a single loaded tank car, to determine the change in potential energies involved. This analysis was then extended to include several empty and several loaded tank cars, to determine the change in potential energies required to initiate domino style derailment in a string of empty and loaded tank cars. The analysis also checked if, once initiated, the change in potential energy would act to propagate or end the domino derailment.

Finally, the first phase included multi-body dynamic simulations of tank cars equipped with standard Type E couplers, and standard Type E double-shelf couplers. The purpose of the simulations was to model domino derailments on strings of tank cars to better understand the domino process, and then to investigate potential solutions to the domino problem.

The second phase of this project was to perform full scale physical testing on short strings of empty tank cars undergoing domino derailments. The purpose of the tests was to gather physical data to support the modeling process, and to test a potential solution for the domino problem.

This report discusses all work from both phases.

2. LITERATURE SURVEY ON LOADED TANK CAR ROLLOVERS

2.1 Background

NRC-CSTT reviewed the National Transportation Safety Board (US) and the Transportation Safety Board (Canada) railroad accident reports in its possession, as well as other reports that were available on the NTSB and TSB websites.

2.2 NTSB Reports

There were 24 accident reports from the NTSB (1993 – current) involving tank cars. In these accidents, the tank cars were sometimes loaded. When the cars derail while travelling at appreciable speeds, they often come to rest in a pileup with the cars positioned perpendicular to the track. This implies that the cars are no longer coupled to one another, either because the couplers have somehow disengaged or because the coupling equipment failed during the derailment. No effort was made in these reports to determine if the tank cars rolled over in domino fashion before piling up; it is probably not possible to do so. In other accidents, loaded tank cars may derail but remain upright. Occasionally, one loaded tank car may roll over without taking adjacent tank cars with it, because of broken coupling equipment.

Few of the NTSB reports mention double-shelf couplers. When they are mentioned, it is usually in a description of the standard equipment required on the type of tank cars involved in the accident. Not one of the NTSB reports mentions a domino-like effect (or similar wording) as a contributing factor to either the cause or severity of any of the derailments. There is seldom a description of the relative positions of the cars post-accident, other than to mention that they were in a pile-up.

2.3 TSB Reports

NRC-CSTT reviewed seventy-three accident reports from the TSB (1993 – current) involving tank cars. The accidents typically involved mixed freight trains that had tank cars in the consists, although there were four cases of unit trains of tank cars. In cases where the train was moving at appreciable speed, the cars were often positioned in a pileup or perpendicular to the track, indicating coupler separation, tear-out or failure. In such cases, it may not be possible to determine if a domino-type rollover initiated or contributed to the severity of the accident.

Brief details from seventeen TSB reports are described below, in which loaded tank cars derailed and rolled over. There are two cases in which double-shelf couplers were stated as the reason for the rollover of some of the loaded cars, seven cases where it seems likely that loaded cars rolled over in domino-type fashion, and eight cases where the details of the report are insufficient to draw a conclusion. In most cases, the number of rolled loaded tank cars is relatively small. There is one derailment in which four loaded tank cars rolled over at near zero-speed, similar to the Clara City incident (although on smaller scale). Based on this information, domino-type rollovers for loaded trains cannot be ruled out although the possibility of a large-scale incident seems remote.

1. **Report R07D0030** reported a derailment in which three loaded tank cars and seven other cars derailed. The report states “Track damage extended for about 1200 feet up to the trailing truck of the first derailed car, GATX 6545 (the 68th car from the head end). The 69th to 73rd cars did not derail; the 74th to 80th cars,

including the three tank cars loaded with sulphuric acid, derailed and came to rest on their sides, down the embankment on the east side of the track”. A schematic in the report shows car 74 tank cars separated from the rest of the train, but cars 75 and 76 (both tank cars) appear close enough to be coupled. It is possible that this is a case of loaded tank cars rolling over in a domino fashion, but it may also be the result of the derailed cars tumbling down the embankment. – **Inconclusive.**

2. **Report R04M0032** reported a derailment involving pressure tank cars loaded with liquefied petroleum gas. The report states “The conductor inspected the rear of the train and determined that 10 cars, the 54th car to the 63rd car from the head end, had derailed in a left-hand curve in the direction of train travel. Nine of the ten derailed cars were pressure tank cars loaded with liquefied petroleum gas (LPG, Class 2.1, UN 1075). The other derailed car was a box car loaded with paper products. Eight of the LPG tank cars rolled over either onto their sides or upside down (photos 1 and 2)”. This could be a case of a domino-type rollover, as Photo 2 shows at least two tank cars rolled onto their sides off the track and positioned longitudinally, possibly still coupled. As well, the position of the tanks cars in the schematic in Appendix A suggests that the cars could have rolled in three separate groups: a box car and a tank car, three tank cars, and four tank cars. The second group of cars had fractured parts that would have allowed them to separate from adjacent cars. The fractures were determined to have occurred due to brittle overstress under torsional load. This strongly points to a domino-type rollover with loaded tank cars. – **Likely.**
3. **Report R04W0148** reported a derailment involving pressure tank cars loaded with anhydrous ammonia; six cars derailed including one hopper and five tank cars. The report states “At the west end of the derailment, the first two derailed cars were tank car ACFX 220149 and covered hopper car FURX 818699, respectively. Both cars derailed all wheels, but remained upright. They were sent to Moose Jaw for further examination. The following three derailed tank cars remained coupled together and came to rest on their sides lying to the north side of the track. At the east end of the derailment, the last derailed tank car, GATX 48058, with the B-end leading, came to rest leaning to the south”. This appears to be evidence of a domino-type rollover of loaded tank cars. – **Likely.**
4. **Report R04Q0040** reported a derailment of unit train of loaded tank cars. Photo 1 of the report shows an aerial view of the post-derailment positions of the cars. There are two tank cars lying on their sides off the track at the bottom left of the photo, possibly still coupled together. There is a gap, followed by two more cars lying on their sides, possibly still coupled together. Then there is a car pileup, followed by three of four more cars that are likely coupled together and are upright on the rails. The report states “The 39th car on the train remained upright 100 m north of the primary derailment site, its leading truck having derailed on the east side of the main track. The preceding eight cars jackknifed and plowed into the peat surface (see Photo 1). The other cars rolled over parallel to the east

- side of the track”. The fact that some cars had rolled over to one side of the track is evidence of a domino-type derailment for loaded cars. – *Likely*.
5. **Report R03V0019** reported a derailment of a unit tank train of loaded glycol cars, which derailed at low speed (and was subsequently struck by another train). Seven of the tank cars had rolled onto their sides. Photo 1 of the report clearly shows the rolled tank cars. – *Likely*.
 6. **Report R03T0157** reported a derailment of a train containing tank cars loaded with sulphuric acid. This report indicates the role the double-shelf couplers played in keeping most of the derailed cars together, but it is also a clear indictment of double-shelf couplers in initiating a domino-type rollover of some of the cars. The report states in the “Other Factual Information” section that “Double-shelf couplers had kept most of the derailed tank cars together, but a separation did occur between the 49th car (PROX 16159) and the 50th car (UTLX 12779)”. The report later states in the “Analysis” section that “Eventually, the train broke apart after the derailed tank cars rolled onto their sides in a chain reaction due to the effect of the double-shelf couplers, which had kept them from jackknifing.” – *Clear*.
 7. **Report R01E0009** reported the derailment of a train containing at least five tank cars loaded with anhydrous ammonia. These five cars derailed; three remained upright and two others rolled on their sides. Something released or failed in the coupling between the second and third cars, but this was not discussed in the report. – *Inconclusive*.
 8. **Report R01W0182** reports the derailment of a train involving three loaded tank cars. The report states “The tank cars loaded with methanol - PROX 41238 (the 97th car behind the locomotives) and CGTX 30093 (the 98th car) - remained coupled on their sides to the south of the track. PROX 41073 (the 99th car), loaded with vinyl acetate, had separated from CGTX 30093 and was leaning at approximately 30° to the south. During the derailment, the A-end coupler of CGTX 30093 had separated from the B-end coupler of PROX 41073 and impacted the B-end of the PROX 41073 tank, severely denting the head. Each tank car was equipped with double-shelf (top and bottom) couplers. These couplers are mandatory for all tank cars. Double-shelf couplers are to prevent tank cars from separating during a derailment, reducing the risk of a tank head puncture from couplers. Subsequent inspection determined that the top shelf of the B-end coupler from PROX 41073 had broken away, allowing the cars to separate”. Had the coupler on PROX 41073 not failed, it may also have rolled onto its side. – *Likely*.
 9. **Report R00D0026** reports the derailment of a train in which three loaded tank cars rolled onto their sides. However, the report does not indicate whether the cars remained coupled together. – *Inconclusive*.
 10. **Report R00T0067** reports a derailment in which double-shelf couplers are stated as being the cause of a near-zero speed rollover of loaded tank cars containing sulphuric acid. The report states “It was determined from the location of the wreckage that the 17th car (UTLX14536) from the locomotives likely derailed first

and the rigid connection of the double-shelf couplers between the tank cars resulted in the derailment of four cars ahead, the 16th, 15th, 14th and 13th cars behind the locomotives”. Figure 2 in the report is a photo of these four tank cars. Two of them may still have been coupled together, the other two are uncoupled.

– **Clear.**

11. **Report R99Q0019** reports a derailment involving a unit train of loaded tank cars. The report indicates that ten cars derailed: “All of the derailed cars were on the north side of the track. The first car had rolled completely over onto its top. The second and third cars were lying on their sides in the ditch parallel to the track. The fourth to seventh cars were lying on their sides, clear of the grade and off the right-of-way. The eighth and ninth cars were on the grade, leaning towards the north-side ditch. The tenth car had the A-end (front) truck derailed, and was upright”. It is not stated if any of these cars remained coupled. Given that the first nine cars came to rest on the same side of the track suggests that a domino-type of incident had occurred. – **Likely.**
12. **Report R99T0256** details a derailment involving a freight train containing nineteen tank cars, four of which were loaded. An empty (cleaned and purged) tank car was reported to have rolled over, as did a loaded tank car to which the empty was coupled. – **Inconclusive.**
13. **Report R99T0298** details a derailment in which a passenger train derailed and jackknifed, causing its locomotive and first coach car to strike the side of a freight car on the adjacent track (just before the freight train had come to a stop), resulting in the rollover of four loaded tank cars. - **Inconclusive.**
14. **Report R98T0292** details the derailment of three tank cars loaded with anhydrous ammonia. It is unclear whether the cars rolled in a domino fashion or not, but one rolled down a twenty foot embankment, one was lying on its side and one remained upright. - **Inconclusive.**
15. **Report R96T0080** details a derailment in which seven cars derailed during a yard collision. Three of the derailed cars were tank cars, one of which was loaded. The loaded car rolled down an embankment. The other two tank cars were residue cars; one was knocked onto its side and the other remained upright. There was no indication if these three cars were initially coupled together or if they were separated by intermediate cars. - **Inconclusive.**
16. **Report R95D0016** details the derailment of a unit train of loaded sulphuric acid cars, twenty-eight of which derailed. The report states “Three cars fell to the west into Petit lac Masketsi, 14 lay inverted near the lake shore and 11 were lying on their sides near the west side of the roadbed”. The train speed was 38 mph immediately prior to a train-initiated emergency brake application. The report does not indicate if any of the cars remained coupled and in line post-derailment, or if they piled up. If all or many of them remained coupled or in line, this would be an example of a large-scale domino-type rollover of loaded tank cars. - **Inconclusive.**
17. **Report R94C0137** details the derailment of a train which contained at least six loaded tank cars. The report states “The last derailed car, UTLX 41717,

remained upright with the trailing truck on the track. The five completely derailed cars came to rest on their sides or inverted south of the track on the track subgrade and in the right-of-way ditch". The report does not state whether the five completely derailed cars remained coupled, but there is also no mention of broken couplers or related components. Given that the rolled cars were on the same side of the track post-derailment, this may be a case of a domino-type rollover for loaded cars. – **Likely.**

3. ENERGY ANALYSIS OF TANK CAR DOMINO ROLLOVERS

3.1 Introduction

NRC-CSTT was tasked to investigate the energy involved in tank car rollovers. An analysis of the potential and kinetic energies involved should provide insight as to whether the domino effect for empty cars could be infinite, and whether it is possible for loaded cars.

A single tank car can roll over in two different modes. The first mode is for the tank car body and the trucks to roll together as a unit about the wheel/rail contact points on one side. This can occur as a result of an external lateral force applied to the tank car body at a height that is not too far above the trucks (for example, at or below the tank centreline, typically at the coupler centreline). In such a case, the car body's centre plate can slide laterally across the centre bowl until the edge of the centre plate is in hard contact with the inside vertical rim of the centre bowl. The external lateral force is then reacted at the centre bowl rim, and ultimately at the wheel/rail interface. This creates an overturning moment on the truck which, if it exceeds the stabilizing moment of the truck weight and the car body weight on the truck, will cause the truck to roll over and take the car body with it.

In the case where no locking centre pin is used, the second mode is for the tank car body to roll on the side bearing (rigid side bearings assumed) until the centre plate separates from the centre bowl; the truck does not initially tip up. This type of motion could occur as a result of a pure torque or a couple applied about the coupler, or because of an external lateral force applied to the car body far above the trucks. Body roll can continue about the side bearing until the body bolster contacts the top chord of the truck side frame, and begins to transfer load to the side frame. This creates an overturning moment, because the load on the side frame is being applied outside of the wheel/rail contact points (for outboard bearing wheelsets). If sufficient load can bear on the side frame, the truck will begin to roll over because the stabilizing moment of the truck weight is not sufficient to counteract the overturning moment. At this instant, there are three pivot points in the system: the wheel/rail contact points (both trucks), the body bolster – side frame contact points (both trucks) and the car body – side bearing contact points (both trucks). Relatively little load is carried on the side bearing and this load decreases as the car body continues to roll onto the side frame. Therefore the system is akin to an inverted double pendulum, which complicates the analysis. The car body and trucks may continue to roll as a rigid assembly about the wheel/rail contact points, or they might roll independently. The car body may also slide off the side bearing, or it may slide off the side frame.

This analysis will examine the energy for the second mode of roll, with the assumption that the car body does not slide on the side bearing or side frame, and that the truck and car body roll together as a rigid assembly once sufficient load is borne on the top chord of the side frame. A single car will be examined first then the analysis will be extended to additional cars. This analysis assumes the cars have no forward speed at any time while the rollover takes place.

3.2 Stages – Empty Tank Car

In order to calculate the energy in the system at any point, we must understand where the centres of gravity are. To do this, we need to examine stages in the body roll process. Stages are differentiated by a change in the path of the motion of the car body and truck, due to different locations of the car body and truck coming into contact.

For the purposes of this analysis there are seven stages and the potential energy will be calculated at each of them. The stages are:

- Stage 1: system sitting undisturbed on level track,
- Stage 2: car body rolls on truck bolsters until the entire car body load is supported on side bearings on rolled side,
- Stage 3: car body continues to roll on side bearings until body bolsters contact the inside corner of the trucks' side frames,
- Stage 4: car body rolls on inside corner of side frames until the car body bolster lies flat on the side frames (truck bolsters are now unloaded) but with vertical load carried at inside corners of side frames on rolled side,
- Stage 5: car body bolster lies flat on the top chord of the side frames on rolled side, but with vertical load carried at outside corners , immediately causing system instability,
- Stage 6: car body and trucks roll together as a rigid body about the wheel/rail contact point until the car body touches the ground,
- Stage 7: truck falls back to the rails.

3.2.1 Stage 1

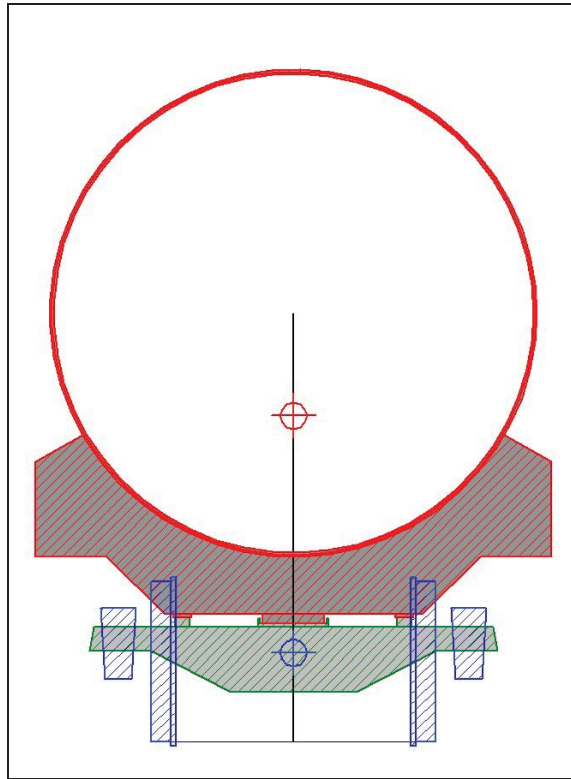


Figure 1: Tank car sitting undisturbed on level track.

In this stage the potential energy of the system is the potential energy of the tank car body and the truck assembly above the datum (taken as the top of the rails (TOR)). It also includes the energy stored in the truck springs due to the weight of the car body and truck bolsters (the spring deflection is the change from the spring free height). Note that the spring rate here is the total rate for the four groups of springs on the car, and that the suspension's friction damping forces are neglected to facilitate a simplified analysis.

Table 1: Empty car energy with respect to the top of the rails, Stage 1.

| Item | CG Height Above TOR, in. | Spring Deflection, in. | | Weight, lb | Spring Rate, lb/in | Energy, in-lb |
|--------------|--------------------------|------------------------|-------|------------|--------------------|------------------|
| | | Left | Right | | | |
| Body | 73.39 | | | 57,500 | | 4,219,925 |
| Trucks | 20 | | | 20,000 | | 400,000 |
| Springs | | 0.573 | 0.573 | | 105,552 | 17,328 |
| TOTAL | | | | | | 4,637,253 |

3.2.2 Stage 2

In this stage, the car body has rolled (counter clockwise for this analysis) sufficiently to just separate the centre plate from the centre bowl. In this condition, the entire load is carried by the side bearings on the rolled side of the trucks. The car body bolster rolls along with the car body.

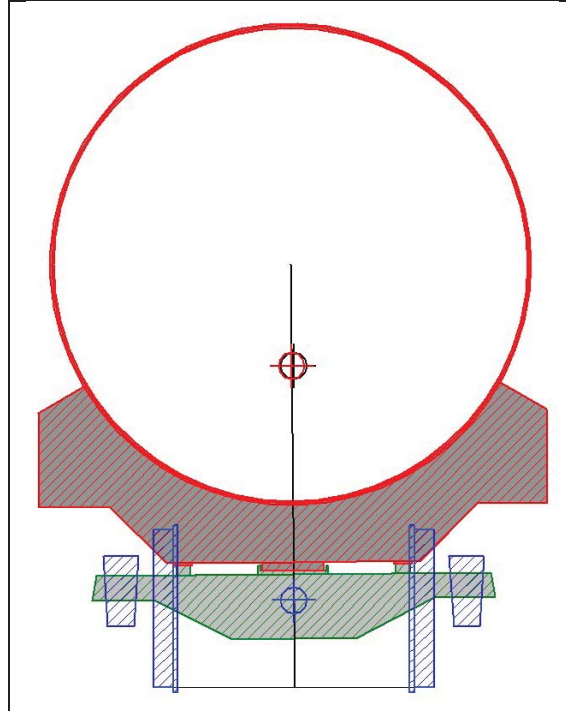


Figure 2: Car body rolled onto the side bearings.

The weight of the car body deflects the truck bolsters on their springs, when the car is undisturbed (Stage 1). Since the car body weight is still entirely supported by the truck bolsters in Stage 2, the motion of the truck bolsters is to roll about their centres, compress the left side springs by an additional amount, and allow the right side springs to extend by the same amount. This motion causes the centre of gravity of the car body to drop slightly and move to the left. The small displacement of the centre of gravity can be seen in Figure 2. The centre of gravity of the truck bolster does not displace. Note that the spring rate in Table 2 is for the two truck spring groups on each side of the car.

Table 2: Empty car energy with respect to the top of the rails, Stage 2.

| Item | CG Height Above TOR, in. | Spring Deflection, in. | | Weight, lb | Spring Rate, lb/in | Energy, in-lb |
|----------------|--------------------------|------------------------|-------|------------|--------------------|------------------|
| | | Left | Right | | | |
| Body | 73.388 | | | 57,500 | | 4,219,810 |
| Trucks | 20 | | | 20,000 | | 400,000 |
| Springs | | 0.940 | 0.206 | | 52,736 | 24,436 |
| TOTAL | | | | | | 4,644,246 |

3.2.3 Stage 3

In this stage, the car body must roll about the outside edge of the side bearings through an angle to bring the car body bolster into contact with the side frame. Contact will occur at the inside edge of the side frame. The geometry of the situation is shown in Figure 3; the black arrow indicates the arc through which the body must roll and the red arrow shows the pivot point.

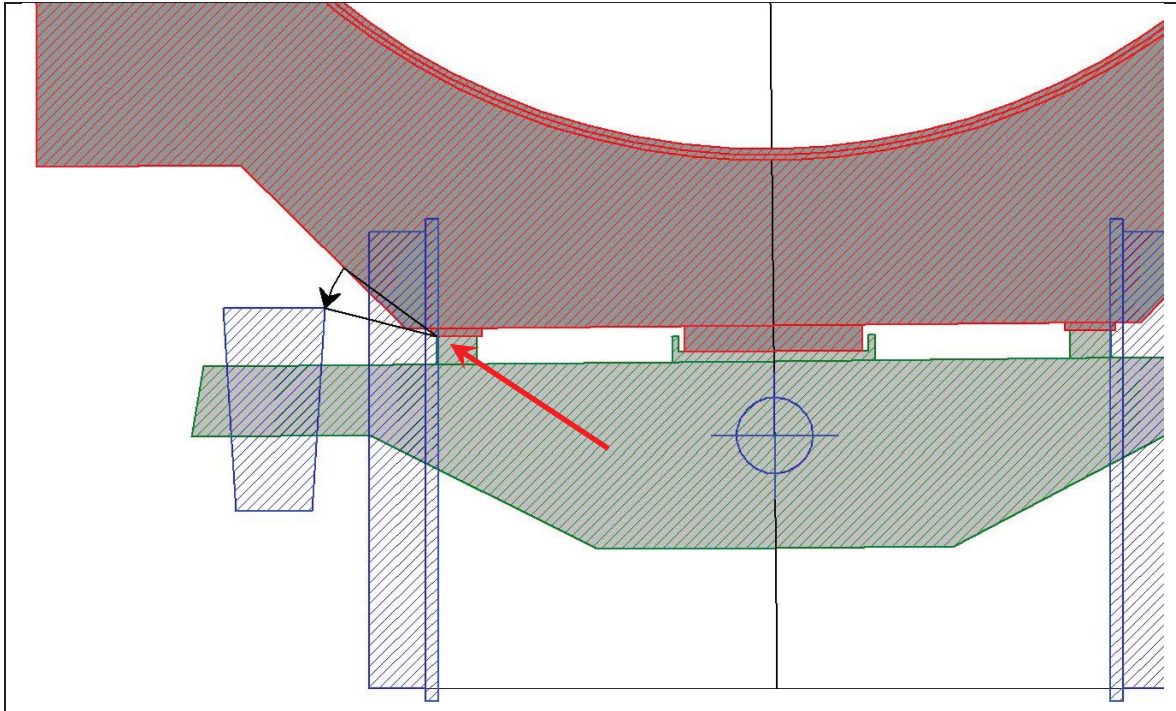


Figure 3: Car body rolls about the side bearings until contact occurs with the side frame.

The actual angle through which the car body will roll in this stage depends on the geometry of the car body bolster. The car body bolster has been drawn using the dimensions found on drawings supplied to NRC-CSTT by GATX for earlier work in this project. Not all dimensions were included, so the angle at the sloped portion of the car body bolster was taken as 45° . It is this part of the body bolster that contacts the side frame. Note that the construction details of the body bolster vary from one tank car design to the next, so contact may occur at different locations on other cars. Based on a 45° body bolster construction angle, the roll angle to bring the body bolster into contact with the side frame is roughly 22° . The car body is just touching the side frame and the load is still on the truck side bearing. Therefore, the truck bolster remains rolled as in Stage 2.

Table 3: Empty car energy with respect to the top of the rails, Stage 3.

| Item | CG Height Above TOR, in. | Spring Deflection, in. | | Weight, lb | Spring Rate, lb/in | Energy, in-lb |
|----------------|--------------------------|------------------------|-------|------------|--------------------|------------------|
| | | Left | Right | | | |
| Body | 79.846 | | | 57,500 | | 4,591,145 |
| Trucks | 20 | | | 20,000 | | 400,000 |
| Springs | | 0.940 | 0.206 | | 52,776 | 24,436 |
| TOTAL | | | | | | 5,015,581 |

The final position of the car for this stage is shown in Figure 4.

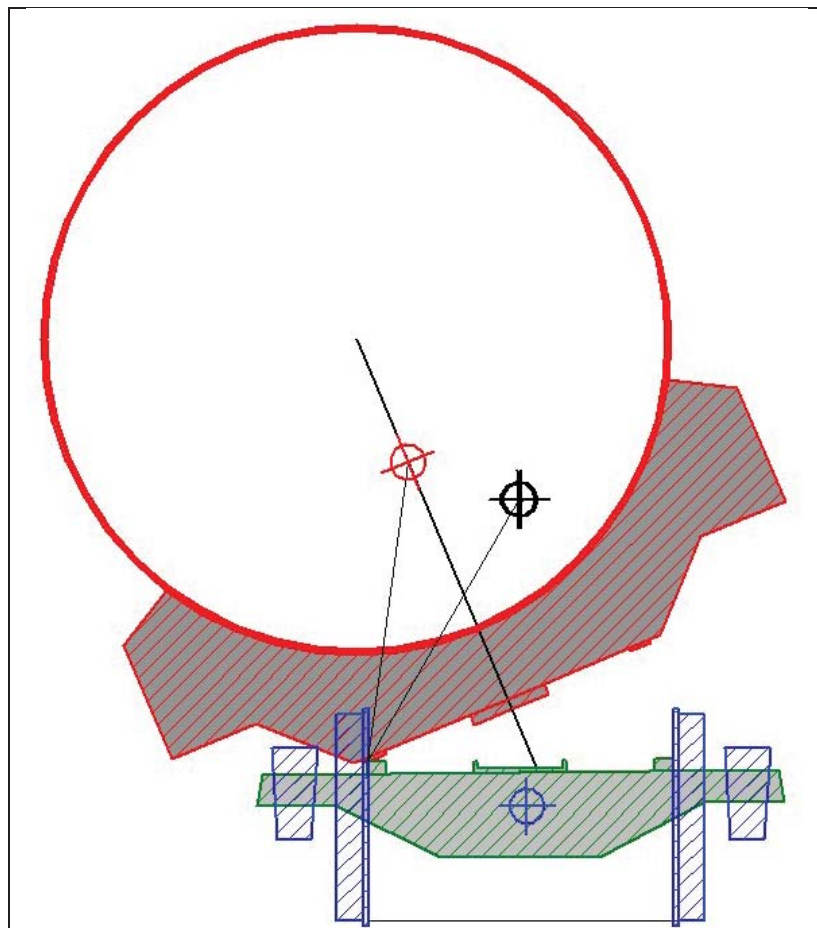


Figure 4: Car body rolled contacting the side frame at the end of Stage 3.

3.2.4 Stage 4

In this stage, the car body must roll about the inside corner of the top chord of the truck side frame through an angle that causes the car body bolster to just lie flat on the top chord of the side frame, while the vertical load (the car body weight) is assumed to still pass through the inside corner of the side frame. The car body is no longer in contact with the truck bolster, so the bolster has rolled back to level and the springs have lifted it vertically to a new static position. The geometry of the situation is shown in Figure 5. The car reaches its maximum potential energy during this stage.

This condition is not yet sufficient to cause the truck to roll about the rail, the vector of the car body weight would have to pass slightly to the outside of the centre of the side frame. The centre of the side frame is at 39.5 in. from track centre, the weight vector would need to be at 40.43 in. from track centre to cause the truck to begin to tip up. For the purposes of this analysis, an infinitesimal increase in roll angle would cause the instantaneous roll centre and car body weight to instantaneously shift to the outside corner of the side frame. This will make the truck unstable.

Table 4: Empty car energy with respect to the top of the rails, Stage 4.

| Item | CG Height Above TOR, in. | Spring Deflection, in. | | Weight, lb | Spring Rate, lb/in | Energy, in-lb |
|-------------------------------|--------------------------|------------------------|-------|------------|--------------------|------------------|
| | | Left | Right | | | |
| Body | 82.171 | | | 57,500 | | 4,724,833 |
| Trucks (less bolsters) | ~ 19.647 | | | 17,000 | | ~ 333,999 |
| Bolsters | 22.000 | | | 3,000 | | 66,000 |
| Springs | | 0.028 | 0.028 | | 52,776 | 43 |
| TOTAL | | | | | | 5,124,875 |

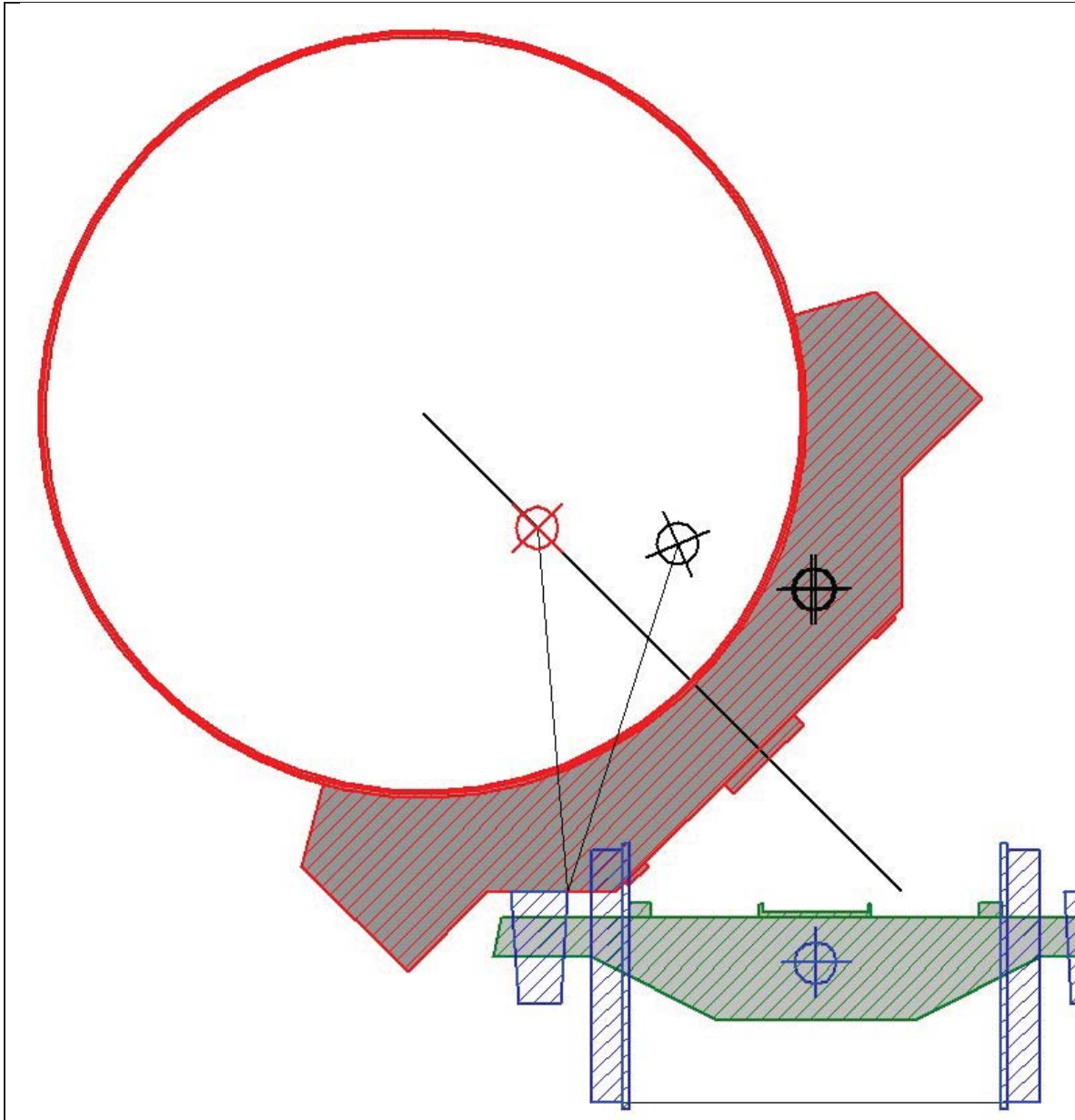


Figure 5: Car body has rolled about the inside corner of the side frame, until the body bolster lies flat on the side frame.

3.2.5 Stage 5

This stage is identical to the previous one, except that the car body weight is now carried at the outside corner of the side frame (Figure 6). Only an infinitesimal amount of roll has occurred during this stage, so the positions of the centres of gravity have not changed. Therefore, the potential energies are also the same as in Stage 4.

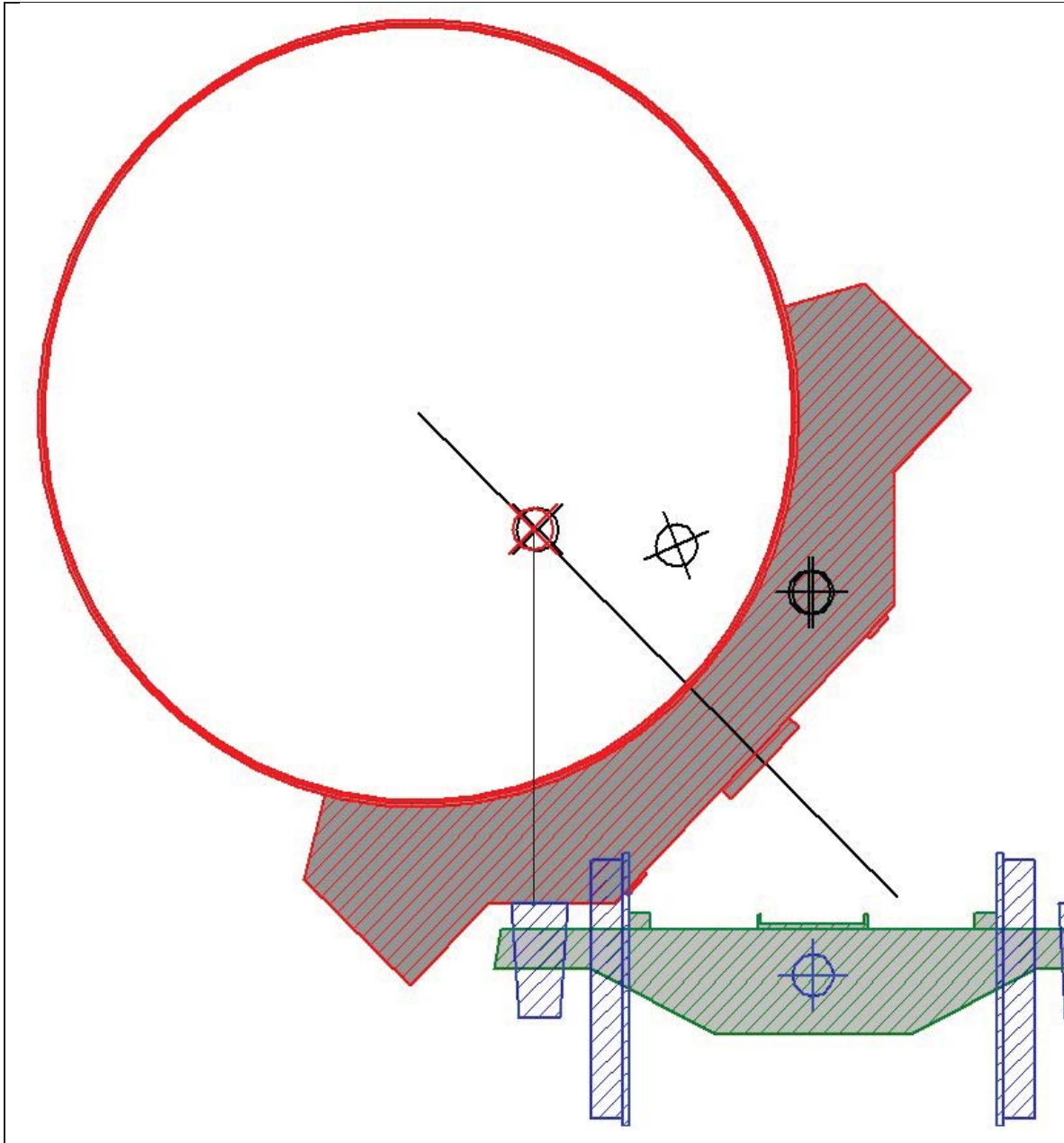


Figure 6: Car body carried on the outside corner of the side frame.

3.2.6 Stage 6

In this stage, the car body would be expected to roll about the outside corner of the top chord of the truck side frame through an angle that brings the car body (or body bolster in this case) into contact with the ground, which is roughly 7 in. below the top of rail. For this to occur, the car body will have rolled 90° from its undisturbed position. However, since the weight of the car body is being carried at the outside corner of the side frame, the truck now has an overturning moment that exceeds the stabilizing moment from its own weight. Therefore, the truck will tip up under the car body. Since the body bolster is

lying flat on the side frame, it is assumed that the truck and car body will roll together as a rigid body with instant roll centre about the wheel/rail contact point.

Table 5: Empty car energy with respect to the top of the rails, Stage 6.

| Item | CG Height Above TOR, in. | Spring Deflection, in. | | Weight, lb | Spring Rate, lb/in | Energy, in-lb |
|----------------|--------------------------|------------------------|-------|------------|--------------------|------------------|
| | | Left | Right | | | |
| Body | 51.207 | | | 57,500 | | 2,944,403 |
| Truck | ~ 35.355 | | | 20,000 | | ~ 707,100 |
| Springs | | 0.028 | 0.028 | | 52,776 | 41 |
| TOTAL | | | | | | 3,651,544 |

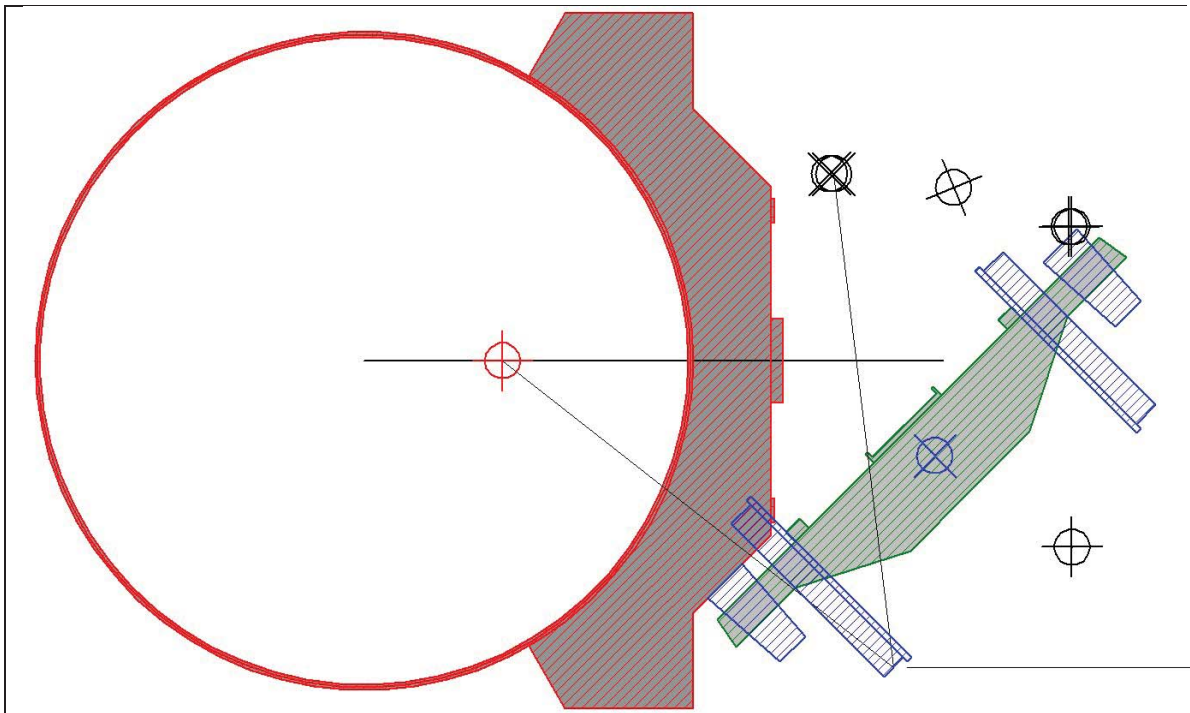


Figure 7: Car body has rolled about the wheel/rail contact points until the body contacts the ground below the TOR.

3.2.7 Stage 7

In the final stage, the body has fallen away from the truck sufficiently to allow the truck to fall back onto the rails (Figure 8). The change in potential energy at this stage comes from the change in height of the centre of gravity of the truck assembly.

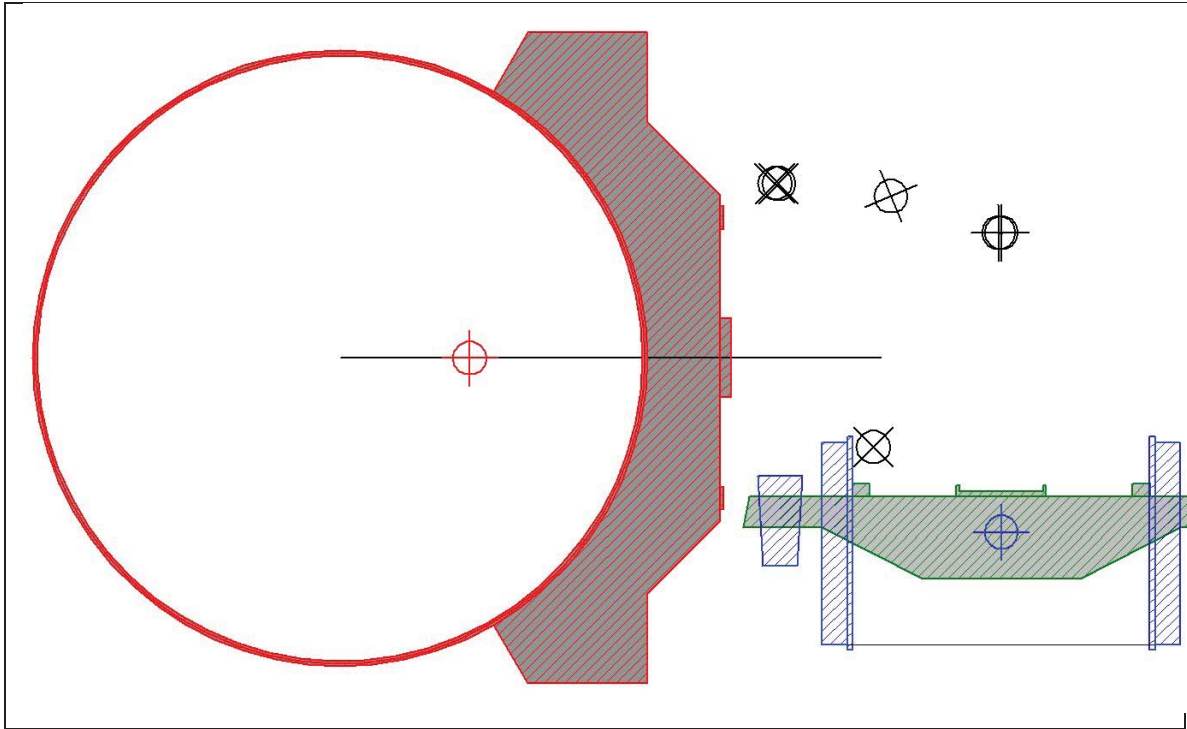


Figure 8: Truck falls back on the rails after the car body has rolled sufficiently far away on the ground.

Table 6: Empty car energy with respect to the top of the rails, Stage 7.

| Item | CG Height Above TOR, in. | Spring Deflection, in. | | Weight, lb | Spring Rate, lb/in | Energy, in-lb |
|----------------|--------------------------|------------------------|-------|------------|--------------------|------------------|
| | | Left | Right | | | |
| Body | 51.207 | | | 57,500 | | 2,944,403 |
| Truck | ~ 20 | | | 20,000 | | ~ 400,000 |
| Springs | | 0.028 | 0.028 | | 52,776 | 43 |
| TOTAL | | | | | | 3,344,446 |

3.3 Analysis – Empty Tank Car

The motion of the centre of gravity of the car body follows a series of circular arcs from one stage to the next. Each arc can be expressed as a function of the radius from the centre of gravity to the pivot point, and the angle through which the centre of gravity rolls. Therefore, the potential energy of the car can be determined analytically at any intermediate point within each stage. The energy stored in the springs can be calculated based on the forces applied to the truck bolster at any intermediate point within each stage.

Based on photographs (provided by Transport Canada) of a tank car derailment at Belleville, Ontario approximately (circa 1998 – 2000), there is evidence to suggest that the angular lag between rolled tank cars, due to torsional free clearance and elastic deflection in the cars' couplers and retainer keys is approximately 18°. (The torsional free slack can vary for different cars depending on the state of wear of the coupler knuckle, retainer key and keyway). This was also seen during the dry run rollover testing of tank cars at NRC-CSTT's facility in mid-August, 2010. The lag angle and the equations which describe the potential energy of a tank car can be combined to allow the examination of the potential energy of several coupled tank cars that are in a dynamic state of domino rollover. This will reveal if the change in potential energy of several empty cars is sufficient to initiate and propagate a domino-style rollover.

If the first tank car were rolled by 90°, the second car would be at 72°, the third car would be at 54°, the fourth car would be at 36°, the fifth car would be at 18°, and a sixth car would be at 0°. Therefore, five tank cars would be active at any time in a domino derailment. As each car rolls from its undisturbed position, its energy would begin to increase, reach a maximum (at roughly 41° roll angle) and then begin to decrease. The change in potential energy of each car from its undisturbed position is shown in Figure 9. Each car would follow the same energy path, lagging the previous car by 18°.

The phase-lagged energy curves can be added together to yield the system energy of the cars. The change in potential energy of the system from its undisturbed state is also shown Figure 9. The system's potential energy reaches a maximum value once the first car has rolled approximately 64°, and the system potential energy decreases after that. Maximum system potential energy is reached before the fifth car begins to roll so only four cars are actually involved.

Once the first car has rolled past 64°, its potential energy is decreasing rapidly and the second car has only just begun to decrease its potential energy. The third and fourth cars are gaining potential energy but at a lesser rate than the decrease in first two cars. This is what enables the rollover derailment to propagate through a train of tank cars; leading cars are continuously transferring energy to subsequent cars.

A necessary condition for the domino effect to begin is that sufficient energy must be transferred to the undisturbed system to roll the first car to 64°; this puts the system at the point of maximum energy (a system meta-stable point). The change in potential energy required is 1,368,743 in-lb above the potential energy for four similar empty cars sitting undisturbed on level track. This increase in potential energy could come from a sideswipe impact with another train. An empty tank car travelling at roughly 6.6 miles/hour has this amount of kinetic energy, as does a loaded tank car travelling at roughly 3.6 miles/hour. In a collision, not all of this energy will be transferred from the striking car to the struck car. Some energy will likely remain in the striking car (it may continue to roll along its track), energy may be used to crumple the tank walls, etc. Therefore, actual collision speeds would need to be higher.

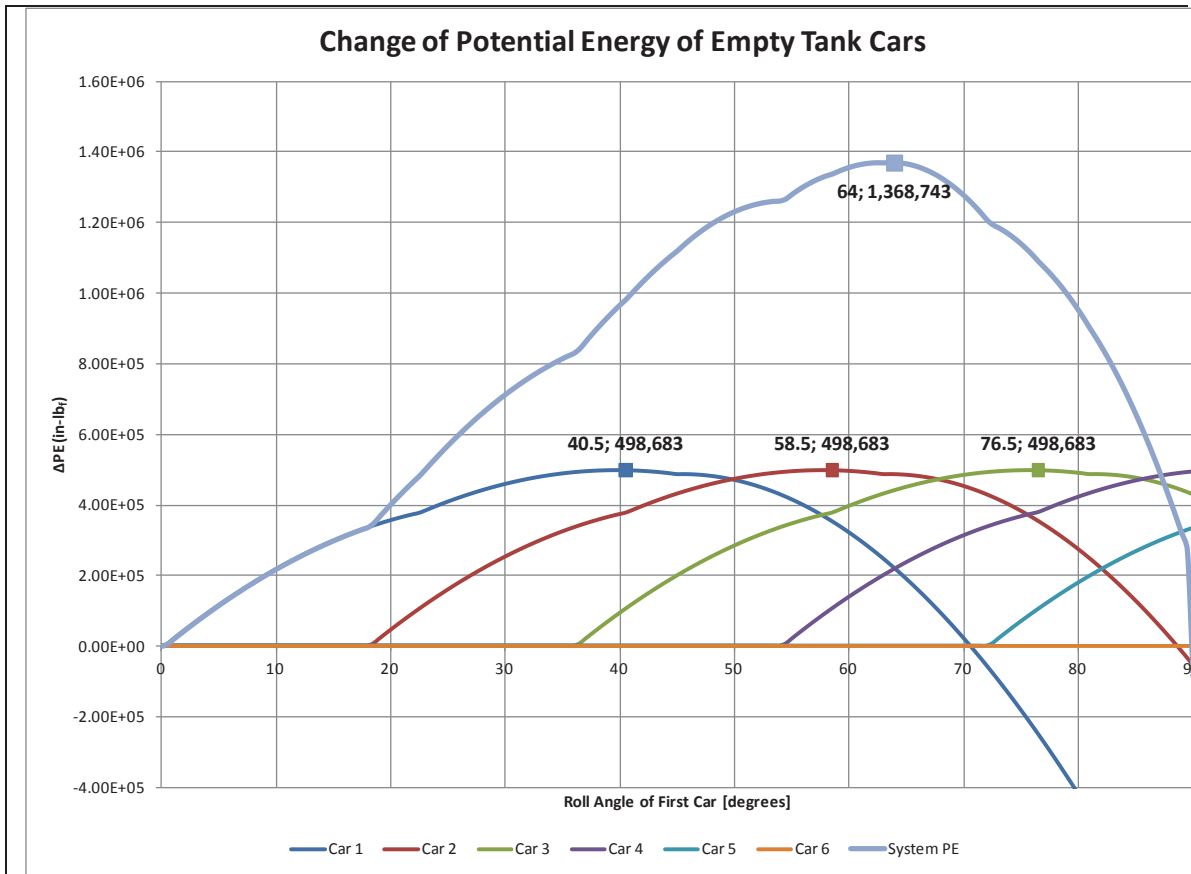


Figure 9: Change in potential energies of empty tank cars and change in total potential energy of a system, as a function of the car body roll angle of the first car.

3.4 Stages – Loaded Tank Car

As with the empty car, we must calculate the position of the centres of gravity of the fully loaded car at various stages of body roll. Stages are differentiated by a change in the path of the motion of the car body and truck, due to different locations of the car body and truck coming into contact.

For the purposes of this analysis there are eight stages for a loaded tank car and the potential energy will be calculated at each of them. The stages are:

- Stage 1: system sitting undisturbed on level track,
- Stage 2: car body rolls on truck bolster until the truck suspension springs have been fully compressed on the rolled side,
- Stage 3: car body load is transferred from the centre plate to the side bearing until the centre bowl just contacts the centre plate without loading it.
- Stage 4: car body continues to roll on side bearing until the car body bolster just contacts the inside corner of the side frame without loading it,
- Stage 5: car body load is transferred from the side bearing to the inside corner of the side frame's top chord, until the side bearings are only carrying the load required to fully compress the suspension springs on the rolled side (the overload

has been relieved). There is no change in car body position, so no change in energy.

Stage 6: car body continues to roll on the side frame inside corner until the side frame has been sufficiently loaded to cause system instability,

Stage 7: car body and truck roll together as a rigid body about the wheel/rail contact point until the car body touches the ground,

Stage 8: truck falls back to the rails.

3.4.1 Stage 1

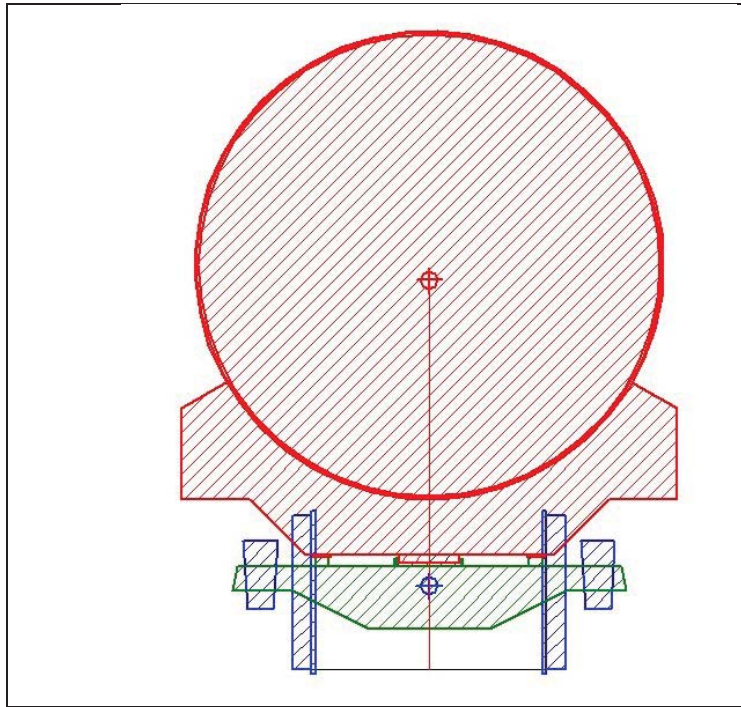


Figure 10: Tank car sitting undisturbed on level track.

In this stage the potential energy of the system is the potential energy of the tank car body, cargo, and the truck assembly above the datum (taken as the top of the rails (TOR)). It also includes the energy stored in the truck springs due to the weight of the car body, cargo, and truck bolsters (the spring deflection is the change from the spring free height). Note that the spring rate here is the total rate for the four groups of springs on the car, and that the suspension's friction damping forces are neglected to facilitate a simplified analysis.

Table 7: Loaded car energy with respect to the top of the rails, Stage 1.

| Item | CG Height Above TOR, in. | Spring Deflection, in. | | Weight, lb | Spring Rate, lb/in | Energy, in-lb |
|----------------|--------------------------|------------------------|-------|------------|--------------------|-------------------|
| | | Left | Right | | | |
| Body | 91.060 | | | 243,000 | | 22,127,682 |
| Truck | 19.651 | | | 20,000 | | 393,008 |
| Springs | | 2.331 | 2.331 | | 105,552 | 286,664 |
| TOTAL | | | | | | 22,807,354 |

3.4.2 Stage 2

In this stage, the car body has rolled (counter clockwise for this analysis) sufficiently to fully compress the truck suspension springs on the rolled (left) side. The weight of the car body deflects the truck bolsters on their springs, when the car is undisturbed (Stage 1). Since the car body weight is still entirely supported by the truck bolsters in Stage 2, the motion of the truck bolsters is to roll about their centres, compress the left side springs by an additional amount, and allow the right side springs to extend by the same amount. This motion causes the centre of gravity of the car body to drop slightly and move to the left. The small displacement of the centre of gravity can be seen in Figure 11.

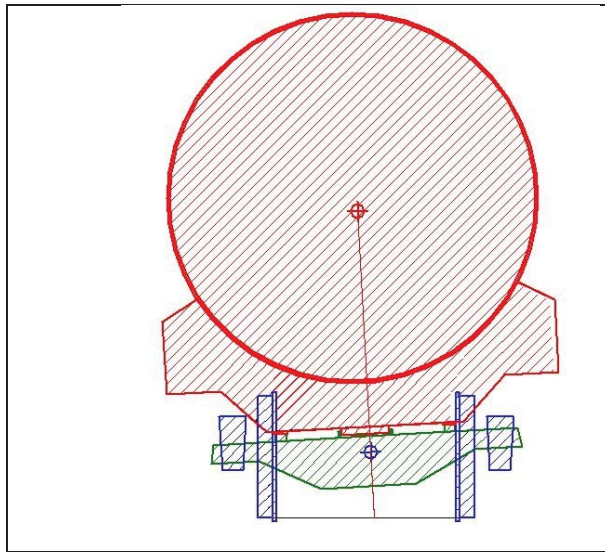


Figure 11: Car body compresses truck suspension springs.

The centre of gravity of the truck bolster does not displace. Note that the spring rate in Table 8 is for the two truck spring groups on one side of the car.

Table 8: Loaded car energy with respect to the top of the rails, Stage 2.

| Item | CG Height Above TOR, in. | Spring Deflection, in. | | Weight, lb | Spring Rate, lb/in | Energy, in-lb |
|----------------|--------------------------|------------------------|-------|------------|--------------------|-------------------|
| | | Left | Right | | | |
| Body | 91.019 | | | 243,000 | | 22,117,617 |
| Truck | 19.650 | | | 20,000 | | 393,000 |
| Springs | | 3.688 | 0.974 | | 52,776 | 283,946 |
| TOTAL | | | | | | 22,894,563 |

3.4.3 Stage 3

In this stage, the car body has rolled (counter clockwise) sufficiently to just transfer the load from the centre plate to the side bearing. In this condition, the entire load is carried by the side bearings on the rolled side of the trucks. This stage is identical to the previous one, except that the car body weight is now carried at the side bearing (Figure 12). Only an infinitesimal amount of roll has occurred during this stage, so the positions of the centres of gravity have not changed. Therefore, the potential energies are also the same as in Stage 2. The red arrow in Figure 12 below shows the side bearing.

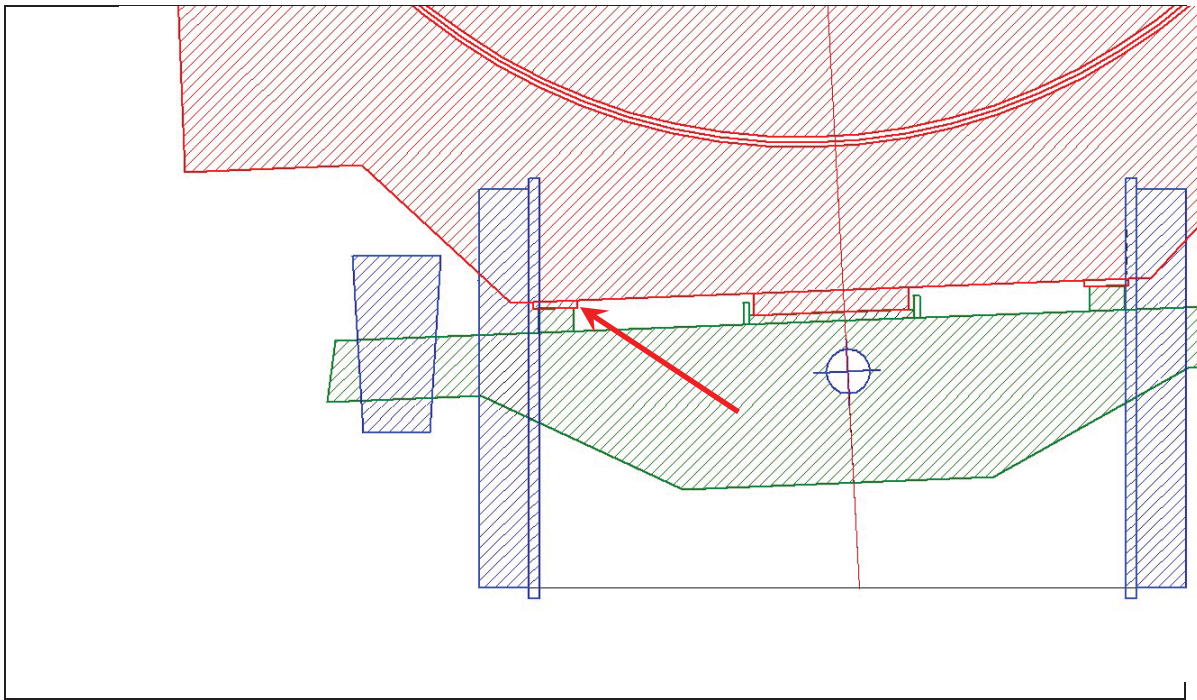


Figure 12: Car body load transferred to side bearing from centre plate.

3.4.4 Stage 4

In this stage, the car body must roll about the outside edge of the side bearings through an angle to bring the car body bolster into contact with the side frame without loading it. Contact will occur at the inside edge of the side frame. The geometry of the situation is shown in Figure 13; the black arrow indicates the arc through which the body must roll and the red arrow shows the pivot point.

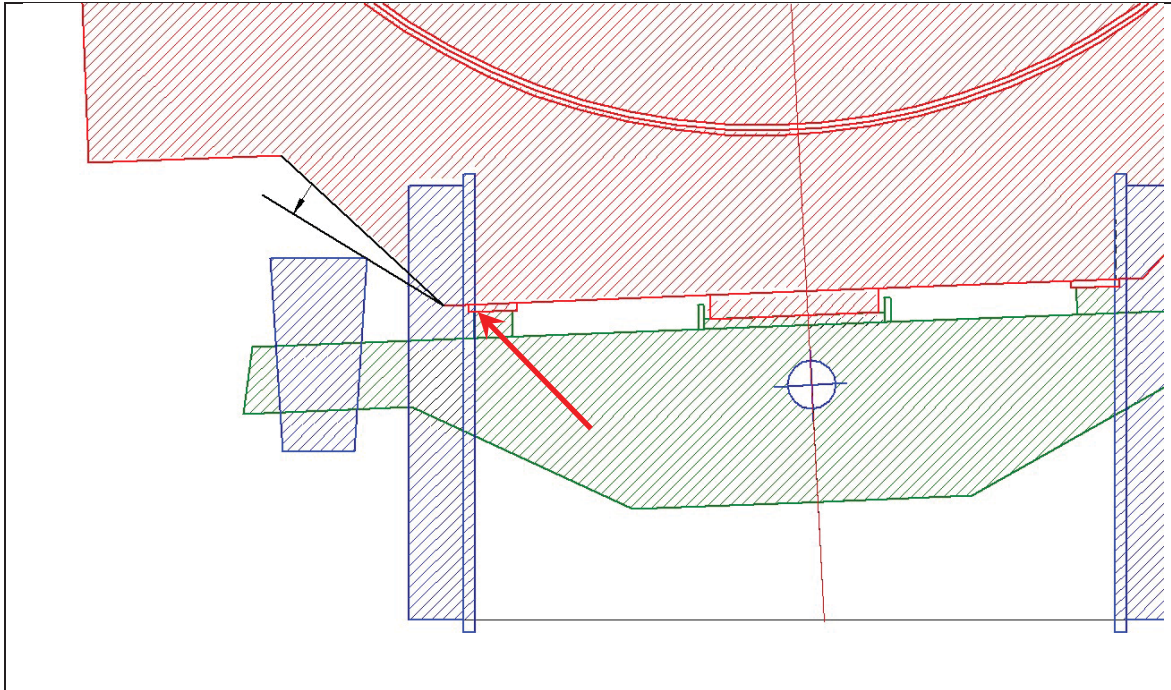


Figure 13: Car body rolls about the side bearing until contacting the side frame.

The actual angle through which the car body will roll in this stage depends on the geometry of the car body bolster. The car body bolster has been drawn using the dimensions found on drawings supplied to NRC-CSTT by GATX for earlier work in this project. Not all dimensions were included, so the angle at the sloped portion of the car body bolster was taken as 45° . It is this part of the body bolster that contacts the side frame. Note that the construction details of the body bolster vary from one tank car design to the next, so contact may occur at different locations on other cars. Based on the extra vertical deflection of the truck bolster on the springs due to the loaded car body and based on a 45° body bolster construction angle, the roll angle to bring the body bolster into contact with the side frame is roughly 7° . The car body is just touching the side frame and the load is still on the truck side bearing. Therefore, the truck bolster remains rolled as in Stage 2.

Table 9: Loaded car energy with respect to the top of the rails, Stage 4.

| Item | CG Height Above TOR, in. | Spring Deflection, in. | | Weight, lb | Spring Rate, lb/in | Energy, in-lb |
|----------------|--------------------------|------------------------|-------|------------|--------------------|-------------------|
| | | Left | Right | | | |
| Body | 93.542 | | | 243,000 | | 22,730,706 |
| Truck | ~ 19.650 | | | 20,000 | | 393,000 |
| Springs | | 3.688 | 0.974 | | 52,776 | 383,946 |
| TOTAL | | | | | | 23,507,652 |

The final position of the tank car at the end of Stage 4 is shown in Figure 14.

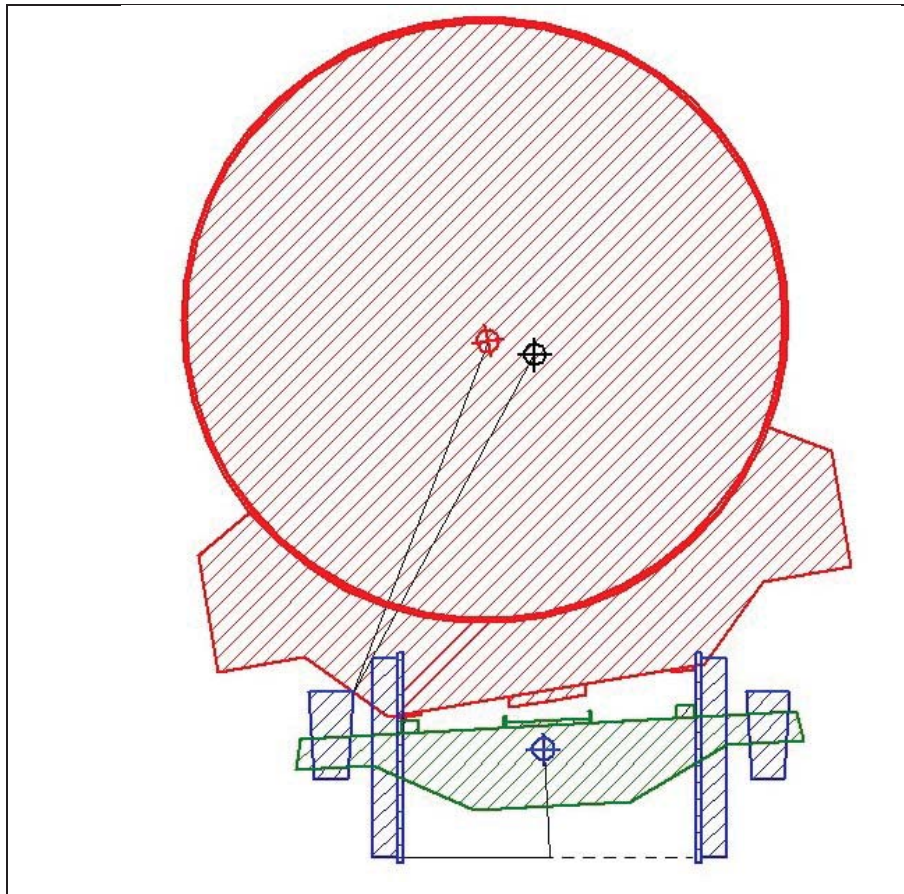


Figure 14: Final position of Stage 4 - car body just contacts inside corner of side frame without loading it.

3.4.5 Stage 5

This stage is identical to the previous one, except that some of the car body weight is now carried at the inside corner of the side frame (Figure 15), relieving the load on the side bearings on the rolled side. The side bearings are now only carrying the load required to fully compress the suspension springs; they are no longer overloaded. Only an infinitesimal amount of roll has occurred during this stage, so the positions of the centres of gravity have not changed. Therefore, the potential energies are also the same as in Stage 4.

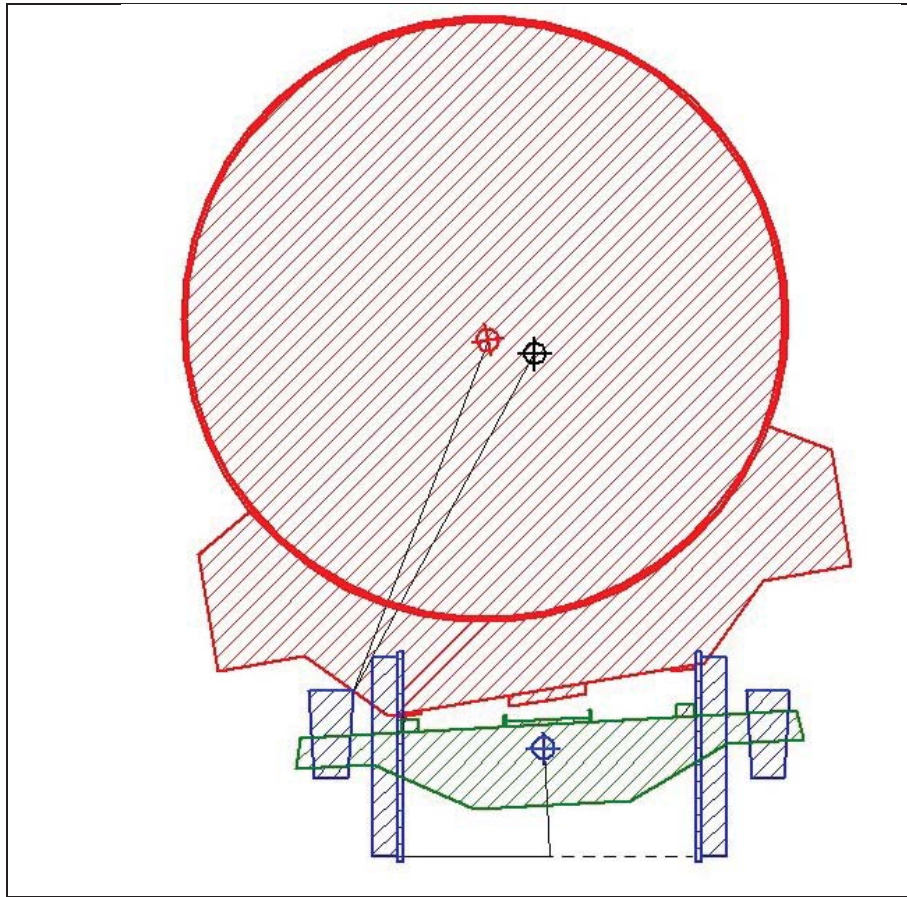


Figure 15: Car body load transferred to inside corner of the side frame.

3.4.6 Stage 6

In this stage, the car body continues to roll on the side frame until the side frame has been sufficiently loaded to cause system instability. As the body rolls, the side bearing on the body bolster moves upward allowing the truck bolster to rise and the suspension springs to extend. However, since more of the weight of the car body is being carried at the inside corner of the side frame, the truck now has an overturning moment that exceeds the stabilizing moment from its own weight. Therefore, the truck will now roll with the car body. The energy at this stage is calculated before the truck starts to roll.

Table 10: Loaded car energy with respect to the top of the rails, Stage 6.

| Item | CG Height Above TOR, in. | Spring Deflection, in. | | Weight, lb | Spring Rate, lb/in | Energy, in-lb |
|----------------|--------------------------|------------------------|-------|------------|--------------------|-------------------|
| | | Left | Right | | | |
| Body | 96.585 | | | 243,000 | | 23,470,199 |
| Truck | 19.650 | | | 20,000 | | 393,000 |
| Springs | | 2.300 | 0.472 | | 52,776 | 145,471 |
| TOTAL | | | | | | 24,008,626 |

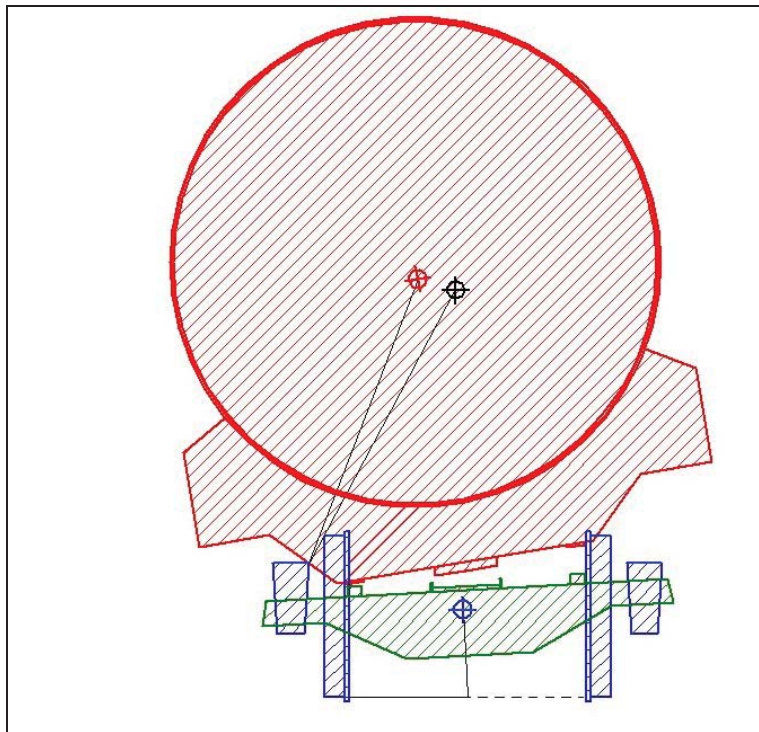


Figure 16: Car body rolls about the side frame until the system becomes unstable.

3.4.7 Stage 7

In this stage, the car body and truck now roll as a single rigid body about the wheel/rail contact points on the rolled side. The angle through which they roll together will bring the car body (or body bolster in this case) into contact with the ground, which is roughly 7 inches below the top of the rails. For this to occur, the car body will have rolled 90° from its undisturbed position.

Table 11: Loaded car energy with respect to the top of the rails, Stage 7.

| Item | CG Height Above TOR, in. | Spring Deflection, in. | | Weight, lb | Spring Rate, lb/in | Energy, in-lb |
|----------------|--------------------------|------------------------|-------|------------|--------------------|-------------------|
| | | Left | Right | | | |
| Body | 38.554 | | | 243,000 | | 9,368,622 |
| Truck | 34.628 | | | 20,000 | | 692,560 |
| Springs | | 0.028 | 0.028 | | 105,552 | 41 |
| TOTAL | | | | | | 10,061,223 |

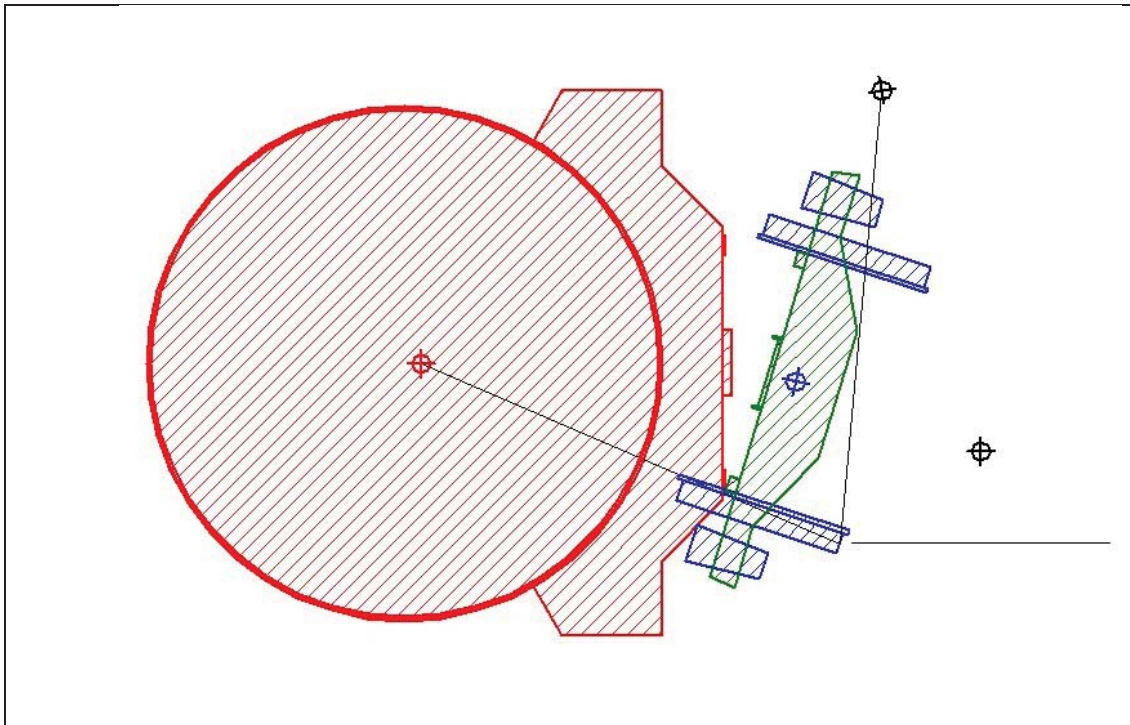


Figure 17: Car body has rolled about the wheel/rail contact points until the body contacts the ground below the TOR.

3.4.8 Stage 8

In the final stage, the body has fallen away from the truck sufficiently to allow the truck to fall back onto the rails (Figure 18). The change in potential energy at this stage comes from the change in height of the centre of gravity of the truck assembly.

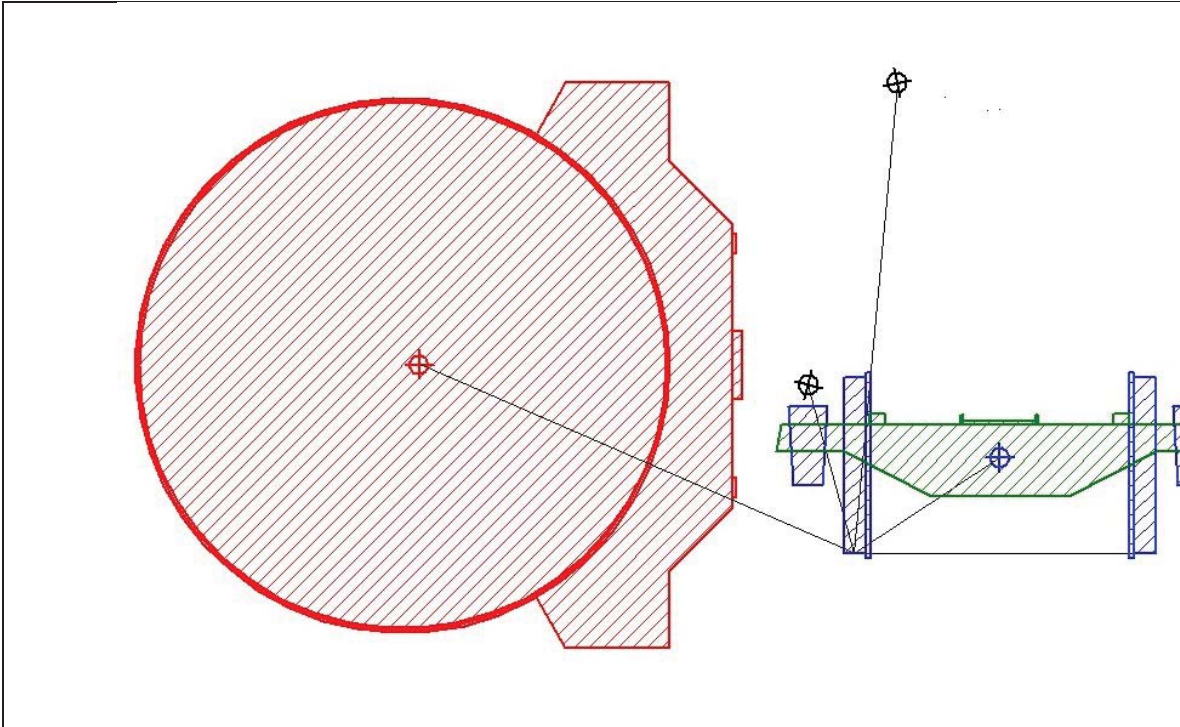


Figure 18: Truck falls back on the rails after the car body has rolled sufficiently far away on the ground.

Table 12: Loaded car energy with respect to the top of the rails, Stage 8.

| Item | CG Height Above TOR, in. | Spring Deflection, in. | | Weight, lb | Spring Rate, lb/in | Energy, in-lb |
|----------------|--------------------------|------------------------|-------|------------|--------------------|------------------|
| | | Left | Right | | | |
| Body | 38.554 | | | 243,000 | | 9,368,622 |
| Truck | 19.650 | | | 20,000 | | 393,000 |
| Springs | | 0.028 | 0.028 | | 105,552 | 41 |
| TOTAL | | | | | | 9,761,663 |

3.5 Analysis – Loaded Tank Car

The motion of the centre of gravity of the car body follows a series of circular arcs from one stage to the next. Each arc can be expressed as a function of the radius from the centre of gravity to the pivot point, and the angle through which the centre of gravity rolls. Therefore, the potential energy of the car can be determined analytically at any intermediate point within each stage. The energy stored in the springs can be calculated based on the forces applied to the truck bolster at any intermediate point within each stage.

The same angular lag (18°) between rolled empty cars is presumed to exist between rolled loaded cars. (It may be slightly larger than 18° , due to a greater elastic component of torsional deflection on account of the higher coupler shank torsional moment being applied for loaded cars. For this analysis, this effect will be neglected.) As before, the lag angle and the equations which describe the potential energy of a tank car can be combined to examine the potential energy of several coupled tank cars that are in a state of roll. This will reveal if the change in potential energy of several cars is sufficient to commence and propagate a domino-style rollover.

If the first tank car were rolled by 90° , the second car would be at 72° , the third car would be at 54° , the fourth car would be at 36° , the fifth car would be at 18° , and a sixth car would be at 0° . Therefore, five tank cars would also be dynamically active at any time in a loaded tank car domino derailment. As each car rolls from its undisturbed position its potential energy would begin to increase, reach a maximum (at roughly 25° roll angle) and then begin to decrease. The change in potential energy of each car from its undisturbed position is shown in Figure 19. Each car would follow the same energy path, lagging the previous car by 18° .

The phase-lagged energy curves can be added together to yield the system energy of the cars. The change in potential energy of the system from its undisturbed state is also shown in Figure 19. The system's potential energy reaches its maximum value once the first car has rolled approximately 32° (marked with a large square), and begins to decrease after that because the loss of potential energy from the first car is more rapid than the increase in potential energy of the second. At 36° , the third car starts to roll and its rising potential energy slows the decrease in the system's potential energy. At 37° , the system potential energy reaches a local minimum and begins to rise again. By 40° , the rate of decrease in potential energy from the first car exceeds the rate of increase from the second and third cars, resulting in a local maximum in the system's potential energy (marked with a large triangle) which has roughly 37,000 in-lb less energy than the absolute maximum. After this, the potential energy of the system only decreases, even as additional cars are picked up.

Maximum system potential energy is reached when the second car has rolled 14° (32° of roll for the first car less 18° of lag between the first and second cars), so only two cars are actually involved in starting the domino progression. The potential energy of the first car is beginning to decrease and the second car is still climbing towards its maximum potential energy. Other cars are not yet involved. The third car body has only rolled by 4° before the system's potential energy is irreversibly in decline.

A necessary condition for the domino effect to begin is that sufficient kinetic energy must be transferred to the undisturbed system to roll the first car to 32° ; this puts the system at the point of maximum potential energy (a system meta-stable point). The energy required is 2,171,892 in-lb. This energy could come from a sideswipe impact with another train. An empty tank car travelling at roughly 8.4 miles/hour has this amount of

kinetic energy, as does a loaded tank car travelling at roughly 4.5 miles/hour. In a collision, not all of this energy will be transferred from the striking car to the struck car. Some energy will likely remain in the striking car (it may continue to roll along its track), energy may be used to crumple the tank walls, etc. Therefore, actual collision speeds would need to be higher.

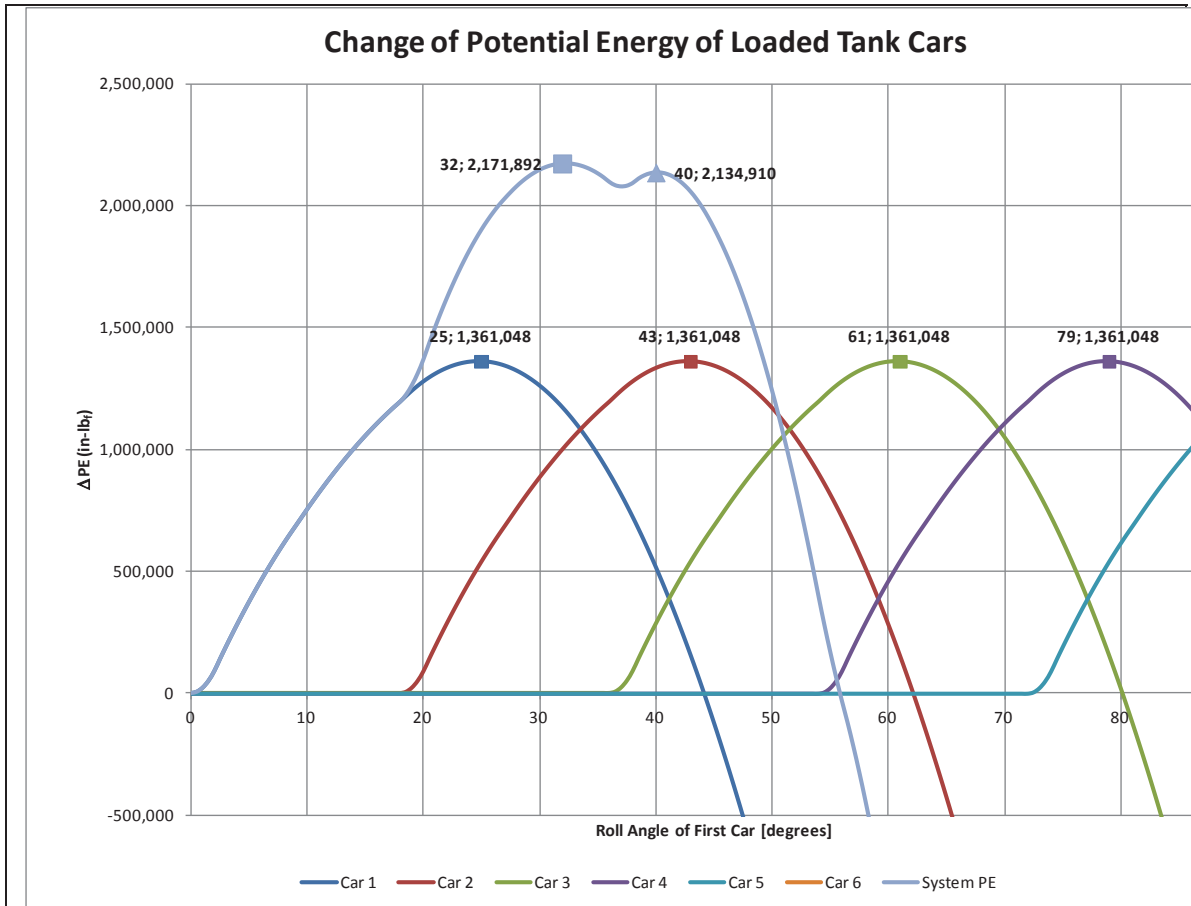


Figure 19: Change in potential energies of loaded tank cars and change in total potential energy of a system, as a function of the car body roll angle of the first car.

3.6 Comparison of Empty and Loaded Cases

The kinetic energy that must be added to the system to initiate a loaded car domino rollover is 1.6 times that required for the empty car case (Figure 20). Fewer cars are required to initiate a loaded car domino derailment. Since the weight of the loaded car compresses the secondary suspension springs far more than does the weight of the empty car, the car body bolster can contact the side frame with much less car body roll. The greater weight of the loaded car body can also transfer enough load to the side frame to destabilize the truck without very much additional car body roll. Therefore, the meta-stable point is reached at a reduced car body roll angle for the first car (32° vs. 64° for the empty car case) and at this point the second car has only rolled by 14°.

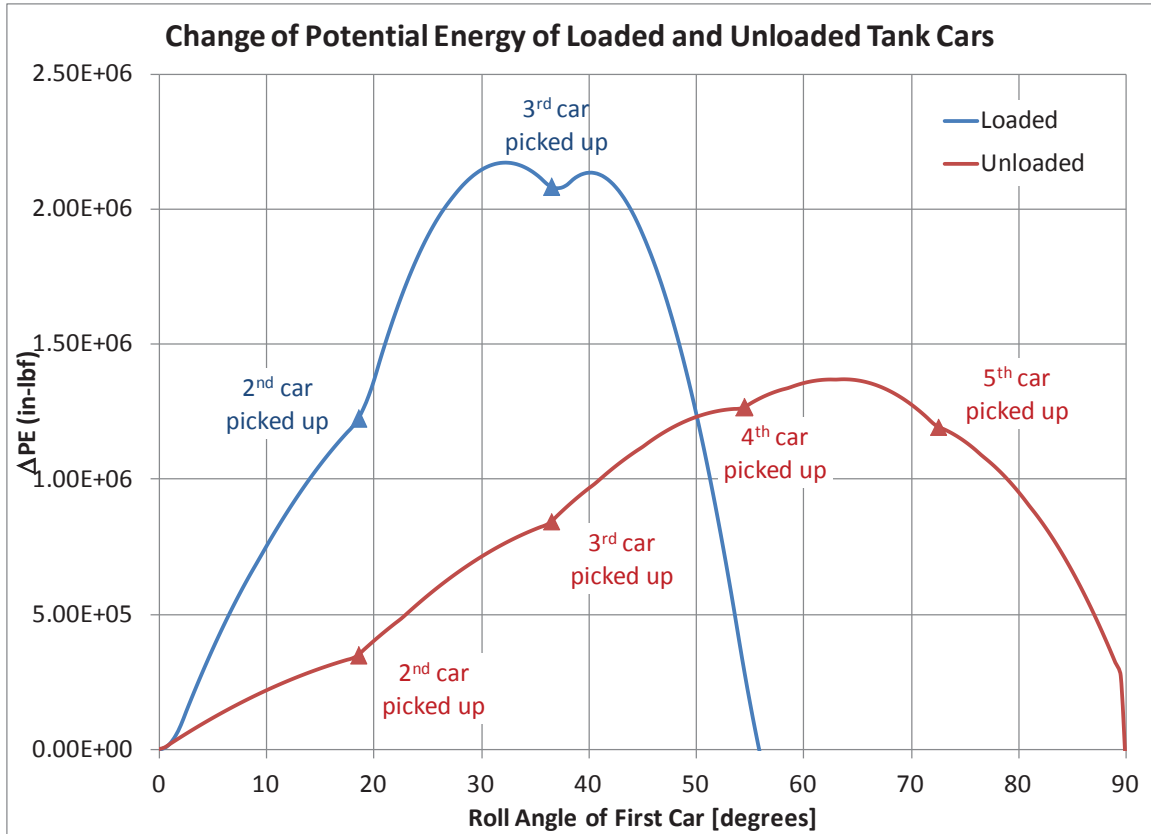


Figure 20: Comparison of system variation in potential energy between loaded and unloaded tank cars.

For either case, it is feasible (purely from an energy point of view) to cause a domino rollover as a result of sideswipe collision with a single car or with a rake of slow moving cars. An example of the latter for empty cars was reported in TSB report R02Q0041.

Not considered in this analysis is the strength of the materials involved. In some of the reports for empty car domino derailments, many cars were involved which implies that there were no failures in components that would have allowed one car to separate from another during the derailment and halt the domino phenomenon. In the reports for the loaded car derailments where a domino effect occurred, a limited number of cars were involved. In some cases, there were loaded car component failures (particularly the coupler carrier iron, coupler key, or coupler shank) that allowed cars to separate and stop the domino effect.

Building on the fact that component failures stopped the domino effect, increasing the amount of energy required to roll over a string of cars could serve as an alternative or addition to the potential solution of a rotary double-shelf coupler (discussed in Section 1 of this report). Increasing the system energy will result in higher stress on the components, effectively making them act as fuses. In order to increase the system energy, the simplest approach is to reduce the amount of angular lag (currently assumed at 18°). Reducing the lag between the cars will force the domino roll to pick up the next cars in the system at a smaller roll angle, adding their weight and resistance to the system. Figure 21 compares the current loaded case analysis with a lag of 18° (blue) to

the unloaded case with a lag of only 11° (red). The energy required to reach the system's meta-stable point is similar in both cases, but seven cars are now involved in the unloaded car string. This alternative solution requires further study: what potential energy level is required to systematically obtain this fuse effect, is it possible to sufficiently reduce coupler roll slack without affecting car operations or increasing puncture risk and are there more efficient or complementary ways to increase the energy to reach the system's meta-stable point?

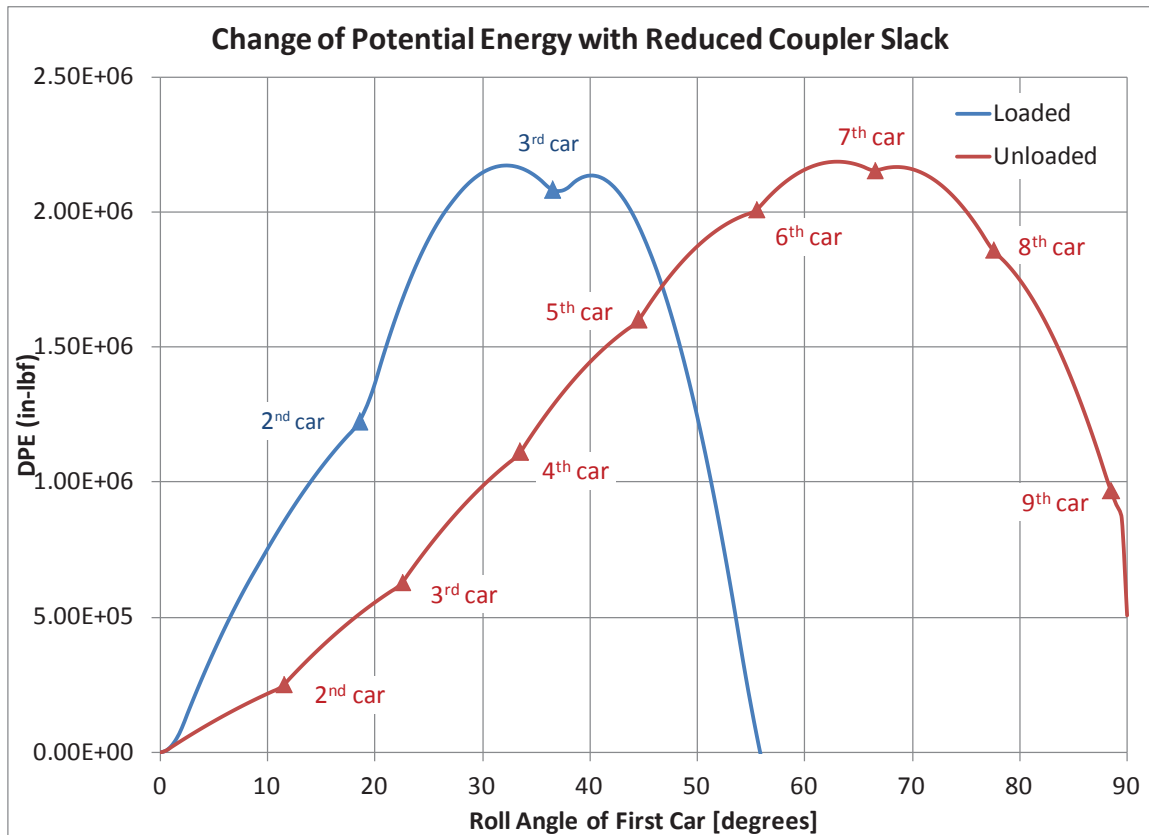


Figure 21: Effect of reducing coupler slack on system energy.

4. VAMPIRE SIMULATION

4.1 Introduction

In September 2007, NRC-CSTT was tasked by TC-TDG to perform an investigation of multiple tank car rollover derailments related to double-shelf couplers, in an effort to better understand the mechanisms involved in the propagation of a multiple empty tank car rollover, and to suggest and examine potential remedies to this problem. NRC-CSTT Report No. CSTT-RVC-TR-157 [1] dated March 2009, presents the investigation results as presented to TC-TDG. The outcome of this investigation identified two mechanisms that likely work in combination. The first mechanism was rollover due to a moment transferred between couplers, and the second mechanism was the transfer of vertical motion and force from a car that is derailing to the adjacent car that is still on the rails.

In January 2010, TC-TDG gave NRC-CSTT a task to perform the following work:

| <u>Task</u> | <u>Description</u> |
|-------------|--------------------|
|-------------|--------------------|

1. Conduct a literature review of loaded tank car rollovers;
2. Conduct an energy analysis to see if there was enough energy for one tank car to roll another over in the empty and loaded conditions;
3. Perform simulations using MBD¹ software of a domino rollover of a string of cars to:
 - a. Simulate the rollover of empty trains equipped with regular couplers, and with double-shelf couplers;
 - b. Calibrate the dynamic model to generate a domino rollover for the double-shelf coupler case;
 - c. Simulate a loaded train equipped with double-shelf couplers to determine if domino-type rollover is possible;
 - d. Investigate the effectiveness of proposed solutions by conducting simulations for tank car unit trains equipped with the proposed coupler systems.

4.2 Simulation Approach

MBD models have been used extensively to evaluate the stability and safety of railcars operating in normal service as they travel along the track. However, there is very limited evidence of their use in predicting car behaviour significantly beyond the point where:

- the wheels lose contact with the track,
- the couplers move through substantial displacements and angles relative to one another,
- the couplers, centre plate and side bearings become disconnected, and the car body leaves the trucks entirely and hits the ground and digs in or slides.

¹ Multi-body dynamics (MBD) is a widely accepted methodology in which the dynamic response of a mechanical system can be estimated by using a computer simulation model in which a number of rigid bodies are connected by springs, dampers, and a variety of other connections, and where the equations of motion are written and solved automatically by the MBD software.

The January 2010 proposal was for the development of a basic MBD model that would take some simple railcar bodies, suspend them on a truck model that is normally used for examining curving and hunting performance, and then incorporate the moment transfer, vertical force, and motion transfer mechanisms that were believed to be key causal factors in the multiple-car rollovers.

NRC-CSTT began work on this task, and delivered results for the literature review (Task 1, discussed in Section 1 of this report) and energy analysis (Task 2, discussed in Section 1 of this report), and a status report on the simulation, at a progress review meeting on 27 May 2010. Task 3 involved the performance of MBD software simulations of a domino rollover of a string of cars. The highlights of the presented simulation work were as follows:

Task 3a: This task was accomplished by building a simple MBD model of three railcars coupled together using VAMPIRE, a commercial MBD package. The model had the following key characteristics:

- A rigid-body mass was used to represent the tank and miscellaneous structure down to and including the body-bolster centre plates, and including the draft gear and couplers, on each of the cars;
- The couplers that join one car body to the next were modeled by a single connection in which the roll rotation is a roll-moment vs. angular displacement taken from measurements reported by Trent et al. [2], a sample of which is shown in Figure 22. The vertical translation of the connection is a similar relationship that allows free vertical translation for the regular and shelf couplers and that incorporates a steel-on-steel stiffness when the shelf couplers run out of vertical travel. The connection also includes steel-on-steel stiffness values for lateral and longitudinal translations, and unconstrained rotations in pitch and yaw;
- Centre bowl and side bearing connections were modeled in a manner that is virtually identical to the accepted methods used in standard freight car MBD modeling, except that the model was altered to allow the connections to separate completely;
- The truck bolsters, side frames, wheels and axles, together with the primary and secondary truck suspension were also modelled in a manner that is identical to the accepted methods used in standard freight car MBD modeling;
- The ground was not modelled in this simulation; Instead, the simulation was simply stopped when one of the cars moved into a position where it would come into contact with the ground; and
- A lateral impact force of 30,000 lb was applied to the centre of one of the car bodies to initiate rollover.

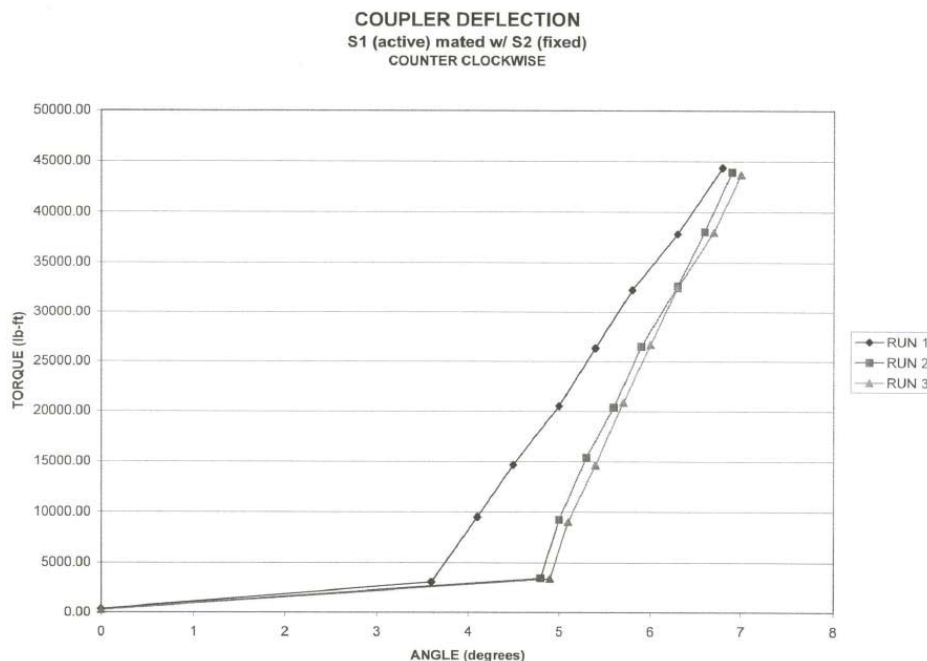


Figure 22: Sample of measured torque vs angular displacement for a shelf (S1) coupler mated with a second shelf coupler (S2), from Trent et al [2].

Constructing the model in VAMPIRE meant that it could be built relatively quickly using existing models and subroutines from other MBD simulations that NRC-CSTT has conducted in the past. However, VAMPIRE always makes small angle assumptions (i.e., that $\sin(\theta) \approx \theta$ and $\cos(\theta) \approx 1$). These assumptions are typically considered reasonable for angles up to about 15 to 20 degrees (where the errors are 3.4% and 6%, respectively), but should not normally be used where angles reach 45 or 60 degrees (where the errors are 29% and 50%, respectively). In this particular case, even though the body roll angles were in the region of 90 degrees when they were approaching the ground, the maximum roll angles in the cases where the cars stayed on the track were always less than about 35 degrees. Thus, for the purposes of performing a quick assessment of the likely effect of rotary couplers, VAMPIRE was considered to provide a reasonable modeling environment. This task was completed.

Task 3b: The parameters in the model were tuned to get the cars to roll off their trucks in a domino manner and end up on the ground beside the tracks in a location similar to that shown in the photographs of actual multiple tank car derailments [1]. NRC-CSTT demonstrated a video to TDG staff of simulations of three simplified car bodies starting on the tracks and ending up with the first car on the ground to demonstrate the extent to which the simulations duplicated the domino rollover described in [1] This task was completed.

Task 3c & Task 3d: These two tasks have not been completed. At the end of the 27 May 2010 meeting, TC-TDG asked NRC-CSTT to stop further work on the dynamic simulation task until after some physical testing was complete. It was believed that information measured in the physical rollover tests could be used to help calibrate the simulation models.

In January 2012, TC-TDG decided not to proceed with any additional simulation work due to budget limitations. Instead, TC-TDG decided to focus their efforts on reviewing NRC's findings from the physical testing and analysis, as it might be sufficient to inform policy decisions, to recommend appropriate risk management practices, or assess if further work is needed.

4.3 Simulation Results

A simulated train consisting of three typical tank cars equipped with typical North American freight trucks was modeled in VAMPIRE. Table 13 shows the major parameters for the tank car and the freight truck.

To simulate a rollover derailment in the field, a dynamic force is applied to Car #1 at the centre of gravity position. The assumed scenario is that a derailed car impacts Car #1 dynamically as shown in Figure 23. The maximum impact force is estimated approximately as 125 kips, which is about 25% of typical impact force observed when a typical empty freight car impacts head-to-head to a string of cars under a speed of around 8 mph. As the purpose of the simulation was mainly to investigate the effect of the double-shelf coupler on a domino rollover, the impact scenario used here is to duplicate one observed in the field. It was believed that the initiation event would have an insignificant effect on the domino behaviour.

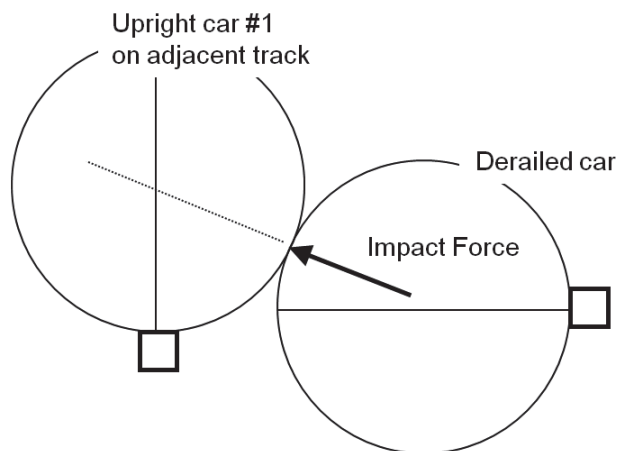


Figure 23: Assumed impact scenario.

Table 13: Major parameters for dynamic simulation.

| Parameter Name | Value |
|--|-----------------------|
| Simulation Speed (mph) | 1 |
| Single Car GRL (lbs) | 598,000 |
| Single Car Body Mass (lbs) | 42,611 |
| Single Car Body Roll Inertia, Ix (lbs-in ²) | 1.09E+08 |
| Single Car Body Pitch Inertia, Iy (lbs-in ²) | 2.32E+08 |
| Single Car Body Yaw Inertia, Iz (lbs-in ²) | 2.23E+08 |
| Single Car Body CG Position from TOR (in) | 95 |
| Distance between Truck Centers (in) | 455 |
| Distance from truck center to coupler face (in) | 95.5 |
| Wheel Diameter (in) | 36 |
| Wheel Base of Truck (in) | 70 |
| Spacing between Journal Center (in) | 79 |
| Center Plate Diameter (in) | 14 |
| Mass of one Bolster (lbs) | 1,467 |
| Roll Inertia of one Bolster, Ix (lbs-in ²) | 9.85E+05 |
| Pitch Inertia of one Bolster, Iy (lbs-in ²) | 1.32E+04 |
| Yaw Inertia of one Bolster, Iz (lbs-in ²) | 9.85E+05 |
| Spacing of Wedge Column Face (in) | 17.5 |
| Mass of one Side Frame (lbs) | 845.5 |
| Roll Inertia of one Side Frame, Ix (lbs-in ²) | 25,480 |
| Pitch Inertia of one Side Frame, Iy (lbs-in ²) | 4.32E+05 |
| Yaw Inertia of one Side Framer, Iz (lbs-in ²) | 4.32E+05 |
| Mass of one Wheelset (lbs) | 2,718 |
| Roll Inertia of one Wheelset, Ix (lbs-in ²) | 1.99E+06 |
| Pitch Inertia of one Wheelset, Iy (lbs-in ²) | 3.50E+05 |
| Yaw Inertia of one Wheelset, Iz (lbs-in ²) | 1.99E+06 |
| Centre Bowl Friction | 0.3 |
| Gap between Center Plate and Center Bowl (in) | 0.0625 |
| Side Bearing Friction | 0.3 |
| Side Bearing Gap (in) | 0.25 |
| Wedge Angle (deg) | 32 |
| Wedge Friction | 0.4 |
| Spring Froup Name | 7D5-3D5 / 2B432-2B433 |
| Axle Adapter Longitudinal Clearance (in) | 0.15 |
| Axle Adapter Lateral Clearance (in) | 0.185 |
| Axle Adapter Friction | 0.4 |
| Wheel Profile | AAR1BW |
| Rail Profile | AREMA Re136 |
| Wheel Rail Friction | 0.4 |
| Rail Gauge (in) | 56.53 |
| Wheelset Back-toBack Spacing (in) | 53.063 |
| Coupler Center Hheight from TOR (in) | 32 |

Two coupler types are used in the VAMPIRE model to connect Car #1 to Car #2 and Car #2 to Car #3. Rotational moment (torque) applied between these couplers is the key connection to transfer energy between cars in the domino rollover. Physical tests for different coupler types, including the double-shelf coupler, have been reported in [2]. The main characteristics of the rotational connection are (1) there exists an 8 - 12 degree clearance before full torque engagement; and (2) the typical rotational stiffness is approximately 10 million inch-pounds per radian. These features have been included in the present VAMPIRE models for regular E coupler and double-shelf coupler connections. Furthermore, the regular E coupler-to-coupler connection is modeled in such a way that the rotational connection (torque) is switched off when the vertical displacement between the two couplers is larger than knuckle height (approximately equal to 15 inches). However, in the case of a double-shelf coupler, no such disengagement in rotational direction is included in the VAMPIRE model due to the knuckle to shelf wall contact. When the vertical displacement between couplers increases to 6.375 inches (approximately equal to the distance between top of knuckle to the bottom surface of the coupler shelf), the vertical steel-to-steel connection between the two couplers will be switched on in the model. Since the above described connections involve complex interaction in vertical and rotational motion directions, they cannot be modeled by the existing connection elements in VAMPIRE software. However, this can be done by employing the user subroutine of VAMPIRE software in which users are allowed to write their code to model special connection features. Therefore, NRC-CSTT has developed special user subroutine codes to describe the above coupler connections and include them into the VAMPIRE model for following simulations.

The completed results obtained are summarized in Figure 24 and Figure 25 for the regular double E coupler case, and in Figure 26 and Figure 27 for the double-shelf coupler case. Figure 24 and Figure 26 are the sequence plots extracted from animation motion obtained from simulations. A cubic box shape is seen in these plots. This is to facilitate easy view of the rotational motion of the car body. As shown in Table 13, the mass moment of inertias used in dynamic calculation are derived from the actual car body shape of tank car, not from the cubic box shape used in animation.

In the case of the regular E coupler, Figure 24 shows that no domino rollover occurs because the coupler disengages. From the animation it can be observed that Car #2 is actually rotated a few degrees at the beginning. This can be seen clearly in Figure 25 where the rotation angles of the three car bodies are plotted, together with the impact force to Car #1 (as shown in Figure 23). This result is in agreement with the general observation that no domino type rollover derailment happened for the tank train equipped with regular E couplers about 30 years ago.

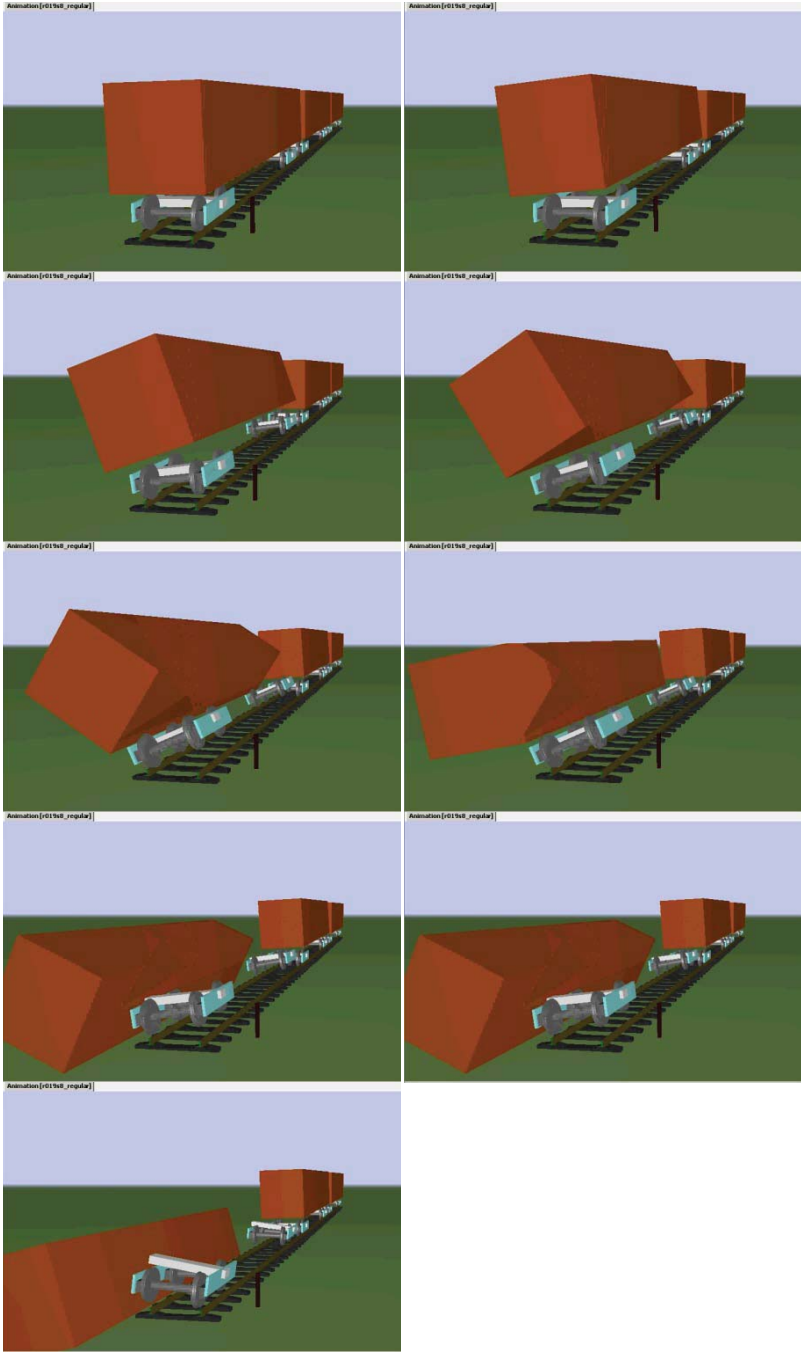


Figure 24: Animations of simulation results for regular Type E coupler case.

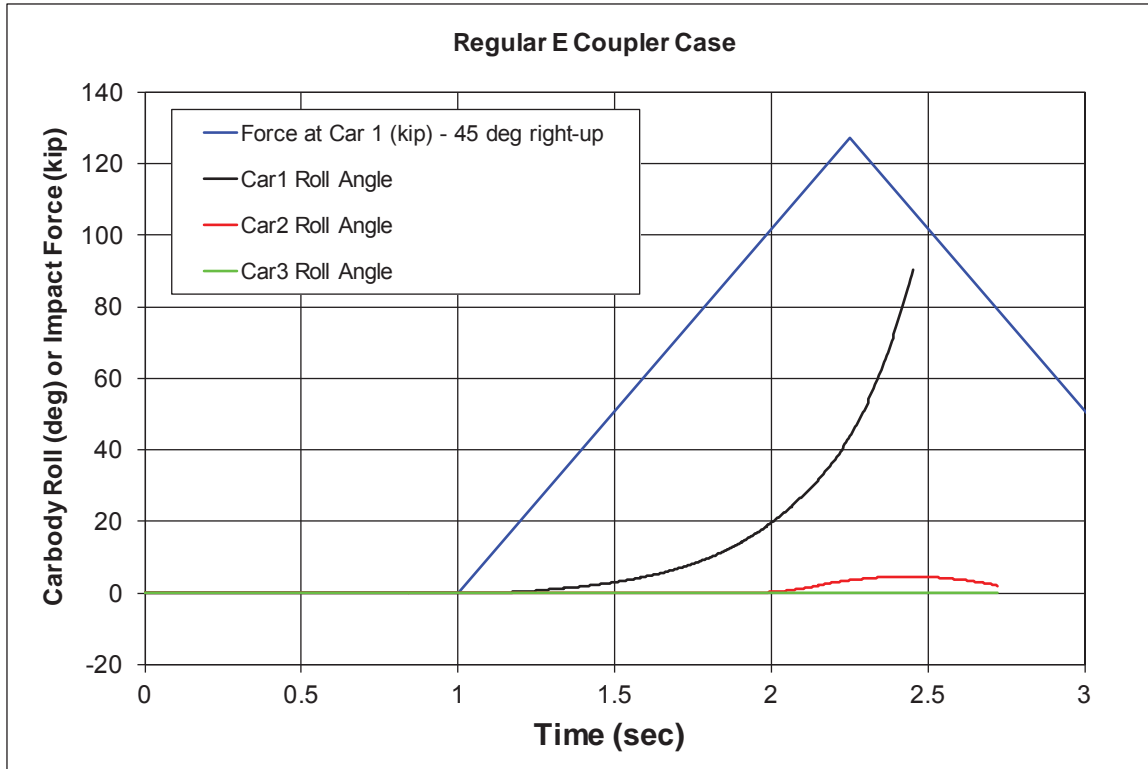


Figure 25: Car body roll angles obtained by simulation for regular Type E coupler case.

Figure 26 shows the domino type rollover when the double-shelf coupler is modeled in the simulation. Figure 27 gives time histories of the angles of the three car bodies. These results indicate the main reason for the domino rollover is the torque transfer between cars through the double-shelf coupler, which cannot be disengaged by the relative vertical motion of two adjacent couplers. The obtained domino rollover is in agreement with the general observation that tank trains equipped with double-shelf couplers are known to suffer domino type derailments. By obtaining the animation motion results shown in Figure 26, the developed VAMPIRE dynamic model shows good potential of the developed coupler models in the user subroutine as well as the whole rollover model. This is despite the limitation VAMPIRE software has that the moment and force are calculated based on small angle assumption (for example using θ to replace $\sin \theta$). The next step will be to assess the impact of small angle assumption to the obtained simulation results by comparing the simulation with the physical test. This was not done as the simulation work was put on hold.

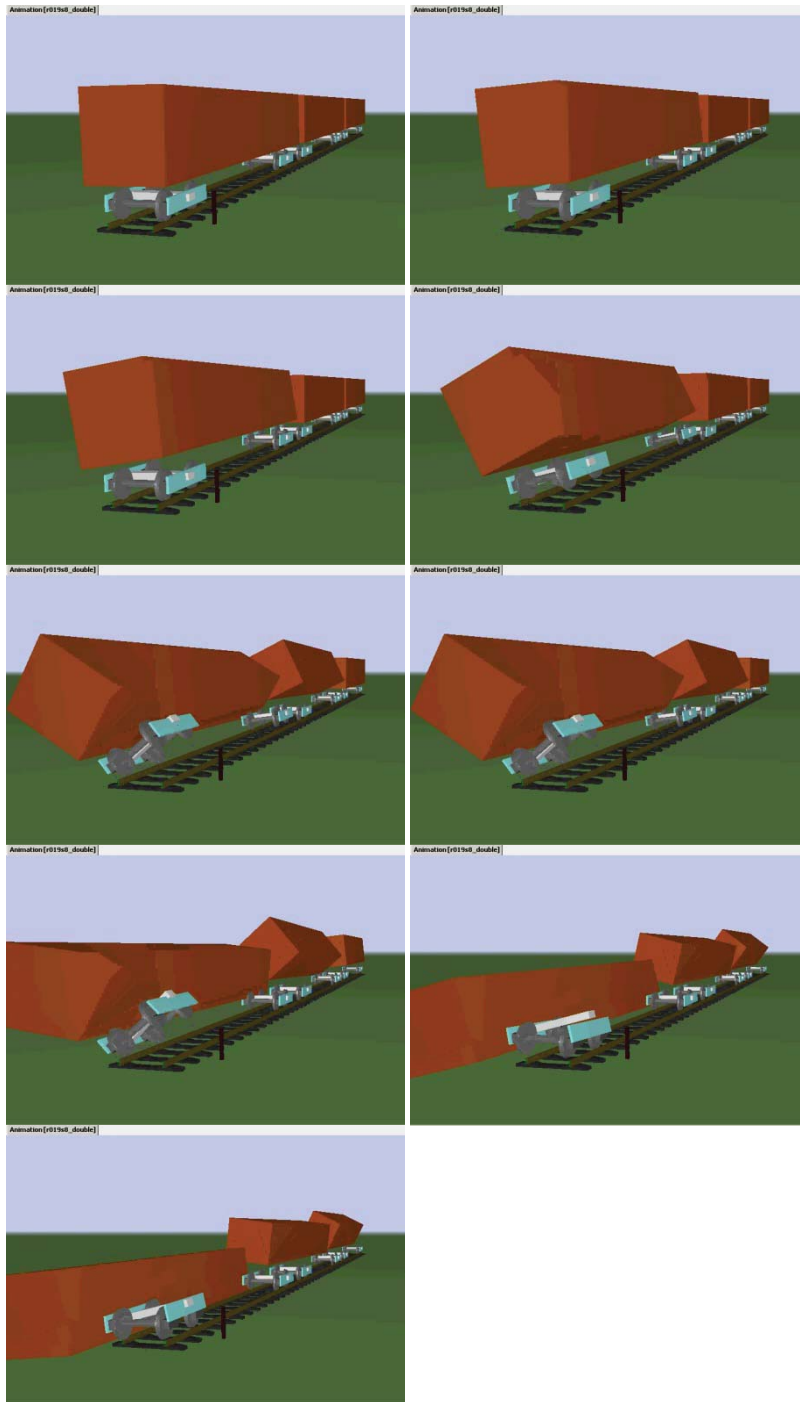


Figure 26: Animations of simulation results for double-shelf coupler case.

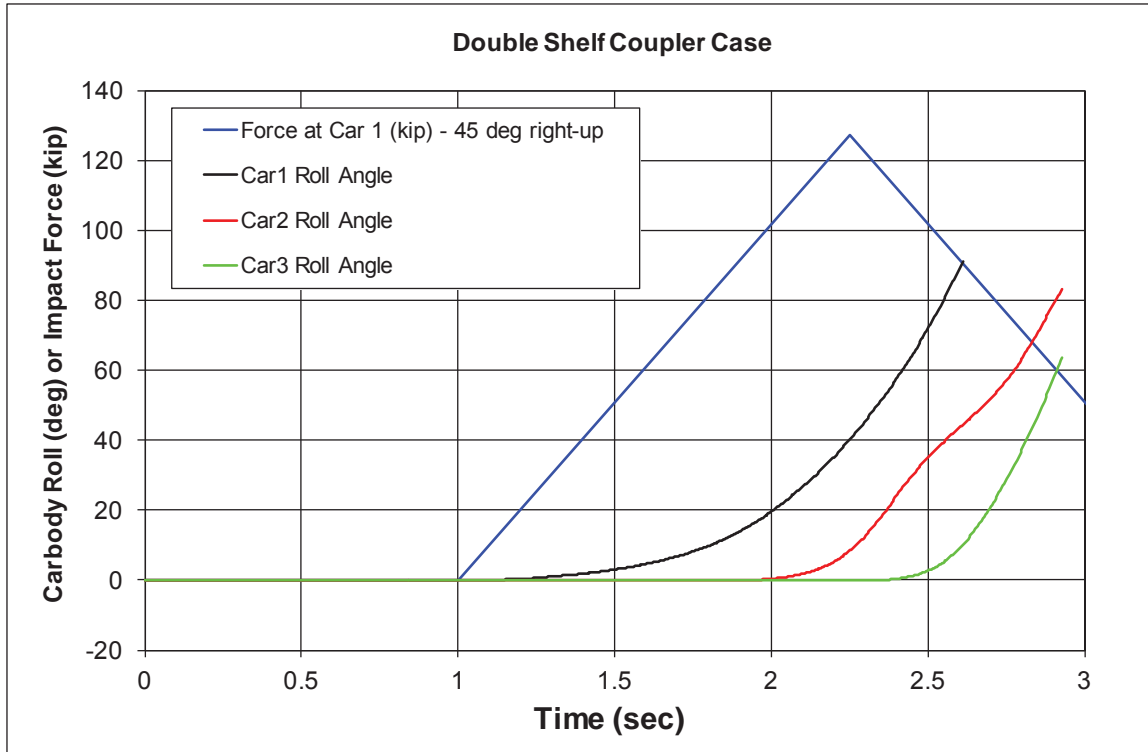


Figure 27: Car body roll angles obtained by simulation for double-shelf coupler case.

4.4 Proposed Dynamic Simulation Work for Future Consideration

After the physical rollover tests were completed, it was proposed that a new set of dynamic simulations be performed that builds on the knowledge gained from the physical rollover tests and the initial rollover simulations.

These new dynamic simulations were proposed to make certain that TC-TDG and NRC-CSTT have an accurate understanding of the underlying causes of domino rollovers, and therefore be in a stronger position to recommend appropriate practices. This could also help support TC-TDG’s risk management decisions regarding the use of a specific coupler system (e.g., establishing the minimum number of rotary double-shelf coupler connections in a string of tank cars) to prevent a domino rollover. These simulations could incorporate information obtained from the physical rollover tests into the simulation models. This would allow a direct comparison of the simulation results with some of the measurements that were made in the physical tests, and would thus provide a much stronger validation.

It was proposed that the simulations be conducted using SIMPACK, a commercial MBD package that is widely used in the passenger rail industry around the world, since it has a much better ability to handle situations where large angle changes occur. Although it can be argued that TC-TDG wants the rotary couplers (or other roll-stabilizing devices) to keep the body roll angles in a region where the roll angles are always small (e.g., less

than about 15 degrees), it may be that every second or third car needs to be equipped with a rotary coupler to achieve this. However, in practice, body roll angles in the region of 35 degrees may still provide an acceptable margin of safety from domino rollover. To accurately predict the car behaviour in the region from 20 degrees up to 35 degrees, it is necessary to make use of commercial MBD software that avoids small angle assumptions. Similarly, if there is a desire to estimate the forces and torques acting on the car bodies as they roll over beyond 20 degrees and up to the point where they impact the ground, then it is essential to use software that avoids small angle assumptions. Also, if there is a desire to optimize the spacing of rotary couplers (e.g., from one on every third car to one on every ten cars), it is important to make use of commercial software that avoids small angle assumptions. Relaxing the rotary coupler spacing will have a very direct impact on the cost that industry experiences in implementing the proposed solution, and thus needs to be examined carefully. These are the key reasons for proposing the use of SIMPACK in place of VAMPIRE for this phase of the investigation.

It was proposed that NRC-CSTT develop simulation models for the Test #1 and Test #2 configurations that were used in the physical rollover tests. Test #1 is the baseline configuration with Type E double-shelf couplers in all locations between all four cars, and Test #2 is a similar configuration but with a rotary coupler at the near end of Car #III as shown in Figure 29. The simulation models will incorporate all four of the tank cars used in the physical tests. The car body weights and centre of gravity heights would be estimated from available data derived from the physical test program. This data would be used to construct the tank car models within SIMPACK.

It was also proposed that a more detailed mathematical coupler model be developed for double-shelf and rotary couplers to better represent the actual geometry of the coupler shanks and pivots, and the way they move laterally, vertically, and in rotation, and then hit physical stops in the sill pockets. These coupler model improvements would be combined with the measured coupler torsional stiffness characteristics from [2], and with relevant data available from the physical rollover tests.

A comprehensive truck model, similar to one used in the Task 3a simulation but valid for large roll angles, would be incorporated into the simulation and would include all the major masses and connection components, such as:

- axle adapters;
- main springs;
- friction wedges;
- side bearing; and
- centre bowl / plate.

The proposed simulation model would also incorporate a comprehensive model for the wheel-rail interface with proper wheel and rail profiles that is virtually identical to that used in the Task 3a simulations.

In selecting an operating environment for the simulations, a tangent track would be modeled and utilized in the simulations. Should the requirement exist, curved track models can also be explored at a later time; however these will not be included in the scope of this proposal.

Provision will be made in the model for the car body bolster to make contact with the top outside portion of the side frame in the rollover process, since this is one of the key events that takes place in all of the physical tests before the tank hits the ground. The model will allow the use of different car body bolster to side frame clearances for each of the cars in the consist. Interaction between the car body bolster and top outside surface of the side frame has a significant effect on rolling a tank car and needs to be included to obtain an accurate assessment of the required rotary coupler spacing.

The simulation model would incorporate interaction between the car bodies and ground that has an elevation that is representative of the elevation that existed for the Test #1 and Test #2 physical tests. This would improve the validation process, and would allow the effect of this parameter to be studied at a later date if necessary.

When simulating the physical tests within SIMPACK, the pulling locations and pulling forces recorded during the physical tests would be used as input into the simulation in place of the impact force that was used in Task 3.

The simulation model would be used to reproduce the key features of car body rollover modes such as domino or non-domino rollover.

The torques and forces between car bodies predicted by the simulations would be compared with those measured during the physical tests.

The simulation models would be improved through two iteration steps to achieve a reasonable agreement between the physical tests and the simulation results.

After the models were validated by the two rollover tests, the models would be used to conduct rollover simulations for the Test #1 and Test #2 configurations, but under a loaded condition in place of the empty condition that existed in the physical tests.

In summary, the proposed simulations would have provided the following key advantages over the Task 3 simulations:

- They would eliminate the small angle assumptions, and thus allow more accurate simulations for cases where the rotary couplers are widely spaced and cars in between them reach body roll angles in excess of 15 degrees but do not roll over;
- They would have a more detailed mathematical coupler model for both double-shelf and rotary couplers to better represent the geometry and behaviour of the actual couplers;
- They would simulate the situation where the body bolster hits the top outside portion of the side frame at moderate roll angles and the side frame produces a destabilizing influence;
- They would include interaction between the car body and ground with a specified elevation;
- They would allow the application of a specific rollover-initiation force at a specified location and direction;
- They would be validated using physical test measurements, including torques and forces between car bodies.
- The models would be used to examine the domino rollover behaviour of the Test #1 (double-shelf couplers alone) and Test #2 (same, but with one rotary coupler) cars, but in a loaded condition rather than the empty condition that they were tested in.

Transport Canada has decided not to move forward with the proposed dynamic simulation work at this time.

4.5 Capabilities and Limitations of the Future Simulation Models

NRC-CSTT was asked by TC-TDG to provide information regarding the capabilities and limitations of the proposed simulation models. TC-TDG has three specific concerns:

1. What will the proposed simulation models provide to TC-TDG?
2. What can the proposed simulation models provide TC-TDG in the future?
3. What will the proposed simulation models not provide TC-TDG in the immediate future?

To address these concerns, Table 14 was prepared for TC-TDG's consideration.

Table 14: Capabilities and limitations of the developed simulation models.

| Request | Capability/Limitation |
|--|---|
| <p>1. What will the proposed simulation models provide TC-TDG?</p> | <p>The proposed simulation models would provide TC-TDG with the following capabilities:</p> <ul style="list-style-type: none"> <input type="checkbox"/> To conduct rollover simulations (virtual tests) for the same consist as physically tested, but under loaded conditions rather than unloaded. <input type="checkbox"/> To reproduce the key features of car body rollover modes such as domino and/or non-domino rollover. <input type="checkbox"/> To validate NRC-CSTT's energy analysis and rollover mechanism, and provide general verification that NRC-CSTT and TC-TDG understand the true causes of the dynamic event, so that stronger recommendations can be made on a solution for implementation by industry. <input type="checkbox"/> To verify torques and forces between car bodies within a consist that is experiencing domino rollover. <p>The simulation models would have limited visual effects, compared with the physical tests. The simulation video would show rollover in a video format from different angles of view.</p> <p>The output of this simulation would be presented as a time-history of events including a numerical factor indicating the car's tendency to roll.</p> |

| Request | Capability/Limitation |
|---|---|
| <p>2. What could the proposed simulation models provide TC-TDG in the future?</p> | <p>The value in using simulation as a complement to physical testing comes from the model's ability to simulate scenarios which are prohibitively expensive or essentially impossible to do using full scale testing.</p> <p>In most cases, a simulation is simply more cost effective once the models have been created and validated. This will allow TC-TDG to investigate other parameters more cost effectively.</p> <p>Some examples of future possible simulation tasks:</p> <ul style="list-style-type: none"> <input type="checkbox"/> trade-offs between having rotary couplers located at different spacings (e.g., every fourth, sixth, or tenth car vs. a current proposed spacing. <input type="checkbox"/> track slope <input type="checkbox"/> track curve <input type="checkbox"/> train consist speed <input type="checkbox"/> wind <input type="checkbox"/> different couplers <p>Future improvements to the fidelity of the simulation model could be made in the following areas if further investigation shows these mechanisms have an important impact on the results:</p> <ul style="list-style-type: none"> <input type="checkbox"/> simulation of the car body sliding sideways off the side bearings and impacting the inside face of the side frame; and <input type="checkbox"/> simulation of the car body being constrained by a long centre pin as it lifts out of the centre bowl on the bolster, with the pin initially behaving like a shear pin, and then later as a pin in bending as the car body rises. |

| Request | Capability/Limitation |
|---|---|
| <p>3. What would the proposed simulation models not provide TC-TDG in the immediate and foreseeable future?</p> | <p>The proposed simulation models would have the following limitations in both the immediate and foreseeable future:</p> <ul style="list-style-type: none"> <input type="checkbox"/> The models would not have every detail from a tank car – only those items that are important to getting a reasonable duplication of domino rollover would be included in the model. Should TC-TDG want more detail, NRC-CSTT can model additional components in detail at an added cost. <input type="checkbox"/> This work would not produce a standalone application that TC can manage/manipulate. <p>The SIMPACK models developed would be retained by NRC-CSTT.</p> |

5. PHYSICAL TESTING

5.1 Introduction

NRC-CSTT was tasked by TC-TDG to develop and undertake a test program in which potential solutions to the problem of multiple tank car rollovers are investigated.

The test program involved full scale testing of empty tank cars as though they were involved in a zero-speed derailment similar to the one that occurred in Clara City, Minnesota in October 2007.

The test program included preliminary testing on a string of three tank cars to determine the most effective way to initiate a domino style rollover on a string of three tank cars, in advance of performing the actual tests. The program also included four full-scale rollover tests.

The first test run involved three tank cars and an extra car to act as the initiating car to which an external force was applied to cause it to roll off its trucks and onto the ground. The roll of this car then started the domino roll effect on the other three cars. All cars were equipped with standard Type E double-shelf couplers. This test represented the baseline case. The cars were instrumented to measure torque and vertical force at the car sills, translational displacements at the sills, angular displacements at various locations on the cars and trucks, and contact between certain components on the couplers, car bodies and trucks. Video cameras were also used to gather visual evidence of the test.

The second test run was a repeat of the first, but the standard coupler of one car was replaced with a rotary coupler that was modified to have a Type E double-shelf coupler head in place of the Type F coupler head. This test investigated the effectiveness of a rotary coupler as a means of halting the progression of a domino rollover in a string of tank cars. The rotary coupler was installed such that it faced the oncoming domino wave as the rollover event progressed through the cars.

The third test run involved five tank cars, with the extra car added to the end of the string away from the initiating car. The rotary coupler was installed so that it faced away from the oncoming domino wave. The car with the rotary coupler was positioned one car further away from the initiating car (compared to the second test), so the domino wave had an increased propagation speed before it reached the rotary coupler. The purpose of the fifth car was to provide the roll restraint that best mimics the domino derailment case of a chain of cars restrained by subsequent cars. No instrumentation was used in this test, but video cameras were used as before.

The fourth test would be a repeat of the third test, but with a minor change. The car with the rotary coupler was originally equipped with Type F coupler heads. As such, its striker castings were fitted with spring-loaded coupler carrier irons. For this test, the carrier iron springs in the end of the car fitted with the rotary coupler were locked in place, to assess their influence on the domino propagation and the ability of the rotary coupler to stop it.

| | Initiating Car | | 1 st Position | | 2 nd Position | | 3 rd Position | | 4 th Position | | |
|----------------------|----------------|--------|--------------------------|--------|--------------------------|----------|--------------------------|----------|--------------------------|--------|----------|
| Test setup overview | | | | | | | | | | | |
| | N | F | N | F | N | F | N | F | N | F | |
| Test #2 setup | | | | | | | | | | | |
| Orientation | B | CSTT-1 | A | A | Car #I | B | A | Car #III | B | A | Not used |
| Sill type | E | | E | E | | E | F | | F | E | |
| Coupler type | E60C | | SE60CC | SE60DC | | SE60CHTE | Rotary | | SE60CC | SE60CC | |

Figure 29: Test #2, dynamic testing - test setup schematic.

Test #3: Perform dynamic testing on five (5) empty tank cars equipped with standard Type E double-shelf couplers, except the far end of Car #III (in the 2nd position) is equipped with the modified rotary coupler as shown in Figure 30. The addition of the fifth car is to increase the speed of the rollover mechanism and provide extra roll restraint for the fourth car.

| | Initiating Car | | 1 st Position | | 2 nd Position | | 3 rd Position | | 4 th Position | | |
|----------------------|----------------|--------|--------------------------|--------|--------------------------|----------|--------------------------|----------|--------------------------|--------|--------|
| Test setup overview | | | | | | | | | | | |
| | N | F | N | F | N | F | N | F | N | F | |
| Test #3 setup | | | | | | | | | | | |
| Orientation | B | CSTT-1 | A | A | Car #I | B | B | Car #III | A | A | CSTT-3 |
| Sill type | E | | E | E | | E | F | | F | E | |
| Coupler type | E60C | | SE60CC | SE60DC | | SE60CHTE | SE60CC | | Rotary | SE60CC | |

Figure 30: Test #3, dynamic testing - test setup schematic.

Test #4: The rotary coupler did not perform as expected during Test #3, and hence Test #4 was undertaken to repeat Test #3 but with a modification to disengage the spring-loaded coupler carrier iron at the rotary coupler draft sill, in an effort to better understand the rotary coupler mechanism in this test configuration. Figure 31 shows an overview of the test setup.


| | | Initiating Car | | 1 st Position | | 2 nd Position | | 3 rd Position | | 4 th Position | | | | | | | | | | |
|----------------------|--|----------------|---|--------------------------|--------|--------------------------|---|--------------------------|--------|--------------------------|---|--------|--------|----------|--|--------|-------|--------|--|-------|
| Test setup overview |  | | | | | | | | | | | | | | | | | | | |
| | N | | F | | N | | F | | N | | F | | | | | | | | | |
| Test #4 setup | | | | | | | | | | | | | | | | | | | | |
| Orientation | B | CSTT-1 | | A | A | Car #I | | B | B | Car #III | | A | A | Car #III | | B | B | CSTT-3 | | A |
| Sill type | E | | | E | E | | | E | F | | | F | E | | | E | E | | | E |
| Coupler type | E60C | | | SE60CC | SE60DC | | | SE60CHTE | SE60CC | | | Rotary | SE60CC | | | SE60CC | SE60C | | | BE60A |

Figure 31: Test #4, dynamic testing - test setup schematic.

5.3 Test Results

5.3.1 Dry Run Testing

On August 17 & 18th, 2010, NRC-CSTT performed a dry run quasi-static rollover test with minimal instrumentation on three (3) empty tank cars (Car #I, Car #II, Car #III). The purpose of this test was to gain a better understanding of the tank car's reaction to rollover inducing forces; as well as providing NRC-CSTT with an opportunity to determine the optimal locations for instrumentation in advance of the full-scale dynamic rollover tests. The tanks were not fully rolled over during these dry run tests.

Five (5) rollover initiation methods were investigated by applying forces at different locations on the first car (Initiation Car), and comparing the cars' reaction to each one. The force was applied at the following locations on the first car:

1. Pulling laterally at the end of the car from centre, as shown in Figure 32.
2. Pulling laterally at the end of the car from top, as shown in Figure 33 (this was *chosen after the dry-run test to be the first preferred method to be used during the dynamic testing*).
3. Pulling laterally at the middle of the car from top, as shown in Figure 34 (this was *chosen after the dry-run test to be the second preferred method to be used during the dynamic testing*).
4. Pulling vertically at the end of the car from jacking pad, as shown in Figure 35.
5. Pulling vertically at the end of the car using a custom-made beam, as shown in Figure 36.



Figure 32: Pulling laterally at the end of the car from centre.



Figure 33: Pulling laterally at the end of the car from top.



Figure 34: Pulling laterally at the middle of the car from top.



Figure 35: Pulling vertically at the end of the car from jacking pad.



Figure 36: Pulling vertically at the end of the car using a custom-made beam.

5.3.2 Test Preparation

Based on the observations during the dry run test, the following tasks were performed prior to the dynamic testing:

1. NRC-CSTT cut holes in the concrete crossing under the rolling side of the far-end truck of the car in the first position and under the near-end truck of the car in the second position to allow the car trucks to roll during testing without the bottom of their side frames riding on top of the concrete crossing, which would change the car behaviour (Figure 37).



Figure 37: Truck almost touching the concrete during the dry-run test (left); and holes in the concrete during testing (right).

2. NRC-CSTT manufactured and installed 12 steel supports to strengthen the tracks at several locations along the test consist during testing; this is to eliminate the possibility of damaging the tracks during testing (Figure 38).



Figure 38: Track support.

3. NRC-CSTT placed several truck tires under each tank car to prevent damaging underground communication cables, and to minimize the damage of the tank cars (Figure 39 and Figure 40).



Figure 39: Cars landing on tires.



Figure 40: Tires under Car #II after the rollover occurred.

5.3.3 Instrumentation

Table 15 lists the make and model of all instruments used during testing. Refer to Appendix A for a complete list of all instrumentation used during Test #1 and Test #2.

Table 15: List of instruments.

| Instrument | Make | Model |
|---|---------------------|---------------------|
| Shear Strain Gauges (Car #I A-end, Car #II A-end, and Car #III A-end) | Micro-Measurements | EA-06-250TK-350 |
| Shear Strain Gauges (Car #III B-end) | Micro-Measurements | SA-06-125TK-350 |
| String Potentiometers | Houston Scientific | |
| | Celeco | MT3A-30E-33-10K-C5A |
| | Intertechnology | PT-101-0030 |
| Inclinometers | Crossbow Technology | CXTA01 |
| Load Transducers | Massload | ML-0700 |

Figure 41 to Figure 49 show the location of the various sensors used during the tests.

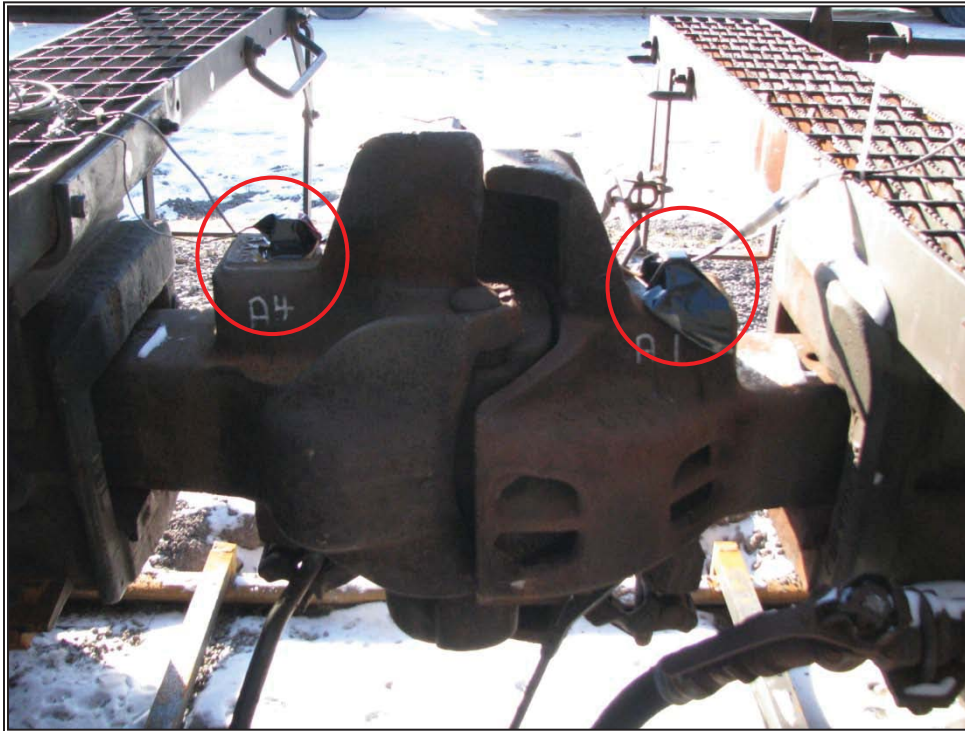


Figure 41: Typical inclinometer location to measure coupler rotation angle.

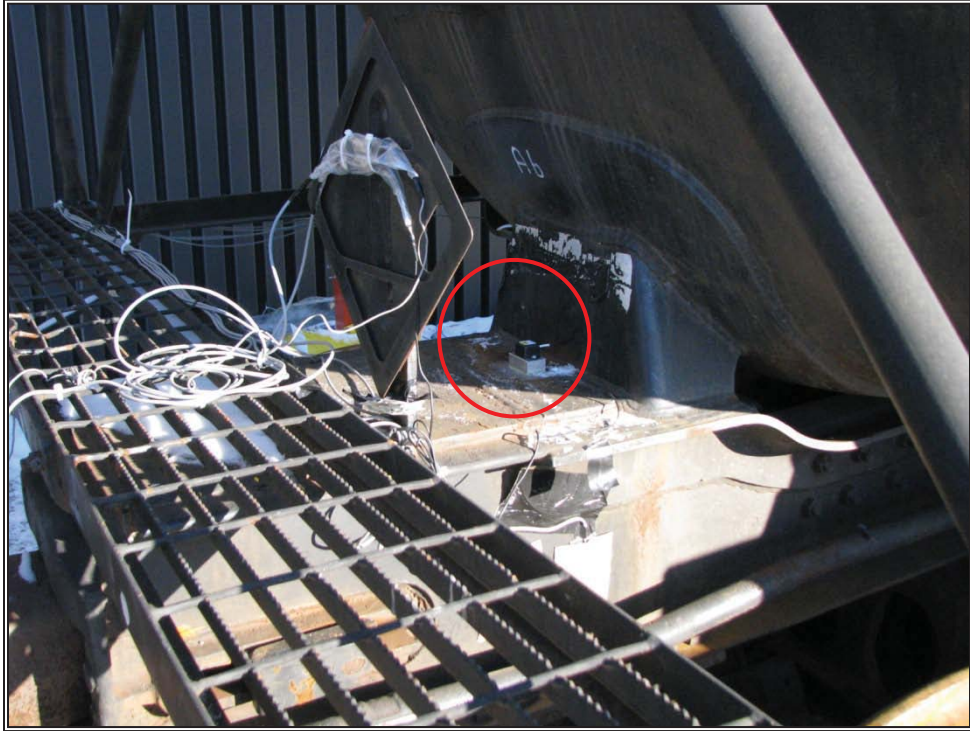


Figure 42: Typical inclinometer location to measure car body rotation angle.

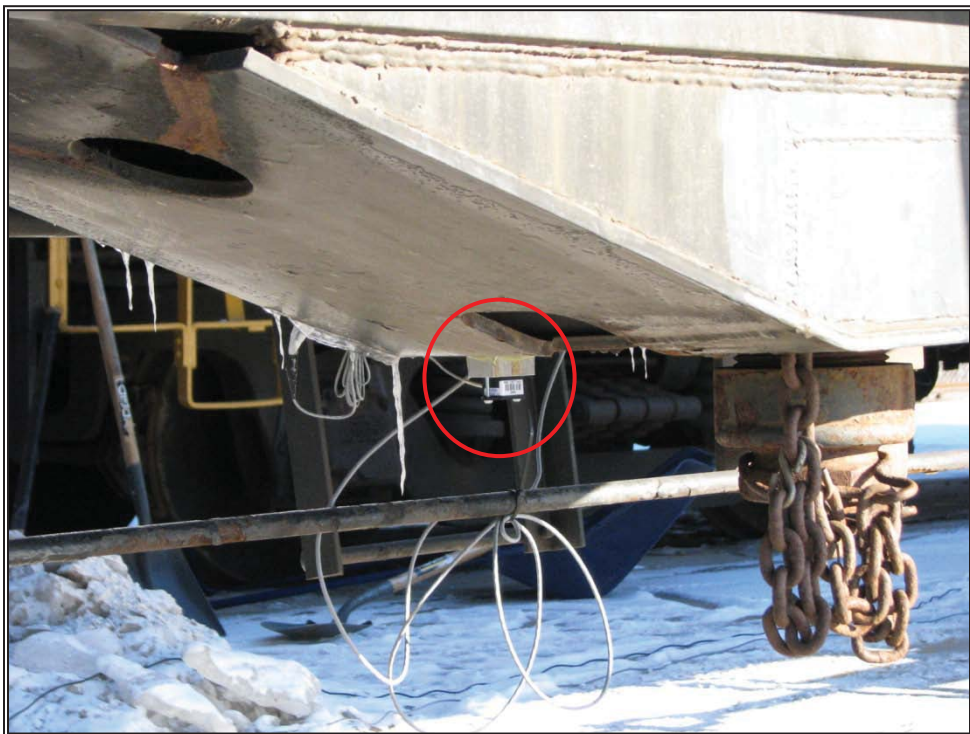


Figure 43: Typical inclinometer location to measure car body pitching angle.

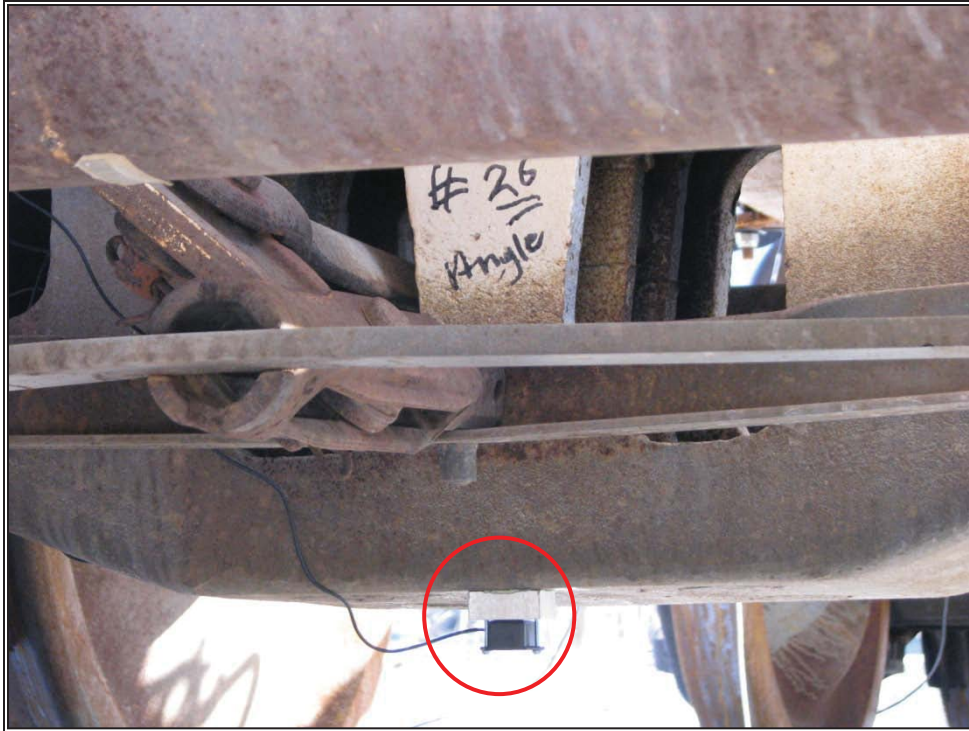


Figure 44: Typical inclinometer location to measure truck bolster rotation angle.

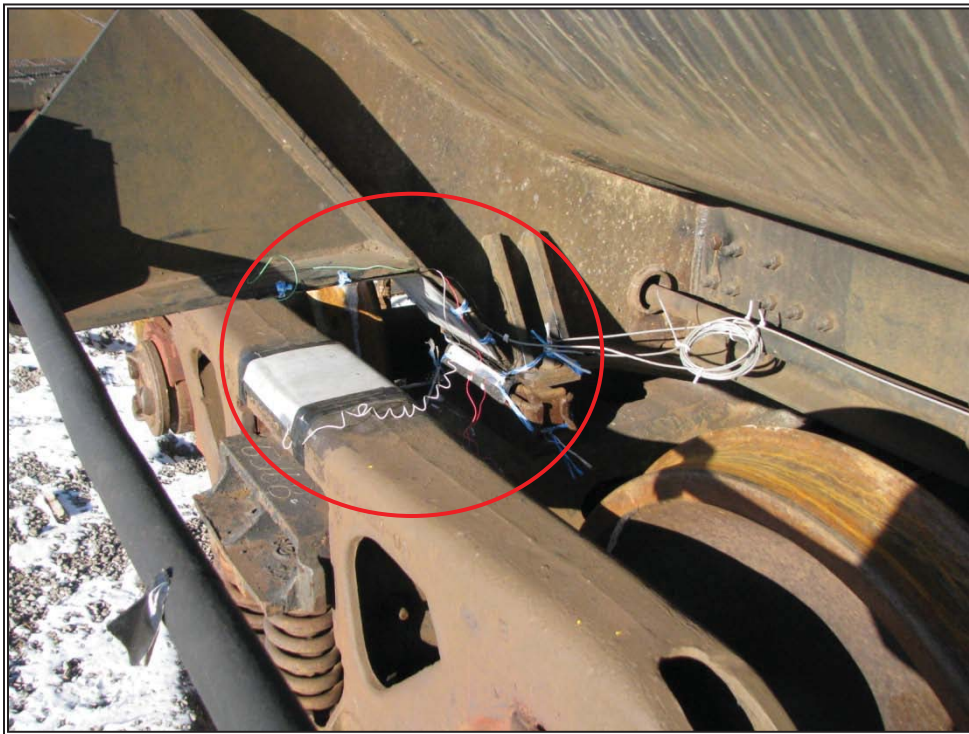


Figure 45: Typical event sensor location to detect contact of body bolster to side bearings, and contact of body bolster to truck side frame (rolled side).

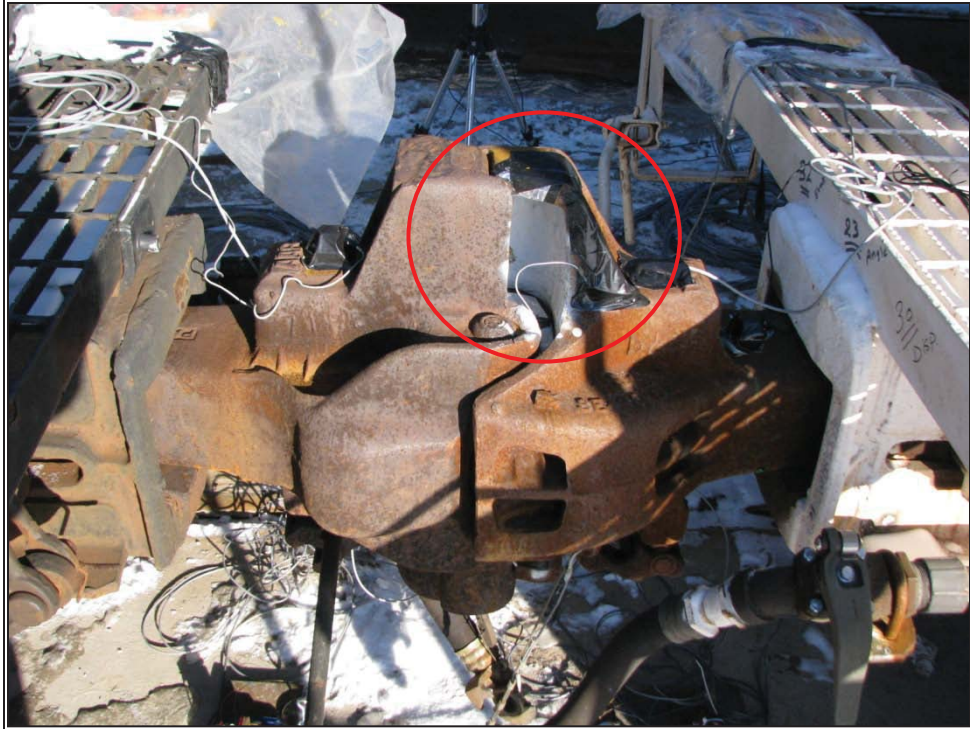


Figure 46: Typical event sensor location to detect shelf/knuckle contact.

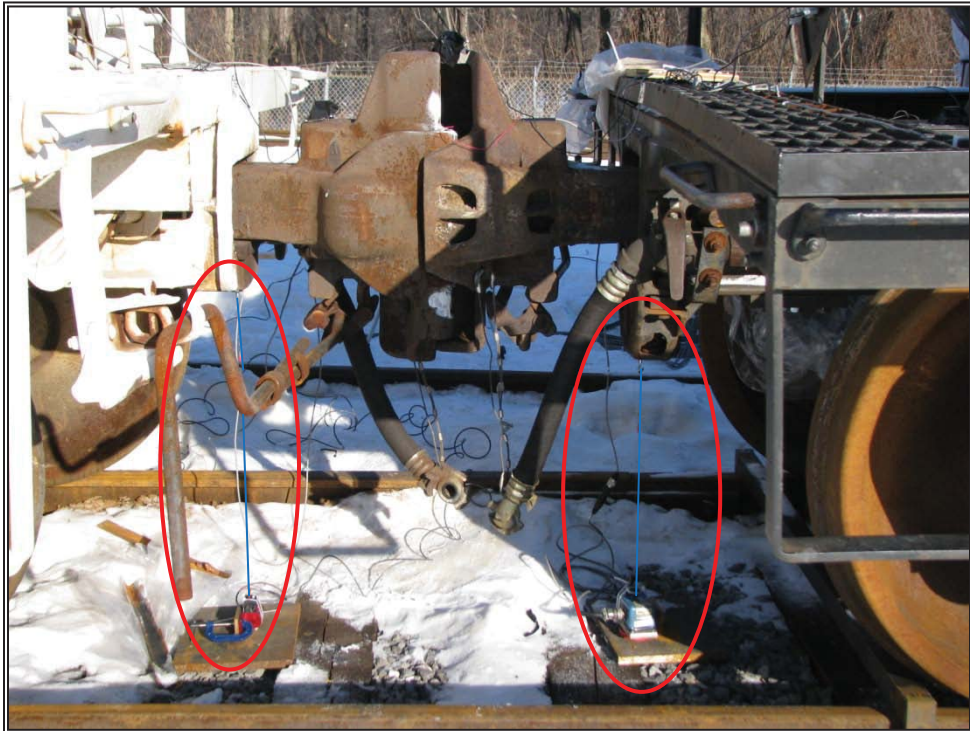


Figure 47: Typical displacement sensor location to measure the height of the draft sill above top of the rail.

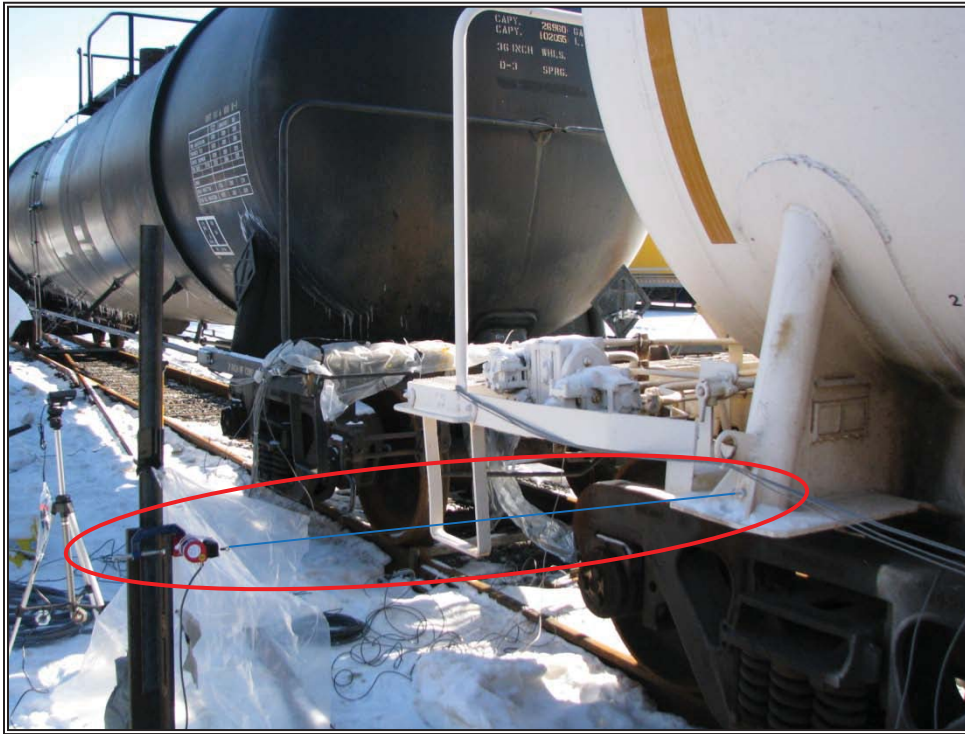


Figure 48: Typical displacement sensor location to measure draft sill horizontal displacement across track.

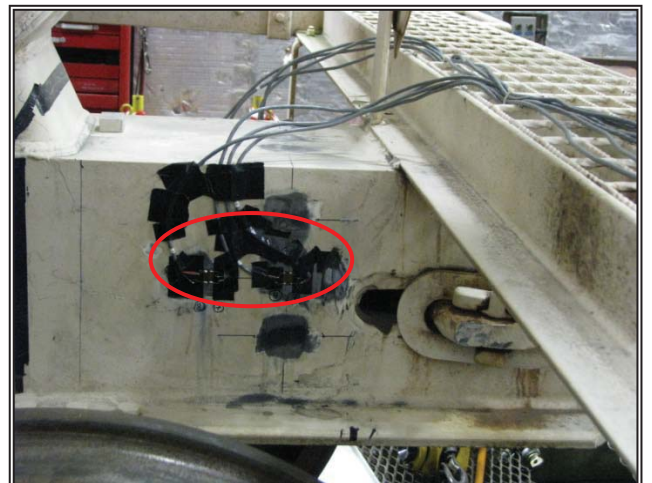


Figure 49: Typical strain gauge locations to measure car vertical load and torque.

5.3.4 Test #1: Baseline Dynamic Testing

Test Setup

On February 22, 2011, NRC-CSTT performed Test #1; a full scale dynamic test on four (4) empty tank cars equipped with standard Type E double-shelf couplers (between coupled cars) throughout the whole test string (Figure 50) to establish the baseline conditions. Cars #I, #II and #III were in the same orientation as for the dry run testing. Various instruments were used to monitor the cars' behaviour. Refer to Appendix A for a full list of instrumentation. Refer to Appendix B for more information about the instrumentation and calibration procedure used to measure vertical forces and torques applied to the tank cars' sills.

The instrumentation described in Appendix A was calibrated and installed, then monitored using a high-speed data acquisition system. The data was sampled at a rate of 250 Hz, and low pass filtered at 50Hz.

Prior to the beginning of the test, all cars were compressed together (no slack between couplers) and hand brakes for all tank cars were released.

Car #III was received with Type F couplers, the coupler at A-end of Car #III was replaced with a double-shelf Type E coupler before testing.

Note: in Figure 50, setup changes between initial car conditions and Test #1 are shown in red. N indicates "near end", while F indicates "far end".

| | | Initiating Car | | 1 st Position | | 2 nd Position | | 3 rd Position | | 4 th Position | |
|---------------------|------|----------------|--------|--------------------------|--------|--------------------------|--------|--------------------------|--------|--------------------------|---|
| Test setup overview | | | | | | | | | | | |
| | | N | F | N | F | N | F | N | F | N | F |
| Test #1 setup | | | | | | | | | | | |
| Orientation | B | CSTT-1 | | Car #I | | Car #II | | Car #III | | Not used | |
| Sill type | E | A | A | B | A | B | A | B | A | B | |
| Coupler type | E60C | SE60CC | SE60DC | SE60CHTE | SE60DC | SE60CC | SE60CC | SE60CC | SE60CC | SF70CC | |

Figure 50: Test #1, dynamic baseline testing - test setup schematic.



Figure 51: Test #1, dynamic baseline testing – test setup.

Due to a few issues related to the weight of the initiating car, and the way the lateral force was applied to the initiating car (pulling laterally at the near end of the initiating car from top), NRC-CSTT was unable to initiate the rollover domino effect on the first attempt (Figure 52).



Figure 52: Test #1, initiating car on ground, failed rollover attempt.

After taking the necessary actions, NRC-CSTT successfully initiated the rollover domino effect on a second attempt (pulling laterally at the near end of Car #1 from top) as shown in Figure 53. In this test the full test string (4 tank cars) rolled over as planned. As the initiating car was lightweight, the force was applied with a slight angle pointing down from the horizontal line to prevent the car from sliding sideways on top of the tracks.



Figure 53: Test #1, pulling laterally at the near end of Car #1 from top.



Figure 54: Test #1, cars after test – side view.



Figure 55: Test #1, cars after test – tail end view.



Figure 56: Test #1, cars after test – initiating end view.

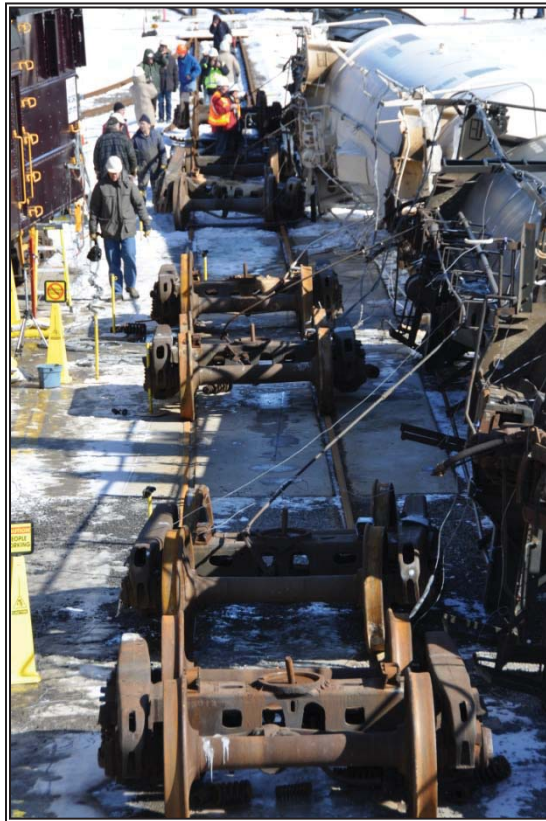


Figure 57: Test #1, cars after test – close up of trucks.



Figure 58: Test #1, cars after test – linked coupler.

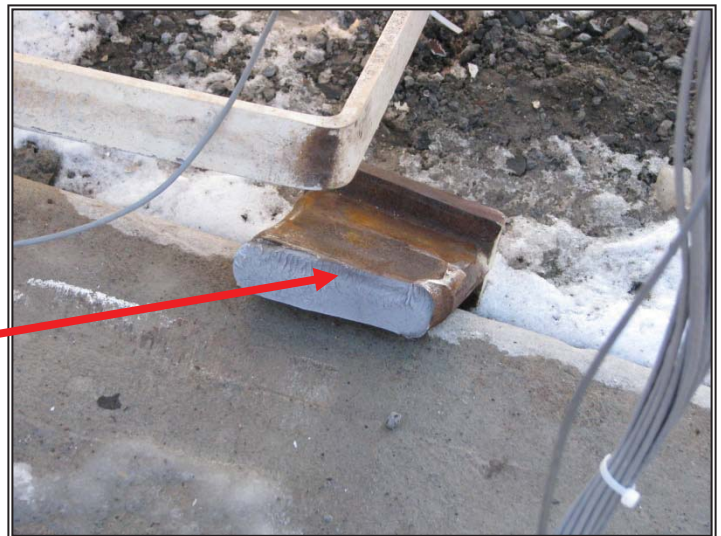


Figure 59: Test #1, broken coupler key of Car #II A-end.

Observations

There were several expectations about the way that the rollover would proceed, given that the tank cars were equipped with conventional Type E double-shelf couplers. **The expectations were:**

1. The far coupler (at the A-end) on the initiating car would undergo shelf/knuckle contact with the near coupler (at the A-end) on Car #I. Refer to Figure 50 for a schematic showing which ends of the cars were coupled, and the meaning of “near” and “far” ends.
2. The near end of Car #I would be lifted vertically and translated laterally by the initiating car.
3. The magnitude of the vertical load applied to a coupler would be half the car body weight.
4. The maximum torque applied to the car body would occur when the centre plate lost contact with the centre bowl. This torque would have a magnitude equal to the car body weight multiplied by the distance between the car body centre and the truck side bearing.
5. The centre plate at near end of Car #I would release from the truck centre pin through a combination of vertical lift and car body roll about the truck side bearing on the rolled side of the car.
6. The body bolster at the near end of Car #I would contact the truck side frame on the rolled side of the car. This would destabilise the body and truck, and both would roll together about the wheel/rail contact points until the body fell to the ground.
7. The truck would drop back down onto the rail, or close to it.
8. The far end of the body would roll about the side bearing, possibly causing the centre pin to bind in the centre plate opening. This would cause the truck to roll with body.

During the first roll attempt, Car #I only partially rolled (to approximately 45°), and Car #II rolled by roughly 12°. When the second (successful) attempt was made at rolling the consist, Car #I and Car #II began from their already partially rolled states. Therefore, to understand how a tank car rolled over during this zero-speed derailment, it is best to examine Car #III during the second roll attempt, as well as the effect Car #II had on Car #III. Some of the effect occurred during the first roll attempt.

The first expectation was that the far coupler (at the A-end) on the initiating car would undergo shelf/knuckle contact with the near coupler (at the A-end) on Car #I. It can be checked by examining the events that were measured on Car #III. These events include knuckle/shelf contact at the couplers between Car #II and Car #III, contact between the body bolster and truck side bearings for both trucks of Car #III, and contact between the body bolster and the top chord of the truck side frames for both trucks of Car #III. Note that Car #III was not equipped with constant contact side bearings (CCSB); therefore there is nominally a gap between the body and the CCSB when the car is sitting on level track.

Events were measured with sensors that produced a zero-value output when there was no contact between the corresponding car components, and a 5 volt output when contact was made. In order to distinguish between the signals in the plot, each was scaled and offset. Integer values correspond to the no-contact condition, real values indicate contact. Figure 60 shows that during the first roll attempt, knuckle/shelf contact (blue line) at the coupling between Car #II and Car #III did not occur.

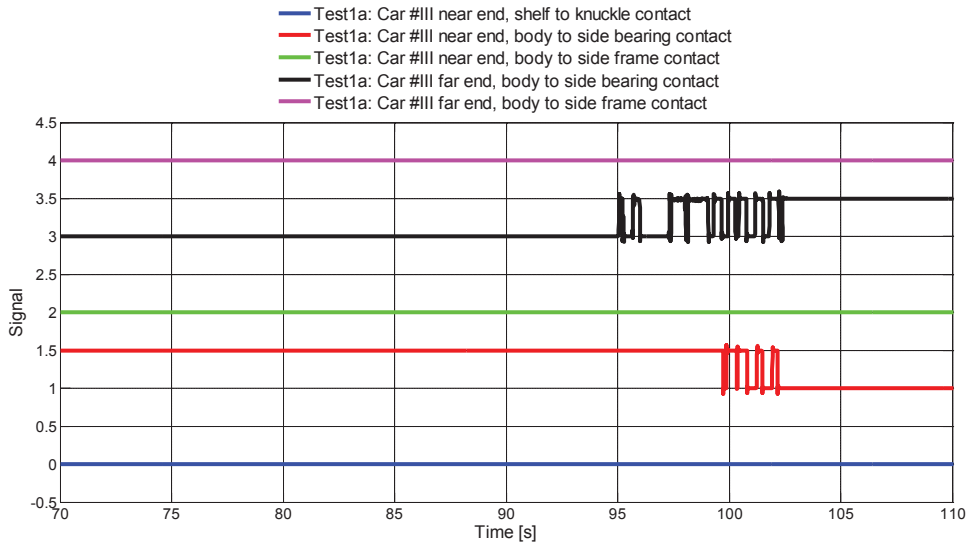


Figure 60: Test #1 first roll attempt, events on Car #III.

Figure 61 shows the same events during the second roll attempt. While Car #III was rolling over and falling off its trucks onto the ground, there was never any knuckle/shelf contact at the Car #II to Car #III coupling.

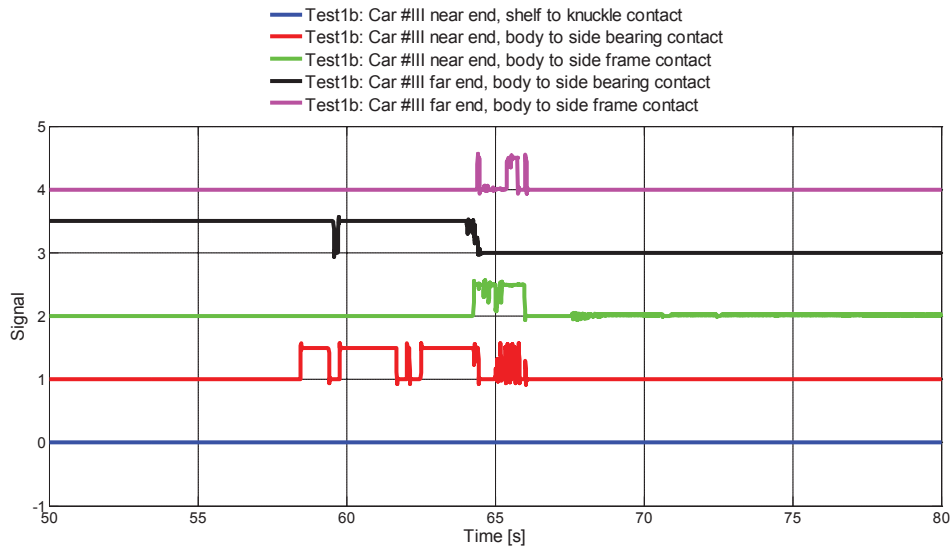


Figure 61: Test #1 second roll attempt, events on Car #III.

During an examination after Test #1, evidence of binding was seen in the form of gouges and rubs on the walls of the coupler head and on the edges of the knuckles (see Figure 62). For Test #1, the forces developed between knuckles and coupler walls were large enough to allow the far-end coupler of each car to lift the adjacent car without the shelves and knuckles bearing the vertical load.



Figure 62: Gouge on wall of far end coupler of Car #I after Test #1.

Therefore, knuckle to shelf contact did not occur as part of the rollover process with Type E double-shelf couplers.

The second expectation was that the near end of Car #I would be lifted vertically and translated laterally by the initiating car. This can be confirmed by examining the displacement data from the string potentiometers at the far end of Car #II and the near end of Car #III. Figure 63 shows displacement data for both ends of Car #II during the first roll attempt. Vertical (green line) and lateral (black line) displacement data for the far end of Car #II indicate that this end of the car was lifted vertically by 5.3 inches, and moved laterally by 7.8 inches. Figure 64 shows that this range of motion was not fully transferred to Car #III. The near end of Car #III was vertically displaced by only 0.7 inches, and laterally displaced by only 1.04 inches.

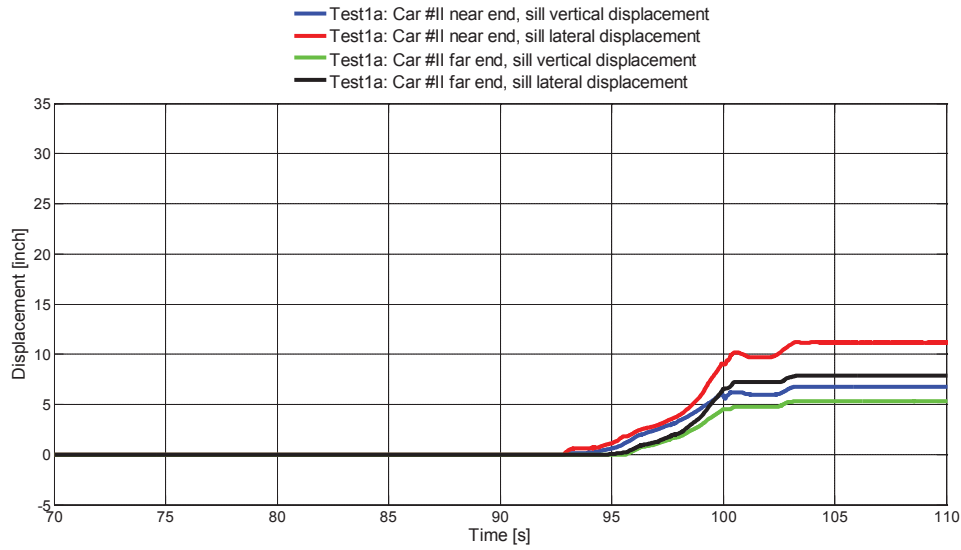


Figure 63: Test #1 first roll attempt, displacements for Car #II.

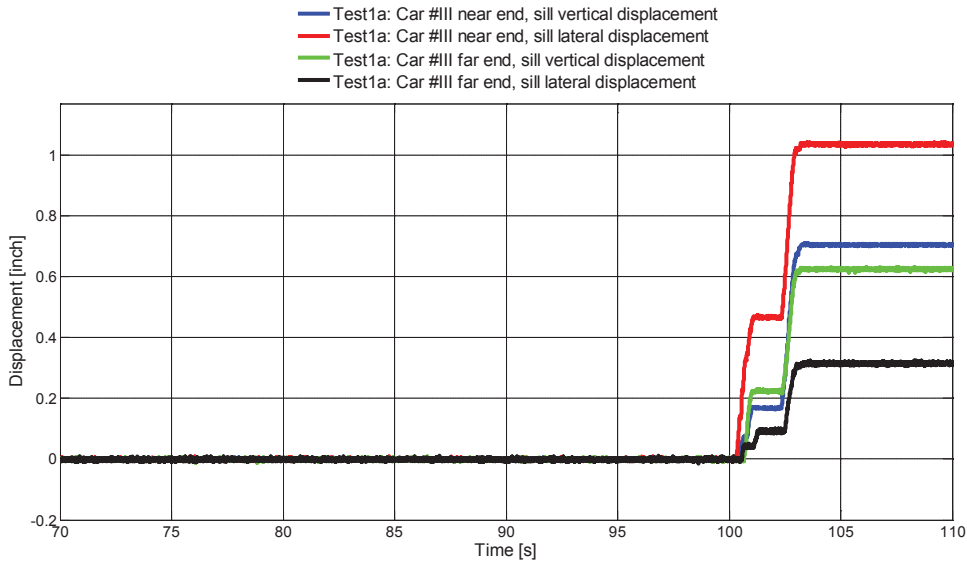


Figure 64: Test #1 first roll attempt, displacements for Car #III.

During the second roll attempt, more displacement at the far end of Car #II and near end of Car #III was observed. These values are plotted in Figure 65 and Figure 66.

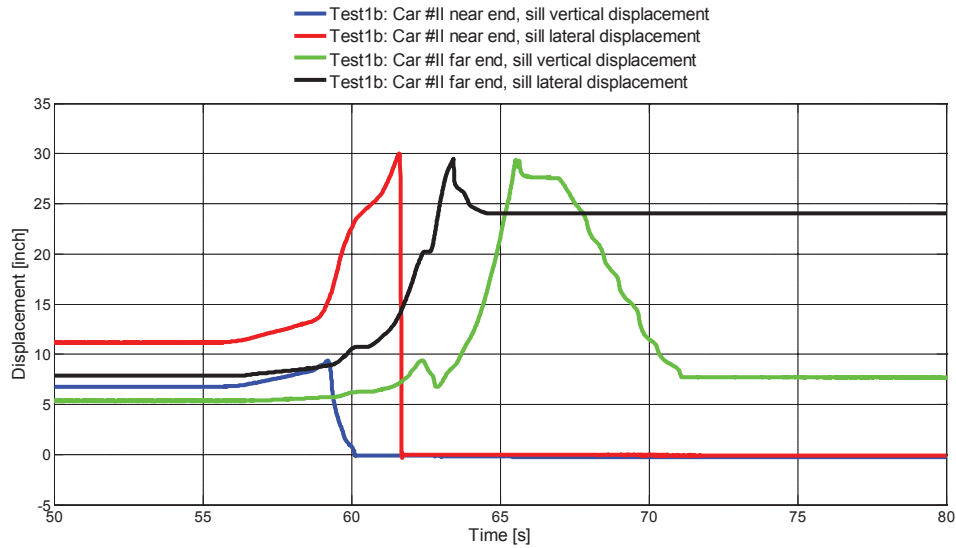


Figure 65: Test #1 second roll attempt, displacements for Car #II.

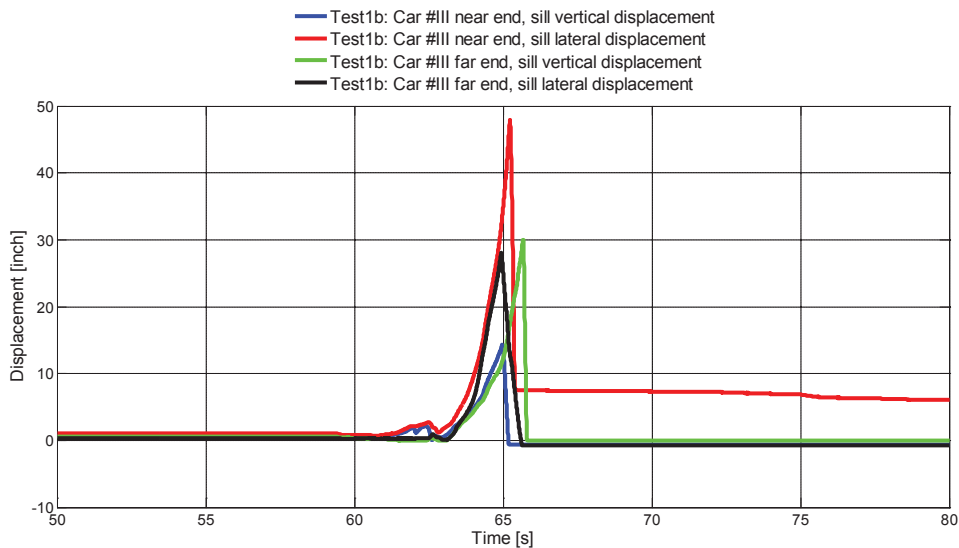


Figure 66: Test #1 second roll attempt, displacement for Car #III.

Figure 65 shows that the far end of Car #II reached a lateral displacement (black line) of 30 inches (the maximum extension for this device), at which point the fuse for this string potentiometer yielded. This end of the car also reached a vertical displacement (green line) of 30 inches before its fuse yielded, but the maximum measured vertical displacement occurred after the maximum measured lateral displacement. This indicates that lateral motion of the car body was occurring more rapidly than vertical motion at this point of the test.

Figure 66 shows that Car #III's vertical displacement at the near end first reached a measured value of 14.3 inches (blue line) before its fuse yielded, the fuse malfunctioned and yielded before the displacement transducer reached its maximum limit. The maximum measured lateral displacement of 47.9 inches was reached a fraction of a second later however the lateral motion was leading the vertical motion at this point in the test. Therefore, the second expectation from the list above did occur.

The third expectation was that a vertical force equivalent to half of the car body weight would be applied to the car as part of the roll process. Figure 67 shows that a peak vertical force of 8,082 lb was applied to Car #III's near-end sill during the first roll attempt.

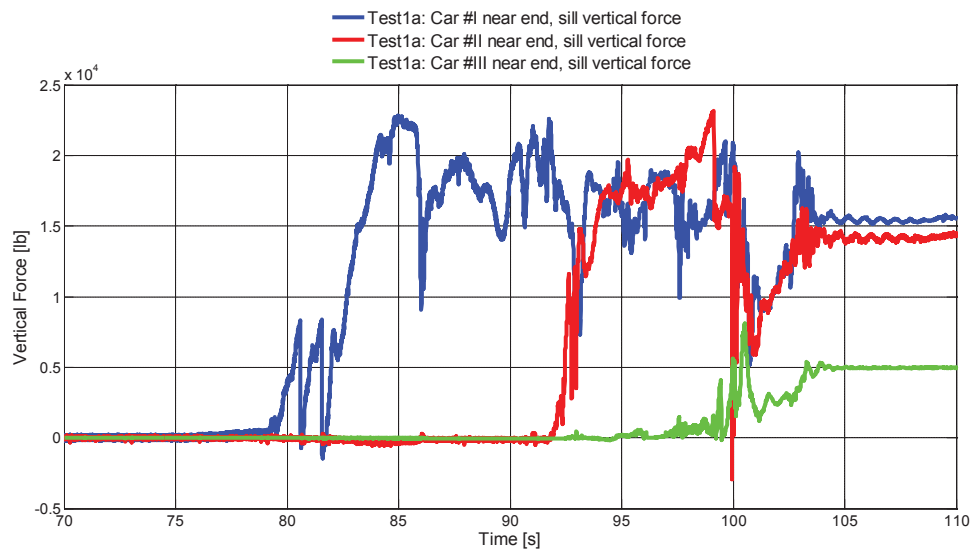


Figure 67: Test #1 first roll attempt, vertical forces on near-end car sills.

Figure 68 shows that the maximum vertical force applied to the near-end sill on Car #III peaked at 29,450 lb. The certificate of construction (supplied by TC-TDG) for this car states its light weight as 71,200 lb. The weight of its 100 ton capacity trucks are taken as 10,000 lb each. Therefore, half of the car body weight is 25,600 lb.

The maximum vertical force measured is therefore 15% greater than half of the car body weight. A review of the video channel (channel 9 from the second roll attempt) that was focused on the near-end Car #III truck shows that the car did not initially lift free of the truck. The car body and the truck were seen to displace laterally toward the rolled side, then the car body began to lift as it rolled and the truck assembly tipped up slightly. The extra vertical load measured at the sill is likely the result of part of the truck weight being carried by the car.

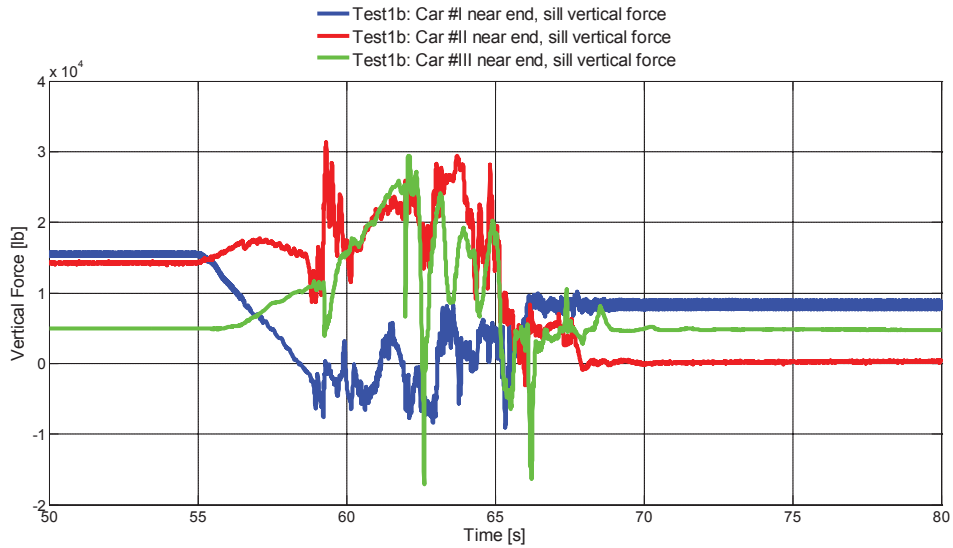


Figure 68: Test #1 second roll attempt, vertical forces on near-end car sills.

The fourth expectation concerned the magnitude of the torque applied to the car body. The torques measured during the test are shown in Figure 69 and Figure 70. Figure 69 shows that the torque applied to Car #III during the first roll attempt was very low, less than 1,000 lb-ft.

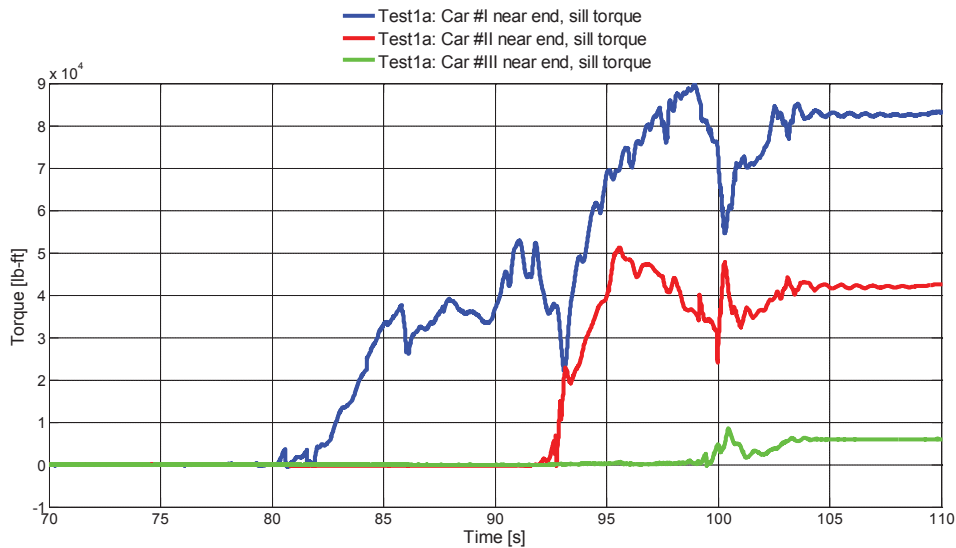


Figure 69: Test #1 first roll attempt, torques on near-end car sills.

During the second roll attempt, the maximum measured torque was 95,730 lb-ft (Figure 70). Torque is expected to be maximum when the centre plates just lose contact with the centre bowls. At this point, the car is assumed to be supported vertically through contact at the side bearings, is held in this position by the torque applied via the coupler shank, and the centre of gravity of the car has only shifted laterally off-centre by a small distance (on the order of 2.4 in. as calculated in the energy analysis described in Section 3.2.2. The distance between the longitudinal centre lines of the truck's centre bowl and its side bearing is 25 inch. The moment required to hold the car in this position is therefore the product of 51,200 lb² and (25 – 2.4 in)/12 in/ft or 96,427 lb-ft; this is very close to the measured value of 95,730 lb-ft.

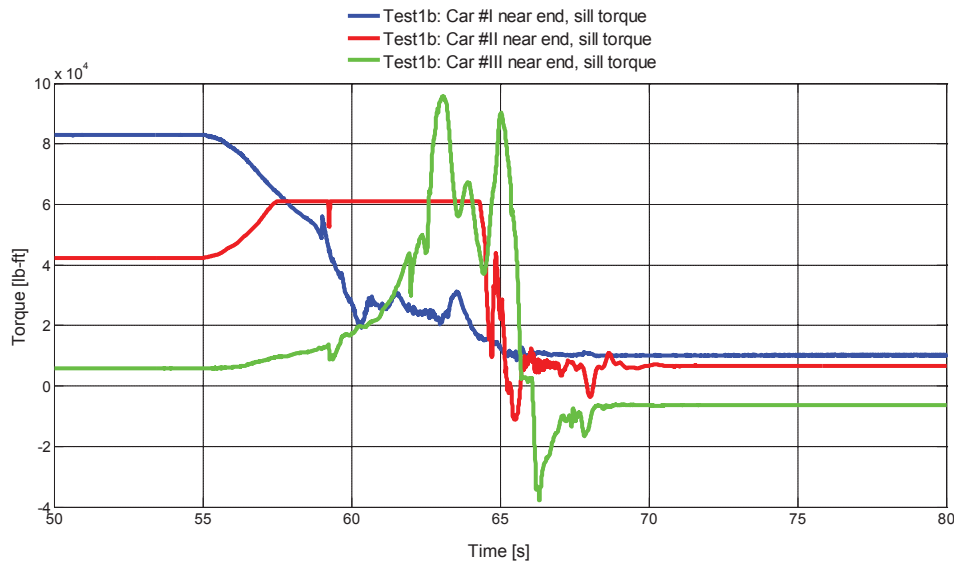


Figure 70: Test #1 second roll attempt, torques on near-end car sills.

The fifth expectation was not something that was directly measured, but elements of it can be seen in the data. It can also be observed in the video channel for the near end of Car #III (channel 9, note there was no video channel for the far end of Car #III). The red oval in Figure 71 shows side bearing contact established at the near end of the car from 62.5 – 64.4 seconds while the car body rolls towards the rolled side. (Car #III did not have constant-contact side bearings, thus there was no initial side bearing contact.) After this time, side bearing contact is lost but the car body continues to roll. Figure 66 shows that at 64.4 seconds, the near end sill of Car #III had displaced vertically by 8 inch, laterally by 17.3 inch and Figure 71 shows that it rolled by 11.8 degrees beyond its starting position. Figure 71 also indicates the car body rolled away from the rolled side (a negative roll angle) from approximately 61 to 63 seconds. The video channel shows the car body is deflecting up and down a few times on the truck suspension prior to rolling towards the rolled side. However, the video does not clearly establish that the car is actually rolling away from the rolled side.

² Tare weight of the tank car assembly (71,200 lb) less the weight of two truck assemblies (10,000 lb each).

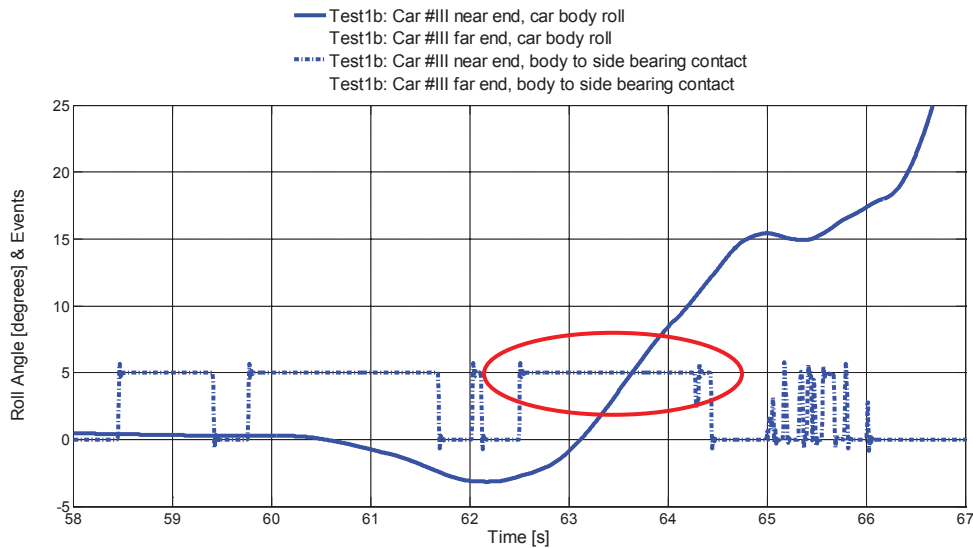


Figure 71: Test #1 second roll attempt, Car #III roll and side bearing contact at near end.

In the video, the centre plate can be clearly seen as it lifts out of the centre bowl and reveals the centre pin. The pin never appears to be caught between the car body and the truck, and therefore the body does not pull the truck laterally by the pin. (Note that the truck did roll (about the wheel-rail interface on the rolled side) somewhat during the rollover process, but it dropped back down on to the rails.) The edge of the opening on the centre plate contacts the pin and tilts it over towards the rolled side, but does not bear on it with enough force to deform the pin. The pin remained in the truck after the rollover had stopped, as shown in Figure 72, leaning to the rolled side but otherwise undamaged.

Therefore, the centre plate at the near end of Car #III was released from its truck's centre pin through a combination of car body roll and vertical displacement.

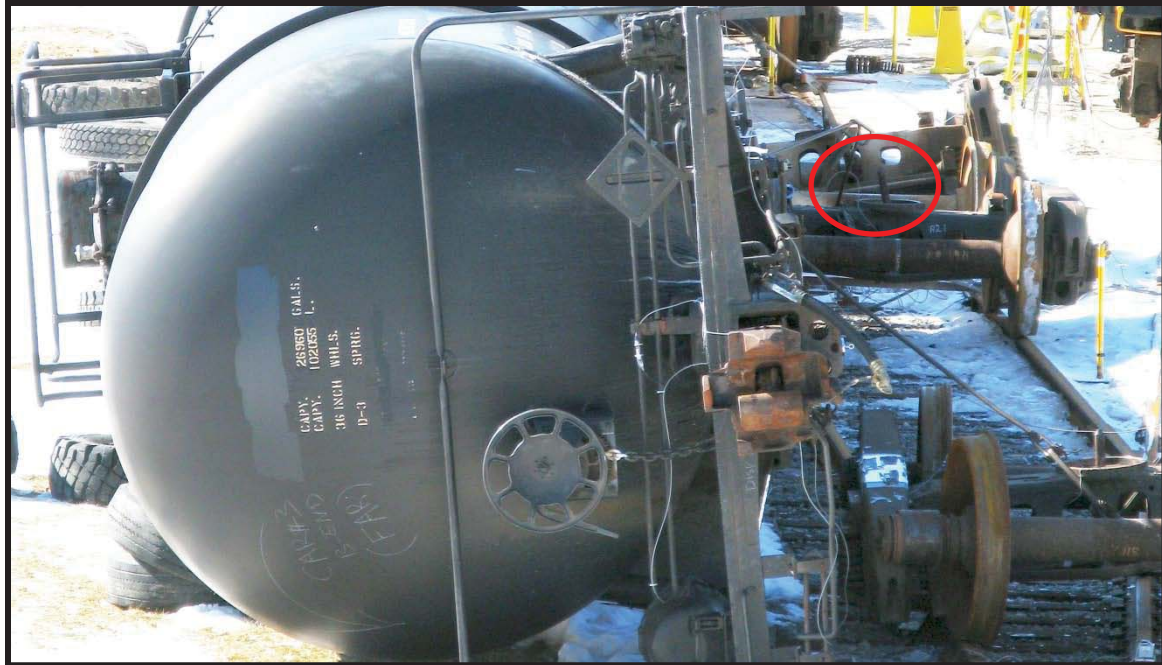


Figure 72: Test #1 second roll attempt, centre pin in Car #111 near truck.

The sixth expectation (contact between the car body bolster and the side frame, resulting in body and truck roll) cannot be clearly seen in the videos, but it can be examined in the data. Figure 73 shows Car #111 body and truck bolster roll angles. It is clear that the trucks do undergo some roll at the same time as the body rolls, but the trucks and car body are not rolling together as a rigid body. Figure 61 showed the events on this car during the second roll attempt. In the figure, it can be seen that contact between the near car body bolster and truck side frame (green line) occurred at 64.2 seconds. At that same time, Figure 73 shows that the near truck bolster began to roll. The security camera video (channel 9) also shows this truck rolling about the wheel/rail contacts on the rolled side. As seen in Figure 73, the near truck only tips up 3 degrees before falling back on the rails. Figure 73 shows that the near truck begins to fall at 66 seconds, which also corresponds to the time (Figure 61) when contact was lost between the car body and truck side frame at the near end.

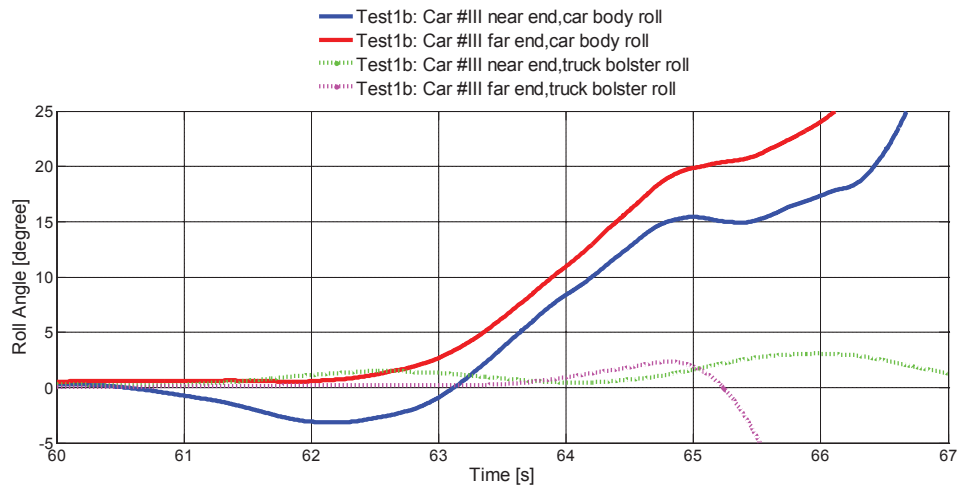


Figure 73: Test #1 second roll attempt, Car #III truck and body roll.

Figure 73 also shows that the far truck begins to roll at about 63.5 seconds, and reaches its peak roll angle of 2.3 degrees at 64.8 seconds. After this, the data signal from the roll sensor saturates and no further meaningful information is available. These times do not correspond to the contact event between the car body bolster and the truck side frame at the far end of the car (Figure 61). Initial contact with the side frame occurs at 64.4 seconds, and it is lost at 64.5 seconds. It is re-established at 65.4 seconds and is lost again at 65.8 seconds. Since the truck begins to roll before body-to-side-frame contact occurs, it may be due to the truck centre pin being caught between the truck bolster and the car body centre plate, allowing the body to pull the truck along as the body rolls. This type of behaviour was seen in the video for the far end of Car #II (video channel 5). In the video, the truck is rolled through a small angle with the car body until the top of the pin breaks free from the centre plate. At this point, the truck drops back down to the rails. Note that there is no video camera at the far end of Car #III to capture this behaviour, but it seems reasonable that the far end of Car #III would behave similarly to the far end of Car #II.

Thus, although contact did occur between Car #III's body and the top chord of the side frame of this car's near end truck, it did not destabilise the truck and cause the car body and truck to roll about the wheel/rail contact points until the car body fell to the ground.

The seventh expectation was that Car #III's near-end truck would drop back down on to the rails. This is shown in the videos (security camera channel 9 video for the near-end truck, and for the far-end truck in "Rollover1-2 South Sync w Clock.mpg"), and in photo evidence (for example, Figure 72). The channel 9 video shows the truck briefly rolling with the body as the body contacts the side frame, followed by the truck falling down on the track. The truck then rolls along the rails toward the camera. The data (Figure 73) for the near-end truck also supports this expectation

The video for the near-end truck of Car #II also shows this behaviour. During the second roll attempt, Car #II's near-end truck initially rolls by a small amount because the centre pin is caught between the body and the truck bolster. The body breaks free of the pin,

and the truck drops back down to the rails. When the body bolster makes contact with the side frame the truck rolls considerably more but falls back to the rail once the car body rolls off the truck.

The videos (first and second roll attempts) for the near-end truck of Car #I also show this behaviour. During the initial roll attempt, the car body and the truck bolster trap the centre pin between them, which causes the truck to roll about the wheel-rail interface on the rolled side. As the roll progresses, the body bolster breaks free of the centre pin and the truck drops back to the rails. In the second roll attempt, the body bolster bears against the truck's side frame and the truck rolls with the body until the body rolls falls off the side frame. At this point, the truck drops back to the rails.

The eighth expectation was that the car body would roll about the side bearing on the far end truck, possibly jamming the centre pin between the truck and car body. The result would be that the truck would roll with the body. The far end car body roll angle and side bearing contact event for Car #III have been plotted for the second roll attempt in Figure 74. Although Car #III was not equipped with constant-contact side bearings, the side bearing gap at the far-end truck on the rolled side was closed up at the start of the second roll attempt. This side bearing remained in contact until 64.0 seconds, at which point the signal became noisy. Contact was lost permanently at 64.4 seconds. The car body began to roll at 62 seconds, and rolled 15 degrees from its starting position before side bearing contact was lost. The truck was also rolling at this time although not as quickly as the car body. It reached a maximum roll angle of 2.3° at 64.8 seconds. The data for the truck bolster roll angle then quickly and smoothly drops to -90°, indicating a problem with the roll sensor. Therefore, there is very limited data available to understand the behaviour of the truck.

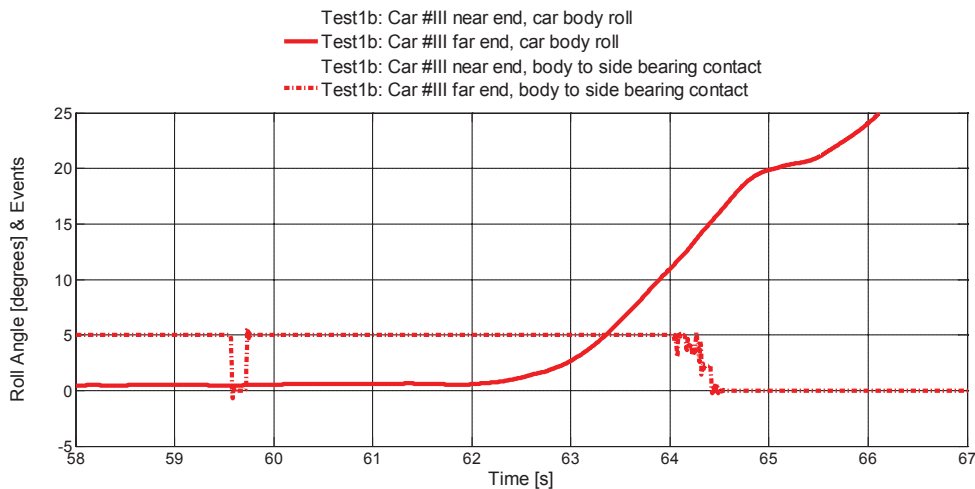


Figure 74: Test #1 second roll attempt, Car #III roll and side bearing contact at far end.

Figure 66 shows that the far end of Car #III began to displace vertically and laterally beginning at 63 seconds. At 64.4 seconds, the car had displaced vertically by only 6.7 inches and laterally by 14.78 inches. This suggests that the centre plate was caught against the pin, which protrudes from the centre bowl by roughly 8 inches.

However, there is no video data to support this suggestion. The centre pin at the far end of Car #III cannot be seen in the “Rollover1-2 South Sync w Clock.mpg” video, and there is no security camera video to show the far-end truck rolling with the car body. The MPEG video does show the truck rolling at the same time as the car body, then falling back to the rail as the car body continues to roll. Figure 73 shows the changing truck bolster roll angle does not keep up with the changing car body roll angle, so it does not seem likely that the truck and car were rigidly connected by the centre pin at any time. After the rollover was completed, the pin remained in an upright position in the far truck. The pin can be seen in Figure 72, near the bottom right of the photo. Note that the far-end truck on Car #I tipped up with the car body, and subsequently fell back down on to the rails. The far-end truck on Car #II only tipped by a small amount as its car body rolled. It violently displaced away from the rolled side as the centre plate broke free of the centre pin, and derailed.

Therefore, the centre pin at the far end of Car #III does not seem to bind between the centre bowl and centre plate and does not cause the car body and truck to roll together as an assembly.

Summary of Observations

- Shelf to knuckle contact did not occur between Car #II (the driving car) and Car #III (the driven car), but a post-test examination of the couplers shows that the knuckles and coupler heads had jammed together. The near end of the driven car was lifted vertically and translated laterally by the driving car. The lateral motion occurs sooner and more rapidly than the vertical motion, meaning the initiating car tends to pull the subsequent car sideways off its near truck.
- The vertical load applied to the sill of the driven car was about 15% greater than half of the car body weight.
- The magnitude of the torque applied to the driven car was essentially identical to the product of the car body weight multiplied by the distance between the rolled car body’s centre of gravity and the centre of the truck side bearing.
- The data shows that the near end of the driven car did roll about its side bearing, reaching 11.8 degrees beyond its starting position. During this period, the near end of the driven car was vertically displaced by 8 inch and laterally by 17.3 inch. Video evidence shows the centre plate lifting free of the pin, but also bumping it and tipping it.
- Contact did occur between the driven car’s body and the near-end truck’s side frame, but the truck and car body did not roll together as a rigid body for any period as a result.
- Both trucks did drop back down to the rails. This was observed in the data for the near end and in the videos for both ends of the driven car. All trucks in the test

did drop back down to the track, although the far-end truck on the driving car finished in a derailed position.

- The far end of the driven car did roll on the side bearings, but there is no evidence to suggest that the pin was caught between the car's centre plate and the truck centre bowl. The truck and car body did not roll together as an assembly.

5.3.5 Test #2: Dynamic Testing With Modified Rotary Coupler – 4 Cars

Test Setup

On March 22, 2011, NRC-CSTT performed Test #2; a full scale dynamic testing on four (4) empty tank cars equipped with standard Type E double-shelf couplers throughout the whole test string except at the near-end of Car #III, where a modified rotary coupler (double-shelf) was installed (Figure 75). The objective of this test was to investigate the modified rotary coupler as a potential solution to reduce the rollover domino effect. Various instrumentation was used to monitor the cars' behaviour. Refer to Appendix A for a full list of instrumentation. Refer to Appendix B for more information about the instrumentation and calibration procedure used to measure vertical forces and torques applied to the tank cars' sills. Refer to Appendix C for the modified rotary coupler manufacturing and installation procedure.

The instrumentation described in Appendix A was calibrated, installed and monitored using a high-speed data acquisition system. The data was sampled at a rate of 250 Hz, and low pass filtered at 50 Hz. Prior to the beginning of the test, all cars were compressed together (no slack between couplers) and hand brakes for all tank cars were released.

Note: in Figure 75, setup changes between Test #1 and Test #2 are shown in red.

| | | Initiating Car | | 1 st Position | | 2 nd Position | | 3 rd Position | | 4 th Position | | | |
|----------------------|------|----------------|---|--------------------------|--------|--------------------------|---|--------------------------|--------|--------------------------|---|--------|----------|
| Test setup overview | | | | | | | | | | | | | |
| | N | | F | | N | | F | | N | | F | | |
| Test #2 setup | | | | | | | | | | | | | |
| Orientation | B | CSTT-1 | | A | A | Car #I | | B | A | Car #III | | B | |
| Sill type | E | | | E | E | | | E | F | | | E | |
| Coupler type | E60C | | | SE60CC | SE60DC | | | SE60CHTE | Rotary | | | SE60CC | Not used |

Figure 75: Test #2, dynamic testing with one modified rotary coupler and 4 tank cars - test setup schematic.

Car #III was chosen for the installation of the modified rotary coupler. This was because the car striker/centre sill design (Type F) was close to the rotary coupler striker/sill design and both sills are equipped with strikers that have front springs. Refer to Appendix C for more information.

NOTE: Car #II and Car #III swapped positions during Test #2, in other words, Car #III during Test #2 was located at the second position, and Car #II was located at the third position.

Based on the observations in Test #1, the force was applied to the initiating car by pulling laterally at the middle of the car from the top. This method distributed the reaction of the applied lateral force to both trucks on the initiating car, preventing the derailment

and damage of the trucks that occurred in Test #1. As the initiating car has lighter weight, forces were applied with a slight angle pointing down from the horizontal line to prevent the car from sliding sideways on top of the tracks.



Figure 76: Test #2, dynamic testing with one modified rotary coupler and 4 tank cars - test setup.

NRC-CSTT was able to initiate the rollover, and the first two tank cars were rolled over onto the ground. The rollover stopped at the modified rotary coupler and the remaining two cars stayed on tracks (Figure 77).



Figure 77: Test #2, cars after test, initiating end – rotary coupler stopped the rollover propagation.



Figure 78: Test #2, cars after test, tail end – rotary coupler stopped the rollover propagation.



Figure 79: Test #2, cars after test, north side – modified rotary coupler junction.



Figure 80: Test #2, cars after test, south side – modified rotary coupler junction.

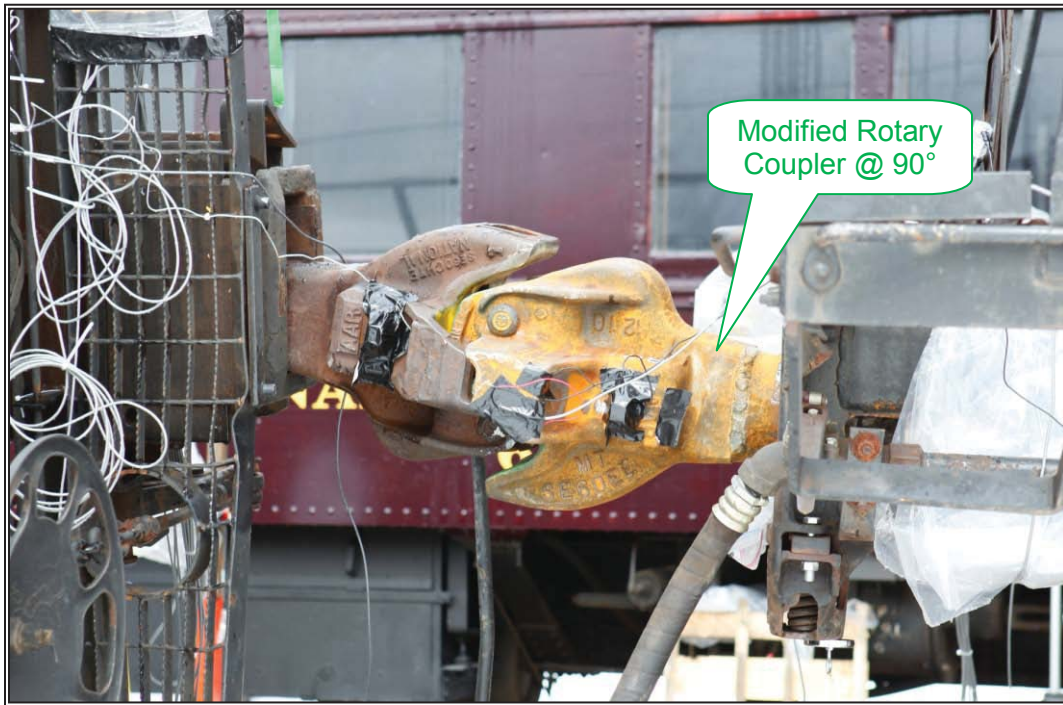


Figure 81: Test #2, rotary coupler after test.



Figure 82: Test #2, rotary coupler orientation after test.

Observations

Prior to undertaking this test, it was not obvious how a rotary coupler would be effective in halting a domino rollover. By design, a rotary coupler allows a railcar (typically an open top gondola) to rotate (roll) about the longitudinal axis of the coupler's shank. When this occurs, the track section on which the gondola is positioned also rotates about the same axis (the car is clamped into a support which forms part of the track section), so the car does not undergo relative motion with respect to the track section.

In a zero-speed domino rollover derailment, NRC-CSTT's assumptions about the manner in which a car would derail included the car body rolling on the truck bolster, on its centre plate, on the side bearing, onto the truck side frame, and finally the car body and truck rolling as a rigid assembly about the wheel/rail contact points. In the order listed, each one of these centres of roll is an increasing distance away from the longitudinal axis of the coupler. If the centre of roll was never along the coupler's axis, it seemed unlikely that the rotary coupler could halt the domino effect. It could still lift the adjacent car, but would not be able to transfer any torque.

In Test #2, the rotary coupler was installed in the near end of the second car in the consist (Car #III). Therefore, the rotary coupler was facing the domino "wave" as it propagated through the consist and its response to the forces and moments applied by Car #I during this test can be examined and compared to the response of the standard double-shelf coupler from Test #1.

As in Test #1, shelf/knuckle contact between Car #I and Car #III was monitored as an event. Since the purpose of the shelves is to deliberately prevent vertical coupler disengagement as a result of a derailment, it was still an expected event despite its non-occurrence during Test #1.

The events on Car #III are plotted in Figure 83. Events were measured with sensors that produced a zero-value output when there was no contact between the corresponding car components, and a 5 volt output when contact was made. In order to distinguish between the signals in the plot, each was scaled and offset. Integer values correspond to the no-contact condition, real values indicate contact. . The black line in the plot shows that there was side bearing contact at Car #III's far-end truck. Although Car #III was not equipped with constant-contact side bearings, the side bearing gap at the far-end truck on the rolled side was closed up at the start of the test.

Shelf to knuckle contact did occur between the knuckle of Car #I and the top shelf of Car #III. Contact was sustained for 7.5 seconds beginning at 105.4 seconds. Contact can also clearly be seen to occur at 31 seconds into the video ("Rotary Coupler.mpg"). This is in contrast to Test #1, where shelf to knuckle contact never occurred because the knuckles bound together.

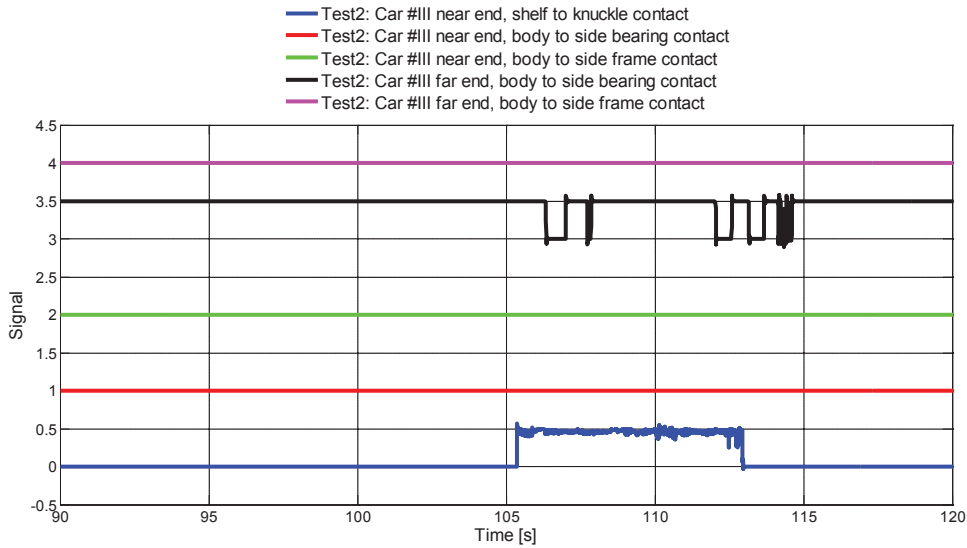


Figure 83: Test #2, events on Car #III.

Figure 84 shows the displacements on Car #I during Test #2. During this test, the lateral movement of the initiating car was more rapid than the vertical movement, at both ends of the car.

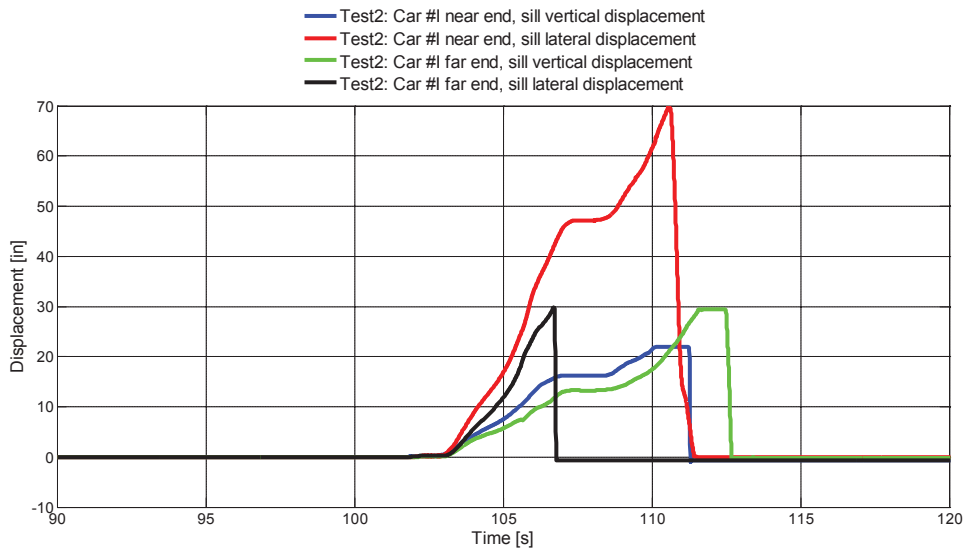


Figure 84: Test #2, displacements on Car #I.

Figure 85 shows the displacements on Car #III. The near end undergoes considerable displacement and the far end does not. This car did not undergo significant roll during the test (roughly 3°), so the effect of car pitch can be seen here as a decrease in the far

end vertical displacement. The far-end centre plate remained in its centre bowl, allowing the car body to yaw about the far end truck. As a result, the far end of the car displaced laterally in the direction opposite to the near end, causing a negative lateral displacement. The near end of Car #III displaced a total of 13.7 inch vertically and 47.7 inch laterally.

The near end of Car #III began to displace at 106.3 seconds; by then the displacements on the far end of Car #I were 10.2 inch vertically and 26.5 inch laterally and the car body had rolled 24°. Therefore, the initiating car must undergo considerable displacement to begin to move the subsequent car if they are joined by a rotary double-shelf coupler that is installed in the subsequent car. In contrast, the far end of Car #III underwent 4.6 inch vertical displacement, 6.9 inch lateral displacement and 10.9° of roll before Car #III began to move during the first roll attempt of Test #1 (with conventional couplers).

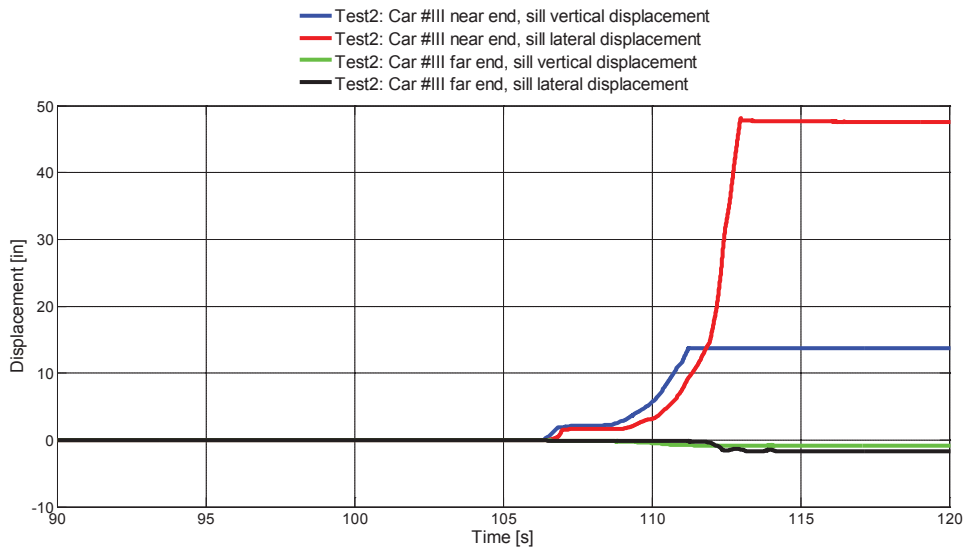


Figure 85: Test #2, displacements on Car #III.

The extra degree of freedom of the rotary coupler delays the transmission of motion to the subsequent car because the coupler knuckles and walls do not bind together. Instead, the top of the knuckle on the initiating car rises until it contacts the upper shelf on the subsequent car. To do this, the initiating car has to undergo greater vertical displacement through lift and car body roll.

The magnitude of the vertical forces applied to the couplers is shown in Figure 86. Note that the far end sill of Car #I was instrumented to measure vertical load; the results are plotted in red. The vertical force on the near end of Car #III is plotted in green. These two forces are almost mirror images of one another until approximately 112 seconds,

when the vertical force on the far end of Car #I begins to decrease to zero. Car #I has rolled by 50° at this point, which means the shear force applied to the sill is now acting diagonally across the sill. The instrumentation was applied to capture forces acting vertically with respect to axes that are fixed to and aligned with the sill; no transverse sill forces were measured and the instrumentation was not calibrated for this. Thus, as the sill rotates, the applied vertical force measured over time may not reflect a true vertical force. Nonetheless, the term vertical force is used to refer to the force measurement returned by the instrumented sill.

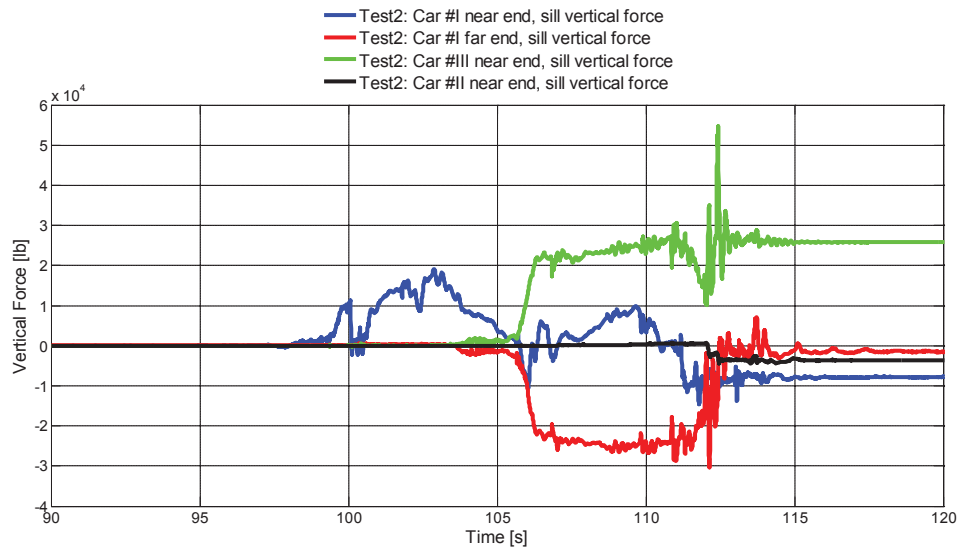


Figure 86: Test #2, vertical forces on car sills.

Figure 86 shows that the vertical forces on the sills of Car #I (far end) and Car #III (near end) fluctuate about 25,000 - 26,000 lb, and the steady state load on the sill of Car #III is 25,760 lb. This is much closer to the half-weight of the body of Car #III (25,600 lb) than was measured during the first test. Since both sills (independently instrumented) produced essentially the same result for the same applied load, the expectation that the coupler of the “driving” car must support the half-weight of the subsequent “driven” car body was confirmed during this test. The presence of a rotary double-shelf coupler in the driven car did not alter the transmission of vertical force from one car to the other.

Since the rotary coupler is designed to roll within the draft sill, it should not be able to sustain a torque. Therefore, the sill on Car #III should not have sustained a torque during the second test unless the coupler was somehow restrained from rolling. By extension, the sill at the far end of Car #I also should not have sustained a torque, because the torque would have to be reacted against Car #III’s near sill through the rotary coupler.

Figure 87 shows the torques applied to the sills of all three cars. In addition to the instrumentation on the sill at the near end of each car, the sill at the far end of Car #I was instrumented to measure torque during this test. Also plotted in this figure are the car body roll angles at the far end of Car #I and the near end of Car #III (roll is plotted in degrees, $\times 10^{-3}$ of the torque scale). Torque is acting at the near end of Car #I and a short time later begins to act at the far end of the car. At the same time, torque in the opposite direction and of much lesser magnitude begins to act on the near sill of Car #III. At approximately 112 seconds, maximum torque of 83,020 lb-ft acts on the far sill of Car #I. At this point, the direction of torque acting on Car #III reverses and begins to rise; the car body also begins to roll towards the rolled side. At 114.3 seconds peak torque of 11,130 lb-ft acts on the near sill of Car #III; Car #I has already contacted the ground. The torques on the far sill of Car #I and near sill of Car #III then decrease (with minor oscillation) to steady state values of roughly 20,000 lb-ft and 7,500 lb-ft respectively.

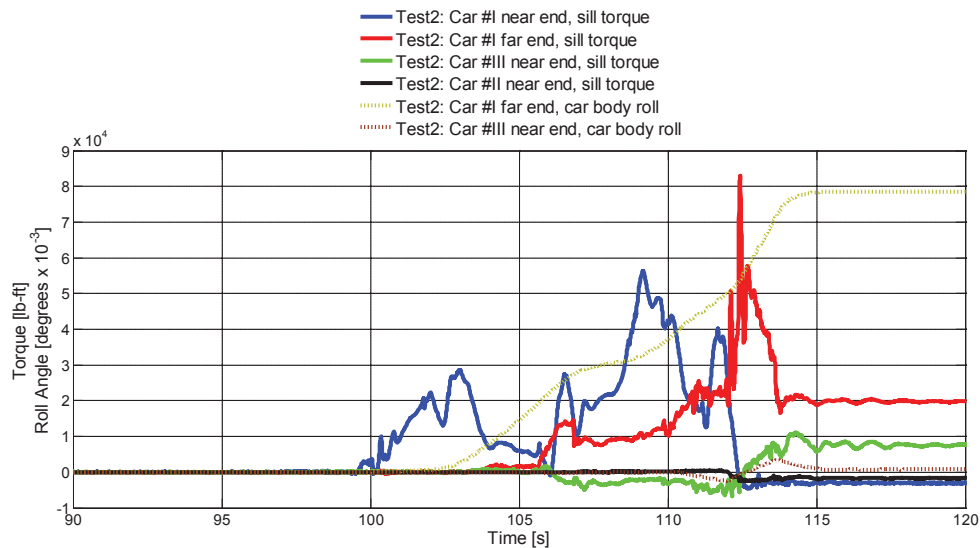


Figure 87: Test #2, torques on car sills.

The torque that acts on the near sill of Car #I is that required to roll Car #I. Figure 87 shows that this torque did not reach its maximum value until Car #I had rolled 33°. By this time, torque was already acting on the far sill of Car #I and on the near sill of Car #III. The maximum torque value on the near sill of Car #I was expected to be the product of 50,600 lb (70,600 lb tare weight of Car #I – 20,000 lb truck weight) and (25 inch – 2.4 inch) / (12 inch/ft) or 95,297 lb-ft. The measured maximum was only 56,250 lb-ft. Therefore, the maximum torque when maximum torque occurred was lesser than expected, and the car body roll angle when maximum torque occurred was greater than expected.

The torque that acts on the far sill of Car #I is that required to roll Car #III, and should be equal in value to the torque that acts on the near sill of Car #III. The maximum torque that acted on the far sill of Car #I was 83,020 lb-ft. This magnitude is unusual for several

reasons. First, it does not coincide with a peak torque measured on the near sill of Car #III (see Figure 87). Second, the torque magnitude from the far end of Car #I is rather large given the expected lack of a reaction torque from the near sill of Car #III due to the rotary connection. Third, the large torque that was measured is roughly 13% less than the maximum torque that was measured on the near sill of Car #III (95,730 lb-ft) during Test #1(second roll attempt); this seems odd since Car #III in Test #2 was the same car as Car #III in Test #1.

The instrumentation on the sills was designed to measure the torsion of the sill section. Torsion would occur when the shank of a Type E coupler was rolled within the sill. Roll of the shank would be restrained by the coupler key which passes through the shank and the sill. The key would bear against the top of the keyway slot on one side of the sill and the bottom of the slot on the other side of the sill. These two forces cause a couple to act on the sill, causing the sill to twist between the keyway slot and the point of attachment of the sill to the tank. The torque instrumentation was installed in this area.

A rotary coupler does not have a key passing through its shank and the sill to prevent rotation. It is therefore free to rotate within its yoke (which is held within the sill, refer to Figure 101 for an illustration of a rotary coupler assembly). The only restraints to rotation are friction in the rotary mechanism and friction between the shank and the sill if there is contact between these two elements.

For these reasons, the low torque magnitude on the near sill of Car #III is not surprising. The rotary coupler shank can be seen in the videos to contact the top of the sill. Torque may be applied to the sill through friction as the shank bears against the top of the sill while the coupler rotates; this could account for the relatively low torque values that were measured given that none were expected. (Note that coupler shank to top of sill contact will occur on all “driven” cars.) However, the instrumentation for torque measurement was specifically calibrated to measure torque as result of sill torsion arising from a couple acting on the edges of the coupler keyway. Torques acting on the sill as a result of frictional interaction between the shank surface and the inner walls of the sill might not be accurately measured and should not be relied upon for analysis.

Figure 83 shows that there was never any contact with the side bearing of the near end truck for Car #III. A review of the videos (both of the coupler and the security camera videos) shows that the car neither lifted nor rolled free of its near truck’s centre pin. The security camera video from channel 6 shows the car body and truck bolster first rising together (50 seconds into the video), then the centre plate partially lifting out of the centre bowl. At 51 seconds, the car body and truck displaced laterally by a small amount toward the rolled side as if the trucks wheels had slid across the rail surface until the wheels on the rolled side were in flange contact with the rail. The car body continues to rise until, at 53 seconds, the bottom of the centre plate is positioned slightly above the rim of the centre bowl. The centre pin is barely visible between the two bodies. At this point, the truck and car body move as an assembly because they are bound together

through the centre pin; the centre of roll for this end of the car is about the wheel/rail contact points of Car #III's near truck on the rolled side.

As the motion progresses, the car body appears to rise more quickly than the truck which suggests the pin is slipping out of one of the bodies. Nonetheless, the truck continues to roll about its wheel/rail contact points as the car body rises until, at 57 seconds, the centre pin breaks free of the centre bowl, the truck is released from the car body and falls back to the rail. The near end car body then displaces laterally as the car body yaws about the centre bowl of its far end truck.

The motion of the near end of Car #III is almost only lateral and vertical displacement. The body underwent very little roll, as seen in Figure 88. The maximum height of the sill was attained slightly before the truck reached its maximum roll angle of 12.9°.

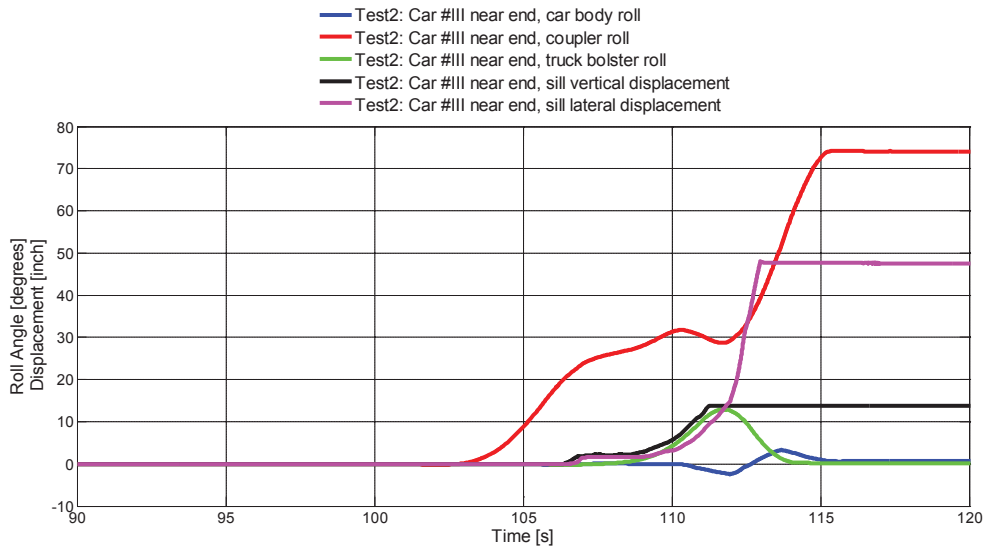


Figure 88: Test #2, motion at the near end of Car #III.

Since the car body did not roll sufficiently, there was never any contact with the side frame of the near end truck. Therefore, this truck was never destabilized and the car body did not roll about the top chord of the side frame until it contacted the ground. The truck did tip up about its wheel/rail contact points on the rolled side. This was due to the lateral force exerted by the centre pin on the opening in the truck's centre bowl. This force was reacted at the wheel/rail contact points. The distance from the top of the rail to the bottom surface of the centre bowl is roughly 25½ inch; this is the moment arm for the lateral force applied through the centre pin. Since the car body's weight was no longer carried on the truck, the only stabilizing moment acting on the truck was its self-weight.

As mentioned above, the security camera video (channel 6) showed slippage occurring between the centre pin and either the car body or the truck or both. Eventually, the pin

broke free of the truck, allowing the truck to drop back to the rails. The force between the centre pin and the opening for the pin in the truck's centre bowl was sufficient to crush the edge of the opening (Figure 89).



Figure 89: Damage to Car #III centre bowl on near truck.

The far end of the car body was initially in contact with the side bearing on the rolled side of the far truck, and briefly lost contact (as seen in Figure 83) as the car body underwent its small roll motion. However, the body never lost contact with the far end truck.

Summary of Observations

- Shelf to knuckle contact did occur between the couplers of Car #I (the driving car) and Car #III (the driven car). This contact was not observed during Test #1.
- The near end of the driven car was lifted vertically by the driving car. More displacement and roll was required from the driving car during this test before the driven car began to move, compared to Test #1. In this test, the driving car's far-end coupler had to be lifted higher to take up the clearance between its knuckle and the top shelf on the driven car's near-end rotary coupler, since binding of the knuckles did not occur in Test #2. The driven car did not displace until after knuckle-to-shelf contact had occurred and the clearance between the top of the rotary shank and the draft sill on the near-end of the driven car was taken up.
- The vertical loads measured on the far sill of the driving car and the near sill of the driven car were in the range of 25,000 – 26,000 lb. This is very close to the

half-weight of the driven car's body. The rotary coupler did not alter the transmission of vertical force between the cars.

- The peak torque acting on the near sill of the driving car was 56,250 lb-ft (39,000 lb-ft less than expected), and it occurred when the body of the driving car was at a greater roll angle than expected (33°). The measured torque acting on the far sill of the driving car was lower than the maximum that was measured during the Test #1, but higher than expected given the expected lack of reaction torque from the driven car.
- The body of the driven car did not lift and roll clear of the centre pin at the near end truck; contact with the truck's side bearing never occurred. The car body's centre plate was stuck on the pin due to the lateral translation of the car. As the driven car continued to rise vertically and move laterally towards the rolled side, the truck rolled about the wheel/rail contacts on the rolled side. The centre pin did finally slip out of the truck bolster, freeing the near end of the car body from its truck and allowing the near end of the body to translate laterally with the far end of the driving car.
- Since the car body did not roll, it never contacted the top chord of the side frame of the near-end truck. Thus, the truck did not roll as a result of a net destabilizing moment. The truck did roll by almost 13° when its centre pin was caught in the truck bolster and car body centre plate as the near end car body displaced laterally.
- Once the centre pin broke free of the truck centre bowl, the near end truck dropped back down on the rails.
- The far end of the car body was initially in contact with the side bearing of the far end truck. Contact was briefly lost as the near end of the car body was moving, but the far end car body remained on its truck.

5.3.6 Test #3: Dynamic Testing With Modified Rotary Coupler – 5 Cars

Test Setup

On July 26, 2011, NRC-CSTT performed Test #3; a full-scale dynamic test on five (5) empty tank cars. All cars were equipped with standard Type E double-shelf couplers, except the far-end of Car #III on which the modified rotary coupler was installed (Figure 90). The rotary coupler was installed in this location instead of the Near-end of Car #III as in Test #2.

The objective of this test was to investigate the modified rotary coupler’s potential to prevent the rollover domino effect when it experiences a more rapid rollover action observed at the far end of the car.

No instrumentation was used during this test, however several video cameras were used to visually record the cars’ behaviour during testing. Prior to the beginning of the test, all cars were compressed together (no slack between couplers) and hand brakes for all tank cars were released.

Note: in Figure 75, setup changes between Test #2 and Test #3 are shown in red.

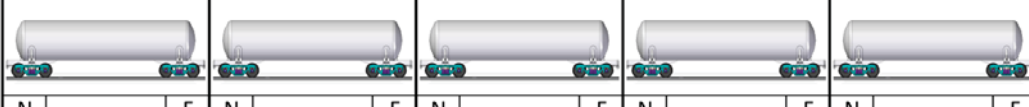
| Test setup overview | Initiating Car | | 1 st Position | | 2 nd Position | | 3 rd Position | | 4 th Position | | | | | | |
|---------------------|---|--------|--------------------------|--------|--------------------------|----------|--------------------------|----------|--------------------------|--------|---------|--------|-------|--------|-------|
| |  | N | F | N | F | N | F | N | F | N | F | | | | |
| Test #3 setup | | | | | | | | | | | | | | | |
| Orientation | B | A | A | B | B | A | A | B | B | A | | | | | |
| Sill type | E | E | E | F | F | F | E | F | E | E | | | | | |
| Coupler type | E60C | CSTT-1 | SE60CC | SE60DC | Car #I | SE60CHTE | SE60CC | Car #III | Rotary | SE60CC | Car #II | SE60CC | SE60C | CSTT-3 | BE60A |

Figure 90: Test #3, dynamic testing with one modified rotary coupler and 5 tank cars - test setup schematic.

A lateral force was applied to the initiating car by pulling laterally at the middle of the car from the top. As the initiating car is lighter weight, forces were applied with a slight angle pointing down from the horizontal line as shown in Figure 92 to prevent the car from sliding sideways on top of the tracks. This method distributed the reaction of lateral forces to both trucks on the initiating car.



Figure 91: Test #3, dynamic testing with one modified rotary coupler and 5 tank cars - test setup.



Figure 92: Test #3, lateral force applied at the middle of the initiating car from the top.

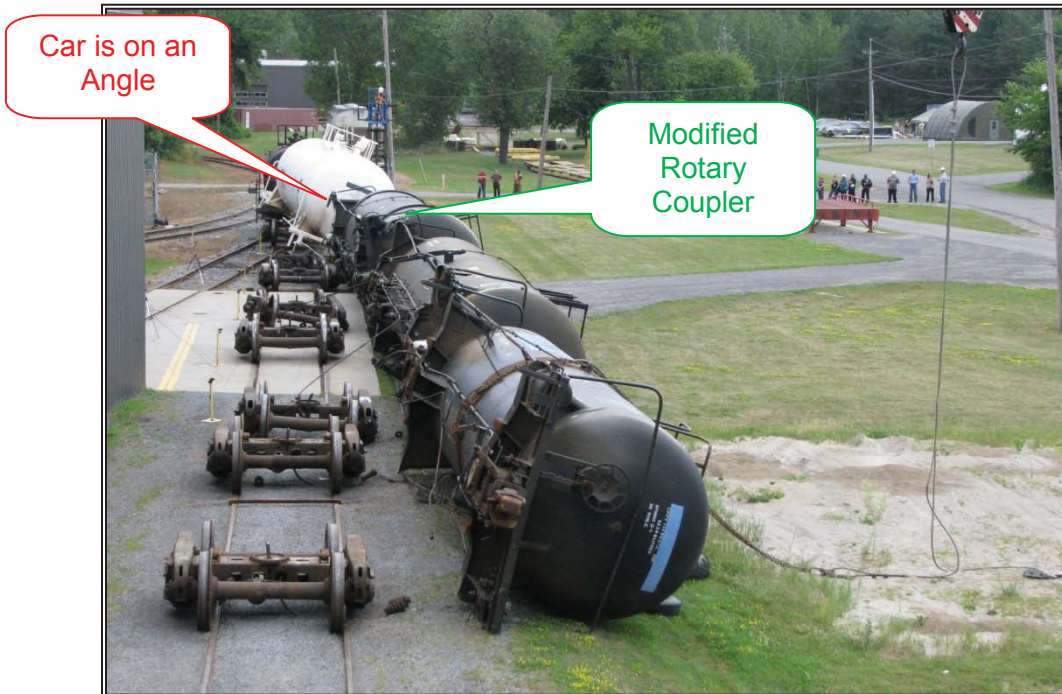


Figure 93: Test #3, cars after test – rotary coupler stopped the rollover propagation.

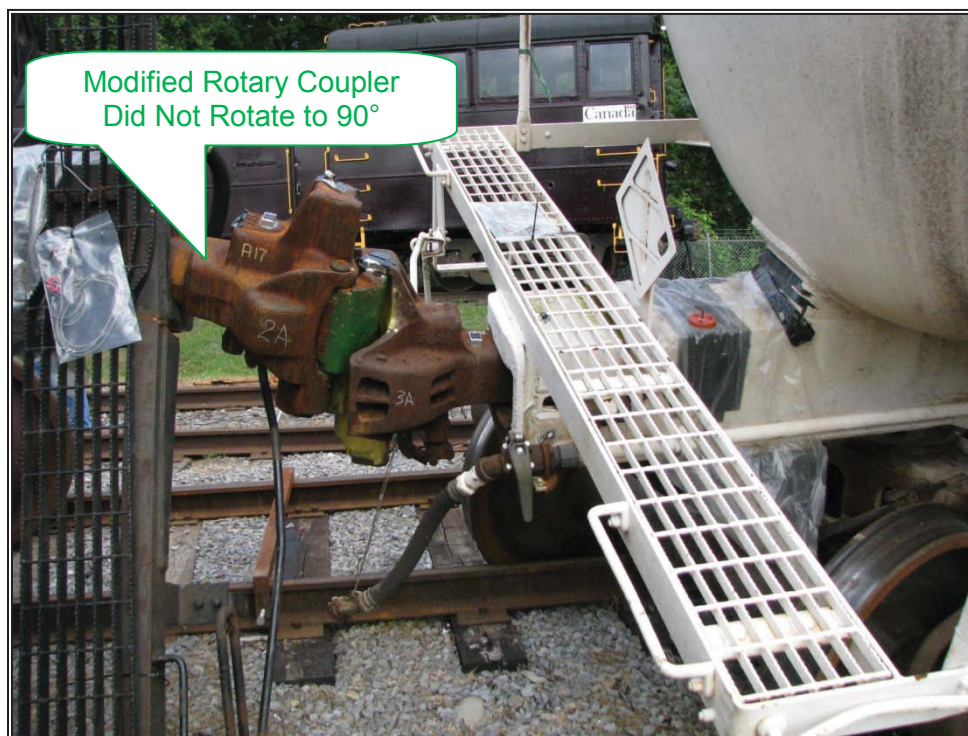


Figure 94: Test #3, rotary coupler after test.

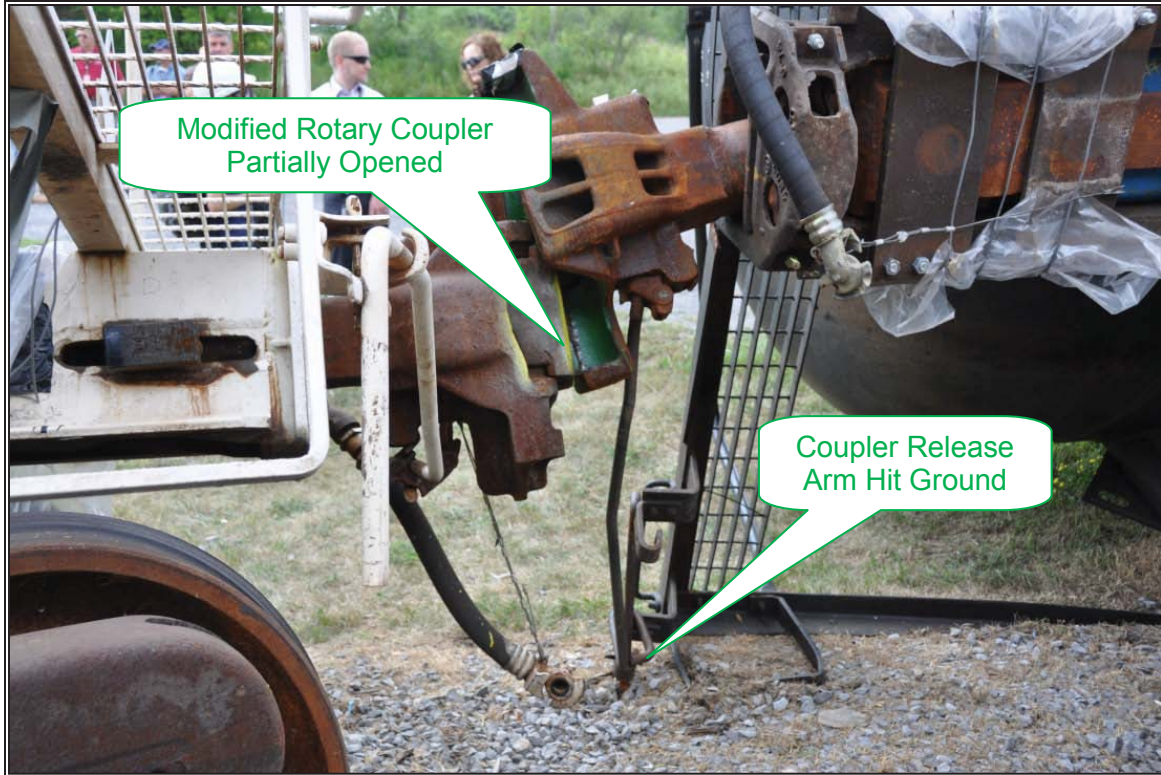


Figure 95: Test #3, rotary coupler partially opened after test, release arm hit ground.



Figure 96: Test #3, rotary coupler partially opened after test.

Observations:

Although the rotary coupler did prevent the rollover from propagating to Car #II and the car in the fourth position, it was noticed that Car #II suffered some rotation that did not happen during Test #2. After further investigation by NRC-CSTT engineers, it was clear that the rotary coupler did not rotate to 90° as was the case in Test #2. The limited rotation that occurred happened only at the beginning of the rollover, and it seems that the rotary coupler was jammed inside the car sill when Car #III (the car in the 2nd position) started to lift Car #II (the car in the 3rd position).

Figure 97 shows a comparison between the rotary coupler behaviour during Test #2 and Test #3. It is clear that in Test #2, the rotary coupler was lifted up and did hit the striker, which limits the vertical motion of the coupler. In Test #3 however, the rotary coupler was pushed down. Because there are springs that support the carrier iron on which the rotary coupler rests, the coupler was allowed much more vertical motion compared to Test #2.

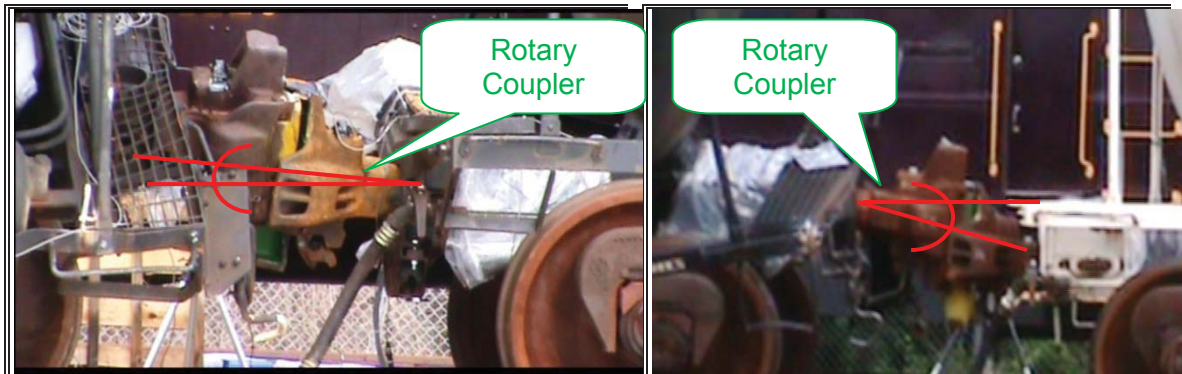


Figure 97: Comparison between rotary coupler position (before lifting the following car) in Test #2 (left) and Test #3 (right).

After Test #3, in order to better understand the effect of the carrier iron springs on the rotary coupler, NRC-CSTT performed a quick test by locking the springs in the compressed position and investigated the rotary coupler behaviour. As shown in Figure 98, the rotary coupler is held at a vertical position by its internal mechanism before the springs are fully compressed, this position is 1 in. lower than the starting position, from 7/8" at the starting position, to 1 7/8" when the coupler is held by its internal mechanism. In other words, the vertical motion of the rotary coupler in the down direction is limited by the internal mechanism and not by the springs.

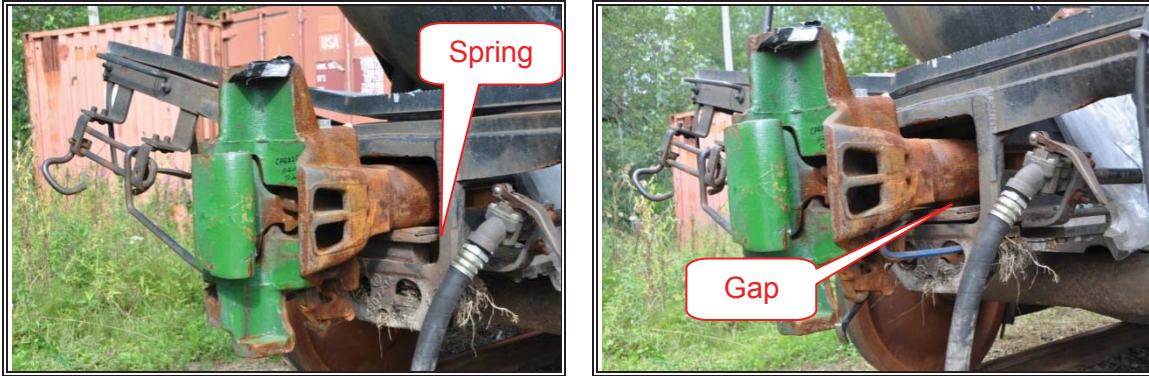


Figure 98: Rotary coupler resting on the bottom springs (left); rotary coupler not touching the springs (fully compressed) (right).

The questions that remained were: what is actually preventing the rotary coupler from moving down, and what is preventing the rotary coupler from rotating?

During the quick test mentioned above, it was noticed that the rotary coupler did not touch either the sill or the yoke when the springs were compressed. Figure 99 shows the gap between the rotary coupler shank and the yoke, both at the top and at the bottom.

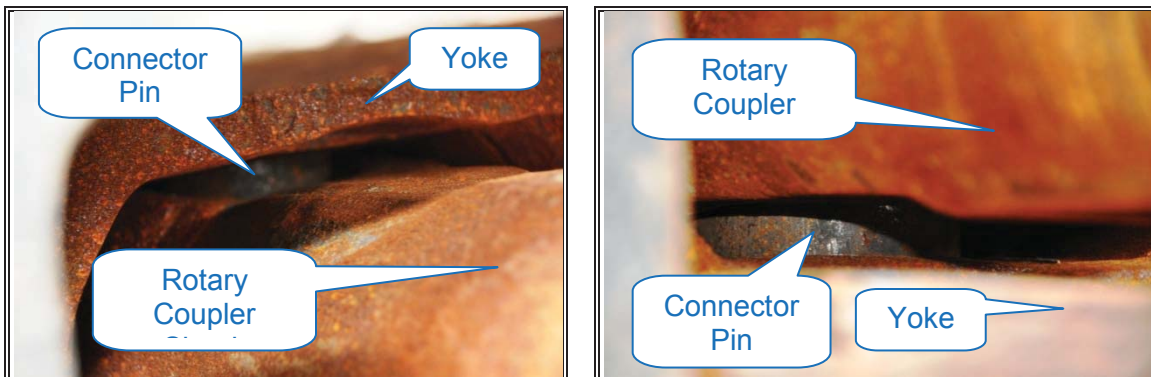


Figure 99: Top gap (left); bottom gap (right).

It is clear that in this case, the coupler is held in position through the connector pin. Figure 100 shows the rear assembly of the rotary coupler where the coupler shank is connected to the connector pin, which in turn is connected to the rotary connector.

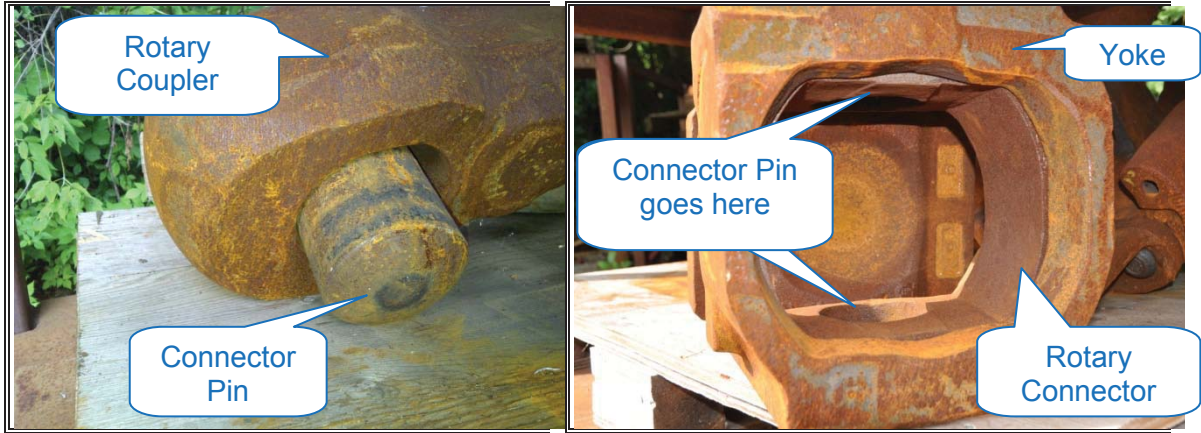


Figure 100: Rear assembly of the rotary coupler.

Figure 101 shows the complete rotary coupler assembly. Indicated in red are the forces acting on the coupler in the down direction, and the force components transferred to the rotary connector through the connector pin. It seems that the forces acting on the rotary connector created a pitching motion inside the yoke. This friction prevented the rotary connector from rotating inside the yoke, causing it to jam, in turn preventing the rotary coupler from rotating fully and freely during the test.

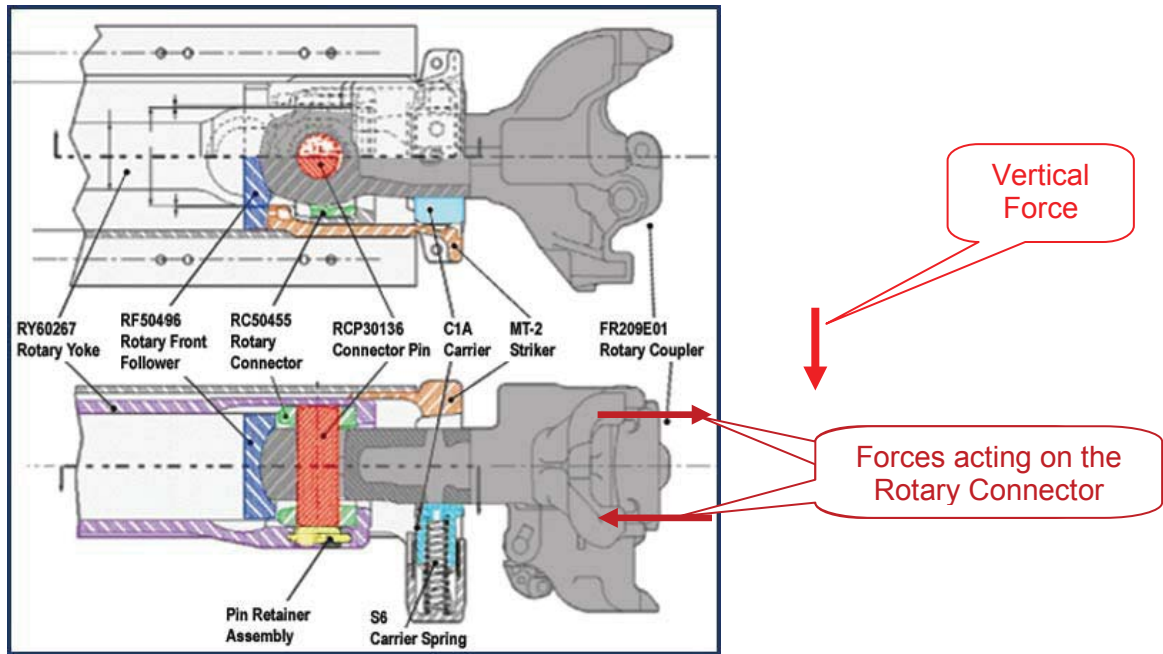


Figure 101: Rotary coupler assembly³.

³ Picture is taken from McConway & Torley LLC website (www.mcconway.com). Picture is used for illustration purpose only.



Figure 102: Car #11 near-end truck.



Figure 103: Car #11 near-end truck.



Figure 104: Car #II after testing.



Figure 105: Car #II far-end truck after testing.

A review of the security camera video (channel 4) shows the near end of Car #III is lifted off its side bearing. It is not clear if the body rolls on its side frame, but the near-end centre plate does clear its centre pin through a combination of lift and roll. The car body then displaces laterally by several inches, possibly striking the side frame. At this point, the near-end truck begins to tip up as the car body continues to roll. The truck reaches approximately 45° before it begins to fall back onto the rails, and the car body continues to roll onto the ground.

The near end of this car was positioned on the concrete apron that leads to one of NRC-CSTT's test buildings. A section of the concrete on the rolled side of the car was removed to prevent interference with the bottom of the side frame.

The far end of Car #III car was positioned off the concrete apron. The channel 5 security camera video shows that the centre plate for the far end of the body clears the centre pin through a combination of lift, roll about the side bearing and small roll about the side frame. The truck bolster can be seen to rise slightly, indicating that it is carrying less of the car body weight; this weight must be transferred to the side frame because there is no other means of supporting this end of the car body. A few frames later, the truck begins to roll about its wheel/rail contact points on the rolled side. The car body and truck do roll together, but not as a rigid assembly; the truck is seen to roll more rapidly than the body causing the centre pin to re-enter the centre plate. Since the truck roll began once the body was contacting the side frame, this demonstrates the destabilising moment that was described and assumed to occur in the energy analysis (see Section 3.2.5 of this report). However, the body and truck roll somewhat independently of one another.

The wheel/rail contact point (on the rolled side of the car) of the outboard wheelset (the wheelset in the truck that is closest to the end of the car) of the truck at the near end of Car #III can be seen in the channel 5 security video, the contact point for the inboard wheelset is out of the frame. The truck continues to roll about the wheel/rail contact point until the flange tip of the outboard wheel on the rolled side is higher than the top of the rail. Finally, the wheel slides towards the field side of the rail head and drops off the rail, the car body falls to the ground, and the truck drops back down to the ground.

In the same video, the near end of Car #II can be seen including the wheel/rail contact points from both wheelsets in the near truck. Car #II's body and truck begin to roll after the far-end truck of Car #III has rolled a few degrees. As the roll on Car #II continues, its near end truck rolls to the point that the flange tip of the outboard wheel is above the rail. The outboard wheel of Car #II's near truck slides off the head of the rail first, followed by its inboard wheel. This occurs at a lesser roll angle of Car #II's truck than of the far-end truck of Car #III. Another few frames are recorded before the outboard wheel of Car #III slides off the rail.

The channel 7 security camera video shows the near end of Car #II. The car body and truck are first seen to slide laterally towards the rolled side, presumably stopping as a result of wheel flange contact with the gauge face of the rail. A few frames later, the car body and truck both begin to roll. At this point, the centre plate is still fully seated within the centre bowl. As roll continues, the edge of the centre plate that is towards the rolled side can be seen to lift clear of the centre bowl but it is not evident if the entire centre plate is out of the centre bowl. As the truck continues to roll, the inboard axle obscures

the view of the centre plate and bowl until the wheels slide off the rail and the truck and car body fall heavily back to the ground together. Car #11's body then bounces up and off the near-end truck. It is at this point that the centre plate finally lifts free of the centre pin, which remains in the truck bolster.

The channel 8 security video shows the far end of Car #11. The video shows the car body rolling (on its constant contact side bearing) to lift the centre plate out of its bowl, revealing the pin. As the roll continues, the pin leans towards the rolled side. The car body slides off its side bearing, causing the pin to lean further then to bend about the edge of the opening in the centre bowl. The video also shows that the near end of the car in the fourth position was lightly disturbed by the motion at the far end of Car #11.

Test #3 was also successful in stopping the progression of the domino derailment at Car #11, the first car downstream of the rotary double-shelf coupler, but the progression was not stopped as convincingly as in Test #2.

5.3.7 Test #4: Dynamic Testing With Modified Rotary Coupler – Blocked Carrier Springs

Based on the previous test work described above and several brainstorming sessions, NRC-CSTT and TC-TDG agreed to proceed with Test #4; a repeat of Test #3, but with restricted motion of the carrier iron springs. The restricted spring motion was accomplished by welding a stopper to prevent it from compressing, which eliminated the possibility of having the rotary connector jamming inside the yoke. The welded stopper limited the coupler vertical motion to ¼” lower than the starting position, which is ¾” above the point at which the internal coupler components prevent further downward motion. This test was a full-scale dynamic test on five (5) empty tank cars equipped with standard Type E double-shelf couplers throughout the whole test string except at the far end of Car #III, where a modified rotary coupler was installed. No instrumentation was used during this test, but several video cameras were used to record car behaviour during testing. Both the initiating car and the car in the fourth position belong to NRC-CSTT’s impact hill anvil string, while Car #I, Car #II, and Car #III were supplied by TC-TDG.

Test Setup

On October 25, 2011, NRC-CSTT performed Test #4; a full scale dynamic test on five empty tank cars. All cars were equipped with standard Type E double-shelf couplers, except the Far-end of Car #III on which the modified rotary coupler was installed (Figure 106). The rotary coupler was installed in this location instead of the Near-end of Car #III as in Test #2.

The objective of this test was to investigate the efficiency of the modified rotary coupler as a potential solution to reduce the rollover domino effect with the rotary coupler carrier springs mechanically isolated.

No instrumentation was used during this test, only several video cameras were used to record the cars’ behaviour during testing. Prior to the beginning of the test, all cars were compressed together (no slack between couplers) and hand brakes for all tank cars were released.

Note: in Figure 75, setup changes between Test #3 and Test #4 are shown in red.

| | | Initiating Car | | 1 st Position | | 2 nd Position | | 3 rd Position | | 4 th Position | |
|----------------------|------|----------------|--------|--------------------------|--------|--------------------------|--------|--------------------------|-------|--------------------------|---|
| Test setup overview | | | | | | | | | | | |
| | | N | F | N | F | N | F | N | F | N | F |
| Test #4 setup | | | | | | | | | | | |
| Orientation | B | CSTT-1 | | Car #I | | Car #III | | Car #II | | CSTT-3 | |
| Sill type | E | A | A | B | B | A | A | B | B | A | |
| Coupler type | E60C | SE60CC | SE60DC | SE60CHTE | SE60CC | Rotary | SE60CC | SE60CC | SE60C | BE60A | |
| | | E | E | E | F | F | E | E | E | E | |

Figure 106: Test #4, dynamic testing with one modified rotary coupler and 5 tank cars - test setup schematic.

As in Test #2 and Test #3 and based on the observations in Test #1, lateral force was applied to the initiating car by pulling laterally at the middle of the car from the top. This method distributed the reaction forces of the applied lateral force to both trucks on the initiating car. As the initiating car is lighter weight, forces were applied with an angle pointing down from the horizontal line to prevent the car from sliding sideways on top of the tracks. The cable is highlighted with a red ellipse in Figure 107.



Figure 107: Test setup showing rollover force application.

Figure 108 shows a close-up of the rotary coupler with the carrier system mechanically isolated.



Figure 108: Rotary coupler with isolated carrier system.

The far end of Car #III was equipped with the modified rotary coupler with the isolated carrier system. The test car's configuration was the same as in Test #3.



Figure 109: Test #4 – five car test consist prior to rollover.



Figure 110: Test #4, five car test consist after rollover – rotary coupler stopped the rollover.

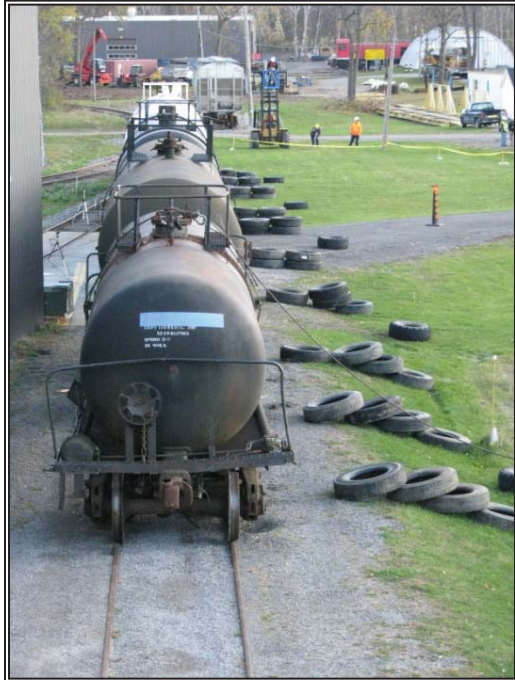


Figure 111: Test #4, dynamic testing with one modified rotary coupler and five tank cars.

Test Setup

NRC-CSTT was able to initiate the rollover, and the first three tank cars were rolled over to the ground. The rollover stopped at the modified rotary coupler. The fourth car's final position was skewed from the track with the leading truck wheels partially buried in the ballast and the trailing truck on the track. The fifth car stayed on tracks (Figure 112).



Figure 112: Test #4, Car #II near-end truck.



Figure 113: Test #4, Car #II far-end truck.



Figure 114: Consist after test, from rolled end.



Figure 115: Final position of modified rotary coupler.

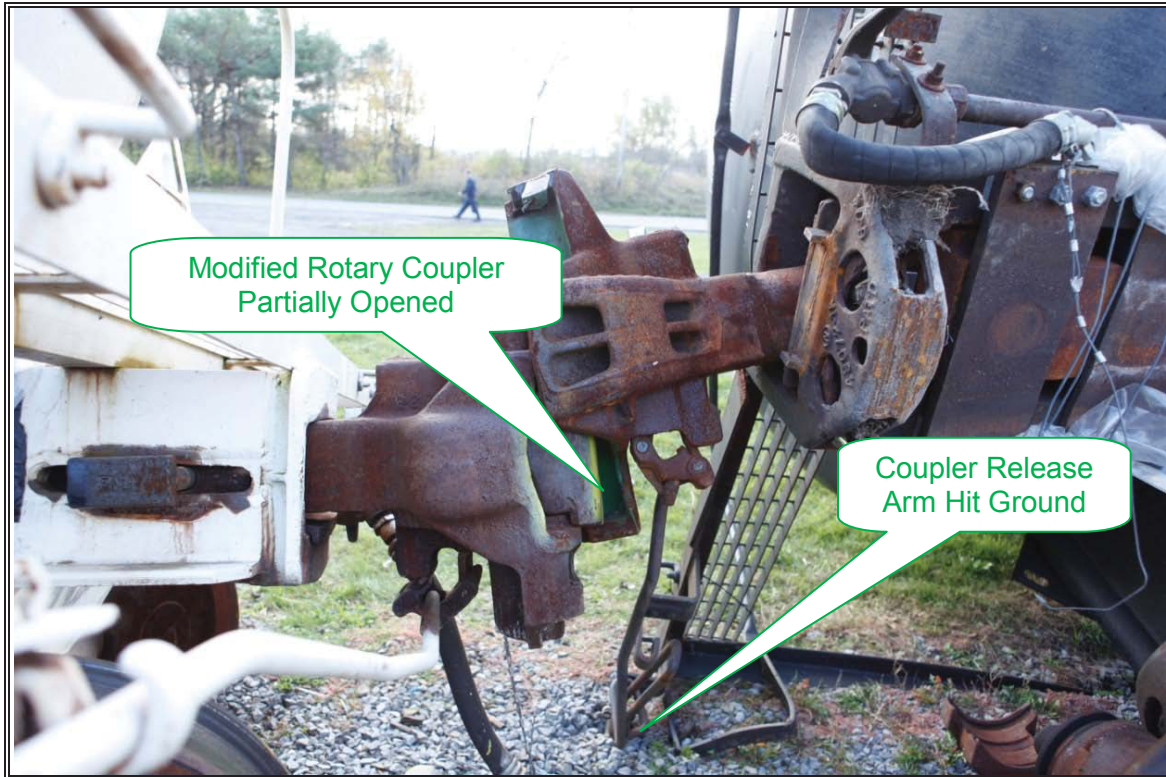


Figure 116: Test #4 modified rotary coupler partially opened after test, release arm hit ground.

Observations from Test #4

The security camera video (channel 4) shows the near end of Car #III is lifted off its side bearing. The near-end centre plate clears the centre pin through a combination of lift and roll and immediately slides laterally by several inches, possibly stopping when it hits the side frame of the truck. At this point, the near-end truck begins to tip up as the car body continues to roll. The truck rolls with the car – not as a rigid body because the truck’s rotational speed varies with respect to the car’s - beyond 45° and then falls back onto the rails as the car body continues to roll onto the ground.

As with Test #3, the near end of this car was positioned on the concrete apron that leads to one of NRC-CSTT’s test buildings. The bottom of the side frame appears to enter the opening that was cut in the concrete in order to allow full motion. The bearing cap on the rolled side of the outboard axle appears to almost contact the ground before the truck falls back on the rails. It does not appear from the video that the truck side frame contacted the concrete before falling back down.

Channel 5 shows the far end of Car #III positioned off the concrete apron. The centre plate at this end of the car clears the centre pin through lift and roll about the side bearing followed by roll about the side frame. While the body cannot be directly seen to roll on the side frame in the video, the rise of the truck bolster indicates that the car body weight has been shifted from the side bearing to the side frame before the pin clears the

centre plate. As described in Section 3.2.5 of this report, the truck only starts rolling when the car body has contacted the side frame and begun shifting its load onto it to create a destabilizing moment.

The truck does not roll up beyond 30° before the outboard wheel on the rolled side slips between the rails. It appears as though a lateral force drives both the car body and the far-end truck across the rails, which allows the wheels on the rolled side to drop between the rails. This is opposite to what was observed in Test #3, where the outboard wheel slid off the rail head to the field side of the rail. The videos also show an abundant quantity of rainwater falling from the truck or car onto the track near the wheel/rail contact point on the rolled side of the far-end truck. This may have reduced the coefficient of friction between the wheels and the rails. At this point, the car body keeps rolling on the side frame until it is on its side on the ground and the truck falls back down. Note that in this test, contrary to Test #3, Car #III's far end wheels slid off the rail before Car #II's near end wheels.

The file (R0275 Rollover4 West_HD.mts) from the high definition video camera that was aimed at the rotary coupler reveals that the near end of Car #II lifts and rolls slightly as the far end truck of Car #III begins to roll, but falls back down on its truck when the outboard wheel of Car #III's far-end truck falls within the rails. As Car #III keeps rolling about the side frame of its far-end truck, Car #II begins to roll again with its car body and truck forming a rigid body since the near-end centre pin is still trapped in the centre plate and bowl. In fact, when looking closely at the HD video, it appears that the car body is not touching the side frame nor the side bearing as it rolls which means the car body is rolling purely about the wheel/rail interface.

Channel 8 appears to show that after the wheel of Car #III's far-end truck falls between the rails, the near end of Car #II is applying very little vertical load to the truck while being rolled. A small gap can be briefly seen between the centre plate and centre bowl which means the truck is briefly unloaded. The gap then only partially closes up, and the edge and bottom of the centre plate on the rolled side of the car are not in contact. Therefore, only lateral force keeps the centre pin inside the centre plate and bowl through friction. The car and truck keep rolling until the lateral motion of the truck is no longer prevented by the flange of the rolled-side wheel on the outboard axle, which has risen above the rail gauge corner. As this wheel slides outside the rails, the truck falls to the ground from under the car body, which frees the pin from the centre plate. The body of Car #III maintains its rolled orientation and its near end falls back onto the truck. It oscillates a few times through a small angular range but does not roll back towards its vertical position, possibly because of the way the car body is supported on both its trucks.

Test #4 was also successful in stopping the progression of the domino derailment at Car #III, the first car downstream of the rotary double-shelf coupler, but the progression was not stopped as convincingly as in Test #2. Mechanically isolating the springs in the rotary coupler's spring-loaded carrier iron did not cause an observable change in the way the domino effect was halted compared to Test #3.

However, any change that could have resulted from isolating the springs might have been completely masked because the wheels of the far-end truck on Car #III slid and fell between the rails, causing Car #III's body and truck to drop as well. Car #III was already

lifting Car #II by its coupler, so Car #II lost some its initial vertical displacement though this effect.

5.4 Explanation of the Domino Rollover Phenomenon and Rotary Coupler Effect

Based on the physical test results, the following observations are given regarding domino rollover with standard Type E double-shelf couplers and rotary couplers.

5.4.1 Domino Rollover Phenomenon – Standard Type E Double-Shelf Couplers

The purpose of the shelves is to limit relative vertical movement between joined couplers so that they cannot disengage. The reduction in the number of tank head punctures during derailments in the years following the introduction of double-shelf couplers points to their effectiveness in keeping derailed tank cars coupled together. Therefore, there was an expectation during Test #1 that knuckle-to-shelf contact would be a necessary event for the domino rollover to proceed. Test #1 was successful in causing the rollover, but a review of the data revealed that knuckle-to-shelf contact did not occur. A subsequent examination of the couplers showed fresh scuffing and gouge marks on the knuckles and coupler walls. The marks indicate that the couplers jammed or bound together as one car and its coupler rotated with respect to the adjacent car and coupler. This binding occurred before the driving coupler moved through the entire shelf-to-knuckle clearance.

Once the couplers were bound together, the driving car could transmit force and torque to the driven car. By not using all the knuckle-to-shelf clearance available, the driving car's motion transferred to the driven car earlier in the rollover process. An earlier transfer of motion enables the body of a driven car to roll on its truck (side bearing and side frame), which makes it easier for the driven car body to disengage from its centre pin. Once this disengagement occurs, the driven car body is free to roll and displace as it follow the motion of the driving car body (which it is constrained to do through the couplers). The driven car will finally roll off its trucks and fall to the ground adjacent to the track. Partway through the roll process, the driven car becomes the driving car for the next car in the consist, and the pattern repeats itself.

Test #1 was an examination of a zero-speed, quasi-static rollover derailment. In an actual rollover derailment, the tank cars will generally have a non-zero velocity. This implies the presence of relative motion between adjacent cars, possibly leading to relative vertical displacements of joined couplers. During an actual derailment of a moving train, it is quite feasible that the knuckles and shelves of joined couplers come into contact, and that forces and moments are not transmitted until this event occurs. However, knuckle-to-shelf contact does not appear to be a necessary condition for a zero-speed domino derailment.

5.4.2 Rotary Coupler Effect – Facing the Oncoming Domino Wave

If the rotary coupler is facing the oncoming domino wave as it did in Test #2, it will restrict the ability of that wave to transmit roll moment to the car carrying the rotary coupler (the driven car). Therefore, as the domino wave lifts the car facing the rotary coupler (the driving car) off its centre plate, the vertical motion at car body centre line of the coupler knuckles does not develop a large couple across the knuckles. The knuckles do not bind together as they did in Test #1, and can therefore slide through the full

extent of the vertical clearance in the coupler until they make contact with the shelves. Once they contact the shelves, the knuckles can then lift the rotary coupler through the clearance (1 inch) between the coupler shank and the underside of the top of the striker casting on the driven car.

This “clearance take-up” reduces the amount of vertical lift the driving car can transfer to the driven car to lift it off its near truck. The driven car’s near-end centre plate might clear the centre pin, allowing the driven car’s body to yaw about the centre plate of its far-end truck. The driven car will remain upright, supported either on the side frame of its near-end truck and/or on the coupler shank of the driving car which has rolled 90° and is lying on the ground. Or, the driven car’s centre plate might not clear the centre pin of its near-end truck by a small amount, causing the driven car’s near truck to roll about the wheel/rail contacts (on the rolled side) until the car body slips off the centre pin, allowing the near truck to fall back to the rails with the car body supported as described above. A different reaction seems to result if the position of the rotary coupler is changed to face away from the oncoming domino wave, as discussed below.

5.4.3 Rotary Coupler Effect – Facing Away from the Oncoming Domino Wave

For Tests #3 and #4⁴, the rotary double-shelf coupler is mounted on the far end of the driving car, and a standard double-shelf coupler is mounted in the near end of the driven car. In this configuration, the rotary coupler is facing away from the oncoming domino wave.

In Test #3, the domino motion causes the driving car’s far-end centre plate to roll out of its centre bowl as its car body rolls on the far-end truck’s side bearing. The driving car continues to roll until the centre plate clears the centre pin, and some of the car body load is transferred to the side frame of the far-end truck. During this body roll, the vertical motion of the rotary coupler on the driving car is absorbed by the vertical clearance available in the double-shelf couplers (6.5 inch), by the vertical depression of the spring-loaded coupler carrier iron on the driving car (1 inch), and by the vertical clearance between the coupler shank and the underside of the striker casting at the top of the draft sill of the driven car (1 inch). Therefore, no vertical motion is yet transmitted to the driven car. During this initial roll of the driving car (before the body of the driven car begins to move), the rotary coupler in the driving car remains at the same angle as the standard coupler in the driven car – horizontal – and the sill of the driving car rotates (roughly 20°) about the shank of the rotary coupler.

Roughly 14° of body roll angle is required for the driving car’s near-end centre plate to clear the end of the centre pin. At that stage of driving car body roll angle, the driving car body centreline is offset laterally from the driven car by roughly 1 inch. Very soon thereafter, the lateral clearance between the coupler shanks and the striker castings on both car bodies will be reduced to zero such that a large lateral force can be transmitted from the driving car to the driven car at coupler centreline height above rail. Due to the lost vertical motion of the double-shelf couplers (and carrier iron spring compression and

⁴ In Tests #3 and #4, there were no transducer measurements taken, so there is no quantitative data to support the following observations. There is only video for each test from the security camera system, which operates at 7 frames per second. Still images from frame grabbing are blurry, and important views during the dynamic action are sometimes blocked by moving truck components passing through the field of view.

coupler shank-to-striker clearance), the driven car was not yet lifted enough for its centre plate to disengage from its near truck centre bowl. Therefore, the lateral force on the driven car's draft sill is reacted at the wheel/rail interface which produces a couple on the driven car's body and its near truck. This causes the driven car and its near truck to roll about the wheel/rail interface on the rolled side, as the driving car's body rolls. The driven car's near truck thus rolls with the driven car's body (centre plate still engaged with the centre bowl) until the effective flange angle between the wheel and the rail is reduced sufficiently to allow the outboard wheelset on the driven car's near truck to derail by sliding over the top of the rail head. At this stage, the driven car's body has rolled roughly 40°.

The driven car's near truck then drops back onto the ground (all four wheels derailed), and the driven car's body rolls back and stops at a roughly 30° roll angle, held at that roll angle by the bent centre pin in the driven car's far truck not able to pass through the hole in the centre plate. The driving car rolled onto the ground at a roughly 90° roll angle. The roughly 60° differential between the two car bodies at the end of the derailment was absorbed by rotation of the rotary coupler in the driving car's sill.

Although the driven car finished with a body roll angle of about 30°, the presence of the rotary coupler terminated the progression of the domino derailment at the driven car, although not as convincingly as in Test #2. It is not clear if the progression of the domino effect would be halted if a rotary coupler were placed many more cars away from the initiating car, where the propagation velocity of the domino wave might be faster than it was during the tests reported here.

The setup in Test #4 was identical to that of Test #3, except that the spring-loaded coupler carrier iron was welded in place. This was done to reduce (or restore) 3/4 in. from the lost vertical motion that the driving car transmits to the driven car.

Despite this change, the result of Test #4 was virtually identical that that of Test #3. However, the expected benefit from isolating the springs might have been completely masked because the wheels of the far-end truck on the driving car slid and fell between the rails, causing the driving car's body and truck to drop as well. The driving car was already lifting the driven car by its coupler, so the driven car lost some its initial vertical displacement though this effect. The behaviour of the driven car during Tests #3 and #4 were very similar. The lateral force that developed across the couplers was again reacted at the wheel/rail contacts on the driven car because the driven car's near-end centre plate did not lift clear of its centre bowl. This caused the driven car body and its near-end truck to roll about the wheel/rail contacts on the rolled side until the effective flange angle was low enough to allow the wheels to slide over the head of the rail towards the rolled side. The driven car body had undergone roughly 40° of roll when this occurred. As before, the driven car's near-end truck dropped to the ground (all four wheels derailed), the car body rolled back to roughly 30°, and the car body had been disturbed on its far end truck. The driving car was on the ground, at a 90° angle. The differential roll had been absorbed by the rotary coupler in the driving car's sill. The effect of mechanically isolating the springs for the rotary coupler's carrier iron was not observable during the test.

5.4.4 Comparison of the Rotary Coupler Effectiveness in Tests #2, #3 and #4

It is important to recognise that there can be very little roll angular displacement between the double-shelf couplers, only what is permitted through the angular slack (approximately 6° - 8°) that is present in the coupler heads and knuckles. Once this slack is taken up, the couplers must roll together.

During Test #2, the driving car's body (Car #I) rolled about its side bearing and side frame. Its far-end draft sill was equipped with a standard Type E double-shelf coupler, which by design, cannot rotate within its sill (note that minor rotation does occur, as a result of dimensional tolerances in the key, keyway openings in the sill, and key slot in the coupler shank). Therefore, as the driving car rolled, its coupler was effectively constrained to roll through the same angular range. The rotary coupler on the driven car (Car #III) also rotated through the same angular range (less the angular slack between couplers), because of the roll constraint across couplers. Since the rotary coupler's sill does not constrain roll, it rotated smoothly and continuously as it followed the driving car's coupler. It did not apply a roll torque to the driven car's body as it rolled, and therefore the driven car's body did not roll.

While the driving car and the two couplers were rolling, the far-end sill of the driving car was displacing vertically and laterally. Some of the vertical displacement was transferred to the near end of the driven car (after vertical slack was taken up), but not enough to completely lift the centre plate free of the truck. As the far-end sill of the driving car displaced laterally, it tried to drag the near-end sill of the driven car with it. The resulting lateral force applied to the driven car's near-end sill was ultimately reacted at the wheel/rail contact points on the rolled side of the driven car's near-end truck. This created a couple, which caused the driven car's near-end truck to roll up about the wheel/rail contact point, but the body did not roll with it. The continued lateral displacement of the driven car's body eventually allowed the centre plate to drag the centre pin out of the rolled truck, allowing the driven car's body to yaw about its far truck. The derailment event ended at this point, with the near end of the driven car supported vertically by its coupler connection to the driving car (which had rolled onto the ground).

During Test #3, the driving car's (Car #III) far-end sill was equipped with the rotary coupler, and the driven car's (Car #II) near-end sill had the standard double-shelf coupler. The driving car's far end rolled about its side bearing and then about its side frame, transferring vertical and lateral displacement to the near end of the driven car. A little more roll of the driving car's body may have occurred before the driven car began to lift, because the driving car's coupler shank would have to bear down on its carrier iron and compress the springs until the spring force was sufficient to resist the load (the coupler shank would reach its maximum downward travel of 1 inch). The effect of the spring-loaded carrier iron is to introduce additional vertical slack in the coupler system.

The driving car's lateral displacement again tried to drag the driven car toward the rolled side, thus applying a lateral force to the driven car's standard coupler. However, contrary to what happened in Test #2, the vertical lift applied to the driven car had not even lifted its near-end centre plate out of the truck centre bowl at this point. The couple from the lateral force acting at the driven car's near-end coupler and the reaction force at the driven car's near-end wheel/rail contact points caused the driven car and its near-end

truck to start to roll about the wheel/rail contact points earlier and with a larger roll moment than in Test #2.

At this point, the driven car's near end coupler was just beginning to roll because the driven car was just beginning to roll. Therefore, the rotary coupler in the driving car had not yet rolled but the driving car itself had rolled about its rotary coupler's shank. Thus, the rotary coupler had absorbed the differential roll of the car bodies. As the rotary coupler rolled within its sill, it could not apply a roll torque through the driven car's coupler and into the driven car's sill. Therefore, the driven car body did not roll on its bolster or side bearings while the driving car rolled.

As the driven car began to roll about its wheel/rail contact points its near-end coupler was constrained to roll with the car body, and the rotary coupler in the driving car was constrained to follow (after angular slack is consumed). The driven car body reached a roll angle of roughly 30° before its centre plate broke free of the centre pin at the near-end truck. Therefore, the driven car's coupler had also rolled roughly 30° with respect to horizontal, as did the driving car's rotary coupler (less angular slack). The body of the driving car was lying on the ground, rolled to roughly 90°. Once again, the rotary coupler had absorbed the roll angle difference between the two cars. The derailment had ended at this point and the driven car remained at a 30° roll angle because both ends of the car body were hung up on the trucks, which prevented the body from rolling back.

Near identical behaviour of the driving and driven car bodies and the couplers occurred during Test #4. Mechanically isolating the carrier iron's springs in the driving car's far-end sill should have reduced the vertical slack that had to be taken up before the driving car could lift the driven car. Thus, the driven car's near-end body should have undergone more lift prior to the application of the lateral force at the coupler. It was not clear from the video that this did in fact occur. The outboard wheel on the far-end truck of the driving car also slid and dropped between the rails, causing the truck on the driving car to drop, and the driving car body to drop with the truck. This could have offset any benefit (in terms of reduced vertical clearance) that occurred by isolating the carrier iron springs on the driving car. Once the derailment process had ended, the driven car was again rolled to a roughly 30° angle while the driving car was lying on the ground, rolled to roughly 90°. The rotary coupler had absorbed the differential roll between the car bodies, and never transmitted a roll torque to the driven car.

When a driving car equipped with a standard double-shelf coupler rolls, its coupler rolls with it. If the driven car is also equipped with a standard double-shelf coupler, the driven car's coupler must also roll and thus will transmit a roll torque to the driven car's body. These are the main differences in the roll behaviour between the first test and the subsequent three tests:

- the standard double-shelf couplers are unable to absorb significant differential roll between the car bodies (they are limited to approximately 18° as a result of angular slack between the coupler heads, and between the shanks and the sills)
- the rotary coupler allows as much differential roll between car bodies as required.
- the standard double-shelf couplers always transmit a torque from the driving car to the driven car's body
- when installed in the near end of a driven car, the rotary coupler cannot transmit a torque to its car body

- when installed in the far end of a driving car, the rotary coupler cannot transmit a torque to the subsequent driven car
- in these zero-speed derailment tests, it was observed that the standard double-shelf couplers bind together before they have consumed the entire knuckle-to-shelf clearance
- in these zero-speed derailment tests, it was observed that the rotary coupler joined to a standard double-shelf coupler allows relative vertical motion that consumes the full knuckle to shelf clearance. This affects the vertical lift of the driven car as follows (compared to the use of standard double-shelf couplers):
 - when the rotary coupler is installed in the near end of the driven car, more roll angle of the driving car must occur before the driven car is lifted – vertical lift is delayed until the knuckle-to-shelf clearance is exhausted
 - when the rotary coupler is installed in the far end of the driving car, vertical lift is delayed until the knuckle-to-shelf and carrier iron spring compression clearances are both exhausted
- in these zero-speed derailment tests, the use of standard double-shelf couplers causes the driving car to roll the driven car on its near-end truck (truck bolster roll, followed by car body rolling on the side bearing then on the side frame)
- in these zero-speed derailment tests, the use of a rotary coupler prevents the driven car body from rolling on its trucks. However, lateral motion of the driving car creates a couple on the driven car and its near-end truck, causing them to roll together

The reason that the third and fourth tests were judged less successful than the second test is because a strong couple acted on the driven car's body and near-end truck assembly before the near end of the driven car body could be lifted clear of its truck. The car body and the near-end truck rolled together until the body violently broke free of the near end truck. By this time, the body had also rolled and slipped on the far end truck, and the derailment event ended with the car body rolled at a 30° angle. The couple is the result of lateral force acting on the near-end sill of the driven car and reacting at the wheel/rail interface of the driven car's near-end truck (the lateral force is transmitted through the centre plate/centre pin/centre bowl interfaces). The lateral force occurs because the far-end sill of the driving car is moving both vertically and laterally as the driving car rolls, and the near end of the driven car is constrained (through the couplers) to follow this motion.

In the second test, the driven car's near-end centre plate was lifted out of the centre bowl, although the pin remained engaged in both bodies. The driven car's rotary coupler was unable to transmit a roll torque to the driven car, therefore driven car did not roll with the driving car even while the driven car's near-end truck was rolling about its wheel/rail contact points.

Insufficient vertical lift of the driven car's body at the near-end truck made Tests #3 and #4 appear less successful than Test #2. In each of these tests, however, the rotary coupler was successful at stopping the domino progression.

5.4.5 Study Limitations

The simulation, physical testing and analyses presented in this report are based on zero-speed (near zero-speed for the simulation) rollover derailments. The effect of speed could not be included in the physical testing or in the energy analysis. Modeling the effect of speed in the simulation would have greatly increased the complexity of the exercise.

The work in this report assumes the tank cars were on level tangent track. The tare weight of the cars was used in all cases, except for the energy analysis where empty and loaded cars were considered. The car in the energy analysis was based on a car that was similar but not identical to (in construction and weight) one of the three tank cars used in the physical testing. The direction of the domino rollover was the same during each physical test. The domino wave always propagated from west to east, and the initiating car was always rolled towards south. Owing to the proximity of buildings by the test track, no testing was possible in other directions. Cars were tested only in their empty state. Loaded testing would have required (for safety reasons) filling the cars with water, but the higher specific gravity of water would have overloaded the cars, and would not been representative of an actual loaded case. Partially filling the cars with water to produce the gross rail load would have introduced dynamic effects due to sloshing of the water; such effects are not present in tanks cars because they are always filled to volume capacity.

As there is no current way to install off-the-shelf load cells between couplers and car sills, the draft sills of several cars were instrumented to measure vertical forces and torque transferred between tank cars. As seen in Appendix B, instrumenting and calibrating the car sills does not provide the same accuracy as off-the-shelf load cells. The force and torque measurements obtained during testing inherit certain error, and were not used in the analysis as absolute values.

6. CONCLUSIONS

6.1 Literature Survey On Loaded Tank Car Rollovers

NTSB reports (24 reports from 1993 – current) provided no information about the nature of the loaded tank car derailments, with respect to the domino derailment phenomenon. These reports seldom mention double-shelf couplers except to say they are standard equipment on tank cars.

The TSB data (73 reports from 1993 - current) included seventeen reports concerning loaded tank car derailments. There are two cases in which double-shelf couplers were stated as the reason for the rollover of some of the loaded cars, seven cases where it seems likely that loaded cars rolled over in domino-type fashion, and eight cases where the details of the report are insufficient to draw a conclusion. In most cases, the number of rolled loaded tank cars is relatively small (2 – 4). There is one derailment in which four loaded tank cars rolled over at near zero-speed, similar to the Clara City incident (although on smaller scale). Based on this information, domino-type rollovers for loaded trains cannot be ruled out although the possibility of a large-scale incident seems remote.

6.2 Energy Analysis – Unloaded and Loaded Cases

The analysis was performed with the assumption that the car body would roll onto the side bearings, then onto the side frame. This would destabilise the truck, causing the car body and truck to roll together as a rigid assembly.

As a single empty tank car rolls from its undisturbed position, its potential energy would begin to increase, reach a maximum (at roughly 41° roll angle) and then begin to decrease.

The system potential energy of a string of empty tank cars can be determined by adding the energy curves of individual cars together, with appropriate angular lag between the cars (taken as 18°). The system's potential energy reaches a maximum value once the first car has rolled approximately 64°, and the system's potential energy decreases after that. Maximum system potential energy is reached before the fifth car begins to roll so only four cars are actually involved.

Leading cars are continuously transferring energy to subsequent cars; this is what enables the rollover derailment to propagate through a train of empty tank cars.

A necessary condition for the domino effect to begin is that sufficient energy must be transferred to the undisturbed system to roll the first empty tank car to 64°; this puts the system at the point of maximum energy (a system meta-stable point).

The change in potential energy required is 1,368,743 in-lb above the potential energy for four similar empty cars sitting undisturbed on level track. This increase in potential energy could come from a sideswipe impact with another train. An empty tank car travelling at roughly 6.6 miles/hour has this amount of kinetic energy, as does a loaded tank car travelling at roughly 3.6 miles/hour.

As a single loaded tank car rolls from its undisturbed position, its potential energy would begin to increase, reach a maximum (at roughly 25° roll angle), and then begin to decrease.

The system potential energy of a string of loaded tank cars can be determined by adding the energy curves of individual cars together, with appropriate angular lag between the cars (taken as 18°). The system's potential energy reaches its maximum value once the first car has rolled approximately 32°, and begins to decrease after that because the loss of potential energy from the first car is more rapid than the increase in potential energy of the second.

Maximum system potential energy for a string of loaded tank cars is reached when the second car has rolled 14°, so only two loaded cars are actually involved in starting the domino progression.

A necessary condition for the domino effect to begin is that sufficient kinetic energy must be transferred to the undisturbed system to roll the first car to 32°; this puts the system at the point of maximum potential energy (a system meta-stable point).

The energy required is 2,171,892 in-lb. This energy could come from a sideswipe impact with another train. An empty tank car travelling at roughly 8.4 miles/hour has this amount of kinetic energy, as does a loaded tank car travelling at roughly 4.5 miles/hour.

The kinetic energy that must be added to the system to initiate a loaded car domino rollover is 1.6 times that required for the empty car case.

The increase in potential energy needed to roll a string of empty tank cars to its meta-stable point increases significantly as the angular slack between couplers reduces. Reducing the angular slack from 18° to 11° raises the change in potential energy to roughly the same value (approximately 2.2 million in-lb) as for a string of loaded tank cars with 18° of angular slack between the couplers.

Increasing the potential energy needed for a string of empty tank cars to roll to its meta-stable point could result in component failure. This could be a fuse between the tank cars, capable of stopping the domino effect before it propagates through many tank cars (such as in a unit train). However, this alternative solution would require further study to determine its effectiveness and feasibility.

6.3 Vampire Simulation

Simulation with the tank cars equipped with standard Type E couplers (no double-shelf) did not result in domino rollover, due to coupler disengagement. This supports historical observations that domino derailments of tank cars did not occur prior to the introduction of double-shelf couplers.

Simulation with the tank cars equipped with Type E double-shelf couplers did result in domino rollover. The main reason was torque transfer between adjacent cars through the double-shelf coupler. This supports general observations that domino rollovers occur on tank cars equipped with double-shelf couplers.

6.4 Physical Testing

All tests were performed with empty tank cars.

6.4.1 Dry-Run Test

- Five different methods for rolling the initiating car were investigated, with respect to their ability to create a domino rollover effect on the empty tank cars. Pulling laterally from the top of the tank at the end of the initiating car furthest away from

the next car was selected as the preferred method. Pulling laterally from the top of the tank at the middle of the initiating car was selected as a back-up method.

- Based on observations during this test, NRC-CSTT
 - o cut sections of concrete out of the concrete crossing to prevent the truck side frames from contacting the concrete, which would influence the behaviour of the cars during the roll process;
 - o manufactured and installed lateral track supports, to prevent track damage during testing;
 - o positioned large truck tires where the tank car would contact the ground, to limit damage to the tank cars, and to prevent damage to underground communications cabling.

6.4.2 Dynamic Test #1 - Baseline with Standard Type E Double-Shelf Couplers – 4 Cars

A review of data obtained through video and instrumentation recorded during the first physical test revealed the following behaviour between Car #II and Car #III:

- Shelf to knuckle contact did not occur between Car #II (the driving car) and Car #III (the driven car).
- The near end of the driven car was lifted vertically and translated laterally by the driving car. The lateral motion occurs sooner and more rapidly than the vertical motion, meaning the initiating car tends to pull the subsequent car sideways off its near truck.
- The vertical load applied to the sill of the driven car was about 15% greater than half of its car body weight.
- The magnitude of the torque applied to the driving car was essentially identical to the product of the car body weight multiplied by the distance between the rolled car body's centre of gravity and the centre of the truck side bearing.
- The data shows that the near end of the driving car did roll about its side bearing, reaching 11.8 degrees beyond its starting position. During this period, the near end of the driving car was vertically displaced by 8 inches and laterally by 17.3 inches. Video evidence shows the centre plate lifting free of the pin, but also bumping it and tipping it.
- Contact did occur between the driving car's body and the near-end truck's side frame, but the truck and car body did not roll together as a rigid body for any period of time as a result.
- Both trucks did drop back down to the rails. This was observed in the data for the near end and in the videos for both ends of the driving car.
- The far end of the driving car did roll on the side bearings, but there is no evidence to suggest that the centre pin was caught between the car's centre plate and the truck centre bowl. The truck and car body did not roll together as an assembly.

6.4.3 Dynamic Test #2 with Modified Rotary Coupler – 4 Cars

A review of data obtained through video and instrumentation recorded during the second physical test revealed the following behaviour between Car #I (the driving car) and Car #III (the driven car):

- Shelf to knuckle contact did occur between the couplers of the driven car and the driving car. This contact was not observed during Test #1.
- The near end of the driven car was lifted vertically by the driving car. More displacement and roll was required from the driving car during this test before the driven car began to move, compared to Test #1. In this test, the driving car's far-end coupler had to be lifted higher to take up the clearance between its knuckle and the top shelf on the driven car's near-end rotary coupler, since binding of the knuckles did not occur in Test #2. The driven car did not displace until after knuckle-to-shelf contact had occurred and the clearance between the top of the rotary shank and the draft sill on the near-end of the driven car was taken up.
- The vertical loads measured on the far sill of the driving car and the near sill of the driven car were in the range of 25,000 – 26,000 lb. This is very close to the half-weight of the driven car's body. The rotary coupler did not alter the transmission of vertical force between the cars.
- The peak torque acting on the near sill of the driving car was 56,250 lb-ft (39,000 lb-ft less than expected), and it occurred when the body of the driving car was at a greater roll angle than expected (33°). The measured torque acting on the far sill of the driving car was lower than the maximum that was measured during the Test #1, but higher than expected given the expected lack of reaction torque from the driven car.
- The body of the driven car did not lift and roll clear of the centre pin at the near end truck; contact with the truck's side bearing never occurred. The car body's centre plate was stuck on the pin due to the lateral translation of the car. As the driven car continue to rise vertically and move laterally towards the rolled side, the truck rolled about the wheel/rail contacts on the rolled side. The centre pin did finally slip out of the truck bolster, freeing the near end of the car body from its truck and allowing the near end of the body to translate laterally with the far end of the driving car.
- Since the car body did not roll, it never contacted the top chord of the side frame of the near-end truck. Thus, the truck did not roll as a result of a net destabilizing moment. The truck did roll by almost 13° when its centre pin was caught in the truck bolster and car body centre plate as the near end car body displaced laterally.
- Once the centre pin broke free of the truck centre bowl, the near end truck dropped back down on the rails.
- The far end of the car body was initially in contact with the side bearing of the far end truck. Contact was briefly lost as the near end of the car body was moving, but the far end car body remained on its truck.

6.4.4 Dynamic Tests #3 and #4 with Modified Rotary Coupler– 5 Cars

No instrumentation was used during the third and fourth physical test, but video data was recorded for both. A review of the video data revealed:

- The far-end centre plate of the driving car cleared its centre pin through a combination of lift and roll about the side bearing and side frame.
- The far-end truck of the driving car tips up as it rolls about its wheel/rail contacts; this occurs after the car body has contacted the side frame.
- The near-end truck and car body of the driven car roll together about the wheel/rail interface.
- The near-end car body of the driven car violently separates from its truck after the two have rolled roughly 30°.
- The adjacent trucks on the driven car and the driving car slide off the rails.
- The derailment events ends with the driven car rolled roughly 30°, and the driving car rolled 90°.
- In the third and fourth physical tests, the domino progression stopped at the rotary coupler, but was not stopped as convincingly as in the second physical test.
- Mechanically isolating the coupler carrier springs in the fourth physical test did not cause an observable change on the test outcome.

A rotary coupler will only rotate when the coupler it is joined to rotates; this is a constraint of all couplers. A car body equipped with a rotary coupler can roll about the rotary coupler's shank even if the rotary coupler is restrained from rolling due to its connection to a standard double-shelf coupler on an adjacent car.

6.4.5 Physical Test Summary

Since a rotary coupler is free to roll within the sill of the car on which it is installed, it is unable to transmit a roll torque to its own car body or through the coupler to which it is joined.

The rolling motion of a driving car's body causes both lateral and vertical displacement at the adjacent, or driven, car body.

Lateral displacement that occurs in advance of vertical displacement causes the driven car's body and truck to roll together as an assembly until the truck slides off the track. This frees the car body from the truck and stops the domino effect from rolling the driven car body further. The zero-speed derailment ends with the driven car body rolled at a significant angle, partially supported by its trucks and possibly by the coupler on the driving car. **This is the domino-halting mechanism in the third and fourth physical tests.**

Vertical displacement that occurs in advance of lateral displacement helps to partially free the driven car's near-end centre plate from its truck before lateral motion causes the driven car's truck to roll about the wheel/rail contact points. The driven car's body does

not roll with its truck, and no roll moment is applied to the driven car's body through the rotary coupler. Therefore, the driven car body does not roll. The zero-speed derailment ends when the driven car's centre plate drags the pin out of the near-end truck, which falls back to the rails. The driven car is suspended by its near end coupler, and sits on its undisturbed far-end truck. **This is the domino-halting mechanism in the second test.**

In the second, third and fourth physical tests, the rotary coupler:

- Absorbed the differential roll between the driving car and the driven car
- Did not transmit a roll torque to either the driving or driven car body

In contrast, standard Type E double-shelf couplers:

- Can only absorb roughly 18° of differential roll (based on angular slack in the coupling system)
- Always transmit a roll torque from the driving car to the driven car's body

Insufficient vertical lift at the near end of the driven car forced the near-end truck of the driven car to roll in order for the near-end car body to follow the lateral motion of the driving car. Since the driven car body was still connected to its near-end truck, the body rolled with the truck. This made the third and fourth tests appear less successful than the second, but the rotary coupler was nonetheless successful at stopping the domino progression in all three tests where it was used.

Table 16: Comparison of key observations from full-scale tests.

| Observation / Question | Test #1 | Test #2 | Test #3 | Test #4 |
|---|--|---|---|--|
| Number of cars involved | 4 | 4 | 5 | 5 |
| Coupler connection | Standard Type E double-shelf couplers | Rotary double-shelf coupler on driven car (Car #III – near end) | Rotary double-shelf coupler on driving car (Car #III – far end) | Rotary double-shelf coupler on driving car (Car #III – far end) - carrier iron constrained |
| Was domino rollover progression stopped and why? | No. Binding of knuckles, large forces developed | Yes Knuckle-to-shelf contact occurs at rotary coupler, | Yes Knuckle-to-shelf contact occurs at rotary coupler | Yes Knuckle-to-shelf contact occurs at rotary coupler |

| Observation / Question | Test #1 | Test #2 | Test #3 | Test #4 |
|------------------------|---|--|--|---|
| | <p>between knuckles and coupler walls, couplers constrained leading to driving cars transmitting large torque to driven cars, causing driven bodies to roll about side bearing and side frames. Trucks tip up as bodies roll on side frames, then fall back to ground when bodies roll off.</p> | <p>delays vertical lift of driven car. Driven car's near-end centre plate only partially lifted out of centre bowl. Driving car unable to transmit a torque to driven car's body, and driven car's body does not roll with its truck. Lateral displacement of driven car causes its centre pin to be dragged out of its truck. Once freed from its truck, the near end of the driven car translates with the driving car as the driving car finishes its roll.</p> | <p>and springs on driven car's coupler carrier iron are compressed. Both further delay vertical lift of driven car. Driving car rolls and translates laterally, dragging driven car with it. Lateral force on driven car's near-end sill is reacted at its near end wheel/rail contacts, creating a couple. Couple causes driven car body and truck to roll together about the rail until truck slides off the rail. Driven car body is now free of its truck, but rolled to a significant angle, supported by its connection to driving car and by its far end truck.</p> | <p>and driving car's far-end truck slides off rails. Both further delay vertical lift of driven car. Driving car rolls and translates laterally, dragging driven car with it. Lateral force on driven car's near-end sill is reacted at its near end wheel/rail contacts, creating a couple. Couple causes driven car body and truck to roll together about the rail until truck slides off the rail. Driven car body is now free of its truck, but rolled to a significant angle, supported by its connection to driving car and by its far end truck.</p> |

| Observation / Question | Test #1 | Test #2 | Test #3 | Test #4 |
|---|--|---|---|--|
| Differential roll angle absorbed by rotary coupler | N/A | Yes, 90° | Yes, ~60° | Yes, ~60° |
| Shelf to knuckle contact (Y/N)? | No | Yes, observed through data and video but only at connection with rotary coupler | Yes, observed through video only, at connection with rotary coupler | Yes, observed through video only, at connection with rotary coupler |
| Driven car vertical clearance / take up before driven car is lifted | Car #I far end: 5.7 inch vertical displacement to lift Car #II Car #II far end: 4.6 inch vertical displacement to lift Car #III | Car #I far end: 10.2 inch vertical displacement to lift Car #III Car #III did not lift Car #II | Estimate Car #I far end as 5.7 inch vertical displacement to lift Car #III Estimate Car #III far end as 11.2 inch vertical displacement to lift Car #II (10.2 inch + 1 inch for carrier iron spring compression) | Estimate Car #I far end as 5.7 inch vertical displacement to lift Car #III Estimate Car #III far end as 10.2 inch vertical displacement to lift Car #II (carrier iron springs isolated) |

| Observation / Question | Test #1 | Test #2 | Test #3 | Test #4 |
|---|---|--|---|---|
| Centre pin clearance (which cars did/did not clear pin) | <p>1st Roll Attempt:</p> <p>Car #I near: Yes</p> <p>Car #I far: Yes</p> <p>Car #II near: No</p> <p>Car #II far: No</p> <p>2nd Roll Attempt:</p> <p>Car #II near: Yes</p> <p>Car #II far: Yes</p> <p>Car #III near: Yes</p> <p>Car #III far: No video.</p> | <p>Car #I near: No</p> <p>Car #I far: Yes</p> <p>Car #III near: Yes</p> <p>Car #III far: No (centre plate stayed in bowl)</p> <p>Car #II near: No video, but body did not roll.</p> <p>Car #II far: No video, but body did not roll.</p> | <p>Car #I near: No</p> <p>Car #I far: Yes</p> <p>Car #III near: Yes</p> <p>Car #III far: Yes</p> <p>Car #II near: No</p> <p>Car #II far: No.</p> | <p>Car #I near: Yes</p> <p>Car #I far: Yes</p> <p>Car #III near: Yes</p> <p>Car #III far: Yes</p> <p>Car #II near: No</p> <p>Car #II far: No video</p> |
| Roll angle at which next car begins to roll | <p>1st Roll Attempt:</p> <p>Car #I at 14.7° when Car #II rolls</p> <p>2nd Roll Attempt:</p> <p>Car #II at 14.5° when Car #III rolls</p> <p>(from data)</p> | <p>Car #I at 57.6° when Car #III rolls slightly.</p> <p>Car #II did not roll.</p> <p>(from data)</p> | <p>Car #I at ~15° - 20° when Car #III rolls</p> <p>Car #III at ~15° - 20° when Car #II rolls</p> <p>Car #II at ~15° - 20° when car in the 4th position is disturbed</p> <p>(based on video observation)</p> | <p>Car #I at ~15° - 20° when Car #III rolls</p> <p>Car #III at ~15° - 20° when Car #II rolls</p> <p>Car #II at ~15° - 20° when car in the 4th position is disturbed</p> <p>(based on video observation)</p> |

| Observation / Question | Test #1 | Test #2 | Test #3 | Test #4 |
|---|--|--|---|---|
| Max vertical loads at key connections | Car #III near end: 29,450 lb | Car #I far end: -30,330 lb Car #III near end: 54,630 lb | No forces measured | No forces measured |
| Max torque measurements at key connections | Car #III near end: 95,730 lb-ft | Car #I far end: 83,020 lb-ft | No torques measured | No torques measured |
| Max vertical displacement at key connections | Car #II far end: 29.4 inch (fuse yielded) Car #III near end: 14.3 inch (fuse yielded) | Car #I far end: 29.5 inch (fuse yielded) Car #III near end: 13.7 inch | No motion measured | No motion measured |
| Max lateral displacement at key connections | Car #II far end: 29.4 inch (fuse yielded) Car #III near end: 47.9 inch (fuse yielded) | Car #I far end: 29.7 inch (fuse yielded) Car #III near end: 48.11 inch | No motion measured | No motion measured |
| Did car body and truck roll together? | Car #I near: Yes Car #I far: No Car #II near: No Car #II far: No Car #III near: No Car #III far: No | Car #I near: Yes Car #I far: No Car #III near: No Car #III far: No Car #II near: No Car #II far: No | Car #I near: Yes Car #I far: No Car #III near: No Car #III far: No Car #II near: Yes Car #II far: No | Car #I near: Yes Car #I far: No Car #III near: No Car #III far: No Car #II near: Yes Car #II far: No |

| Observation / Question | Test #1 | Test #2 | Test #3 | Test #4 |
|---------------------------------------|---|---|--|--|
| Condition of trucks after test | Car #I near: Derailed Car #I far: On rails Car #II near: On rails Car #II far: Derailed, apart Car #III near: On rails Car #III far: On rails, apart | Car #I near: Derailed Car #I far: On rails Car #III near: On rails Car #III far: On rails Car #II near: On rails Car #II far: On rails | Car #I near: Derailed, apart Car #I far: On rails Car #III near: Derailed, apart Car #III far: Derailed, apart Car #II near: Derailed Car #II far: On rails | Car #I near: Derailed Car #I far: On rails, apart Car #III near: On rails Car #III far: Derailed Car #II near: Derailed Car #II far: |
| Other key points? | Coupler key sheared off at Car #II near end | Domino rollover stopped convincingly | Domino rollover stopped | Domino rollover stopped |

7. REFERENCES

1. Caldwell, R. Ladubec, C., Krzyzanowski, M., Liu, Y. and Caldwell, N. Investigation of Multiple Tank Car Rollover Derailments Related To Double-shelf Couplers and its Solutions. NRC Report No. CSTT- RVC-TR-157, National Research Council Canada, March 2009.
2. Trent, R., Prabhakaran, A., and Sharma, V. Torsional Stiffness of Railroad Coupler Connections, Sharma & Associates, Inc. Sponsored by U.S. Department of Transportation, Federal Railroad Administration, Washington. Report No. DOT/FRA/ORD-10/13. November 2010.

APPENDIX A INSTRUMENTATION LIST

Table 17: Instrumentation channels and sensors.

| Ser. | Type | Measured Parameter | Car# | Location | Comments | Fig # |
|------|---------------|--------------------|----------------|-------------------|--|------------|
| 1 | Load Cell | Lateral | Initiating Car | Top of car, N-end | Lateral force from the crane | |
| 2 | Strain Gauges | Vertical | Car #I | Draft sill, N-end | Vertical force from initiating car to Car #I | Figure 117 |
| 3 | Strain Gauges | Vertical | Car #II | Draft sill, N-end | Vertical force from Car #I to Car #II | Figure 117 |
| 4 | Strain Gauges | Vertical | Car #II | Draft sill, F-end | Vertical force from Car #II to Car #III | Figure 117 |
| 5 | Strain Gauges | Torque | Car #I | Draft sill, N-end | Torque from Initiating car to Car #I | Figure 117 |
| 6 | Strain Gauges | Torque | Car #II | Draft sill, N-end | Torque from Car #I to Car #II | Figure 117 |
| 7 | Strain Gauges | Torque | Car #II | Draft sill, F-end | Torque from Car #II to Car #III | Figure 117 |
| 8 | Displacement | Vertical | Car #I | Draft sill, N-end | Height of draft sill above top of rail | Figure 118 |
| 9 | Displacement | Vertical | Car #I | Draft sill, F-end | Height of draft sill above top of rail | Figure 118 |
| 10 | Displacement | Vertical | Car #II | Draft sill, N-end | Height of draft sill above top of rail | Figure 118 |
| 11 | Displacement | Vertical | Car #II | Draft sill, F-end | Height of draft sill above top of rail | Figure 118 |
| 12 | Displacement | Vertical | Car #III | Draft sill, N-end | Height of draft sill above top of rail | Figure 118 |
| 13 | Displacement | Vertical | Car #III | Draft sill, F-end | Height of draft sill above top of rail | Figure 118 |
| 14 | Displacement | Lateral | Car #I | Draft sill, N-end | Draft sill horizontal disp. across track | Figure 118 |
| 15 | Displacement | Lateral | Car #I | Draft sill, F-end | Draft sill horizontal disp. across track | Figure 118 |
| 16 | Displacement | Lateral | Car #II | Draft sill, N-end | Draft sill horizontal disp. across track | Figure 118 |
| 17 | Displacement | Lateral | Car #II | Draft sill, F-end | Draft sill horizontal disp. across track | Figure 118 |
| 18 | Displacement | Lateral | Car #III | Draft sill, N-end | Draft sill horizontal disp. across track | Figure 118 |
| 19 | Displacement | Lateral | Car #III | Draft sill, F-end | Draft sill horizontal disp. across track | Figure 118 |

| Ser. | Type | Measured Parameter | Car# | Location | Comments | Fig # |
|------|-------|--------------------|----------|-------------------|--|------------|
| 20 | Event | Vertical | Car #I | Shelf, N-end | Shelf/knuckle contact, Initiating car-Car #I | Figure 119 |
| 21 | Event | Vertical | Car #II | Shelf, N-end | Shelf/knuckle contact, Car #I-Car #II | Figure 119 |
| 22 | Event | Vertical | Car #III | Shelf, N-end | Shelf/knuckle contact, Car #II-Car #III | Figure 119 |
| 23 | Event | Vertical | Car #I | Side frame, N-end | Contact of body bolster to truck side frame, rolled side | Figure 120 |
| 24 | Event | Vertical | Car #I | Side frame, F-end | Contact of body bolster to truck side frame, rolled side | Figure 120 |
| 25 | Event | Vertical | Car #II | Side frame, N-end | Contact of body bolster to truck side frame, rolled side | Figure 120 |
| 26 | Event | Vertical | Car #II | Side frame, F-end | Contact of body bolster to truck side frame, rolled side | Figure 120 |
| 27 | Event | Vertical | Car #III | Side frame, N-end | Contact of body bolster to truck side frame, rolled side | Figure 120 |
| 28 | Event | Vertical | Car #III | Side frame, F-end | Contact of body bolster to truck side frame, rolled side | Figure 120 |
| 29 | Event | Vertical | Car #I | Side frame, N-end | Contact of body bolster to side bearings, rolled side | Figure 120 |
| 30 | Event | Vertical | Car #I | Side frame, F-end | Contact of body bolster to side bearings, rolled side | Figure 120 |
| 31 | Event | Vertical | Car #II | Side frame, N-end | Contact of body bolster to side bearings, rolled side | Figure 120 |
| 32 | Event | Vertical | Car #II | Side frame, F-end | Contact of body bolster to side bearings, rolled side | Figure 120 |
| 33 | Event | Vertical | Car #III | Side frame, N-end | Contact of body bolster to side bearings, rolled side | Figure 120 |
| 34 | Event | Vertical | Car #III | Side frame, F-end | Contact of body bolster to side bearings, rolled side | Figure 120 |

| Ser. | Type | Measured Parameter | Car# | Location | Comments | Fig # |
|------|-------|--------------------|----------------|-----------------------|------------------------------|------------|
| 35 | Angle | Pitch | Car #I | Middle of centre sill | Car body pitching angle | Figure 121 |
| 36 | Angle | Pitch | Car #II | Middle of centre sill | Car body pitching angle | Figure 121 |
| 37 | Angle | Pitch | Car #III | Middle of centre sill | Car body pitching angle | Figure 121 |
| 38 | Angle | Roll | Car #I | Draft sill, N-end | Car body rotation angle | Figure 122 |
| 39 | Angle | Roll | Car #I | Draft sill, F-end | Car body rotation angle | Figure 122 |
| 40 | Angle | Roll | Car #II | Draft sill, N-end | Car body rotation angle | Figure 122 |
| 41 | Angle | Roll | Car #II | Draft sill, F-end | Car body rotation angle | Figure 122 |
| 42 | Angle | Roll | Car #III | Draft sill, N-end | Car body rotation angle | Figure 122 |
| 43 | Angle | Roll | Car #III | Draft sill, F-end | Car body rotation angle | Figure 122 |
| 44 | Angle | Roll | Car #I | Truck bolster N-end | Truck bolster rotation angle | Figure 122 |
| 45 | Angle | Roll | Car #I | Truck bolster F-end | Truck bolster rotation angle | Figure 122 |
| 46 | Angle | Roll | Car #II | Truck bolster N-end | Truck bolster rotation angle | Figure 122 |
| 47 | Angle | Roll | Car #II | Truck bolster F-end | Truck bolster rotation angle | Figure 122 |
| 48 | Angle | Roll | Car #III | Truck bolster N-end | Truck bolster rotation angle | Figure 122 |
| 49 | Angle | Roll | Car #III | Truck bolster F-end | Truck bolster rotation angle | Figure 122 |
| 50 | Angle | Roll | Initiating Car | Coupler, F-end | Coupler rotation angle | Figure 123 |
| 51 | Angle | Roll | Car #I | Coupler, N-end | Coupler rotation angle | Figure 123 |
| 52 | Angle | Roll | Car #I | Coupler, F-end | Coupler rotation angle | Figure 123 |
| 53 | Angle | Roll | Car #II | Coupler, N-end | Coupler rotation angle | Figure 123 |
| 54 | Angle | Roll | Car #II | Coupler, F-end | Coupler rotation angle | Figure 123 |
| 55 | Angle | Roll | Car #III | Coupler, N-end | Coupler rotation angle | Figure 123 |

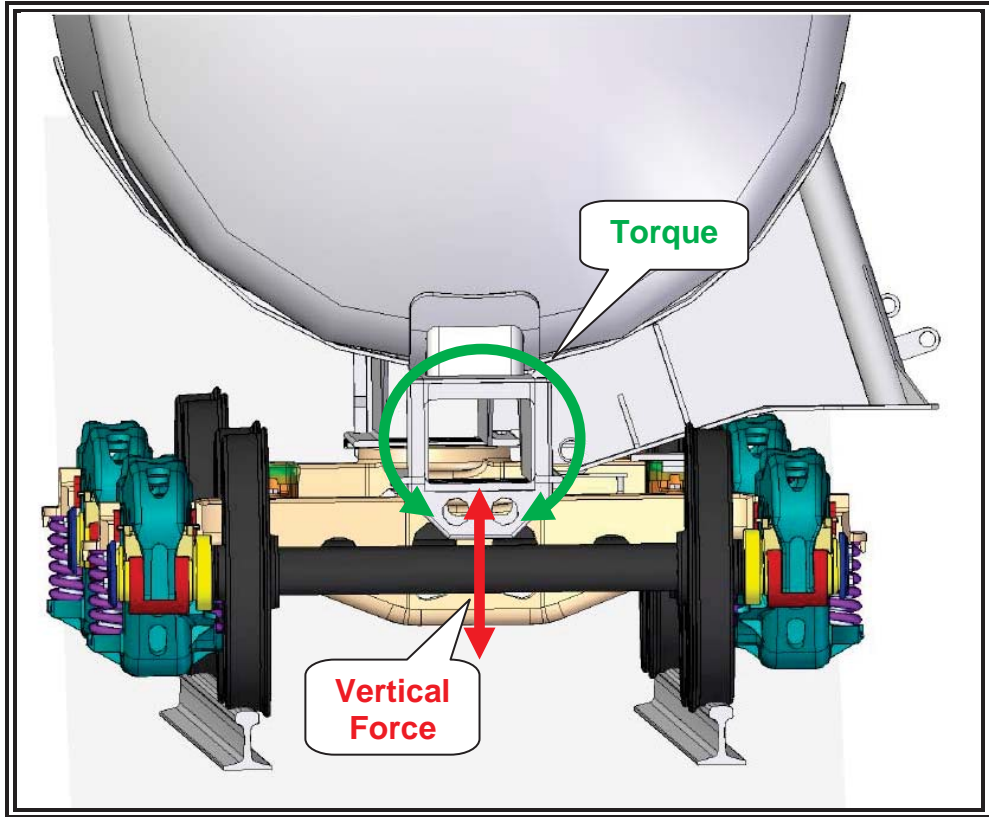


Figure 117: Draft sill vertical force and torque measurements.

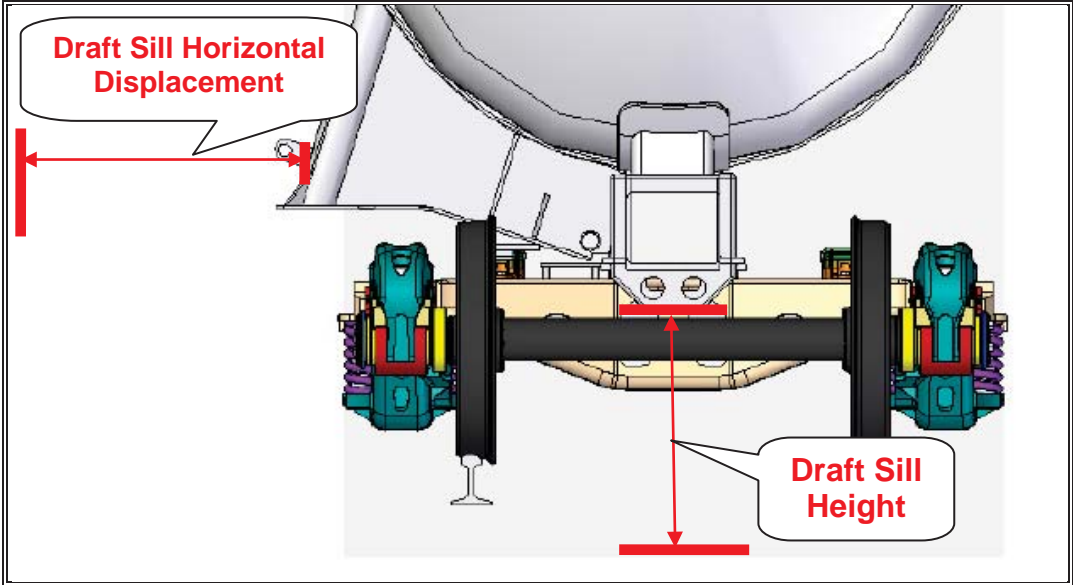


Figure 118: Draft sill displacement measurements.

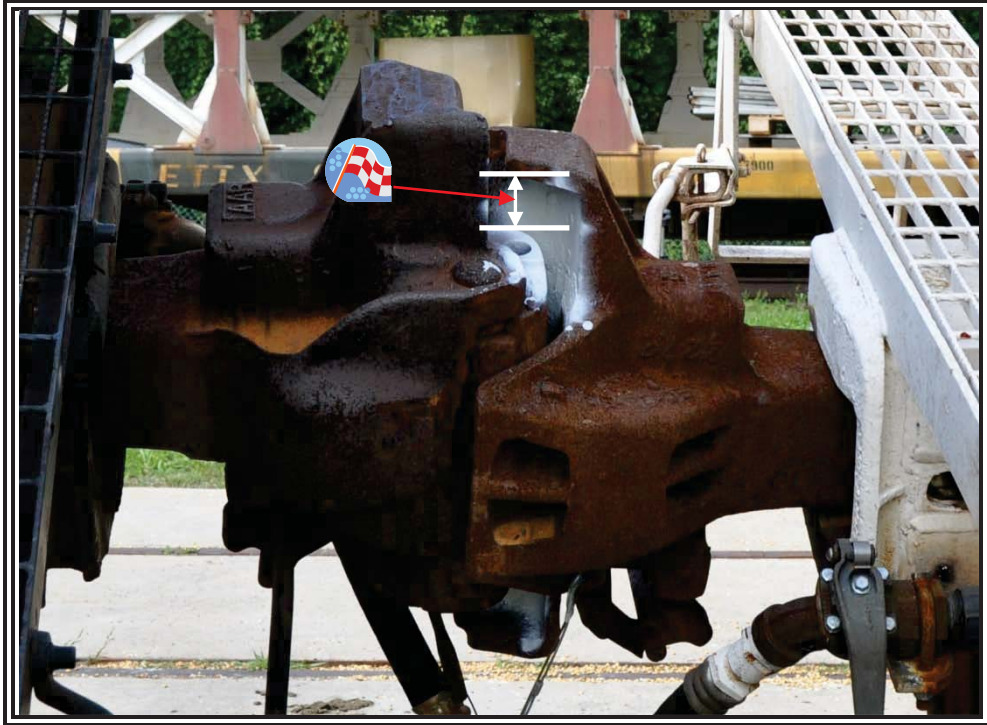


Figure 119: Contact between a knuckle and shelf.

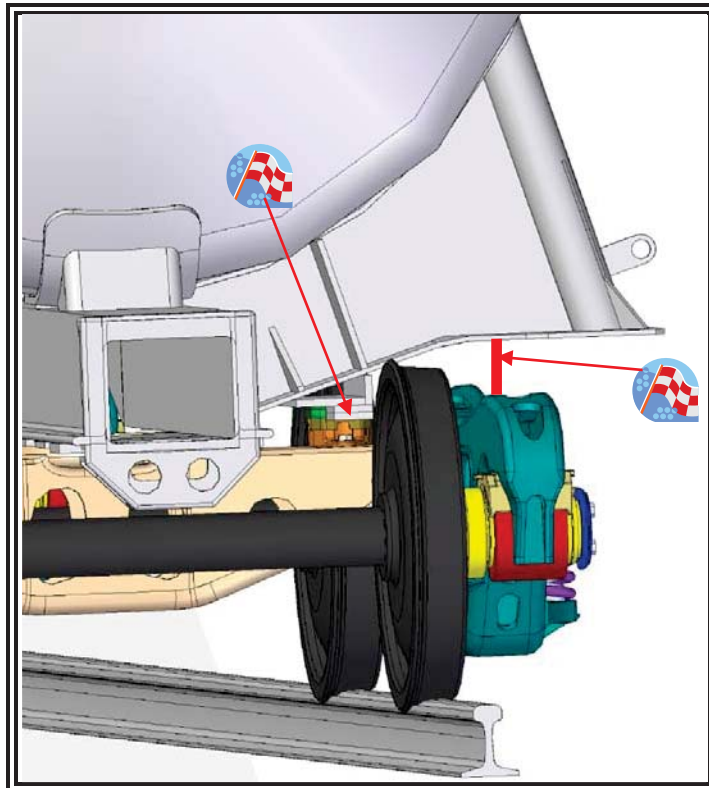


Figure 120: Contact of body bolster to truck side frame and side bearings.

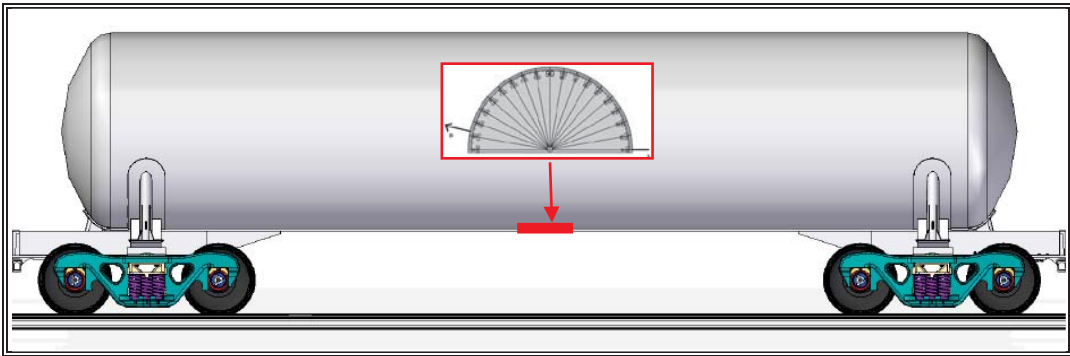


Figure 121: Car body pitching.

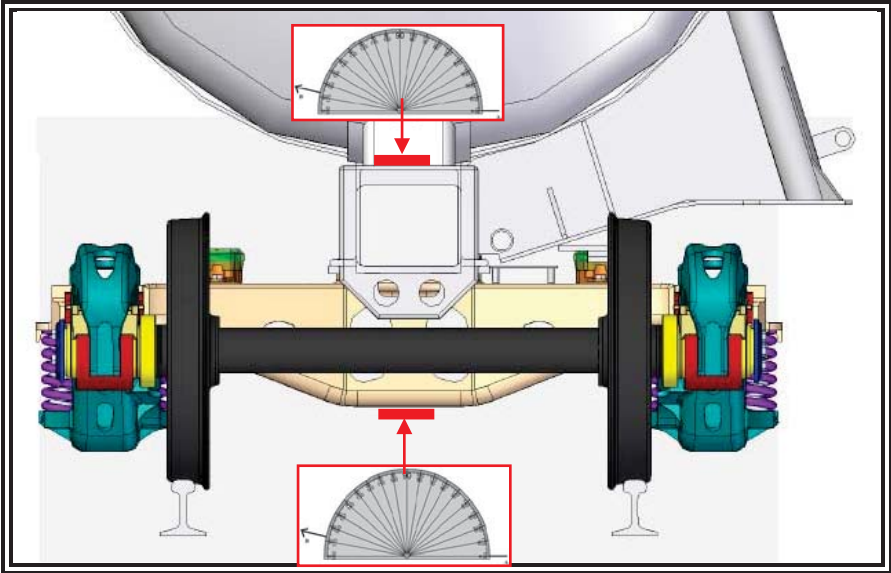


Figure 122: Car body and truck bolster rotation angle.

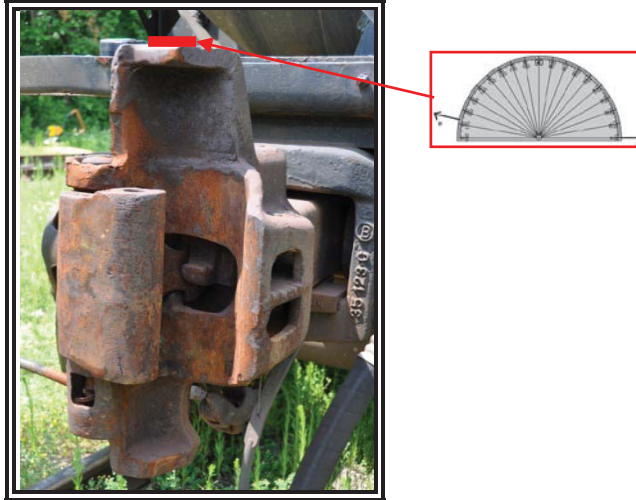


Figure 123: Coupler rotation angle.

APPENDIX B TANK CAR DRAFT SILL CALIBRATIONS

B.1 Strain Gauges Location Investigation

In an effort to find the best location for installing strain gauges to convert the tank car draft sill into a load cell to measure both vertical force and torque applied to the coupler, NRC-CSTT affixed several gauges to the car centre sill at the locations shown on Figure 124. One set of gauges (SG1, SG2, SG3, SG4, SG9 and SG10) was intended to measure the total torque applied to the coupler, and another set of gauges (SG5, SG6, SG7, SG8) was intended to measure the vertical force applied to the coupler.

All strain gauges are manufactured by VISHAY. Different gauges were used as follows; SG1, SG2, SG3, and SG4 are shear gauges (P/N EA-06-250TK-350). SG5, SG6, SG7 and SG8 are uniaxial gauges (P/NCEA-06-250UW-350). SG9 and SG10 are full bridges (P/N CEA-06-250US-350).

NRC-CSTT's engineers determined the strain gauge locations based on their previous experience in the instrumentation of railway cars, and by consulting with Intertechnology Inc., a company that designs load cells.

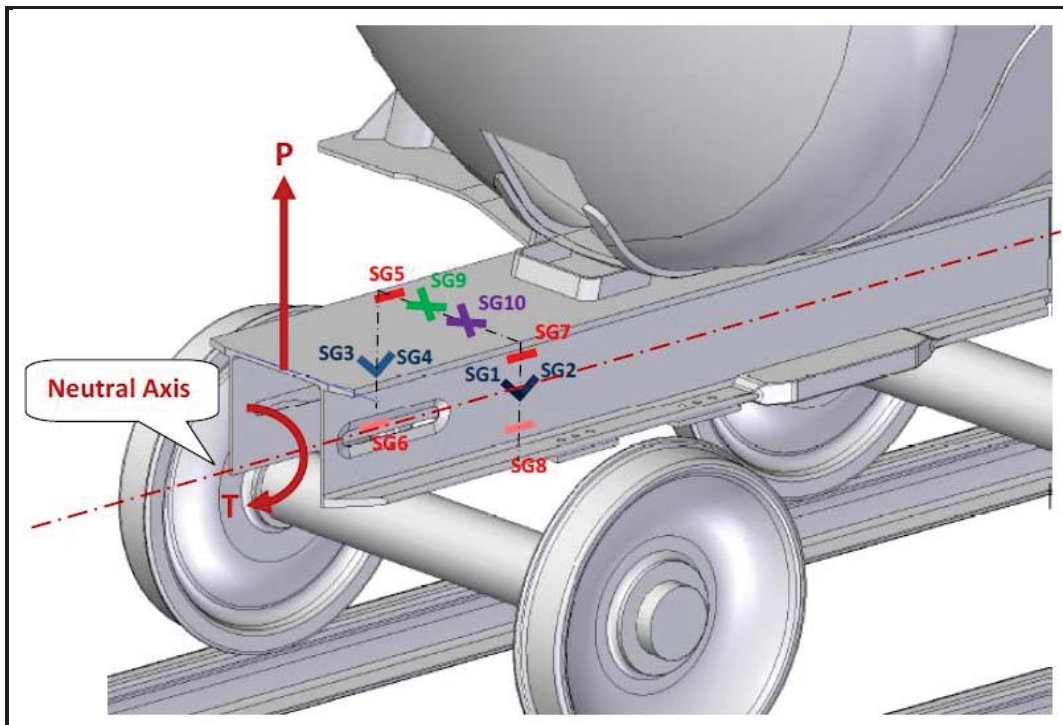


Figure 124: Preliminary strain gauge locations on draft sill.

Based on preliminary test results, NRC-CSTT found that shear strain gauges SG1-SG4 produces better results for torque measurements, but had some difficulties with the vertical force calibration. NRC-CSTT decided to perform FEA analysis to find the most adequate location for the strain gauges of the draft sill of each tank car. It was found that shear strain gauges as arranged similarly to SG1-SG4 but at different longitudinal position gave good results for vertical calibration.

Figure 125 below shows the various strain gauge arrangements used to instrument the tank car draft sill during the preliminary instrumentation phase.

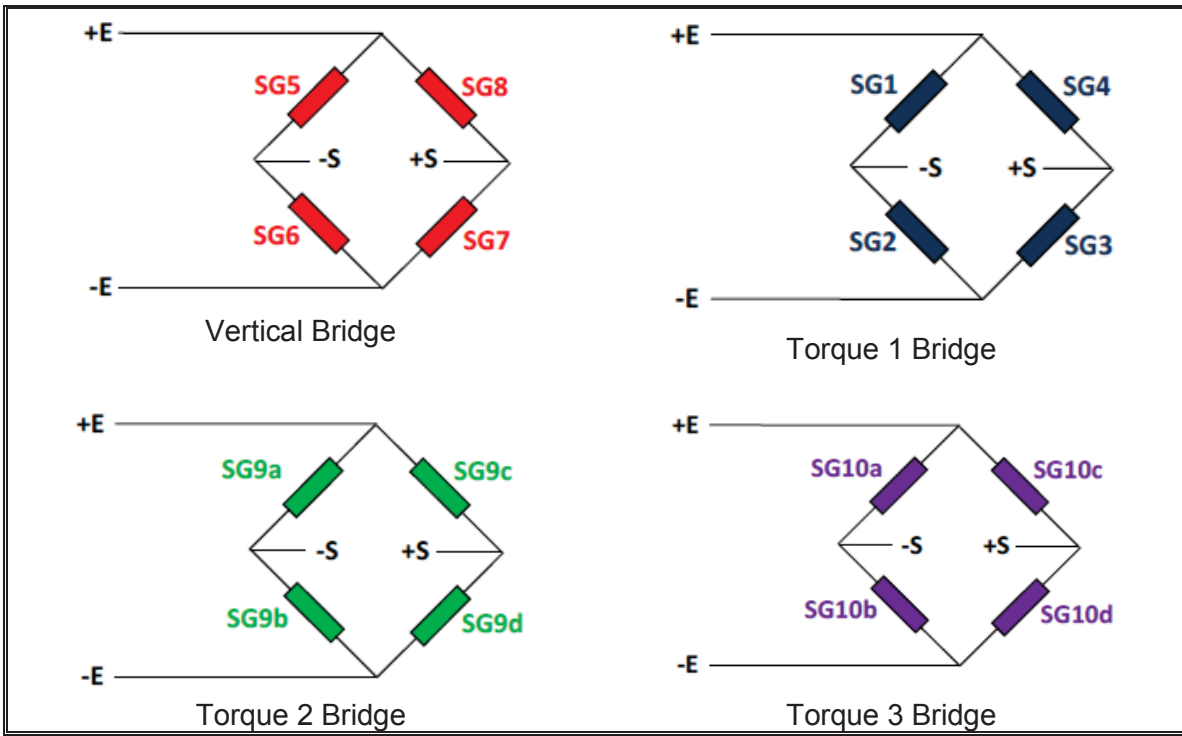


Figure 125: Preliminary strain gauge bridge wiring diagrams.

B.2 Final Strain Gauge Locations

Figure 126 shows typical strain gauge locations on the tank car draft sill to measure both vertical force and torque applied to the coupler. Strain gauges locations SG1-SG4 and SG5-SG8 are changed based on the FEA analysis that was performed on each tank car's draft sill.

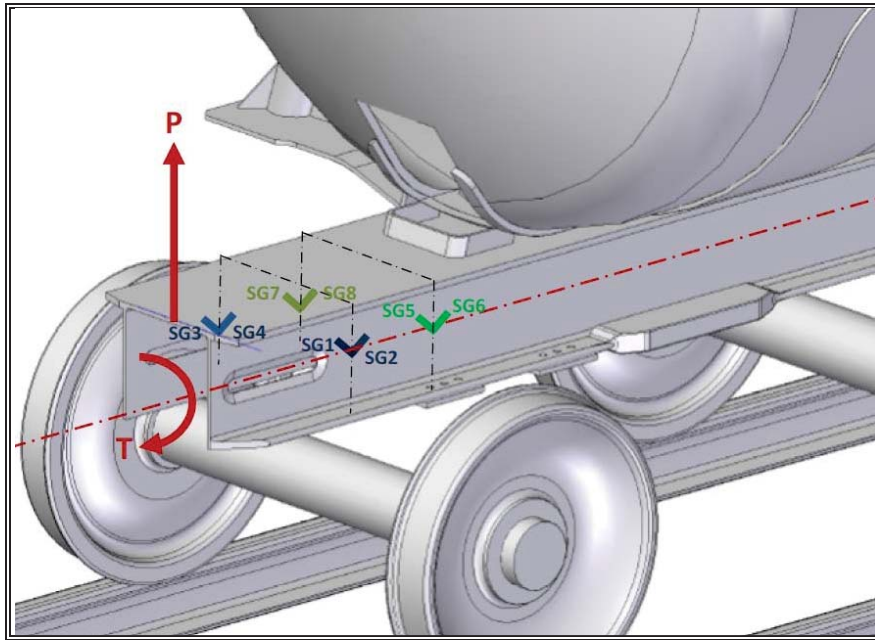


Figure 126: Typical strain gauge locations on draft sill.

The selection of the best strain gauge locations was based on achieving the best sensitivity while minimizing crosstalk between vertical and torque measurements. Figure 127 shows a side view for the strain gauge locations on the draft sill of tank Car #III as identified by the FEA analysis for both vertical force and torque measurements.

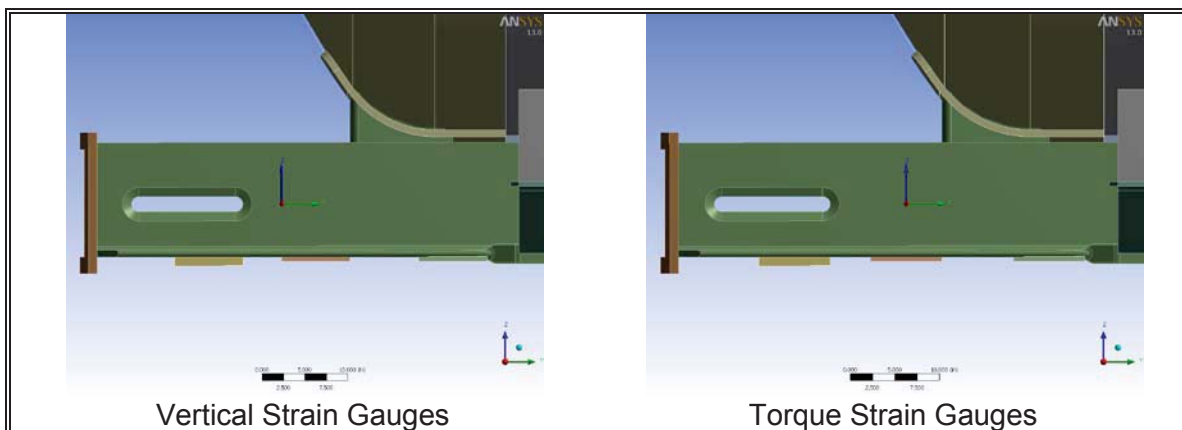


Figure 127: Strain gauge locations on Car #III draft sill.

Figure 128 shows a close up of the SG3 and SG4 shear strain gauges.

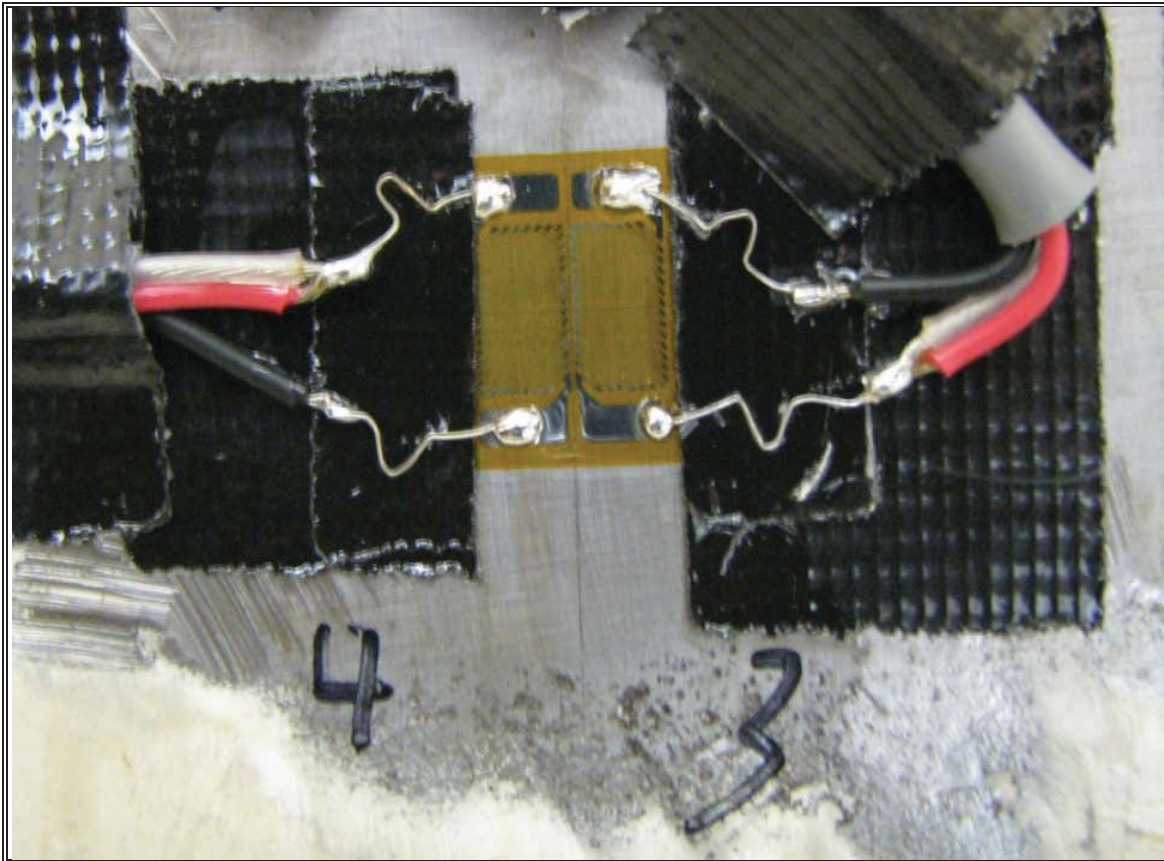


Figure 128: Strain gauges SG3 & SG4 on Car #II draft sill.

B.3 Calibration Procedure

B.3.1 Calibration Beam

NRC-CSTT prepared a calibration beam to facilitate the force and torque application to the car centre sill. A standard coupler head was removed and an 11-foot steel tube was welded horizontally to the coupler shank at the head location. The forces applied to the beam during calibration generated the same loading through the sill as the forces normally applied to the coupler head, and at the same distance from the car body. Figure 129 shows the calibration beam attached to the tank car.

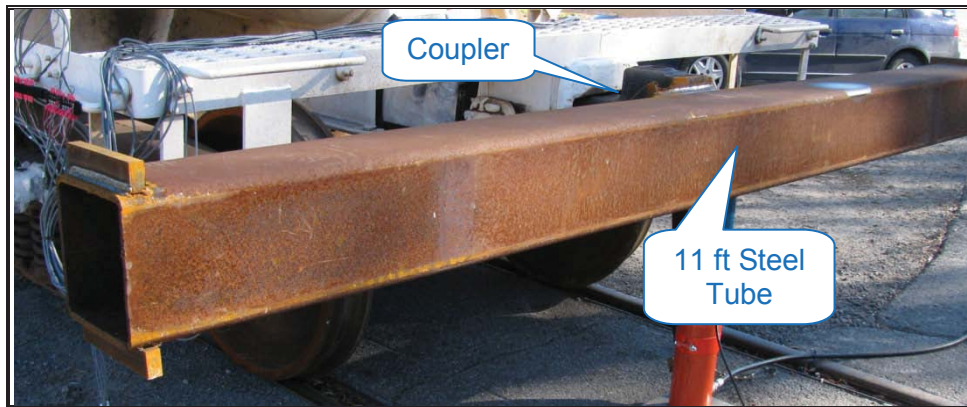


Figure 129: Calibration beam.

B.3.2 Vertical Calibration Procedure

An overhead crane with a calibrated load cell was used to lift the car vertically from the centre of the calibration beam (also the car's lateral centre) while monitoring and recording the load cell and the strain gauge outputs. The calibration beam was lifted until it no longer rested on the car to set the zero reference of all strain gauges. Then the car was completely lifted up with a total vertical load of around 20,000 lb as recorded by the load cell. Figure 130 shows a typical setup during the vertical calibration.

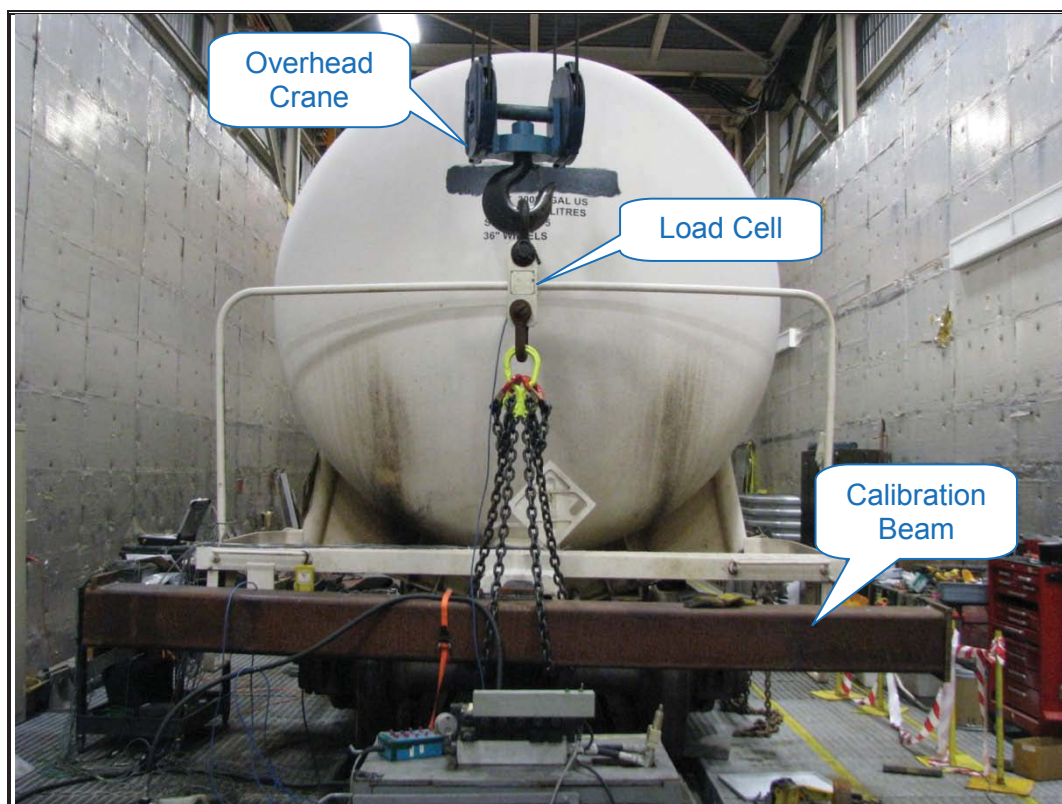


Figure 130: Typical vertical force calibration setup.

B.3.3 Torque Calibration Procedure

To apply torque to the car draft sill, two hydraulic cylinders were used to apply forces to the calibration beam in opposite directions (upward and downward) at 62 inch from the centreline of the calibration beam at each end. Both forces were applied through load cells to measure the forces received by the calibration beam. Refer to Figure 131.

An electric hydraulic pump was used to drive both hydraulic cylinders to gradually apply the upward and downward forces. Three inclinometers were used to monitor the beam's horizontal angle and the vertical angle of both hydraulic cylinders during the torque calibration to correct the torque force applied to the car draft sill, as described below.

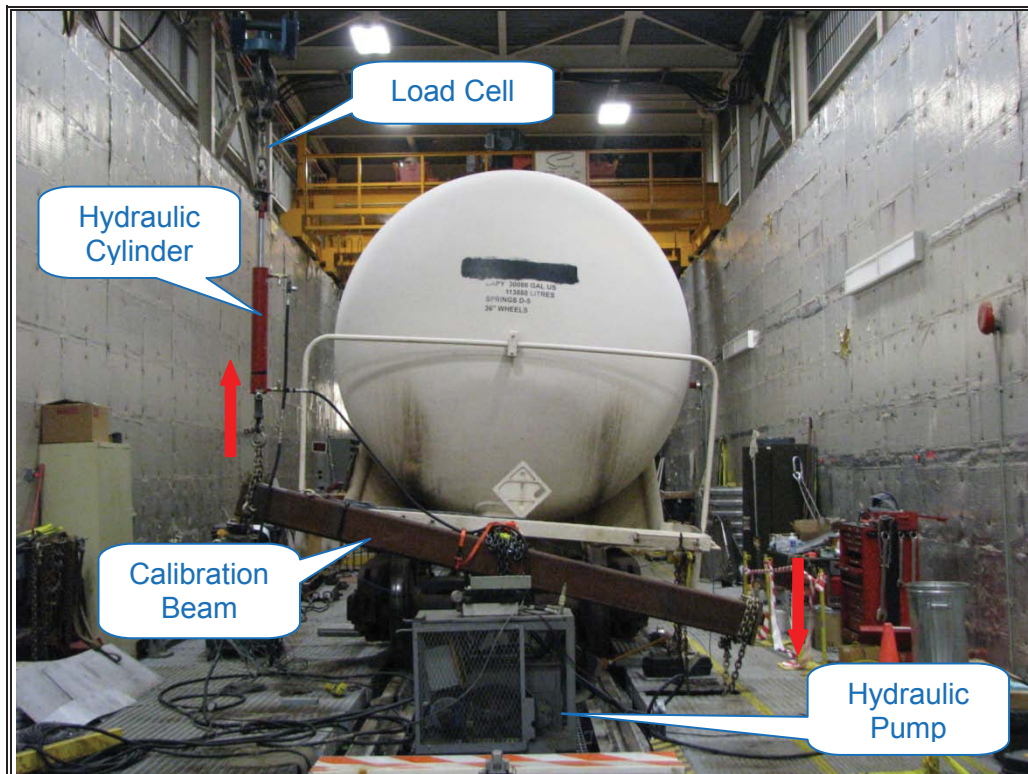


Figure 131: Torque calibration setup.

The calibration beam will start at zero angle (horizontal) and the torque can be simply calculated by the following equation:

$$\text{Torque (ft.lb)} = (F1*5.17\text{ft}) + (F2*5.17\text{ft})$$

where:

- F1 : Downward force as recorded by the load cell
- F2 : Upward force as recorded by the load cell
- 5.17: The 62 in distance from the load to the car centre

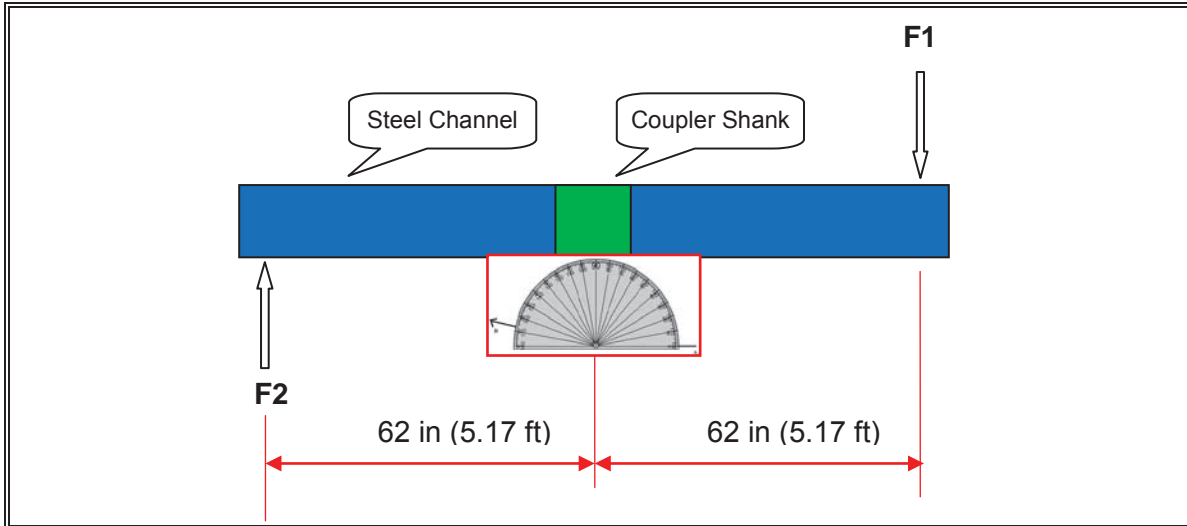


Figure 132: Torque calculations - beam at angle zero.

During torque application, the calibration beam will start rotating which creates an angle with respect to horizontal, and the applied forces will no longer be perpendicular to the calibration beam. To compensate for the change in angles and to obtain the force components that will generate torque on the car draft cell, three inclinometers were installed on the calibration beam, the upward force cylinder, and the downward force cylinder (refer to Figure 132). The torque calculations will be as follows:

$$\text{Torque (ft.lb)} = (F1 \cos(\theta_L - \theta_B) * 5.17\text{ft}) + (F2 \cos(\theta_R - \theta_B) * 5.17\text{ft})$$

where:

- F1 : Downward force as recorded by the load cell
- F2 : Upward force as recorded by the load cell
- 5.17: The 62 in distance from the load to the car centre
- θ_B : The beam angle relative to horizontal as shown below
- θ_R : The hydraulic cylinder angle relative to vertical as shown below
- θ_L : The hydraulic cylinder angle relative to vertical as shown below

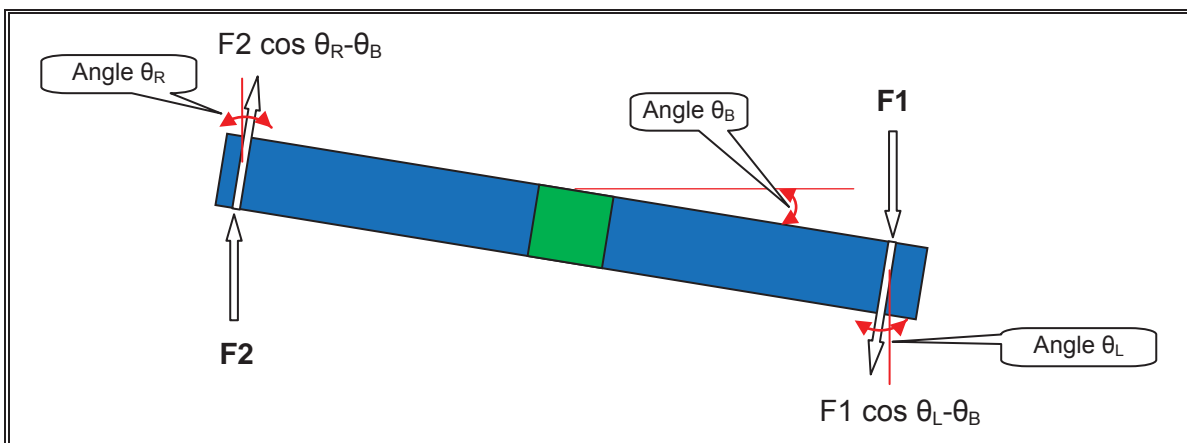


Figure 133: Torque calculations - beam at angle θ .

B.4 Calibration Results

B.4.1 Disclaimer

The instrumentation was applied to capture forces acting vertically with respect to axes that are fixed to and aligned with the sill; no transverse sill forces were measured and the instrumentation was not calibrated for this. Thus, as the sill rotates, the applied vertical force measured over time may not reflect a true vertical force. Nonetheless, the term vertical force is used to refer to the force measurement returned by the instrumented sill.

B.4.2 Vertical Force Calibration Results

Table 18 summarizes the vertical force calibration results for each draft sill of the three tank cars, along with the maximum applied vertical forces during calibration, and the % error in the calculated vertical force measurements. The table also shows the error in calculated torque measurements at the maximum applied vertical force; this error is a result of the crosstalk between forces. During Test #1, the A-end of Car #III was calibrated to measure upwards vertical force, then it was calibrated to measure downwards vertical force after installing the rotary coupler during the subsequent tests. As there are no torque measurements with the rotary coupler installed, the crosstalk effect on torque channel was ignored, and was represented by N/A in Table 18.

Table 18: Tank car draft sill vertical force calibration results.

| Car # | Car End | Vertical Force Calibration | | | | |
|----------|----------------------|--|---|---|--|---|
| | | Calibration Factor ($\mu\text{V}/1,000$ lbs) | Maximum applied vertical force (lbs) | % error in calculated vertical force | Maximum absolute error in calculated torque measurements (ft*lbs) at the maximum applied vertical force | % error in torque channel at the maximum applied vertical force ⁽¹⁾ |
| Car #I | A-End | 54.5209 | 19,283 | 1.8% | 3,217 | 3.6% |
| | B-End | -81.3967 | 19,430 | 2.3% | 2,028 | 2.3% |
| Car #II | A-End | 110.7002 | 19,595 | 2.0% | 2,167 | 2.4% |
| Car #III | A-End (Upwards) | 138.5457 | 19,405 | 3.9% | 2,289 | 2.5% |
| | A-End (Downwards) | -169.3481 | 19,164 | 3.4% | N/A | N/A |

1- Full scale torque of 90,000 ft*lb was used to calculate the % error in calculated torque measurements.

Figure 134 shows a general overview of the calculated vs. applied vertical forces during the calibration of Car #1 A-end draft sill.

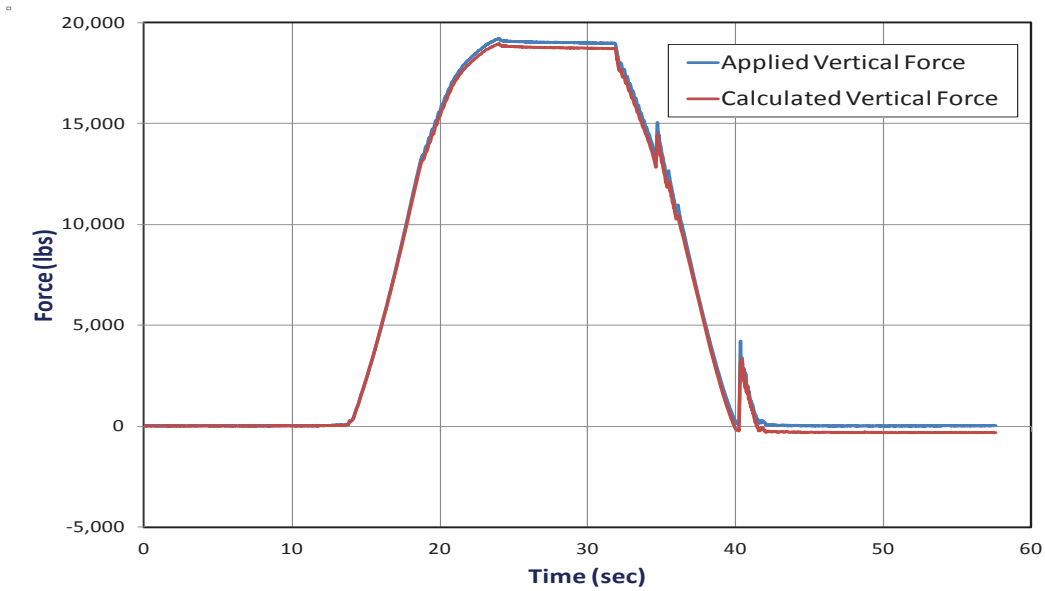


Figure 134: Calculated and applied vertical forces – Car #1 A-end.

Figure 135 shows an example of the relationship between the % error in the calculated vertical force measurements and the applied vertical force.

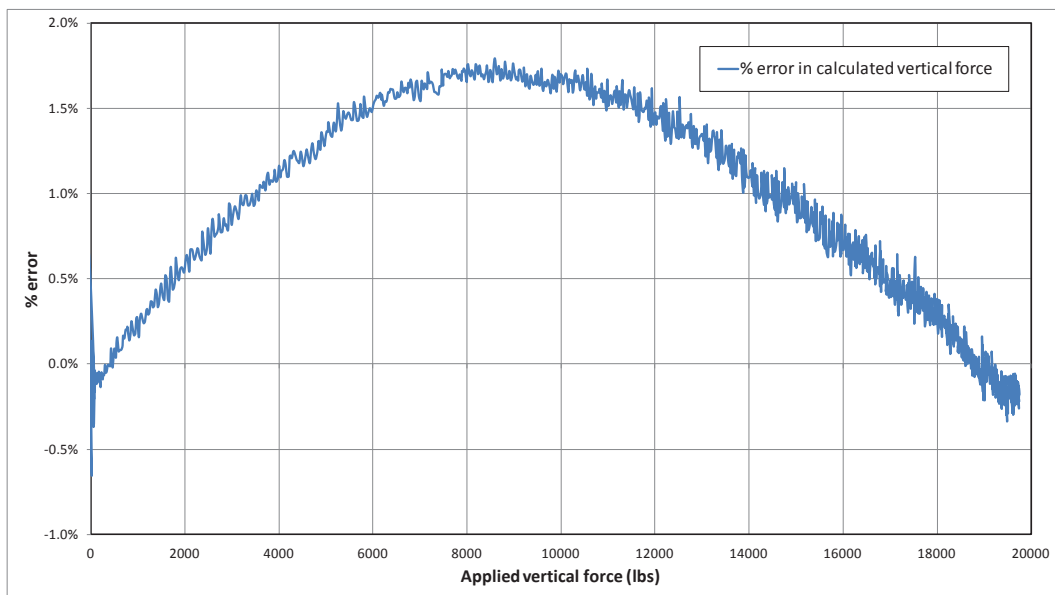


Figure 135: Percent error in calculated vertical force measurements – Car #1 B-end.

Figure 136 shows an example of the relationship between the crosstalk error (% full scale) in the torque channel due to vertical force application.

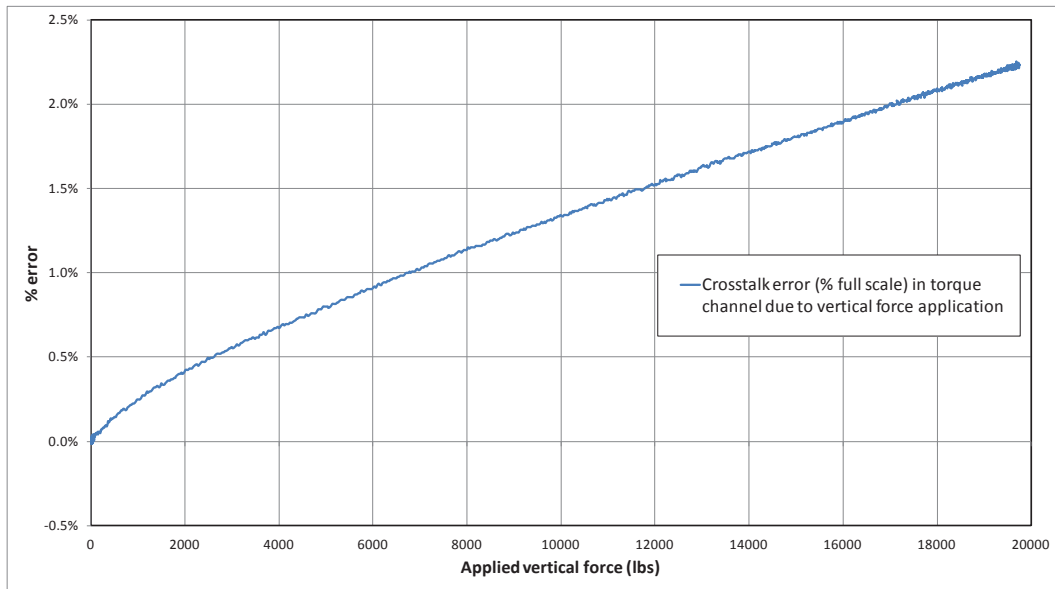


Figure 136: Percent crosstalk error in torque measurements – Car #1 B-end.

B.4.3 Torque Calibration Results

Table 19 summarizes the torque calibration results for each draft sill of the three tank cars, along with the maximum applied torque during calibration, and the % error in the calculated torque measurements. The table also shows the error in calculated vertical force measurements at the maximum applied torque, this error is a result of the crosstalk between forces. During Tests #2, 3 and 4, the B-end of Car #I was calibrated to measure the torque between Car #I and Car #III where the modified rotary coupler was installed. The crosstalk (% full scale) error in the vertical force channel due to the torque application was found to be over 50% (indicated in red). For this reason, during these tests, vertical force measurements between Car #I and Car #III was obtained from the A-end of Car #III, and the torque measurements was obtained from B-end of Car #I.

Table 19: Tank car draft sill torque calibration results.

| Car # | Car End | Torque Calibration | | | | |
|----------|---------|--|------------------------------------|---------------------------------|---|---|
| | | Calibration Factor ($\mu\text{V}/1,000\text{ft}^*\text{lbs}$) | Maximum applied torque (ft*lbs) | % error in calculated torque | Maximum absolute error in calculated vertical force measurements (lbs) at the maximum applied torque | % error in vertical force channel at the maximum applied torque ⁽²⁾ |
| Car #I | A-End | 75.6132 | 91,102 | 2.0% | 2,806 | 14.8% |
| | B-End | 77.6432 | 98,420 | 7.4% | 9,809 | 51.6% |
| Car #II | A-End | 178.8444 | 94,679 | 3.6% | 1,163 | 6.1% |
| Car #III | A-End | 146.9251 | 92,036 | 3.6% | 1,079 | 5.7% |

2- Full scale vertical force of 19,000 lb was used to calculate the % error in calculated vertical measurements.

Figure 137 shows the calculated vs. applied torque during the calibration of Car #1 A-end draft sill. The divergence between both forces occurs when releasing the applied torque due to the difficulties in controlling the same oil flow through both hydraulic cylinders, which creates sudden movement of the car body. Only the applying torque portion was used for calculating the torque calibration factors.

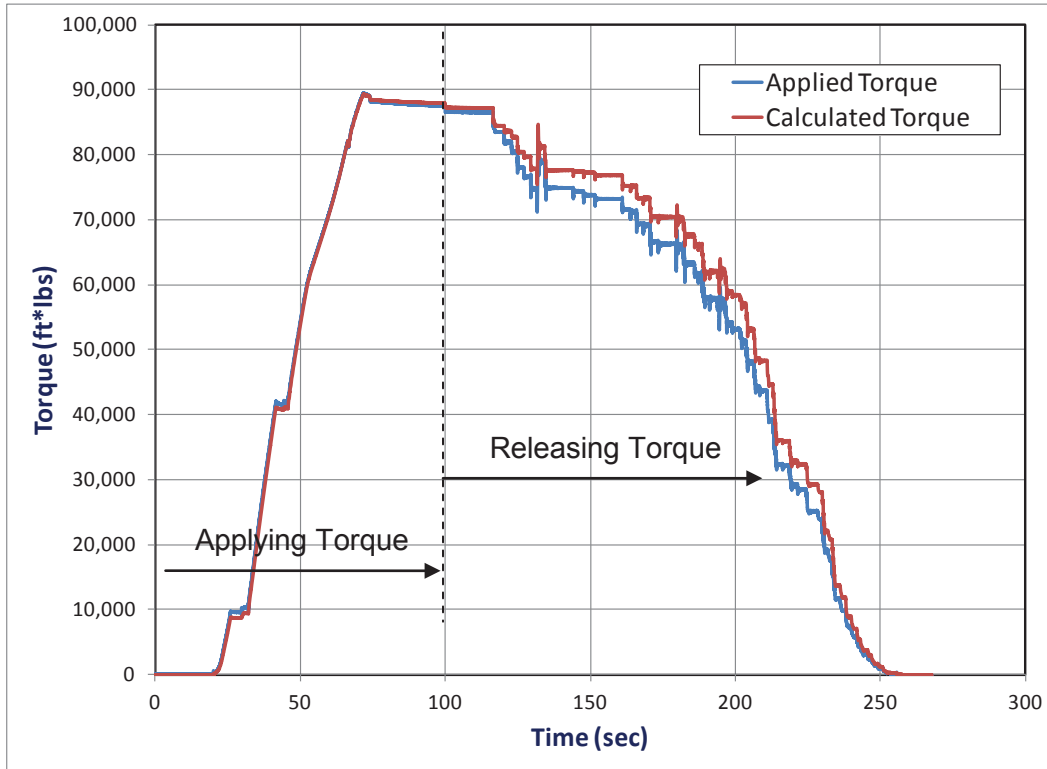


Figure 137: Calculated and applied torque – Car #1 A-end.

Figure 138 shows an example of the relationship between the % error in the calculated torque measurements and the applied torque.

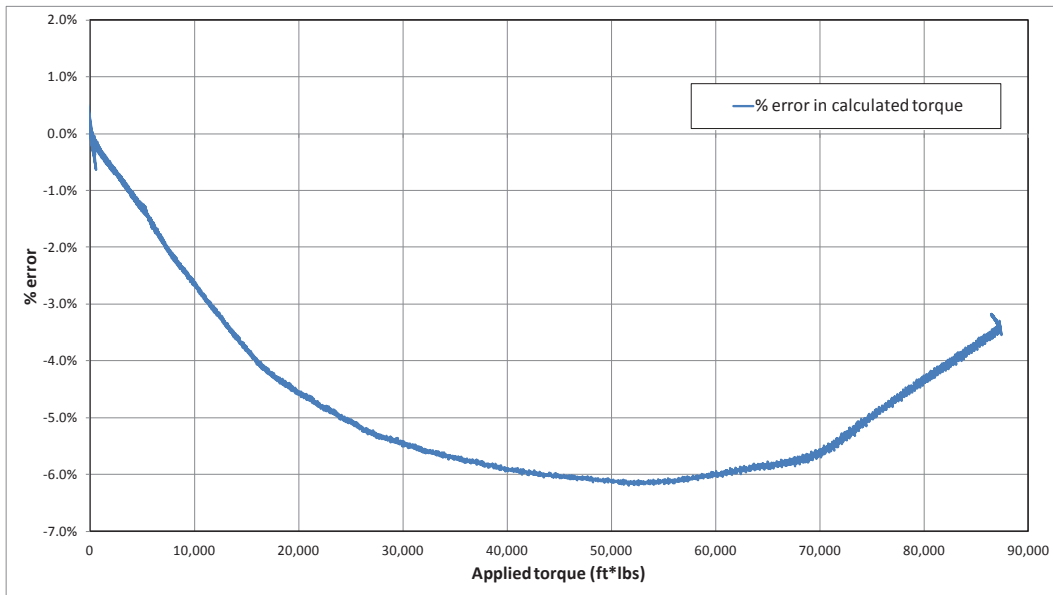


Figure 138: Percent error in calculated torque measurements – Car #1 B-end.

Figure 139 shows an example of the relationship between the crosstalk error (% full scale) in the vertical force channel due to torque application.

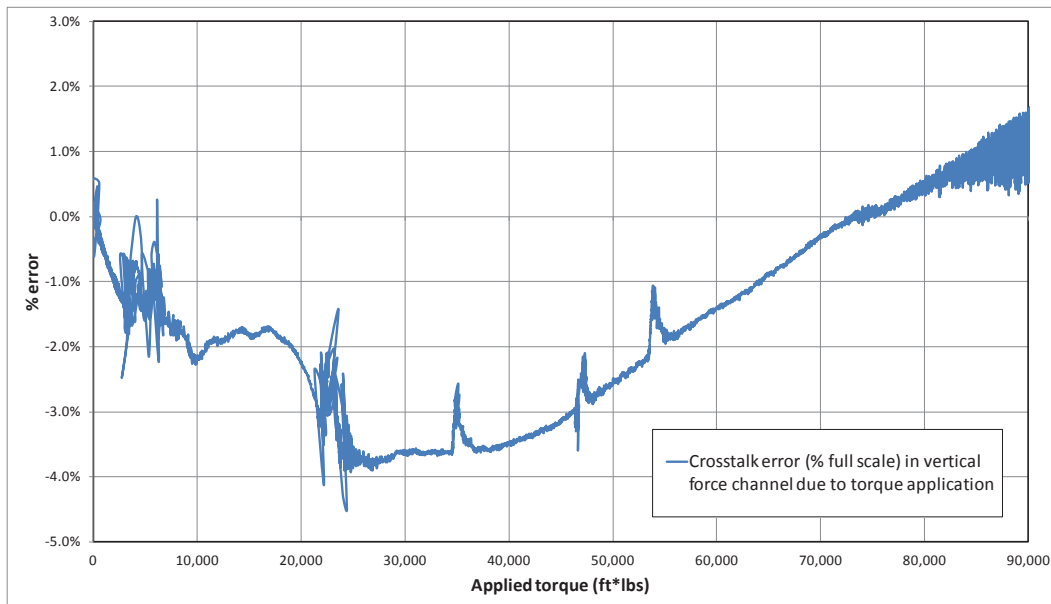


Figure 139: Percent crosstalk error in vertical force measurements – Car #1 A-end.

**APPENDIX C MODIFIED ROTARY COUPLER MANUFACTURING AND
INSTALLATION**

C.1 Coupler Modification

NRC-CSTT prepared a modified rotary coupler to be used during Test #2, Test #3, and Test #4. The modification included the purchase of a rotary coupler and a rotary coupler yoke, and the purchase of a standard Type E double-shelf coupler. NRC-CSTT modified the couplers by cutting off the standard Type E double-shelf coupler's head and welding it to the rotary coupler shank after removing the rotary coupler's head. Figure 140 shows a schematic for the modification.

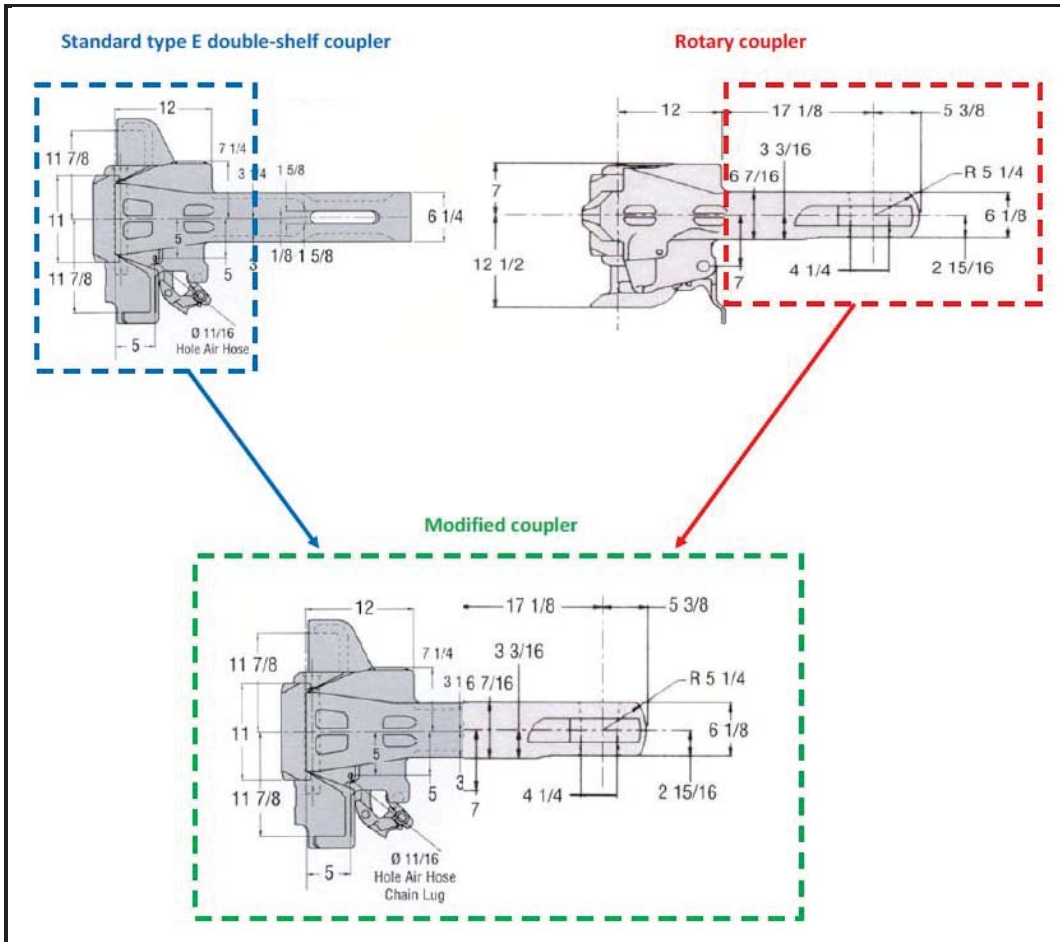


Figure 140: Rotary coupler modification schematic⁶.

Figure 141 shows the steps taken to manufacture the modified rotary coupler.

⁶ Pictures are taken from McConway & Torley LLC website (www.mcconway.com). Pictures are used for illustration purpose only.



Figure 141: Modified rotary coupler manufacturing.

C.2 Coupler Installation

A comparison between Type E sill/striker and Type F sill/striker revealed that Type E sill/striker is too small to allow the rotary coupler to rotate. Figure 142 shows a schematic for the rotary coupler shank inside a Type E sill/striker. The widest diameter of the rotary coupler shank is 7 1/8" and the Type E sill maximum clearance is only 7".

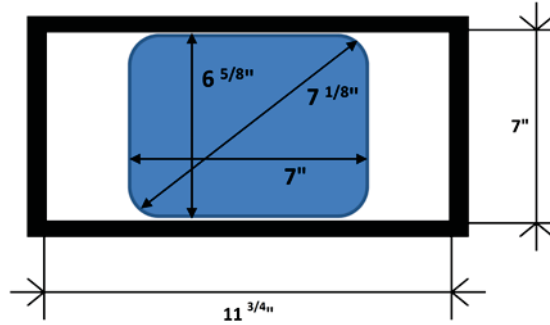


Figure 142: Modified rotary coupler inside Type E sill/striker.

The Type F sill/striker is very comparable to the rotary coupler sill/striker as both of them have a wider opening that allows the rotary coupler to rotate as intended. The Type F striker is also similar to the rotary coupler striker as both of them have carrier springs. Figure 143 shows a schematic for the rotary coupler shank inside a Type E sill/striker.

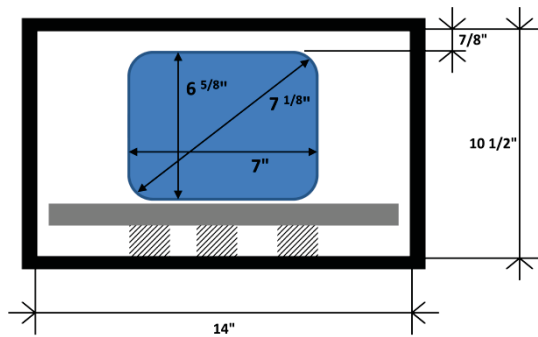


Figure 143: Modified rotary coupler inside Type F sill/striker.

While installing the rotary coupler yoke inside the Type F sill, a small part of the front lugs had to be cut to accommodate the yoke as shown in Figure 144 and Figure 145.

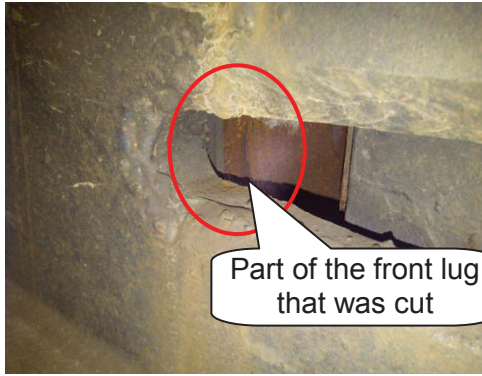


Figure 144: Sill before modification.



Figure 145: Sill after modification.

The rotary coupler yoke was 1 in. larger than the Type F yoke, and for this reason, a 1 in. spacer was required between the car sill and the draft gear carrier plate to lower the carrier plate as shown in Figure 146.



Figure 146: Insertion of 1 in. spacer below the yoke

APPENDIX D TANK CAR WEIGHTS AND DIMENSIONS

Table 20: Tank car weights and dimensions used in simulation.

| Parameter | Unit | Car #II | Car #III | Car #I |
|--|------|---------|----------|--------|
| Light weight | lb | 71000 | 71200 | 70600 |
| Loaded CG above top of rail | in | 86.15 | 82.1 | 85.61 |
| Tank inner diameter | in | 113.125 | 110.25 | 108 |
| Shell thickness | in | 0.449 | 0.46875 | 0.4375 |
| Head thickness | in | 0.4375 | 0.4375 | 0.4375 |
| Gross rail load | lb | 263000 | 263000 | 263000 |
| Truck cap | ton | 100 | 100 | 100 |
| Spring travel | in | 3.6875 | ?? | 3.6875 |
| Draft sill above top of rail | in | 26.5 | 20.5 | x |
| Top of side frame above top of rail | in | 31 | 31.25 | same |
| Lateral position of inside of side frame from truck centre | in | 38 | same | same |
| Side frame top chord width | in | 8 | same | same |
| Centre plate above TOR | in | 26 | same | same |
| Vertical clearance, coupler shank to underside of striker, A-end | in | 1 | 1 | 0.75 |
| Vertical clearance, coupler shank to underside of striker, B-end | in | 0.875 | 1.5 | 0.75 |
| Side bearing type | | CCSB | rollers | CCSB |
| Distance, pulling face to striker, A-end | in | 16.25 | 18 | 16.75 |
| Distance, pulling face to striker, B-end | in | 16.75 | 18.25 | 15.75 |
| Vertical distance, knuckle to shelf top, A-end | in | 6.625 | 6.5 | 6.75 |
| Vertical distance, knuckle to shelf bottom, A-end | in | 6.25 | 6.75 | 6.5 |
| Vertical distance, knuckle to shelf top B-end | in | 6.5 | 6.75 | 6.75 |
| Vertical distance, knuckle to shelf bottom B-end | in | 6.75 | 6.5 | 6.5 |
| Length across strikers | in | | | |
| Truck wheelbase | in | 70 | 70 | 70 |
| Truck centre distance | in | 575 | 552.5 | 573 |

APPENDIX E TANK CAR AND TRUCK COMPONENT TERMINOLOGY

Car body bolster – a structural member on the underside of the car body at each end, which transmits the car body load to the truck.

Centre bowl – a flat-bottomed circle with a raised edge located at the centre of the truck bolster, in which the centre plate sits.

Centre pin – a steel pin which passes through the centre bowl and centre plate at both ends of the car, for the purpose of transmitting longitudinal force from the car body to the truck in the event that the centre plate momentarily rises above the centre bowl.

Centre plate – a short circular steel plate that is located at the centre of the bottom of the car body bolster.

Coupler – the component installed at both ends of all rail cars to enable one car to be joined to another, and to transmit longitudinal force from one car to another.

Coupler carrier iron springs – when Type F couplers (which greatly restrict relative vertical movement) are installed on rail cars, the coupler carrier iron is vertically supported on springs to compensate for the loss of relative vertical motion.

Coupler carrier iron: a cross-member at the bottom front of the draft sill which bears the weight of the portion of the coupler that extends beyond the draft sill, prevents the coupler head from drooping and provides a wear surface for the coupler to slide on.

Coupler key – a flat steel member that passes through the draft sill and the coupler shank, and prevents rotation of the coupler shank within the draft sill. Only used on Type E couplers.

Coupler knuckle – a part of the coupler head which pivots about a vertical pin between open and closed positions. It engages with the knuckle on a mating coupler, and then mechanically locks in the closed position, thus joining two rail cars together.

Coupler shank – the part of the coupler immediately behind the coupler head which extends into the draft sill.

Coupler: shelf, knuckle, key, shank, carrier iron, carrier springs

Double-shelf coupler – a coupler having an upper shelf and a lower shelf cast integral with the coupler head, the purpose of the shelves being to constrain relative vertical movement and prevent unintentional disengagement of the couplers

Draft sill – structural component used on tank cars to carry the couplers and to transmit in-train forces between cars.

Side bearings – surfaces on the truck bolster which come into contact with corresponding surfaces on the car body bolster for the purpose of limiting car body roll with respect to the truck bolster, and for reducing/controlling truck hunting.

Side frame – the structural members on the left and right side of a truck that transmit the car body and truck bolster weight to the wheelsets.

Tank car body – cylindrical vessel in which the liquid or gaseous product is stored on this type of freight car

Truck bolster – a support member that transmits the weight from the car body bolster through suspension springs to the truck side frames.

Truck springs – the elements installed in each side frame which support the weight of the car body and its lading.

Truck – the assembly under both ends of a conventional freight car which supports the car body and enables it to roll along the track.